AN ABSTRACT OF THE THESIS OF

Dante L. Knapp for the degree of Master of Interdisciplinary Studies in Applied Anthropology, Soil Science, and Applied Anthropology presented on June 20, 2014.

Title: Paleoenvironmental Reconstruction of Late Pleistocene and Holocene Human Ecologies: A Case Study of Phytoliths from the Lower Salmon River Canyon, Idaho.

Abstract approved: _____

Loren G. Davis

Archaeological excavations of the Cooper's Ferry site in the Lower Salmon River Canyon, Idaho, have revealed a stratified record of cultural occupation, spanning the late Pleistocene and early Holocene periods. The purpose of this study was to contribute to the understanding of cultural adaptive strategies represented in the archaeological record at this site, as part of the larger ongoing research agenda for the Cooper's Ferry locale. In order to develop a human ecological perspective of the late Pleistocene and Holocene environments associated with the archaeological record, datasets examining past environmental conditions are required. This study advances these datasets through the analysis of late Pleistocene and Holocene phytolith assemblages derived from both the Cooper's Ferry site and within the Lower Salmon River Canyon.

In total, 129 samples were processed for phytolith analysis from four stratigraphic sections—SR 23, SR 27, SR 34, and the north wall of Unit A—at Cooper's Ferry. Through comparisons of the phytolith assemblages obtained for this study with other

locally available paleoenvironmental proxy records, this study facilitates the reconstruction of the biophysical environment of the Lower Salmon River Canyon during the late Pleistocene and Holocene periods, thus contributing to a contextualized human ecological model. Results show that the Lower Salmon River Canyon provided a variety of economic opportunities and constraints associated with grass- and shrub-step vegetative communities during these periods. Findings also indicate the ways in which phytolith analyses may be applied in the development of locally derived paleoecological models that can be used to address questions regarding human behavior in the archaeological record.

Paleoenvironmental Reconstruction of Late Pleistocene and Holocene Human Ecologies: A Case Study of Phytoliths from the Lower Salmon River Canyon, Idaho

by
Dante L. Knapp

A THESIS

submitted to

Oregon State University

in partial fulfillment of
the requirements for the
degree of

Master of Arts in Interdisciplinary Studies

Presented June 20, 2014
Commencement June 2015

Master of Arts in Interdisciplinary Studies thesis of Dante L. Knapp presented on June 20, 2014

APPROVED:

Major Professor, representing Applied Anthropology

Director of the Interdisciplinary Studies Program

Dean of the Graduate School

I understand that my thesis will become part of the permanent collection of Oregon State University libraries. My signature below authorizes release of my thesis to any reader upon request.

Dante L. Knapp, Author

ACKNOWLEDGEMENTS

The author expresses sincere appreciation to the following individuals and entities that made this thesis possible: To the Department of Anthropology; School of Language, Culture, & Society; the Department of Crop & Soil Sciences; and the Graduate School for ongoing support and opportunities. To my primary advisor, Dr. Loren G. Davis, for his endless guidance, encouragement, expertise, and the applied prospects he has provided me that have made me the archaeologist I am today. To my committee members—Drs. Jay Noller and Leah Minc—for their guidance and leadership. To faculty from the Departments of Anthropology and Crop & Soil Science for their ongoing mentorship and offerings. To my colleagues at Oregon State University and across the country for their friendship and inspiration. To the community of Cottonwood, Idaho for their steadfast hospitality. To David Sisson, District Archaeologist of the Bureau of Land Management, Cottonwood Resource Area Office for allowing me to sample the stratigraphic sections at SR-23, SR-27, and SR-34. To James Knobbs for providing the raft and guiding skills for one of the most enjoyable work commutes. To my family and especially my mother, Kate Sloan, for their love, care, and endless encouragement to follow my passions. Finally, to my amazing wife Courtney Everson for her endless support and encouragement through this process; you are truly an amazing woman and I could not be the man I am without you.

TABLE OF CONTENTS

TABLE OF CONTENTS (Continued)

Page

TABLE OF CONTENTS (Continued)

LIST OF FIGURES

LIST OF FIGURES (Continued)

LIST OF TABLES

LIST OF APPENDICES

Chapter 1. Introduction

Previous geoarchaeological investigations of the Cooper's Ferry site, in western Idaho's lower Salmon River canyon (LSRC), have identified a stratified record of cultural occupation spanning the late Pleistocene and early Holocene (LP/EH) epochs (Butler 1969; Davis 2001a; Davis and Schweger 2004). Davis conducted test excavations of the site in 1997 by opening up a 2x2 meter unit (Unit A) in efforts to establish chronometric controls in addition to understanding site function and culture change during the LP/EH (Davis 2001a; Davis and Schweger 2004). The 1997 excavation revealed a stratified archaeological record dating as early as 11,370-11,410 yr BP to 7,300 yr BP with an associated assemblage of non-fluted Western Stemmed projectile point technology (Davis 2001a; Davis and Schweger 2004). The proposed antiquity of Cooper's Ferry is controversial given that site's assemblage reflects either a pre-Clovis or co-Clovis cultural tradition present in the Far West, which calls the traditional Clovis First model into question.

A growing body of archaeological research has challenged the validity of the Clovis First model over the last two decades, as pre-Clovis sites have become accepted by the larger archaeological community (Adovasio and Pedler 2013; Collins et al. 2013; Dillehay 2013; Jenkins 2013; Waters 2013). Dillehay (1989) argues that a non-Paleoindian cultural occupation at the Monte Verde site in South America pre-dates Clovis by 1,000 years. In the Pacific Northwest, the Paisley Fivemile Rockshelter site, located in southern Oregon, has provided some of the earliest and most definitive evidence of human occupation in the New World in the form of human coprolites dated to 12,450 yr BP (Gilbert et al. 2008; Jenkins 2007; Jenkins et al. 2010; Jenkins et al.

2012). Paisley has revealed a high-resolution chronometric record, derived from 190 radiocarbon dates, that spans from 12,450 to 2,295 yr BP (Jenkins et al. 2012). In addition to the dated coprolites, Paisley has also yielded Western Stemmed projectile points that date to a period of 11,070 to 11,340 yr BP (Jenkins et al. 2012). This is highly significant as it represents the first accepted evidence of a Western Stemmed points radiocarbon dated to a period that pre-dates or co-occurs with Clovis ages of 10,800-11,050 yr BP (Waters and Stafford 2007).

In light of this new evidence from Paisley, it is plausible to argue that the ages of the LP component of the Cooper's Ferry site are correct and represent the presence of non-fluted Western Stemmed point-bearing peoples in the LSRC ca. 11,370 yr BP (Davis 2001a; Davis and Schweger 2004). One could also argue that the assemblages from Paisley and Cooper's Ferry are related in so much as they represent people in the American Far West who are utilizing Western Stemmed projectile points at time pre-dating or contemporaneous with Clovis. If these assumptions are true then sites such as Cooper's Ferry and Paisley Fivemile Rockshelter may reflect some of the earliest peoples to enter into the New World sometime after or even before the last glacial maximum ca. 20,000- 18,000 yr BP (Madsen 2004).

Beginning in the summer of 2009, the Cooper's Ferry site was revisited as part of a multiyear research project undertaken by Dr. Loren G. Davis of Oregon State University in cooperation with the Bureau of Land Management and the Nez Perce Tribe. Under the current research design, Davis (2009:1) is attempting to address a number of larger questions, including: 1) what is the cultural chronology of the site's early

occupation; 2) what are the possible evolutionary links between fluted Paleoindian and nonfluted Western Stemmed Tradition/Paleoarchaic technologies, and; 3) what adaptive strategies were employed by the earliest Plateau peoples? It is these larger research questions that will inform and guide on-going and future investigations at Cooper's Ferry and within the LSRC at large.

Research Objectives

The objectives of this project are focused on addressing aspects of the third question guiding archaeological research at Cooper's Ferry and the LSRC, which aims to expand upon our current understanding of the adaptive strategies employed by the earliest peoples occupying the southern Columbia River Plateau and the LSRC. In order to understand the adaptive strategies employed by prehistoric hunter-gatherers we require knowledge of past ecological conditions within the LSRC (Davis 2001a). Local ecological conditions within the LSRC would have provided prehistoric hunter-gatherers with a variety of economic opportunities and constraints. The archaeological record of the LSRC reflects the adaptive strategies employed by these early groups within this ecological context of various opportunities and constraints. Therefore, to better understand the adaptive strategies reflected in the archaeological record requires the development of locally derived data sets that provide a means of measuring paleoecological conditions and change through time (Butzer 1982; Davis 2001a; Piperno 2006; Rovner 1971).

This study aims to address questions of paleoecological conditions and change through time with the analysis of locally derived phytolith records within the LSRC.

Interpretation of the phytolith records allows for the development of an inferential model of potential hunting and gathering opportunities that existed within the LSRC in the vicinity of the Cooper's Ferry site by reconstructing the paleovegetative conditions (Piperno 2006; Rovner 1971). By building and expanding on existing phytolith data sets from the LSRC (Davis and Collins 2009; Somer 2003) it is possible to provide perspectives on the LP/EH ecologies associated with the LSRC earliest occupations. These perspectives will help to establish a contextual framework that permits a greater understanding of the adaptive strategies reflected in the archaeological record.

Ecological Context and Archaeology

In order to understand the human behavioral systems and adaptive strategies implemented by prehistoric hunter-gatherer groups of the southern Columbia River Plateau a contextualized understanding of the environment in which they were adapted is required. It is this local and regional environment that would have provided various economic opportunities and constraints in which the adaptive strategies were implemented. Within the framework of evolving paleoecological contexts associated with the climatic changes of the late Pleistocene and Holocene epochs it is possible to examine human behavior, adaptive strategies, and cultural evolution as reflected in the archaeological record.

Butzer (1982) proposed a contextual approach to archaeological research, which provides a sound theoretical framework for addressing these types of questions. Butzer's "contextual" archaeological paradigm promoted interdisciplinary research that combined methodologies from the physical, biological, and social sciences with the primary goal of

contextualizing the human ecosystem, which was viewed as the intersection of cultural systems and the biophysical environment. Butzer (1982:6) states that:

> [The] primary goal of environmental archaeology should be to define the characteristics and processes of the biophysical environment that provide a matrix for and interact with socioeconomic systems, as reflected, for example, in subsistence activities and settlement patterns.

It is this approach that provides a viable means of developing a conceptual framework for understanding human-environmental interactions by modeling paleoecological contexts at different temporal and spatial scales. Butzer goes on to outline three subsidiary fields of research that could provide a contextual interpretation of the human ecosystem which include: 1) geoarchaeology, 2) archaeometry, and 3) bio-archaeology.

Contextual Archaeology of the Columbia River Plateau

The development of a contextually based, conceptual framework of human-environmental interaction and paleoecological modeling of the Columbia River Plateau and LSRC requires locally derived paleoenvironmental and geologic data sets (Davis 2001a). It these data sets that allow a broader reconstruction of the biophysical environment that would have provided the matrix in which cultural systems operated in and adapted to.

The knowledge base and understanding of paleoenvironmental conditions of the Columbia River Plateau comes from a variety of environmental proxy records such as palynology studies (Barnosky 1985; Barnosky et al. 1987; Mack et al. 1978a, 1978b, 1979, 1983; Mehringer et al. 1977; Whitlock and Bartlein 1997; Whitlock 1992), geomorphological and geological studies (Chatters and Hoover 1992; Davis 2001a; Davis and Muehlenbachs 2001), stable isotopes (Davis et al. 2002), paleozoology (Graham and

Grimm 1990; Meatte 1986), and phytolith analysis (Blinnikov 2005; Blinnikov et al. 2001, 2002; Davis and Collins 2009; Eccleston 1999; Somer 2003). Despite this large dataset many of these studies (e.g., palynology) are derived from upland sites and do not necessarily reflect characteristics and composition of riparian zones located within the canyon bottoms of Columbia River Plateau drainages. Of the studies listed above only a few directly address these questions of riparian environments and ecologies (Chatters and Hoover 1992, Davis 2001; Davis and Muehlenbachs 2001; Davis et al 2002; Somer 2003).

This project will utilize phytolith analysis to build upon the existing phytolith datasets that have been derived from stratigraphic sections within the LSRC between Hammer Creek and Cooper's Ferry (Davis and Collins 2009; Somer 2003). Previous studies have validated the application of phytolith analysis from stratigraphic and archaeological contexts within the Columbia River Plateau (Blinnikov 1999, 2005; Blinnikov et al. 2001, 2002; Davis and Collins 2009; Eccleston 1999; Somer 2003). Phytolith data obtained from stratigraphic sections SR-23, SR-27, SR-34 and the north wall of Unit: A at the Cooper's Ferry site will provide a direct measure of the vegetative ecologies that existed in the LSRC the late Pleistocene and Holocene. The phytolith data can then be compared with other paleoenvironmental proxy records that have been established within the LSRC in order to model paleoecological conditions within the LSRC during this time period.

Chapter 2. Environmental and Cultural Context of the Columbia River Plateau

Physiographic Setting and Modern Environment

The lower Salmon River canyon (LSRC) is located in west-central Idaho, within southern portion of the Columbia River Plateau physiographic province. The southern Columbia River Plateau is a large region bounded to the west by the Cascade Mountains, to the east by the Bitterroot and Rocky Mountains, to the north by the Okanogan Highlands and to the south by the Basin and Range physiographic province (Figure 2.1).

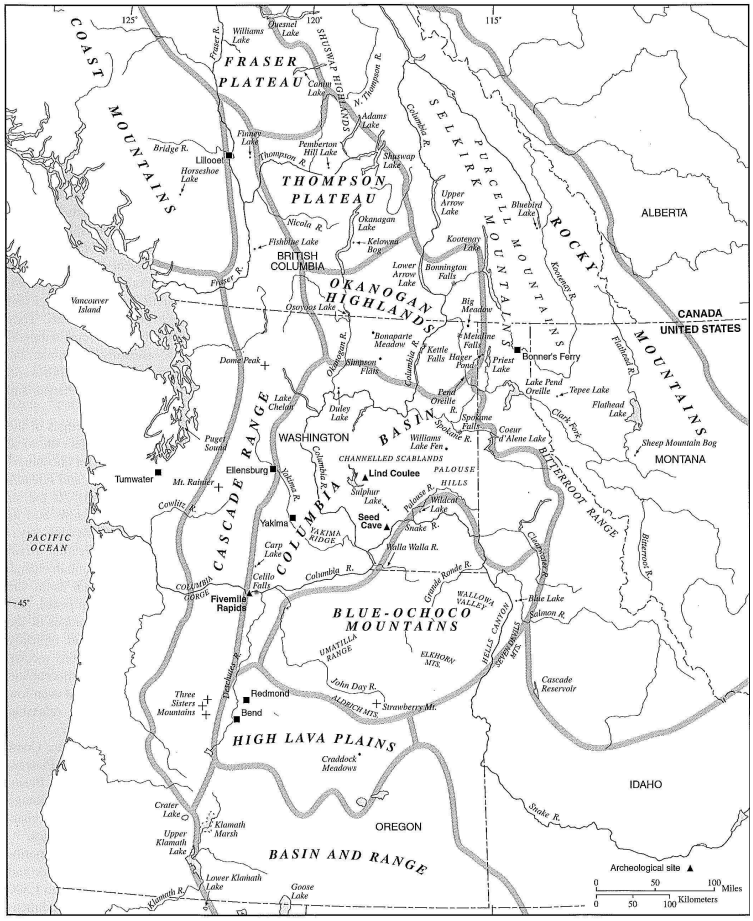

Figure 2.1 Physiographic subprovinces of the Columbia River Plateau and surrounding regions (from Chatters 1992)

Physiography of the Columbia River Plateau

The Columbia River Plateau is characterized by large expanses of flood basalts that were laid down between 17 and 6 million years ago during the late Miocene and early Pliocene (Bonnichsen and Breckenridge 1982; Maley 1987). These expansive flood basalts originated from a north to northwest trending fissure that opened along the eastern edge of the Columbia River Plateau, which allowed flows to overrun and infill the existing topography of the region covering roughly 50,000 km^2 (Bonnichsen and Breckenridge 1982; Holden 1974; Mckee 1972; Reidel 1978). Five episodes of activity can be identified in the stratigraphy of these basalt flows, from youngest to oldest they are defined as the: 1) Imnaha Basalt (17-16.5 ma), 2) Picture Gorge Basalt (16.5 ma), 3) Grande Ronde Basalt (16.5-14.5 ma), 4), Wanapum Basalt (14.5-13.5 ma) and 5) Saddle Mountain Basalt (13.5-6 ma) (Maley 1987). Subsequent folding, faulting, and erosional processes operating during Pleistocene have transformed these nearly horizontal flood basalts into the present day ranges, basins, plateaus and uplands that characterize the southern Columbia River Plateau (Freeman et al. 1945).

The southern Columbia River Plateau physiographic province has been sub-divided into two ecoregions defined as the Columbia Basin and Blue Mountains (Figure 2.2) (Omernik 1987; USEPA 2003). The LSRC and study area are situated within the Blue Mountains ecoregion. The Blue Mountains ecoregion is characterized as a complex group of mountain ranges and dissected uplands that is bounded to the east by the contact between the flood basalts and adjacent Northern Rockies and Idaho Batholith, to the west

by the Eastern Cascades, to the south by the Northern Basin and Range and the Snake River Plain, and to the north by the Columbia Basin ecoregions.

The Blue Mountains ecoregion covers most of central and northeastern Oregon as well as small portions of southeastern Washington and west-central Idaho. This ecoregion contains surficial geologic and sedimentary deposits that reflect a complex history of erosion, deformation, and deep dissection (Freeman et al. 1945; Omernick 1987). The Blue Mountains consists of a group of complex mountain ranges and gently warped uplands composed of flood basalts, which have been deeply incised by the major drainages and tributaries of the Salmon, Snake, and Grande Ronde rivers.

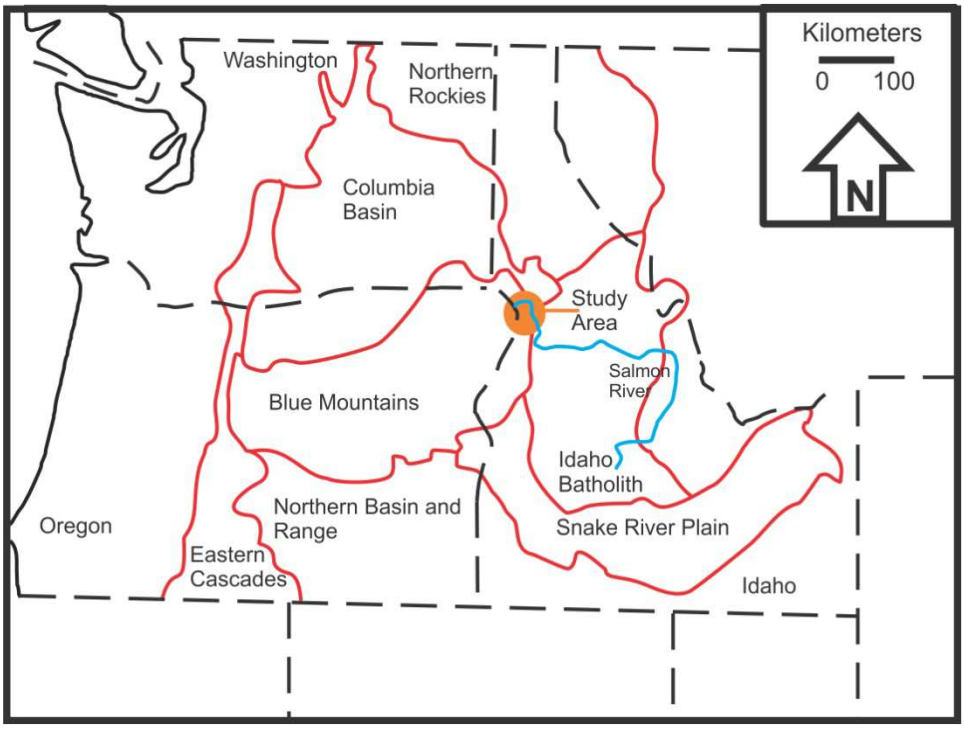

Figure 2.2 Map of southern Columbia River Plateau ecoregions. Study area is located within the orange circle (adapted from Omernick 1987; USEPA 2003)

The study area for this project encompasses an area of the LSRC from Hammer Creek (ca. river mile 53) downstream to Rock Creek (ca. river mile 39) (Figure 2.3). Within this section of the river the description above is very evident as the river is found at an elevation of roughly 432-390 meters above sea level (masl) between Hammer and Rock Creek, while the surrounding canyon walls reach an elevation of roughly 1,060-1,375 masl. The deep canyon transitions into gently rolling upland prairies such as Camas Prairie, to the north of canyon, and Joseph and Doumecq Plains to the southwest.

Natural Vegetation

Given the varied physiographic nature of the Columbia River Plateau, the local vegetation distribution is largely dependent upon local temperature, precipitation, slope aspect, and elevation. A great deal of ecological diversity has been reported within the region (Daubenmire 1970; Daubenmire and Daubenmire 1968; Franklyn and Dyrness 1988; Kuchler 1964), which has allowed for the development of seven broad vegetation groups defined as shrub steppe, bunchgrass steppe, woodland transition, xeric montane forest, mesic montane forest, subalpine forest, and montane meadows (Chatters 1998) (Figure 2.4). The LSRC is situated within bunchgrass steppe, which has also been referred to as the ‘Palouse Prairie’ by Gould and Shaw (1983) and as steppe and shrub-steppe by Kulcher (1964). Recent studies of Idaho’s ecological contexts have been reported and define vegetative zones that conform to those described above in the form of grasslands and shrublands (Scott et al. 2002).

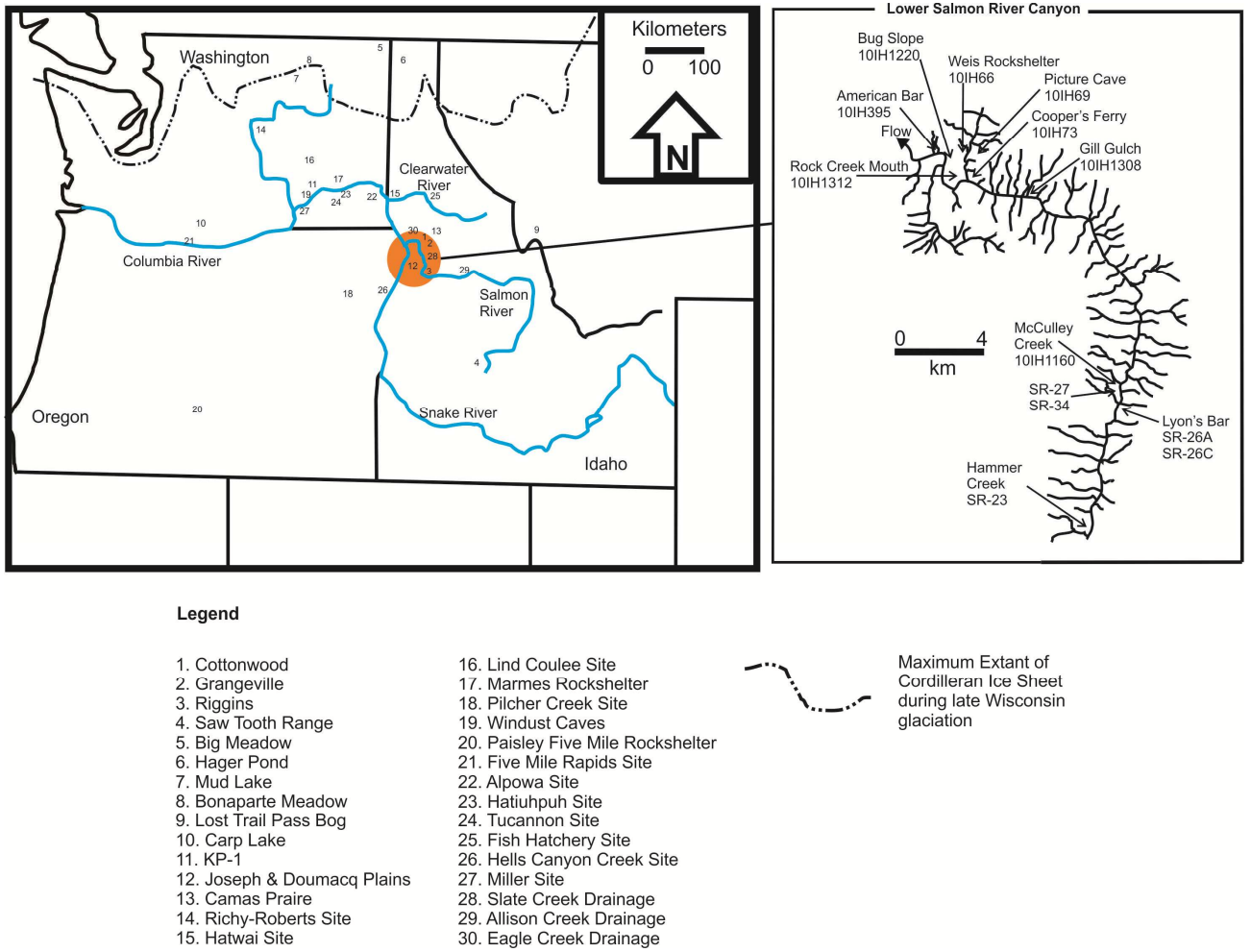

Figure 2.3 Locations of sites discussed in the text.

The vegetation found within the bunchgrass steppe is characterized as C_3 grasslands. These grasslands are comprised of principle species such as *Agropyron spicatum* (bluebunch wheat grass), *Festuca idahoensis* (Idaho fescue), and *Poa secunda* (Sandberg's bluegrass) with occasional *Artemisia tridentate* (sagebrush) (Franklyn and Dyrness 1988; Kuchler 1964). Additional associates include a variety of annual bromes

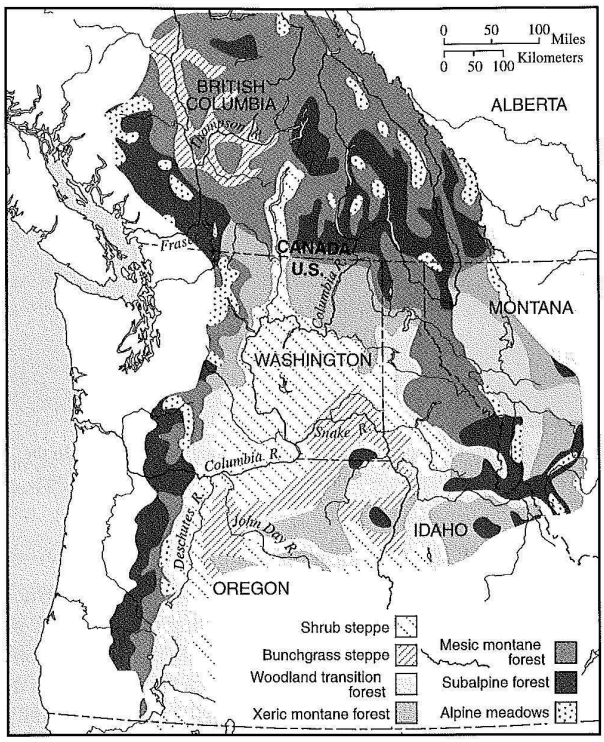

Figure 2.4 Vegetation regions of the Columbia River Plateau (from Chatters 1992).

(*Bromes tectorum, B. japonicus, B. brizaeformis, B. commutatus, and B. rigidus),* arrowleaf balsamroot (*Balsamorhiza sagittata),* and yarrow (*Achillea millefolium).* Additionally, there are isolated stands of ponderosa pine (*Pinus ponderosa)* and Douglas-fir (*Pseuduotsuga menziesii)* found at higher elevations on north- and west-facing slopes

and in consistently active drainages. Active tributary drainages and side canyons also provide habitat for a variety of herbaceous species including hackberry (*Celtus douglasii)*, smooth sumac (*Rhus glabra*), ninebark (*Physocarpus malvaceous*), mountain mahogany (*Cerocarpus ledifolius*), and hawthorn (*Crataegus douglasii*) (Daubenmire 1970; Daubenmire and Daubenmire 1968; Franklyn and Dyrness 1988; Kuchler 1964)

Climate

These semi-arid grassland and steppe communities are supported by varied climatic conditions depending on the given location (Table 2.1). The bottom of the LSRC experiences annual mean maximum and minimum temperatures ranging from 19.2° C (66.5° F) to 5.5° C (41.9° F) with annual precipitation rates of 42.7 cm (16.81”) of rainfall and 17.53 cm (6.9”) of snowfall as measured at Riggins, ID. This is contrasted with the data derived from high elevation weather stations from both Cottonwood and Grangeville, ID. Cottonwood stations reveal annual mean maximum and minimum temperatures ranging from 13.2° C (55.8° F) to 3.1° C (37.6° F) with annual precipitations rates of 56.57 cm (22.27”) of rainfall and 97.54 cm (38.4”) of snowfall. Grangeville stations record annual mean maximum and minimum temperatures ranging from 14.4° C (58° F) to 1.7° C (35° F) with annual precipitation rates of 59.69 cm (23.5”) of rainfall and 121.92 cm (48”) of snowfall (Western Regional Climate Center 2012).

Table 2.1 Summary of annual climatic data derived from nearby weather stations (adapted from Western Regional Climate Center 2012)

Station	Rainfall (annual cm)	Snowfall (annual cm)	Mean annual high (°C)	Mean annual low (°C)
Riggins	42.7	17.53	19.2	5.5
Cottonwood	56.57	97.54	13.2	3.1
Grangeville	59.69	121.92	14.4	1.7

Cultural Chronology of the Columbia River Plateau and Lower Salmon River

The Columbia River Plateau has a long history of archaeological research that began in the early 19th century as nonsystematic excavations were conducted by amateur antiquarians. This type of archaeology persisted until the early 20th century after which research became more systematic as archaeologists worked to construct culture-histories that could explain the temporal and spatial contexts of recovered assemblages (Daugherty 1956; Lohse and Sprague 1998). Following World War II archaeological research began to expand beyond simply describing the temporal and spatial context of the material record and strived to provide a means of researching and explaining the human behavior represented by the material record. Additionally, researchers started to focus on problems related to the larger cultural systems that operated in the past (i.e. settlement patterns, subsistence and social organization) (Lohse and Sprague 1998).

In the 1960s and 1970s many archaeological investigations were conducted within the Columbia River Plateau as salvage projects focused on recovering archaeological data from sites that would soon be flooded by dam development along the Columbia River

(Lohse and Sprague 1998). The data collection allowed for the development of regional cultural chronologies (Ames et al. 1998; Leonhardy and Rice 1970; Rice 1972; Roll and Hackenberger 1998). The following discussion will use a modified version of the chronology developed by Ames et al. (1998) and will provide a regional overview of the archaeological record of the Columbia River Plateau.

Culture History of the Columbia River Plateau

The Early Prehistoric Period >12,000 – 7,000 yr BP

Ames et al. (1998) identify the earliest parts of the archaeological record of the southern Plateau as Period 1, which they further subdivide into Period 1A (11,500-11,000 yr BP) and Period 1B (11,000-7,000/6,400 yr BP). Period 1A is associated with Clovis point technology recovered from the Richey-Roberts Clovis Cache located in central Washington (Merhinger 1989). The cache contained some of the largest fluted point forms recovered from an archaeological site. The antiquity of the site is largely based on the dates of Clovis sites from other regions of North America (i.e. southwestern United States). Waters and Stafford (2007) have provided an updated chronology for the Clovis Tradition, which places Clovis between 13,125 and 12,925 yr BP. The Richey-Roberts Clovis Cache has a relative date of <13,120 yr BP assigned to it based on the association of Glacier Peak tephra with the underside of fluted points and accepted Clovis chronology (Mehringer and Foit 1990; Waters and Stafford 2007). However, the association is tentative and the tephra is identified as silica grains adhering to the underside of some of the points and as such the dates should be taken with caution and not as an absolute age.

Within the Columbia River Plateau, artifact assemblages of the Western Stemmed Tradition (WST) (Bryan 1980, 1988) are the earliest known archaeological assemblages within buried contexts. WST assemblages have been recovered from sites such as Cooper's Ferry (Butler 1969; Davis and Schweger 2004), Hatwai (Ames et al. 1981; Sanders 1982), Lind Coulee (Daugherty 1956; Irwin and Moody 1978; Kirk and Daugherty 2007), Marmes Rockshelter (Hicks 2004; D. Rice 1972), Pilcher Creek (Brauner 1985), and Windust Caves (H. Rice 1965). Collectively, these sites provide evidence of a non-fluted lithic technology in the southern Columbia River Plateau that is contemporaneous with and possibly older than Clovis. This non-fluted, WST technology contains large shouldered and stemmed, and unstemmed lanceolate points that have been recovered from sites referenced above (Ames et al. 1998). Recently, the antiquity of WST assemblages has been recorded at Paisley Five Mile Rockshelter, which is located in southern Oregon along the northern edge of the Great Basin. Jenkins et al. (2012) reported the ages of deposits that contained western stemmed points, which dated to 11,070 to 11,340 yr BP. This is significant in that Paisley provides some of the earliest and widely accepted dates associated with the WST (Jenkins et al. 2012). The age of WST at Paisley is similar to the dates recovered from Cooper's Ferry where Davis and Schweger (2004) reported that stemmed points dated to 11,370 to 11,410 yr BP. The data appears to reflect a non-fluted lithic tradition operating in the Far West that was either contemporaneous with Clovis or pre-dates it entirely.

Leonhardy and Rice (1970) developed a regional cultural chronology for the Lower Snake River region of southeastern Washington. Their regional framework

identifies the earliest period as the Windust Phase (11,000-8,000 yr BP), which is characterized by the assemblages of stemmed and unstemmed lanceolate points like those discussed above.

Period 1B (11,000-7,000/6,400 yr BP) is characterized as the Post-Clovis cultural period by Ames et al. (1998); however, there is a continuation in some of the artifact types identified in Period 1A, namely the continued use of stemmed and unstemmed lanceolate points up until roughly 9,000 yr BP. After 9,000 yr BP projectile point forms become more standardized as laurel-leaf shaped forms predominate the record (Ames et al. 1998). These leaf shaped forms are also known regionally as Cascade points, named after their associated Cascade Phase (8,000-4,500 yr BP), which was proposed by Leonhardy and Rice (1970). After 7,800 yr BP additional point forms are added to toolkits and identified as large side- and corner-notched projectile points, which are also referred to as Northern Side Notched and Bitterroot points (Ames et al. 1998). The introduction of side- and corner-notched point forms to the lithic assemblages was used Leonhardy and Rice (1970) to further subdivide the Cascade Phase into Early (8,000-7,000 yr BP) and Late (7,000-4,500 yr BP) subphases. Period 1B artifact assemblages also contain additional lithic technologies such as cobble tools, utilized flakes, scrapers, gravers and burins, and cores. A variety of bone implements have been recovered from Period 1B sites. For example both barbed and non-barbed bone points have been recovered from the Lind Coulee site (Daugherty 1956; Irwin and Moody 1978; Kirk and Daugherty 2007), while Marmes Rockshelter contained small bone needles (Hicks 2004). Additional bone and antler tool technology consists of bone awls, antler wedges and

antler tines. Evidence of fishing technology (harpoons and stone net weights) has been recovered from the Fivemile Rapids and Roadcut sites (Aikens et al. 2011; Ames et al. 1998).

The archaeological record pertaining to Period 1 occupations has been argued to reflect the larger cultural patterns of the Plateau. These early cultures are described as broad-spectrum hunter-gatherers who utilized a wide range of natural resources as they maintain high rates of annual and seasonal mobility (Ames et al. 1998). High mobility allowed these groups to effectively exploit a variety of seasonally abundant resources within the region. The lack of formal dwellings and/or structures is thought to reflect a highly mobile culture that maintained low population densities as these groups moved through the landscape (Ames 1988; Ames et al. 1998). The technological systems utilized by these groups are characterized as highly flexible systems that allowed these groups to exploit a variety of floral and faunal resources as they moved from one location to the other (Ames et al. 1998). These groups exploited a number of resources, depending upon the given location, including riverine resources (i.e. both anadromous and non-anadromous fish species, river mussel, and riparian fauna) and terrestrial resources (i.e. deer, elk, and pronghorn), and edible root crops (i.e. camas bulbs) (Ames et al. 1998; Chatters and Pokotylo 1998).

The Middle Prehistoric Period 7,000 - 3,900 BP

Ames et al. (1998) define Period II (7,000/6,400-3,900 yr BP) as a continuation of Period I cultural patterns. However, there are a number of changes that occur during Period II that allow it to be differentiated from the earlier Period I assemblages. The

changes observed relate to changes in both the settlement and subsistence patterns of groups occupying the southern Columbia River Plateau during this period. One of the significant changes to the settlement patterns is the appearance of semisubterranean pit houses in the region (Ames et al. 1998). Semisubterranean pit houses were observed at Alpowa (Brauner 1976), Hatwai (Ames et al. 1981), and Hatiuhpuh (Brauner and Stricker 1990; Chance et al. 1989). The dates associated with the pit houses from these three sites span a period from 5,200 to 4,400 yr BP respectively. However, House 6 at the Hatwai site is associated with a date of 5,825 yr BP and Houses 2 and 3 from the Hatiuhpuh are dated to a period as late as 3,800 yr BP (Ames et al. 1998). These dates from Hatwai and Hatiuhpuh expand the temporal range associated with the use of semisubterranean pit houses in the Columbia River Plateau. The shift to the use of housing structures is argued to reflect in a change in the mobility patterns of these groups. These new settlement patterns and use of houses suggests that groups are becoming more sedentary as they are opting to invest in constructing and maintaining these structures (Ames et al. 1998; Chatters 1989).

Changes in the artifact assemblages of Period II are interpreted as reflecting adaptations of the larger subsistence and settlement strategies utilized by the groups occupying the Columbia River Plateau. For example, the assemblages recovered from the Hatwai site that are associated with Period II contain substantial ground stone technologies thought to be part of processing system used for exploiting plant resources (i.e. edible roots and seeds) (Ames et al. 1998; Ames and Marshall 1980; Chatters and Pokotylo 1998). Ground stone technology included hopper mortar bases, flat milling

stones and anvils, which are prevalent in the pit houses excavated at Hatwai and Alpowa. These technologies are heavy and not suitable for long distance transport and are also argued to reflect a shift towards increased sedentism and reduced mobility of Plateau groups (Ames et al. 1998; Chatters 1989).

Lithic technologies undergo some changes during Period II as well, while Cascade, Bitterroot, Northern Side Notched points continue to be utilized the frequencies of these point forms decreases when compared to assemblages from Period I (Ames et al. 1998). Sometime after 5,800 yr BP projectile point forms exhibit more variability as some styles become localized. For example, side-notched forms known as Hatwai-eared points, which have a characteristic notch found low on the side; they also have rounded shoulders, a convex base, and a thick cross-section (Ames et al. 1998). Leonhardy and Rice (1970) identity a form known regionally as the Snake River Corner Notched type; these corner-notched forms have expanding stems and barbed shoulders. Additionally, Ames et al. (1998) point out that edge ground cobbles and prepared cores are less prevalent when compared to the preceding Period I artifact assemblages.

Some aspects of the subsistence strategies employed by these groups remain the same between Periods I and II. For example, continued exploitation of terrestrial game (i.e. deer, elk, pronghorn) is observed in the faunal records recovered from Period II sites like Marmes Rockshelter (Hicks 2004), Hatwai (Ames et al. 1981), Windust Caves (Leonhardy and Rice 1970; Rice 1972), and Alpowa (Brauner 1976). Faunal assemblages also contain an abundance of other small and large mammal remains, fish remains (both anadromous and non-anadromous species), and river mussel shell (Ames et al. 1998;

Chatters and Pokotylo 1998). As discussed above it is also argued that plant based subsistence strategies were of increasing importance during this period (Ames and Marshall 1980).

The archaeological record of Period II reflects a continuation of some cultural systems that were in place during Period I, while also providing evidence that some systems underwent marked change. The record suggests that groups reduced their mobility and became semisedentary as they adopted the use of semisubterranean pit houses. The increased use of ground stone technology and intensified exploitation of plant based resources are also believed to reflect these larger changes of settlement and subsistence strategies implemented by hunter-gatherer groups in the Columbia River Plateau (Ames et al. 1998; Chatters and Pokotylo 1998).

Late Prehistoric Period 3,900 – 250 BP

Ames et al. (1998) define Period III (3,900-250 yr BP) as one marked by widespread use of semisubterranean pit houses, intensified exploitation of both fish (i.e. salmon) and edible root crops (i.e. camas), food storage, and changing land use patterns. By 2,500 yr BP pit houses are abundant in the southern Plateau and believed to be part of a larger “winter village” pattern (Ames et al. 1998; Ames and Marshall 1980; Swanson 1962). The winter village pattern is argued to represent a shift from a foraging based hunter-gatherer subsistence system to a collector based hunter-gatherer subsistence system (Chatters and Pokotylo 1998) as groups were able to secure seasonally abundant resources (i.e. salmon and camas) in bulk, which could be processed and stored for future use. After 1,500 yr BP new forms of housing appear in the Plateau as groups begin to

differentially adopt the use of long-house structure over the pit house structure (Ames et al. 1998).

Period III has been further subdivided by Ames et al. (1998) on the basis of changes in projectile point forms, settlement patterns, and the introduction of the horse. These subdivisions are identified as subperiods IIIA (3,900-2,500 yr BP), IIIB (2,500-1,500/1,000 yr BP), and IIIC (1,500/1,000-250 yr BP). Each subperiod will be discussed below.

Subperiod IIIA (3,900-2,500 yr BP) is identified in the record by the intensified occupation of sites such as Hatwai (Ames et al. 1981) and Alpowa (Brauner 1976), which remain occupied through contact with Europeans ca. 1700 A.D. Projectile point forms associated with this subperiod include Hatwai-eared and Snake River Corner Notched types identified at the end of Period II as well as small numbers of laurel-leaf shaped points. While a continuation of projectile point forms is observed during this subperiod the overall frequencies are low when compared to other artifacts in the assemblage. Notably, higher frequencies of cobble tools, fishing equipment, and ground stone technology characterize the assemblages from subperiod IIIA sites (Ames et al. 1998). Subsistence practices are characterized by limited faunal assemblages from this subperiod, which reflect a continued and intensified use of deer. Groups also took advantage of elk, pronghorn, birds, martin, beaver, and fish (Atwell 1989).

Subperiod IIIB (2,500-1,500/1,000 yr BP) sites are found along almost all the major drainages in the southern Plateau. Much of the information pertaining to this subperiod comes from sites situated along the Snake, Clearwater, and Columbia Rivers.

This includes sites such as Alpowa (Brauner 1975), Tucannon (Nelson 1966), Fish Hatchery (Sappington 1988), and Hells Canyon Creek (Pavesic 1986). The continued use of pit houses identified in the earlier periods intensifies during this subperiod. Artifact assemblages from this subperiod exhibit a number of changes as projectile point frequencies increase dramatically compared to subperiod IIIA, while new point forms replace older forms from the previous periods (Ames et al. 1998). For example, Hatwai-eared projectile point forms disappear from the record during this subperiod, while Snake River Corner Notched forms remain. Large basal-notched projectile point forms appear in association with the Snake River Corner Notched forms during the initial part of this subperiod. After 2,300 yr BP these projectile point forms are replaced by smaller varieties of corner and basal notched points, which are thought to be part of a bow and arrow technology (Ames et al. 1998). Additional characteristics of the artifact assemblages from this subperiod are increased frequencies of fishing equipment (net weights, leisters, and harpoons) and ground stone technologies (Ames et al. 1998). Subsistence activities during this subperiod are reflected by faunal assemblages that are dominated by deer remains, indicating the continued exploitation of deer as observed in the previous subperiod IIIA. Oddly, the second most abundant faunal remains are derived from bison and it is thought that groups began exploit this new resource at the expense of elk, which was a major component of subperiod IIIA faunal assemblages. Fish remains continue to be the third most abundant part of the faunal record recovered from subperiod IIIB sites (Ames et al. 1998).

Subperiod IIIC (1,500/1,000-250 yr BP) is characterized by a change in settlement patterns as groups begin to adopt longhouses as the preferred housing structure at the expense of pit house forms. However, it is noted that adoption of longhouses occurred in different spatial and temporal contexts during this subperiod (Ames et al. 1998). Groups also began to aggregate in large villages and towns at strategic locations near the confluence of major drainages. For example, the Miller site (Cleveland 1976; Schalk 1983) is located on Strawberry Island in the Snake River just above the confluence of the Snake and Columbia Rivers. The Miller site contained evidence of several hundred pit houses that ranged in size from 3 meters to over 20 meters in diameter (Cleveland 1976; Schalk 1983). The smaller corner and basal notched projectile point forms observed during subperiod IIIB persist into subperiod IIIC, however, they get smaller and are still thought to be part of a bow and arrow technology (Ames et al. 1998). Subsistence patterns associated with this subperiod reflect a shift back to strategies observed during subperiod IIIA as deer, elk, and fish dominate the faunal assemblages. While bison is represented during this period, they occur in lower frequencies when compared to subperiod IIIB. The end of this subperiod is marked by European contact and the introduction of the horse on the Columbia River Plateau at approximately 1720 A.D. (Ames et al. 1998).

Culture History of the Lower Salmon River

The first cultural chronology for the LSRC was developed by B. Robert Butler (1968). Butler's (1968) chronology is largely based on the excavations of five sites within the LSRC; this includes Weis Rockshelter (10IH66), McLaughlin Flat (10IH67), Picture

Cave (10IH69), Cooper's Ferry (10IH73), and Double House (10IH80). Butler's chronology spanned the last 7,400 yr BP and was divided into four cultural phases, these are labeled as the Craig Mountain Phase (7,400-3,500 yr BP), Grave Creek Phase (3,500-2,100 yr BP), Rocky Canyon Phase (2,100-600 yr BP), and Camas Prairie Phase (600-150 yr BP).

The initial chronology developed by Butler was evaluated and revised by Davis (2001b) on the basis of new information obtained from seven sites within the LSRC. Between 1997 and 2000 excavations were conducted at Cooper's Ferry (10IH73), American Bar (10IH395), Bug Slope (10IH1220), McCulley Creek (10IH1160), Rock Creek Mouth (10IH1312), Rock Creek Bridge (10IH2491), and Gill Gulch (10IH1308) (Davis 2001b; Dickerson 1997). Davis (2001b) integrated the new data obtained from these sites and expanded upon Butler's original chronology. Davis adds an additional two phases to Butler's chronology as well as refining the chronology of the Craig Mountain and Grave Creek Phase's. The updated chronology spans the last 11,500 yr BP and is divided into six cultural phases, these are labeled as Cooper's Ferry I Phase (11,500-11,000 yr BP), Cooper's Ferry II Phase (11,000-8,400 yr BP), Craig Mountain Phase (8,400-3,500 yr BP), Grave Creek Phase (3,500-2,000 yr BP), Rocky Canyon Phase (2,000-600 yr BP), and Camas Prairie Phase (600-150 yr BP) (Davis 2001b).

Cooper's Ferry I Phase (11,500-11,000 yr BP)

The Cooper's Ferry I Phase is the earliest of the new phases proposed by Davis (2001b) and is identified from the assemblages recovered from the lower portions of the Cooper's Ferry site (10IH73). This phase is characterized by the presence of a stemmed

point technology (Davis and Schweger 2004), which is similar to other stemmed point assemblages from the Columbia River Plateau (Daugherty 1956; Ames et al. 1981; Hicks 2004; Leonhardy and Rice 1970). A pit cache was excavated down into the basal gravels of the site; this cache contained four stemmed projectile points, one uniface, two cores, two blades, and one hammerstone. Additional artifacts associated with this phase include unifaces, bifaces, multidirectional cores, modified flakes, and debitage. This phase represents the earliest use of the site, which is interpreted as limited occupations by groups accessing the riparian zone of the LSRC.

Cooper's Ferry II Phase (11,000-8,400 yr BP)

This phase is also identified at the Cooper's Ferry site (10IH73) and includes a lithic assemblage characterized by both stemmed and lanceolate points. Additional tools associated with this phase include large scrapers, bifaces, modified flakes, and hearth features. This phase represents a continued and intensified use of the riparian zone near the site as artifact densities increase and living surfaces can be identified, which are associated with fish remains and expedient tool technology (i.e. modified flakes) (Davis 2001b).

Craig Mountain Phase (8,400-3,500 yr BP)

The Craig Mountain Phase defined by Butler (1968) was updated in light of new information recovered from excavations at American Bar (10IH395) and Cooper's Ferry (10IH73), which allowed Davis (2001b) to place the lower boundary of the phase at ca. 8,400 yr BP. This phase is characterized by leaf-shaped projectile points, which dominate the assemblages, in addition to antler wedges and edge-ground cobbles. Side-notched

projectile point forms are identified during this phase at Weis Rockshelter (10IH66) and Gill Gulch (10IH1308) in association with middle Holocene-aged deposits (Butler 1968; Davis 2001b). The record associated with this phase indicates a continued and intensified use of the LSRC riparian zone and associated resources. Faunal assemblages indicate that subsistence strategies were utilizing river mussel and deer in higher frequencies, with possible exploitation of bison. Butler (1968) reported that the teeth from two bison were recovered from Weis Rockshelter, suggesting that limited hunting of bison may have occurred during this phase.

Grave Creek Phase (3,500-2,000 yr BP)

Once again, new information allowed Davis (2001b) to refine the original chronology proposed by Butler (1968) and place the upper limit of the Grave Creek Phase at ca. 2,000 yr BP. This phase is characterized by a marked increase in the frequencies of Bitterroot side-notched point forms at the expense of leaf-shaped point forms (Butler 1968). Ground stone tool technology appears during this phase, possibly reflecting an increased use of plant based food resources such as camas (Davis 2001b). The record associated with this phase reflects the continued and intensified use of the LSRC as groups begin to heavily occupy floodplain and alluvial fan sites situated along the riparian zone. Groups are expanding their diet breadth and integrating additional plant resources during this time as reflected by the increased frequencies of grinding and milling stones (Davis 2001b). Davis (2001b) places the upper limit of this phase at ca. 2,000 yr BP on the basis of observed changes in both the archaeological geological record of the LSRC.

Rocky Canyon Phase (2,000-600 yr BP)

During the Rocky Canyon Phase, a number of new socioeconomic adaptations are observed in the archaeological record of the LSRC. Most notably, pit houses appear in the record during this phase and are associated with dense accumulations cultural debris (i.e. lithic and subsistence debris) and intensified occupation of the LSRC (Butler 1968; Davis 2001b). Davis (2001a; 2007) argues that the lower Salmon River experienced an episode of channel erosion that was caused by fault activity near the confluence of Rock Creek and the Salmon River. The geologic activity caused the Salmon River to adjust its gradient and flow, which resulted in the formation of the rivers modern fluvial context (Davis 2001a). It is argued that the new fluvial context of the river improved the local salmon fishery and allowed seasonally strong and reliable runs of anadromous fish (i.e. salmon and steelhead), which in turn allowed groups to adopt new settlement, subsistence, and technological strategies (Davis 2007). In addition to pit houses, other changes observed in the archaeological record during this phase include the appearance and predominance of smaller corner-notched projectile point forms while frequencies of Bitterroot side-notched points are much lower. Other artifacts associated with this phase include fishing gear, such as net weights and bone tools, ground stone technology, and ornamental beads made of bone and shell. A variety of terrestrial resources were being exploited for subsistence purposes during this phase as reflected in the faunal assemblages, which include remains from deer, elk, and mountain sheep in addition to river resources such as salmon and mussels (Butler 1968; Davis 2001b).

Camas Prairie Phase (600-150 yr BP)

This final phase represents the establishment of the ethnographic patterns of the Nez Perce. Groups continue to utilize pit house structures as they occupy riparian zones located along the LSRC. Projectile point forms undergo further changes as small basal- and corner-notched point forms dominate assemblages associated with this phase. Changes in groundstone technology are reflected by presence of hopper and mortar bases during this time. Groups are making contact with Europeans and trading goods with one another. A glass bead was recovered from the Rock Creek Mouth Site (10IH1312), which provides evidence of such trading.

Chapter 3. Paleoenvironments of the Southern Columbia River Plateau and LSRC

Current understanding of the paleoenvironmental conditions that operated within the Columbia River Plateau during the late Pleistocene and into the Holocene are derived from a variety of proxy records. Proxy records allow for indirect measures of past environmental conditions such as temperature, aridity, and vegetative composition through the analysis of materials such as stable isotopes of carbon and oxygen. Additionally, direct measures of paleoenvironmental contexts can be derived from sources such as surficial geology and geomorphology, pedological studies, palynology and phytolith analysis, and entomogical studies. The following sections will discuss the results of studies such as these that have been conducted within the Columbia River Plateau. Together they provide a basis for interpreting and discussing late Quaternary paleoenvironmental change in the region.

It is important to point out that many of the studies that will be discussed below originate from sites that are found at elevations higher than the LSRC. Thus, they are interpreted as reflecting larger regional scale paleoenvironmental contexts. However, a few studies have been conducted at lower elevation sites allowing for more direct measures of conditions that operated in low elevation sites both in and outside of the riparian zone. As such the following discussion of paleoenvironmental research will be arbitrarily sub-divided into high elevation studies (>500 masl) and low elevation (<500 masl) studies.

High Elevation Paleoenvironmental Records

High elevation (>500 masl) late Quaternary records are largely derived from palynological studies of cores derived from upland lake and bog sites. Additional studies have examined the surficial geology to elicit information regarding the Pleistocene glacial history of the region. The results of such studies will be summarized below.

Glacial History

The Columbia River Plateau has experienced a tremendous amount of change since the last glacial maximum ca. 18,000-22,000 BP. Both regional and local environments within the Plateau were subjected to influences related to continental and alpine glaciations. Floral and faunal communities in the region reflect changes in both coverage and composition as glacial retreat occurred into the terminal Pleistocene. Due to these influences it is important to provide an overview of the glacial history of the surrounding LSRC prior to discussion of regional and local paleoenvironmental proxy records.

During the Wisconsinan glacial period, large portions of North America were covered by two continental ice sheets, the Cordilleran and Laurentide, in addition to alpine glaciers. Beginning ca. 29,000 BP, the Cordilleran ice sheet began to advance from the interior of Canada (Clark et al 2001). Between 19,000 and 23,000 yr BP, continental glaciers had advanced to their maximum extent with portions of the Cordilleran ice sheet extending into Idaho, Montana, and Washington (Sherard 2006; Waitt and Thorson 1983).

During this maximum southward extension of the Cordilleran ice, the Purcell Trench Lobe inundated the Clark Fork River drainage, which allowed formation of glacial Lake Missoula (Breckenridge 1989; Waitt and Thornson 1983). Glacial Lake Missoula experienced repeated episodes of filling and draining as periodic failures in the ice dam allowed for catastrophic flood events that are responsible for creation of the Channeled Scablands in eastern Washington in addition to other erosional and depositional features observed in affected regions (Figure 3.1) (Alt and Hyndman 1989; Breckenridge 1989; Bretz 1929; Chambers 1984; Waitt and Thorson 1983). Evidence of these flood events is argued to be present within the lower Salmon River near its confluence with the Snake River. Davis (2001a) reports that flood deposits were identified within the lower 10 miles of the Salmon River at the "back-eddy bar" location by Webster et al. (1982), who associated the deposits with the earlier Bonneville flood that occurred ca. 14,500 yr BP (O'Connor 1993). However, Davis (2001a) suggests that this assignment of the deposits to the Bonneville flood may be incorrect and are actually associated with Missoula flood events. Thus, the lower Salmon River, above river mile 10, was not affected by Pleistocene flood events.

During the terminal Pleistocene, glacial retreat caused the Cordilleran ice sheets to recede northward of the present day Canadian border. While the continental ice sheets had retreated, the region surrounding the LSRC still experienced alpine glaciations in the higher elevations of the surrounding mountain ranges. Several studies have identified and described glacial deposits within the region that reflect a complex history of advance and retreat of alpine glaciers spanning from the LGM (ca. 19,000-23,000 yr BP) and into the

late-glacial period (ca. 17,000-11,000 yr BP) (Chadwick et al. 1997; Dort 1965; Gosse et al. 1995; Licciardi et al. 2001, 2004; Thackray 2001; Thackray et al. 2004).

Figure 3.1 Map showing the location of Glacial Lake Missoula and extent of the flood path (from Digital Geology of Idaho Website).

During the terminal Pleistocene, glacial retreat caused the Cordilleran ice sheets to recede northward of the present day Canadian border. While the continental ice sheets had retreated, the region surrounding the LSRC still experienced alpine glaciations in the higher elevations of the surrounding mountain ranges. Several studies have identified and described glacial deposits within region that reflect a complex history of advance and retreat of alpine glaciers spanning from the LGM (ca. 19,000-23,000 yr BP) and into the late-glacial period (ca. 17,000-11,000 yr BP) (Chadwick et al. 1997; Dort 1965; Gosse et al. 1995; Licciardi et al. 2001, 2004; Thackray 2001; Thackray et al. 2004).

Alpine glaciation within the Sawtooth Mountains influenced the formation of an extensive moraine belt that extends along the southeastern portion of the Sawtooth range Thackray et al. (2004). The surficial geology of these moraines was mapped and dated to allow for a chronological interpretation of glacial history within the region. Thackray et al. (2004) describe two periods of interest in which alpine glacial advancement was detected. The first episode occurred around ca. 16,900 yr BP; while the second episode is defined by the youngest moraines dated to ca. 14,000 yr BP. This data indicates that periods of alpine glacial advancement occurred well beyond the LGM and into the late-glacial period.

Further research regarding the nature of alpine glaciations within the region of the LSRC have been reported by Dort (1965), who provides discussion on the lower elevation limits of alpine glacial ice (Table 3.1). It should be noted that adequate chronological context of these glacial deposits is lacking. While the data do indicate that alpine glaciers influenced the region at large, the LSRC was never covered in glacial ice during the Wisconsinan glacial period; however, it is expected that local hydrology of the Salmon River would have been influenced by the glacial activity described above.

Palynological Records

Quaternary paleoenvironmental data pertaining to the Columbia River Plateau comes largely from palynology studies (Barnosky 1985; Barnosky et al. 1987; Mack et al. 1978a, 1978b, 1979, 1983; Mehringer et al. 1977; Sea and Whitlock 1995; Smith 1983; Whitlock 1992; Whitlock and Bartlein 1997).

Table 3.1 Lower elevation limits of glacial ice within study area of the LSRC (adapted from Dort 1965)

Location of Deposits	Location Description	Lower Elevation Limit of Glacial Ice
45°30'N/115°30'W	Buffalo Hump Area, Idaho County	1,525 m
45°30'N/115°30'W	Dixie Area, Idaho County	Above 2,130 m
45°30'N/116°W	Florence Area, Idaho County	To 1,675 m, locally to 1,220 m.
45°30'N/116°W	Warren Area, Idaho County	To 1,675 m, rarely at 1,220 M.
45°30'N/116°W	Secesh Basin, Idaho County	To 1,830 m. 1,220 m nearby. Cirques above 2,285 m.
46°N/115°30'W	South/Middle Forks of the Clearwater River, Idaho County	To 1,070 m forming Piedmont glaciers.

Analysis of fossil pollen assemblages allows for the inference of past ecological and environmental conditions. Within this framework it is possible to assess the vegetative composition of paleolandscapes in a given region (i.e. arboreal versus non-arboreal). These records can also provide information regarding vegetative composition

through time, which is very powerful when it comes to discussing landscape evolution within a given regional context.

Some limitations do exist in palynological studies; one such limitation is the resolution capabilities of fossil pollen (Beaudoin 1993, 1999). Pollen assemblages allow for various levels of taxa identification; for example pollen can indicate the presence of Poaceae (grasses) but does not distinguish subfamilies (i.e. Chloridoideae vs. Panicoideae vs. Pooideae) within the Poaceae family (Pearsall 2010). In contrast, pollen can be used to identify subgenus members Pinaceae family. For example, haploxylon pine pollen (i.e. *Pinus monticola* and *P.albicaulis*) can be distinguished from diploxylon pine pollen (i.e. *P. ponderosa* and *P. contorta*) (Whitlock and Bartlein 1997). Additional limitations of these regional pollen studies are that the fossil pollen assemblages are obtained from forested upland lakes and bogs or they are located some distance away from the study area (i.e. the Carp Lake pollen sequence is located along the southwestern portion of the Columbia River Plateau). It has been noted by other researchers that these records may not provide an adequate measure of ecological conditions operating within the lower elevation riparian contexts of major drainages such as the Salmon and Columbia Rivers during the late Quaternary period (Blinnikov 1999; Blinnikov et al. 2001, 2002; Davis 2001a; Somer 2003).

Given the various strengths and limitations of pollen analysis it is still a valuable proxy for measuring paleoenvironmental context and change within the Columbia River Plateau during the late Quaternary period. The following summary of palynological

studies from the Pacific Northwest will provide a framework for understanding the paleoenvironmental record of the region over the last 12,000 yr BP.

A pollen record spanning roughly the last 12,000 yr BP was recovered from the Big Meadow locality in Pend Orielle County, Washington (Mack et al. 1978a). The site is situated at an elevation of 1,040 masl and was inundated by the Cordilleran ice sheet during the LGM (ca. 19,000-23,000 yr BP). As a result of glacial inundation the core provides a record of post-glacial vegetation within the area.

Low rates of pollen influx are indicated in the basal portions of the core, which indicates a predominance non-arboreal vegetative cover. Until roughly 9,700 yr BP the core indicates high proportions of *Artemisia* and Poaceae pollen with little pine pollen. Mack et al. (1978a) interpreted the record as indicative of a tundra-like landscape dominated by grass and sagebrush with little forest cover that would have been cooler and wetter than today. Between roughly 9,700 to 3,300 yr BP the pollen record indicates a significant increase in diploxylon pine pollen (i.e. *Pinus ponderosa*) while Poaceae pollen decreases in abundance. This is interpreted as a shift from a tundra-like landscape to a developed pine forest with grass understory by 3,300 yr BP (Mack et al. 1978a). Climatic conditions during this period are characterized as warmer and drier than present. The record indicates a period of increased moisture and cooler temperatures following 3,300 yr BP as the pollen assemblage shows an increase and predominance of both *Picea* and *Abies* types (i.e. spruce and fir species). Following this period of cooler temperatures and increased moisture the record indicates a shift towards modern vegetative conditions

with the presence of *Tsuga heterophylla* (western hemlock), *Abies* (spruce), and *Picea* (fir) (Mack et al. 1978a).

Mack et al. (1978b) also examined a pollen core from Hager Pond located in Bonner County, Idaho. Hager Pond is situated at an elevation of 860 masl and contains a record that encompasses >9,500 yr BP to present. The pollen sequence is similar to the record derived from the Big Meadow locality and has been divided into five zones of vegetative and environmental change.

The earliest period, zone 1, dates to roughly 9,500 to 8,300 yr BP and is characterized by predominance of diploxylon pine pollen with additional contributions coming from *Abies*, *Artemisia*, and *Picea.* Additionally small amounts of Cyperaceae and Poaceae were identified in the core (Mack et al 1978b). Further investigation of the assemblage allowed for the identification of *Pinus albicaulis* (whitebark pine), which suggests climatic conditions that were both cooler and moister than present. Mack et al. (1978b) argue that the presence of *P. albicaulis* at Hager Pond during this time frame represents an elevation depression of local vegetation during the glacial and post-glacial periods. As glacial ice retreated it is thought that vegetation would slowly follow, reclaiming higher elevation sites now free of ice.

The next period identified, zone 2, spans a period between 8,300 to 7,600 yr BP. During this period the pollen record indicates an increase in non-arboreal pollen as Poaceae pollen predominates the assemblage. The percentage of *Pinus* pollen types is lower than the earlier period. The assemblage is argued to reflect a period of warming and drying (Mack et al. 1978b). These conditions are believed to have persisted until

3,000 yr BP. A third period, zone 3, is identified between 7,600 to 3,000 yr BP within the record. This period reflects abundant diploxylon pine, plus *Pseudotsuga menziesii* (i.e. Douglas-fir) and *Artemisia*. During this same period the record reflects decreases in Poaceae pollen that coincides with increases in other types mentioned above. It is believed that the initial warming and drying observed in the period between 8,300 to 7,600 yr BP continued into the next period and persisted until about 3,000 yr BP (Mack et al. 1978b).

A fourth period, zone 4, is identified between 3,000 to 1,500 yr BP. This period consist of a pollen assemblage that suggest a climatic reversal to conditions that were both cooler and moister than the previous period associated with zone 3 as well as present day conditions. It is characterized by a marked increase and predominance in *Picea*, *Abies*, and *Pinus* pollen types while at the same time *Artemisia* and Poaceae pollen types occur as minor components of the assemblage (Mack et al. 1978b). After 1,500 yr BP the final period, zone 5, is identified by the onset of modern vegetation. The assemblage is dominated by *Tsuga heterophylla* pollen with smaller contributions of *Abies*, which characterizes the current vegetation cover in the area today (Mack et al. 1978b).

Another pollen sequence examined by Mack et al. (1979) was obtained from Mud Lake and Bonaparte Meadow, which is located in Okanogan Valley, Washington at an elevation of 1021 masl. It too, provides a record that is dated to 11,000 yr BP, which yields information regarding post-glacial vegetative patterns within the Columbia River Plateau. The early record derived from the core indicates that as glacial retreat occurred pioneering species were comprised of *Artemisia* and haploxylon pine pollen types (Mack

et al. 1979). Additional contributors to the pollen assemblage at this time were Poaceae and Cyperaceae. The assemblage during this time is interpreted as a representation of steppe like vegetation with climatic conditions that were cooler and moister than present (Mack et al. 1979).

Conditions persisted until a period of roughly 10,000 yr BP after which, a shift in the pollen assemblage is observed. The assemblage is characterized by high quantities of *Artemisia* and Poaceae with additional contributions derived from diploxylon pine pollen (Mack et al. 1979). The increase in *Artemisia* along with the presence of diploxylon pine pollen is argued to represent a climatic shift towards conditions that were both warmer and drier than the prior period discussed above. These climatic conditions persisted until roughly 4,700 yr BP; however there is an observed change in the pollen assemblage that occurred around 7,000 yr BP. This period is indicated by an increase in *Artemisia* and Poaceae pollen with minor amounts of diploxylon pine and *Carex* pollen types (Mack et al. 1979). It is believed that this is a continuation of the warming and drying trend identified in the previous beginning ca. 10,000 yr BP.

Following 4,700 yr BP the pollen record indicates a dramatic shift in vegetation at the site. It is at this time that diploxylon pine pollen dominates the assemblage, which suggests a shift to fully forested conditions; additional contributions were derived from *P. ponderosa* and *P. menziesii* (Mack et al. 1979). This is described as the onset of modern vegetative conditions, which can be observed within the locality today. Mack et al. (1979) indicate that the pollen sequences and vegetative histories observed in the Big Meadow and Hager pond pollen cores (Mack et al. 1978a, 1978b) do not fully match the

sequence derived from Mud Lake and Bonaparte Meadow. Specifically, they address the fact that the sequence from Mud Lake and Bonaparte Meadow does not indicate a period of climatic reversal in which conditions became cooler and moister prior to the onset of modern conditions. This brief shift to cooler and moister conditions was observed in both the Big Meadow and Hager pond records. The differences observed in the sequences from the studies are attributed to differential effects related to the local latitude, topography and hydrological contexts of each site (Mack et al. 1979).

Mehringer et al. (1977) reported a record spanning the last 12,090 yr BP that was recovered from a core taken from the Lost Trail Pass Bog site. Lost Trail Pass Bog is situated at an elevation of 2,152 masl in the Bitterroot Mountains of Montana. The earliest portion of the record (ca. 12,000 yr BP) is dominated by *Artemisia* and Poaceae pollen types, which are indicative of a sagebrush steppe like landscape (Mehringer et al. 1977). After 11,500 yr BP a dramitic shift is observed in the pollen record. The shift is characterized by decreases in *Artemisia* and Poaceae types which are replaced with pine types along with minor contributions derived from *Abies* (Mehringer et al. 1977). These first two periods of the pollen record reflect conditions that were cooler and moister than present. These conditions persisted until 7,000 yr BP after which climatic conditions became warmer and drier compared to the earlier periods. These drier and warmer conditions spanned a period from 7,000 to 4,000 yr BP and are reflected in the pollen record by decreases in both *Pinus* and *Picea* types while *Pseudotsuga-Larix* became more abundant (Mehringer et al. 1977). After 4,000 yr BP there is an observed decrease in pollen contributions derived from *Pseudotsuga-Larix* while *Pinus* and *Picea* types come

to dominate the assemblage. This shift suggests that conditions became cooler and moister than the previous period. After this point modern vegetation communities become well established and very little change is detected in the pollen sequence. However, it is noted that shortly after 2,000 yr BP haploxylon pine pollen dominates the record, at the expense of *Pseudotsuga-Larix* types, into modern times (Mehringer et al. 1977).

Another pollen record spanning the last 125 kyr BP was recovered from Carp Lake, Washington (Whitlock and Bartlein 1997). Carp Lake sits at an elevation of 714 masl along the western margin of the Columbia River Plateau and lies within the transition range of low elevation *Artemisia* steppe and higher elevation *P. ponderosa* forest. As stated above the pollen record spans the last 125 kyr BP and has been divided into 11 different zones, with zone 1 being further subdivided into zones 1a and 1b (Whitlock and Bartlein 1997). Given the fact that the research interests of this thesis are focused on late Pleistocene and Holocene environmental conditions of the LSRC the following summary of the Carp Lake pollen data will be limited to zones 1 through 3, which spans the last 30.9 kyr BP to present (Whitlock and Bartlein 1997).

Zone 3 of the Carp Lake pollen sequence spans a period from 30.9 to 13.2 kyr BP and provides a record of conditions that persisted during the LGM and into the late-glacial period. The pollen record from zone 3 is characterized by high frequencies of *Artemisia* and Poaceae pollen types, with minor amounts of arboreal taxa comprised of *Pinus* pollen types (Whitlock and Bartlein 1997). The authors suggest that the assemblage form zone 3 is indicative of a cold dry steppe environment comprised of

sagebrush and grasses. They also note that during the late-glacial period there is small increase in *Picea* types, probably derived from stands of *P. engelmannii* near the site (Whitlock and Bartlein 1997). This period is also associated with the coldest and driest conditions observed in the 125 kyr BP sequence.

The subsequent zone 2 from Carp Lake spans a period from 13,900 to 9,100 yr BP. Zone 2 is characterized by a sharp decrease in *Artemisia,* while *Pinus* types become more prevalent (Whitlock and Bartlein 1997). The authors suggest that the sequence reflects a shift to warmer and drier conditions associated with the establishment of an early Holocene forest-steppe environment comprised of grasses and mixed pine.

Zone 1 from Carp Lake has been sub-divided into zones 1a and 1b on the basis of changes within the assemblage as modern forested conditions took hold in the Carp Lake vicinity. Zone 1b spans a period from 9,100 to 3,900 yr BP and is characterized by a dramatic increase in *Pinus* types at the expense of Poaceae. Arboreal taxa at this time comprise 75-80% of the total assemblage, which is argued to represent the establishment of a *P. ponderosa* and *Quercus* (oak) forest (Whitlock and Bartlein 1997). Climatic conditions are interpreted as warmer and drier than present.

Zone 1a from Carp Lake spans a period from 3,900 yr BP to present. This period reflects the establishment of modern conditions with the continuation of forest development. The pollen record indicates a continued increase in *P. ponderosa* contributions in addition to the presence of *P.menziesii,* interpreted as the onset of the ponderosa pine and Douglas-fir forests that exists in the region today (Whitlock and Bartlein 1997). Additionally, localized areas of increased moisture supported stands of

Abies grandis, *P. monticola*, and *T. heterophylla*, while lower elevations supported an oak forest (Whitlock and Bartlein 1997). The increase in Poaceae types is argued to represent the presence of low elevation grasslands and isolated areas of grass cover in forest openings.

The late Quaternary paleoenvironmental pollen studies discussed above clearly indicate periods of changing climatic and ecological conditions within the Columbia River Plateau region. These pollen studies provide powerful proxies for interpreting the timing and nature of these environmental changes at regional scales. However, it has been argued that these proxy records are not adequate for addressing questions of paleoenvironmental context and change within the context of low elevation (<500 masl) riparian zones like that of the LSRC (Blinnikov 1999; Blinnikov et al. 2001, 2002; Davis 2001a; Somer 2003). The pollen studies discussed above all came from sites with elevations >700 masl and distances in excess of 400 km from the LSRC study area, so it is reasonable to argue that those records may not accurately reflect conditions operating in the LSRC over the last 20,000 yr BP.

Low Elevation Paleoenvironmental Records

To date, a limited number of studies have addressed the paleoenvironmental contexts of low elevation (<500 masl) sites, both within and outside of riparian contexts. A variety of environmental proxy records are available from studies on stable isotopes and grain size analysis (Davis and Muehlenbachs 2001; Davis et al. 2002; Stevenson 1997), paleopedological analysis (McDonald and Busacca 1992), entomological analysis (O'Geen 1998) and phytolith analysis (Blinnikov 1999, 2005; Blinnikov et al. 2001,

2002; Davis and Collins 2009; Somer 2003). These studies have been used to develop high-resolution frameworks for interpreting the nature and timing of paleoenvironmental change both in the Columbia River Plateau region at large (Blinnikov 1999; Blinnikov et al. 2001, 2002) and specifically within the context of the LSRC (Davis and Collins 2009; Davis and Muehlenbachs 2001; Davis et al. 2002; Somer 2003). The following section will summarize the results of these various studies. However, discussion of the phytolith studies mentioned above will be provided in Chapter 4.

Additionally, note that these low elevation studies comprise two locations: 1) the LSRC study area encompassing the area from Hammer Creek Recreation Site downstream to American Bar, and 2) the KP-1 Loess Section, located in southeastern Washington. The records from each location will be discussed separately.

Lower Salmon River Canyon Stable Isotope and Grain Size Analyses

Isotopic analysis of oxygen and carbon can provide a proxy measure of paleoenvironmental conditions and can be interpreted as measures of temperature and rainfall patterns (Amundson et al. 1988; Cerling 1984, 1992; Cerling and Quade 1993). The basis of this interpretation assumes that the signature of $\delta^{18}O$ contained in pedogenic carbonate is an indicator of meteoric water composition. Within natural environmental systems the ^{16}O isotope evaporates preferentially when compared to the heavier ^{18}O isotope. What this means is that increases in the $\delta^{18}O$ signature of pedogenic carbonate represents periods of increased aridity. Measures of $\delta^{13}C$ also derived from pedogenic carbonate are interpreted as an indicator of the relative proportions of plants that utilize the C_4 photosynthetic pathway compared to plants utilizing the C_3 photosynthetic

pathway (Cerling 1999). It is generally recognized that C_4 plants are relatively drought tolerant when compared to their C_3 counter parts (Piperno 2006). This distinction between C_3 and C_4 plant communities can be useful when attempting to reconstruct paleoenvironmental contexts of a given location. Cerling (1999) discusses this process further and provides baselines for interpreting the signature of $\delta^{13}C$ derived from pedogenic carbonate sources. Notably Cerling (1999:457) points out processes of enrichment in pedogenic carbonate, which causes the signature to vary when compared to those derived from soil organic matter. Cerling (1999) goes on to describe a range of pedogenic $\delta^{13}C$ values for completely C_3 and C_4 ecosystems. Values reported form pedogenic carbonates in C_3 systems range from about -9 to -12‰ $\delta^{13}C$, while those from C_4 systems range from about 1 to 3‰ $\delta^{13}C$ (Cerling 1999:457). $\delta^{13}C$ studies cannot resolve species populations; however they can provide proxy measures of the relative proportions of C_3 and C_4 plant populations within a given environment.

Davis and Muehlenbachs (2001) and Davis et al. (2002) conducted paleoenvironmental studies in the LSRC. Davis et al. (2002) examined the stable oxygen and carbon isotopes signatures of pedogenic carbonate samples obtained from six stratigraphic sections in the LSRC. Sediment grain size analysis was also conducted on the same sections. Together the data sets have been used to construct a high-resolution framework for interpreting late Pleistocene and Holocene terrestrial climate and vegetation patterns between 20,000 and 2,000 yr BP.

Late Pleistocene environmental conditions are characterized by Davis et al. (2002) who identify declining $\delta^{18}O$ and $\delta^{13}C$ signatures prior to 20,000 yr BP, which are

interpreted as reflecting the cold wet conditions associated with the LGM. Local floral communities are dominated by C_3 plants, which are indicated by negative $\delta^{13}C$ values. Late Pleistocene conditions following 20,000 yr BP are marked by oscillating $\delta^{18}O$ and $\delta^{13}C$ values along with varied rates of fine sand influx (Davis et al. 2002). The variability measured in the data set indicates a brief episode of increased aridity that is followed by a shift back to colder conditions ca. 12,000 yr BP.

The late Pleistocene-early Holocene transition (LP/EH) is characterized by extreme variability within the isotope record. Between 11,000 and 10,000 yr BP the isotopic values indicate dramatic shifts in climatic conditions and vegetative composition with warmer and drier conditions ca. 10,500 yr BP to colder and wetter conditions ca. 10,000 yr BP (Davis et al. 2002). Following 10,000 yr BP the record indicates a period of relative vegetative stability as $\delta^{13}C$ values show little variability, which lasts until 9,000 yr BP. However, during this period between 10,000 and 9,000 yr BP the $\delta^{18}O$ record indicates fluctuations in temperatures as the $\delta^{18}O$ values range from 18 to 25‰ (Davis et al. 2002).

Following the LP/EH transition middle Holocene environmental conditions are established and characterized the LSRC from 9,000 to 5,700 yr BP. This period is characterized by reduced variability in the $\delta^{13}C$ values derived from sources located both on canyon slopes and tributary floodplains (Davis et al. 2002). The data is interpreted as reflecting a period that was warmer and drier than prior environmental conditions as well as present day conditions.

During the late Holocene between 5,000 and 2,000 yr BP the isotope record indicates a shift to cooler and wetter conditions as both $\delta^{13}C$ and $\delta^{18}O$ values decline within floodplain deposits (Davis et al. 2002). These conditions supported greater percentages of C_3 flora and persisted until 2,000 yr BP. Following 2,000 yr BP the Salmon River experienced an episode of down-cutting as channel incision reorganized the hydrological system (Davis 2001a) and established the modern gradient of the Salmon River. It is argued that this episode of channel incision is detectable in the isotopic data, as sharp increases in $\delta^{13}C$ values reflect an increase in C_4 flora (Davis et al. 2002). Channel incision lowered the water table of the floodplain, which in turn lowered the available moisture for local C_3 flora (Davis 2001a; Davis et al. 2002).

Another isotopic study conducted in the LSRC by Davis and Muehlenbachs (2001) examined $\delta^{18}O$ values obtained from the shells of *Margaritifera falcata* (river mussel). Shells sampled from three archaeological sites provided $\delta^{18}O$ values from late Pleistocene to Holocene sediments. Modern *M. falcata* shells were sampled to provide a baseline $\delta^{18}O$ value (13.6‰), which was then compared to values derived from the archaeological sites (Davis and Muehlenbachs 2001). Values below the modern baseline of 13.6‰ reflect periods of increased precipitation and those above the baseline reflect periods of decreased precipitation; the data set represents a record of late Pleistocene to Holocene precipitation patterns in the LSRC (Davis and Muehlenbachs 2001).

The *M. falcata* record indicates that precipitation patterns in the Salmon River basin were not stable during the late Pleistocene and early Holocene. The $\delta^{18}O$ values from this time period fluctuate indicating periods of increased aridity punctuated by

periods of increased precipitation (Davis and Muehlenbachs 2001). Middle to late Holocene portions of the record contained $\delta^{18}O$ values that indicate a period of increased precipitation. These wetter conditions persisted until roughly 1,800 yr BP after which modern conditions became established as the values closely track the baseline (Davis and Muehlenbachs 2001).

KP-1 Paleoenvironmental Record

The KP-1 loess section is located in the Columbia Basin of southeastern Washington. The section is exposed as a large road-cut along the Kahlotus-Pasco Highway at an elevation of 410 masl. KP-1 is one of the most extensively studied deposits of loess within the Palouse region of Washington State (McDonald and Busacca 1992). The 12.5 meter thick section of loess provides a record of paleoenvironmental data spanning the last 100,000 years (Berger and Busacca 1995; Richardson et al. 1997). Additional research has been conducted on stable isotopes (Stevenson 1997) and fossil cicada burrows (O'Geen 1998), which help to inform reconstructions of the paleoenvironmental conditions in the area. The following discussion will summarize the paleoenvironmental data from KP-1 that pertains to conditions associated with the LGM to present.

Pedological studies identified four paleosols within the 12.5 m section. These soil-stratigraphic units are identified as the Devils Canyon Soil, the Old Maid Coulee Soil, the Washtucna Soil, and the Sand Hills Coulee Soil (McDonald and Busacca 1992). A series of thermoluminescence (TL) dates were obtained from two different studies in efforts to establish a chronology for KP-1 (Berger and Busacca 1995; Richardson et al.

1999). The TL dates were integrated with other regional tephra and pedological studies to establish the site chronology and an age-depth model for KP-1 (Berger and Busacca 1995; Blinnikov et al. 2001; Busacca et al. 1992; McDonald and Busacca 1992; Richardson et al. 1999).

The two paleosols of interest pertaining to late Pleistocene and Holocene environmental conditions of the Columbia River Plateau are the Washtucna and Sand Hills Coulee Soils (McDonald and Busacca 1992). The Washtucna Soil complex is identified at 216 to 425 cm depth and contains a well-developed light-gray petrocalcic horizon (Bkqmb) (McDonald and Busacca 1992). The Washtucna Soil complex is argued to have formed during the LGM due to its stratigraphic position, which is below Mount St. Helens (MSH) set S tephra dated to 15,500 yr BP (Crandell et al. 1981). TL samples taken from the upper portion of the soil complex, below the overlying MSH set S tephra returned dates of 20,400±2,400 yr BP (Berger and Busacca 1995) and 17,200±1,900 yr BP (Richardson et al. 1997). A lower limiting age of 46,000±6,300 yr BP was obtained from a TL sample taken at ca. 500cm depth within a portion of weakly altered loess that directly underlies the Washtucna Soil complex (Berger and Busacca 1995).

Both Stevenson (1997) and O'Geen (1998) provide additional paleoenvironmental data associated with the Washtucna Soil complex. Examination of ^{18}O and ^{13}C values derived from pedogenic carbonates samples were used to infer past climatic conditions (Stevenson 1997). The isotopic data suggests that conditions associated with the LGM and the formation of the Washtucna Soil complex were dry and cold ca. 20,000 yr BP after which conditions started to trend towards wetter and slightly warmer until roughly

15,000 yr BP (Stevenson 1997). O'Geen (1998) examined the traces of fossil cicada burrows contained within the loess of KP-1 and used this data as a proxy to measure the abundance of sagebrush. This is based on the fact that cicada larvae spend much of their life cycle underground feeding on roots of overlying vegetation. Through the study of modern analogue sites, O'Geen (1998) established that cicada burrows comprise about 19% of the rooting zone below sagebrush steppe communities compared to grasslands and coniferous forests in which burrows account less than 2% of the rooting zone. Cicada burrow data was recovered from the upper 550 cm of the KP-1 section (45,000 yrs to present) and provides a measure of sagebrush vegetative history in the Columbia River Plateau. The highest percentage of burrow activity was observed within the Washtucna Soil complex at a depth of 225-400 cm, which corresponds to roughly 20,000 to 33,000 yr BP (O'Geen 1998). During this time frame burrow abundance is at its highest accounting for over 90% of the total volume sampled between 225-400 cm depth. After 20,000 yr BP the burrow activity drops dramatically with burrows accounting for less than 10% of the volume sampled between 0-225 cm depth (O'Geen 1998). The data is argued to represent LGM conditions that were colder and drier than present. These conditions favored the expansion of sagebrush steppe vegetative communities as reflected in the cicada burrow data set. Following the LGM conditions become warmer and wetter allowing grassland communities to expand at the expense of sagebrush.

The Sand Hills Coulee Soil is the upper most paleosol identified at 110 to 210 cm depth and characterized as a weakly developed soil that contains a distinctive carbonate horizon (Bk) (McDonald and Busacca 1992). The Sand Hills Coulee Soil overlies both

the Washtucna Soil complex and the MSH set S tephra, which suggests that it formed sometime after 15,000 yr BP during the LP/EH transition. Additional chronologic data was obtained from TL samples taken directly above the MSH set S tephra. Berger and Busacca (1995) report an age of 17,000±2,800 yr BP while an age of 14,000±2,400 yr BP was reported by Richardson et al. (1997), which are used to support the timeframe of soil development. Isotopic data indicates a shift from the cold dry conditions of the LGM to wetter cool conditions of the LP/EH (Stevenson 1997). After 15,000 yr BP the isotopic values indicate the onset of modern conditions, which are characterized as warm and dry. Cicada burrow activity drops dramatically after 20,000 yr BP accounting for less than 10% of the total volume sampled between 0-225 cm depth (O'Geen 1998). The data suggests that during the LP/EH the climate was trending towards wetter and slightly warmer conditions compared to LGM climatic conditions (McDonald and Busacca 1992; Stevenson 1997). These conditions favored the expanse of modern grassland communities at the expense of sagebrush, which is supported by the cicada burrow activity (O'Geen 1998).

Chapter 4. Phytolith Analysis and Paleoenvironmental Reconstruction: Methodological and Theoretical Considerations

Since their initial discovery in the early 19th Century, phytoliths have been used to describe plant communities from a variety of environmental and temporal contexts. Phytoliths are particles of hydrated silica that form within living plant tissue, which very in size and morphology depending on plant species and plant part, and can be used to identigy plant taxa (Pearsall 2010; Piperno 2006). Following plant tissue decay, these particles become part of the sedimentological, pedological, and/or archaeological record of a given area. These particles can be extracted from sediments and soils, which can then be used to measure vegetative conditions of a given context. As a result of their durability in sediments and soils, phytoliths have been used as fossil indicators in a variety of paleoenvironmental and archaeological studies (see Blinnikov 2005; Blinnikov et al. 2001, 2002; Carbone 1977; Fredlund et al. 1998; Fredlund and Tieszen 1994, 1997; Pearsall 2010; Piperno 1984, 1985, 1988, 2006; Powers and Gilbertson 1987; Rovner 1971).

As a result of a long and varied history in phytolith research, there is a large body of literature that discusses the history and development of phytolith analysis. Most prominently, Powers (1992), Pearsall (2010), and Piperno (1988, 2006) provide detailed discussions on the history and development of this research field. The following section will briefly discuss the major developments and discoveries that have occurred in phytolith research over the last 150 years.

Discovery and Development of Phytolith Analysis

Piperno (2006:2-4) identifies four stages within the history of phytolith research that characterize the discovery, development, and evolution of phytolith analysis within the context of environmental and archaeological studies. The stages are labeled as the Discovery and Exploration Stage (1835-1895 A.D.), Botanical Phase of Research (1895-1936 A.D.), Period of Ecological Research (1955-1975 A.D.), and the Modern Period of Archaeological and Paleoenvironmental Research (1978 to present).

The discovery of phytoliths first occurred during the early 19th Century when a German botanist G.A. Struve (1835) published his dissertation on phytoliths observed in modern plants. However, much of the credit regarding initial phytolith studies is attributed to the German naturalist Christian Gottfried Ehrenberg, a pioneering microbiologist. Ehrenberg (1841, 1854) had reported observations of numerous siliceous bodies that were contained in soil samples from a variety of natural contexts, including fine dust collected by Charles Darwin form the sails of the H.M.S. Beagle (Piperno 1988, 2006; Powers 1992). These observed siliceous bodies were named “Phytolitharia” by Ehrenberg who went on to develop the first classification system that allowed taxonomic distinctions to be made (Piperno 1988, 2006).

The Botanical Phase of phytolith research that occurred during the early 20th century was largely focused on descriptions of phtyolith production within modern plants. Efforts were made to examine many members of the plant kingdom as research focused on the production, morphology, and taxonomic affinity of phytoliths (Piperno 1988, 2006). The results of these systematic studies resulted in some of the first published

drawings and descriptions regarding phytolith morphology in a variety of plants. German archaeologists Netolitzky and Schellenberg also began to embrace the use of phytolith studies in archaeological research for the first time, as they were able to recover phytoliths from ceramics and ash features from Old World sites (Piperno 2006). Most of the literature produced during this time was in German, which left many English-speaking scientists unaware of the advances that were being made within this growing field. The dissemination of research was dampened even further during World War II as conflict caused scientific communities to flee and/or focus attention elsewhere (Piperno 1988, 2006; Powers 1992).

Phytolith research experienced a revival during the 1950s when a growing number of researchers in the fields of soil science, ecology, and botany began to embrace and promote the use of phytolith studies within the context of larger modern ecological and paleoecological studies. A growing body of literature focused on the production and morphology of phytoliths within the Poaceae (grass) family (Geis 1978; Metcalfe 1960; Parry and Smithson 1958a, 1958b, 1964, 1966; Twiss et al. 1969). Twiss et al. (1969) published a seminal study in which they presented a morphological classification system that allowed subfamily identifications to be made in the Poaceae family. This classification system is still used today by many researchers, although it has been modified slightly to allow the integration of additional phytolith forms as well as to account for changes in grass taxonomy.

Other ecologically focused studies of the time examined the production of phytoliths within deciduous and coniferous tree species. Researchers examined the

production of phytoliths in modern deciduous and coniferous tissue samples, which were then compared to assemblages derived from modern soil samples from these two forest types (Baker 1959; Geis 1973; Klein and Geis 1978; Norgen 1973; Witty and Knox 1964). North American scientists then began to use phytoliths in late Quaternary paleoecological studies and found that they could be utilized as reliable paleo-indicators of forest and grassland communities (Jones et al. 1963; Parry and Smithson 1958a, 1958b; Rovner 1971).

During the late 1970s, phytolith analysis expanded further as it established roles within the fields of archaeological and paleoenvironmental research. Archaeologists and ecologists both began to seriously examine the production and morphology of phytoliths in a wide range of economically and ecologically significant plant taxa (Piperno 2006). Phytoliths became recognized as independent proxy measures of paleoenvironmental conditions at large, as well as a measure of prehistoric plant use and domestication practices. Much of this work focused on phytolith production within the Neotropical forests of the Americas (Pearsall 1978, 1982, 1989; Piperno 1984, 1985a, 1985b, 1985c, 1988, 1989; Piperno et al. 1985). This body of research confirmed the applicability of phytolith analysis as a means of identifying domesticated and cultivated New World crops like maize (*Zea mays*), squash (*Cucurbita* spp.), and arrowroot (*Maranta arudinacea*) (Piperno 1988, 2006; Pearsall 2010).

By the 1990s, it was widely recognized that phytolith analysis had a place within late Quaternary research because it provided a proxy measure of past environmental conditions and also allowed archaeologists to examine aspects of human environmental

interaction. It was previously shown that phytoliths could be obtained from a variety of temporal and spatial contexts, which could be used in conjunction with pollen data or on its own as phytoliths are routinely recovered from contexts that are inadequate for pollen studies (Carbone 1977; Fredlund 1986; Kurmann 1985; Piperno 1985a, 1988, 2006; Rovner 1971). This period saw many advances as researchers began to publish phytolith data from a variety of regional contexts, such as North America (Blinnikov 2005; Blinnikov et al. 2001, 2002; Bozarth 1992, 1993; Cummings 1992; Fredlund and Tieszen 1994, 1997; Mulholland 1993; Mulholland and Rapp 1992a, 1992b;), American Tropics (Pearsall 2010; Piperno 1995, 1998, 2001), southern China (Zhao 1998; Zhao and Piperno 2000), and New Zealand (Kondo et al. 1994). As researchers expanded geographic and taxonomic investigations of phytolith production, they also advanced the methodological procedures related to the extraction and analysis of phytoliths (Coil et al. 2003; Horrocks 2005; Lentfer and Boyd 1998, 1999, 2000; Lentfer et al. 2003; Madella et al. 1998; Pearsall 2010; Piperno 2006).

Phytolith Formation and Deposition: From Plants to Soil

The production of phytoliths is a process that begins with the absorption of monosilicic acid (H_4SiO_4) from ground water by overlying vegetation. The monosilicic acid present in ground water is largely determined by the pH conditions of a given area. Conditions with a pH value of 9 or lower permit the production of monosilicic acid and favor phytolith production (Mulholland and Rapp 1992a; Pearsall 2010; Piperno 2006). The soluble silica in ground water is absorbed by the roots of plants and carried through

the plant via the xylem, which then becomes deposited in various locations of the plant as silicon dioxide (SiO_2) (Piperno 2006).

Research has shown that the process of silica uptake and deposition within plants is both a passive and active process in which the plant exerts some level of control regarding the quantities of silica absorbed and locations of silica deposition (Piperno 2006). Passive uptake occurs as plants uptake silica through ground water, which is then carried through the vascular system and laid down in a nonselective manner. Active transport, in contrast, occurs as the plant is actively expending metabolic energy to facilitate both the uptake and allocation of silica within its vascular system (Piperno 2006). While it is believed that a combination of passive and active processes of silica absorption influence the phytolith production in many plants, it is also recognized that some plants have root based mechanisms that act as barriers to silica absorption (Piperno 2006).

Following the absorption of monosilicic acid, phytolith formation occurs as transpiration causes the soluble silica to precipitate as solid form of amorphous silicon dioxide. Typically, the deposition of silica is restricted to three locations in the plant: cell walls, cell lumen, and intercellular spaces (Piperno 1988, 2006). The cell walls may become impregnated with silica through a process called membrane silicification, which can cause silicification of epidermal, mesophyll, and xylem cells. The second location of silica deposition is the interstitial space bounded by the cell wall, also known as the cell lumen. Silica is deposited within the lumen, filling the space completely in some cases.

The third location of deposition occurs in the intercellular spaces of the plant tissue (Parry and Smithson 1958a; Piperno 2006).

There are a number of different theories regarding the function of silica in living plants (Pearsall 2010; Piperno 1988, 2006; Sangster et al. 2001). Sangster et al. (2001) suggests that the silica largely functions as structural aids and defensive mechanisms. In this context, silica has been an important component of the evolutionary history of plants because it has facilitated increased reproductive success. Structurally, silica is utilized to strengthen and support plant tissue, which can improve the plants photosynthetic capabilities. For example, the increased support and rigidity of the upper leaves in *Oryza* sp. (rice) permits more sunlight to reach the lower portions of the plant. Defensively, silica plays a role as a mechanical barrier to herbivores and insects by increasing the toughness of the plant tissue and/or seeds, which discourages herbivory. The silica also acts as a barrier to pathogenic fungi that may cause disease and decay, and may also serve as a barrier thought to mitigate the negative effects of certain heavy metals like aluminum and manganese (Piperno 1988, 2006)

Typically, phytoliths are deposited into soils and sediments as plants die and the tissue decays in place where they are released into the uppermost portions of the soil or sediment of a given location. These contributions from all local vegetation are deposited together over time at a given site and form a phytolith assemblage. Stratified records of past vegetative conditions develop in those places where phytolith assemblages and other sediments accumulate over long periods of time.

Additional depositional processes influencing assemblage formation include transport via humans and animals, fire, wind, and water (Fredlund and Tieszen 1994; Piperno 2006). Research has shown that the combined effects of wind and fire can cause increased movement and aeolian deposition of phytoliths as they become liberated from the ignited plant tissue and transported as windblown dust. Darwin's study of dust from the sails of the H.M.S. Beagle revealed the role of wind transport in the dispersal of phytoliths (Piperno 2006; Powers 1992). Piperno (1988) studied horizontal transport within the landscape and collected a number of surface samples from different forested areas in Panama, and found that phytolith movement was typically less than 20 meters. However, Fredlund and Tieszen (1994) studied transport within the Great Plains and found that anywhere from 30-70% of the assemblage had been transported from outside of the local sample site. Phytoliths are also transported via fluvial processes (Piperno 2006). Humans and animals also play a role in horizontal transportation. Herbivores consume and transport plant matter via their dung, which contains undigested phytoliths from outside areas depending upon the mobility of the given animal. Like animals, humans can actively transport plants and plant products as they move through the landscape, which may skew the phytolith assemblages of cultural sites when non-local and economically significant plant types may be over-represented (Pearsall 2010; Piperno 2006).

Clearly, there are a number of natural and cultural processes that are responsible for the formation of phytolith assemblages in a given location. However, the assemblage is still thought to reflect the average vegetative composition present during periods of

stability and soil formation, which is referred to as inheritance by Fredlund and Tieszen (1994). Simply put, inheritance refers to the processes of continued deposition of phytoliths to a stable surface, which forms assemblages that provide a measure of long-term vegetative composition for a given area. Thus, phytoliths remain a viable indicator fossil for late Quaternary paleoenvironmental studies at local and regional spatial scales (Fredlund and Tieszen 1994; Piperno 2006; Pearsall 2010).

Finally, there are a couple taphonomic processes that may influence assemblage preservation of phytoliths, including chemical and mechanical degradation that may occur following deposition. It is recognized that phytoliths are susceptible to dissolution when conditions permit pH values of nine or greater. In other words, highly alkaline conditions can cause phytoliths to either fully or partially dissolve into solution as monosilicic acid (Piperno 2006). The extent of dissolution is also influenced by the degree of silification that occurred in the plant. It is known that some plant types (e.g. *Ulmaceae*) contain both weakly and partially silicified phytolith forms that are more susceptible to degradation (Bozarth 1992, 1993; Mulholland and Rapp 1992a; Pearsall 2010; Piperno 2006). Mechanical degradation can occur as phytoliths become broken and/or abraded over time as a result of transport via agents such as wind, water, fire, and animals. Again, weakly or partially silicified phytoliths may be more susceptible to mechanical damage associated with transport. Despite the potential for damage and loss in assemblages, phytoliths have been successfully recovered and identified in geologic deposits upwards of 60 million years in age (Jones 1964).

Classification of Phytoliths as Paleoenvironmental Proxies

Rovner (1971) was among the first archaeologist to promote and test the applicability of phytoliths as a means for paleoecological reconstruction within the context of a larger archaeological research agenda. Archaeology has a long history of collaboration and interdisciplinary research, which integrates methods and data derived from paleontological, geological, pedological, and paleobotanical studies. Rovner (1971) argues that there are both advantages and disadvantages associated with each of these individual subfields of study, including phytoliths, and, therefore, reconstructions should integrate multiple independent lines of evidence when available. Rovner (1971: 343-344) goes on to state:

> For any fossil system to be useful to the archaeologist at least three criteria must be met. The material must withstand decomposition, exhibit sufficient morphological differences to be of taxonomic significance, and provide sufficient quantities to reflect the nature of the entire assemblage from which it is derived.

Phytoliths fulfill Rovner's (1971) criteria because they are preserved in a wide range of environmental contexts; they are recoverable in large quantities in wide range of environmental contexts; and they exhibit taxonomically distinct morphologies. A number of studies have validated the applicability of phytolith assemblages as indicators of vegetative cover (e.g., forest versus grassland) at a variety of temporal and spatial contexts (Beavers and Stephen 1958; Blinnikov et al. 2001, 2002; Jones and Beavers 1964; Jones et al. 1963; Klein and Geis 1978; Norgen 1973; Parry and Smithson 1958; Witty and Knox 1964).

Twiss et al. (1969) proposed one of the first morphologically based classification systems that allowed subfamily identification within the Poaceae (grass) family. The system permitted identification of Chloridoid, Panicoid, and Festucoid grasses based on the presence and frequencies of morphologically distinct short cell grass phytoliths (Figure 4.1). While updated, this system is still in use today and will be discussed in more detail in the following sections.

Twiss et al. (1969) and Rovner (1971) both recognized that there were problematic overlaps in the morphology of short cell grass phytoliths between different subfamilies, which is a phenomenon Rovner (1971) termed “redundancy”. In other words, some phytolith shapes are observed in many different plants. Another problem related to classification is known as “multiplicity”, in which multiple phytolith morphologies are present within one plant (Rovner 1971).

These issues related to redundancy and multiplicity could potentially cause misinterpretations of assemblage data. However, these issues can be mitigated through adequate sampling and counting procedures that are based on observations derived from reference collections (Pearsall 2010; Piperno 2006; Rovner and Russ 1992). Classification systems used for paleoenvironmental reconstruction should, thus, be based on observed phytolith data derived from modern tissue and sediment samples in addition to fossil assemblages derived from archaeological and/or geological contexts from within the region of study (Mulholland 1989; Pearsall 2010; Piperno 2006).

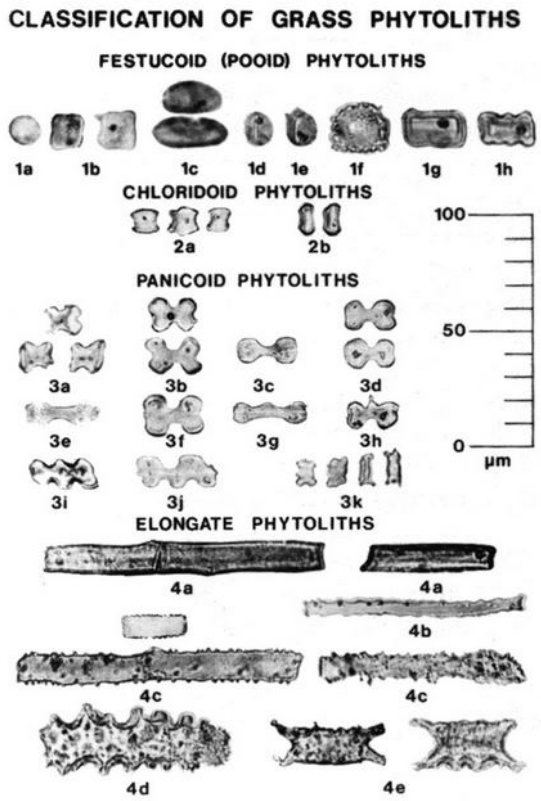

Classification of Grass Phytoliths

I) Festucoid Class
1b. Rectangular
1c. Elliptical
1d. Acicular, variable focus
1e. Crescent, variable focus
1f. Circular crenate
1g. Oblong
1h. Oblong, sinuous

II) Chloridoid Class
2a. Chloridoid
2b. Thin Chloridoid
3k. Crenate

III) Panicoid Class
3a. Cross, thick shank
3b. Cross, thin shank
3c. Dumbbell, long shank
3d. Dumbbell, short shank
3e. Dumbbell, long shank, straight or concave ends
3f. Dumbbell, short shank, straight or concave ends
3g. Dumbbell, nodular shank
3h. Dumbbell, spiny shank
3i. Regular, complex dumbbell
3j. Irregular, complex dumbell

IV) Elongate Class (no subfamily characteristics)
4a. Elongate, smooth
4b. Elongate, sinuous
4c. Elongate, spiny
4d. Elongate, spiny with pavement
4e. Elongate, concave ends

Figure 4.1 Grass phytolith classification system (adapted from Twiss et al. 1969).

Grass Phytolith Morphology and Classification

The production and morphology of Poaceae or grass phytoliths has been extensively studied in many different regions of the world over the last 50 years (see Blinnikov 2005; Brown 1984; Fredlund and Tieszen 1994, 1997; Metcalfe 1960; Mulholland 1989; Mulholland and Rapp 1992b; Norgren 1973; Piperno 2006; Twiss et al. 1969; Witty and Knox 1964). As a result of this research, morphological classification systems have been developed that allow subfamily identifications of grasses on the basis of short cell morphology. The use of grass short cell morphologies as a proxy for reconstructing grassland composition and modeling grassland evolution through time has been validated within late Quaternary ecological and archaeological studies (Blinnikov et al. 2001, 2002; Fredlund and Tieszen 1994, 1997; Fredlund et al. 1998; Mulholland and Rapp 1992b; Piperno and Pearsall 1993, 1998; Twiss 1992).

As discussed earlier, Twiss et al. (1969) presented one of the first classification systems (Figure 4.1) that permitted identification of grass subfamilies (Panicoideae, Chloridoideae, and Pooideae) within the Great Plains of North America. Following the work of Metcalfe (1960), they recognized that certain phytolith short cell morphologies were associated with the (then) three grass subfamilies and proposed the following classification system. The subfamily Panicoideae (tall grasses) was characterized by the production of bilobates (originally called ‘dumbbells’) and cross-shaped phytoliths, which they grouped as the Panicoid Class. The subfamily Chloridoideae (short grasses) produced abundant saddle shaped phytoliths that were grouped as the Chloridoid Class. The subfamily Pooideae, formerly called Festucoideae, was characterized by the

production of circular, oval, and rectangular shaped phytoliths, which they grouped as the Festucoid Class. A fourth class of long cell phytoliths was recognized in all three of the subfamilies examined. These long cell varieties were grouped as the Elongate Class, which is characteristic of the Poaceae family. However, they do not permit subfamily classification within the system (Twiss et al. 1969).

The original system developed by Twiss et al. (1969) has been updated due to new information regarding phytolith morphology and production within the Poaceae family (Brown 1984; Fredlund and Tieszen 1994; Mulholland 1989;), which has allowed for higher levels of taxonomic resolution to be obtained. Additionally, recent studies undertaken by the Grass Phylogeny Working Group (GPWG 2001) have updated and revised the Poaceae Taxonomy, which now recognizes twelve subfamilies compared to the original three subfamilies recognized by Twiss et al. (1969). The subfamilies recognized by the GPWG (2001) are: Anomochlooideae, Pharoideae, Puelioideae, Bambusoideae, Ehrhartoideae, Pooideae, Aristidoideae, Danthonioideae, Arundinoideae, Chloridoideae, Centothecoideae, and Panicoideae. Analysis of short cell phytolith production and morphology within the twelve subfamilies indicates that some shapes are still characteristic to a given subfamily (Piperno 2006).

Revisions to the Twiss et al. (1969) short cell classification system have refined the ability to reconstruct grassland composition to the subfamily level within the context of North America. Brown (1984) demonstrated that the subfamily Pooideae produced characteristic “long wavy trapezoids”, also referred to as “crenates” (Fredlund and Tieszen 1994) (Figure 4.2), and “short trapezoids”, also referred to as “rondels”

(Fredlund and Tieszen 1994; Mulholland 1989) (Figure 4.2). These forms can be used to identify members of the Pooideae subfamily (e.g. *Poa*, *Festuca*, and *Agropyron*) (Piperno 2006), which is an important and abundant grass flora of temperate zones in both hemispheres (Twiss 1992).

The subfamily Panicoideae produces characteristic lobate and polylobate forms that Twiss et al. (1969) named “dumbbells” and “crosses”. The lobate and polylobate forms are distinguished by two or more disk-like lobes, which are connected by a pronounced shaft-like mid-section (Brown 1984; Fredlund and Tieszen 1994; Mulholland 1989; Piperno 2006). Commonly referred to as bilobates, Fredlund and Tieszen (1994) recognized that “Panicoid-type” bilobates exhibited a characteristic degree of symmetry that could be used to distinguish them from the *Stipa*-type bilobate forms produced by members of the Aristidoideae subfamily (Figure 4.2). *Stipa*-type bilobates are characterized by a lack of symmetry and when viewed in cross-section, they exhibit a trapezoidal shape (Fredlund and Tieszen 1994).

Cross forms are still considered characteristic of the Panicoideae subfamily; however, it is recognized that their production is not exclusive to Panicoideae (Brown 1984; Mulholland 1989; Piperno 2006; Twiss et al. 1969). For example, there are a variety of cross shapes produced by the subfamilies Bambusoideae and Arundinoideae; though they can be distinguished from Panicoideae forms on the basis of their three-dimensional morphologies and global distribution (Piperno 2006; Piperno and Pearsall 1998; Twiss 1992). These forms can be used to identify members of the Panicoideae

subfamily (e.g. *Andropogon* and *Panicum*), which is the dominate tall grass flora of the Great Plains in North America (Piperno 2006; Twiss 1992).

The subfamily Chloridoideae produces abundant and characteristic saddle shaped forms (Figure 4.2) that have been observed by many researchers (Brown 1984; Fredlund and Tieszen 1994; Metcalfe 1960; Mulholland 1989; Piperno 2006; Piperno and Pearsall 1998; Twiss et al. 1969). Their work has shown that saddle shaped short cells can be used to identify the short grasses of the Chloridoideae subfamily (e.g. *Bouteloua*), which are important drought tolerant species of the short grass prairies of North America (Twiss 1992).

A variety of other phytolith shapes (e.g., long cell or elongate types, bulliform, hairs, and trichomes) have been identified in the Poaceae family. Twiss (1992) presents an updated version the original 1969 classification system that includes two new classes: Fan-shaped and Point-shaped phytoliths identified by Sase and Kondo (1974) (Figure 4.3). These forms have also been referred to as bulliforms and trichomes (Mulholland 1989; Pearsall 2010; Piperno, 2006). The elongate class of Twiss et al. (1969), also referred to as elongate plates (Brown 1984), are still considered to be characteristic of the Poaceae family at-large, but lack further taxonomic resolution. While these additional forms do not allow identification of Poaceae to the subfamily level, they can still be used as a reliable indicator of grassland environments relative to forested environments (Piperno 2006).

Phytolith Morphology and Classification in Non-grasses

A number of studies have examined phytolith production within pteridophytes

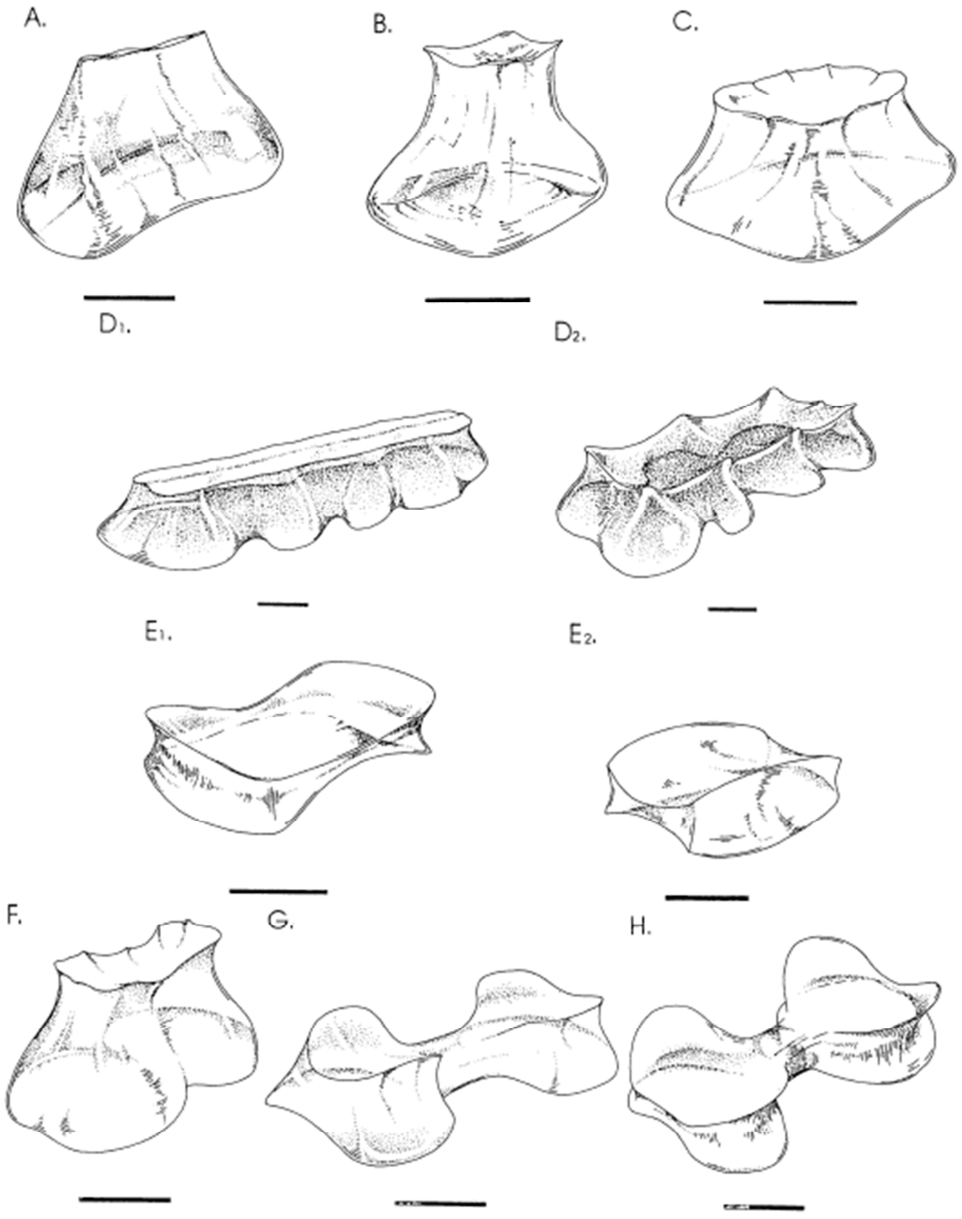

Figure 4.2 Additional grass short cell phytolith morphotypes: A, Keeled Rondel; B, Conical Rondel; C, Pyramidal Rondel; D_1 and D_2, Crenate; E_1 and E_2, Saddle; F, *Stipa*-type; G, Simple Lobate; H, Panicoid-type. Bar scale equals 5 nm (from Fredlund and Tieszen 1994).

Figure 4.3 Grass phytolith classification. Pooid (festucoid) phytoliths, Class1; Chloridoid phytoliths, Class 2; Panicoid phytoliths, Class 3; Elongate phytoliths, Class 4; Fan-shaped phytoliths, Class 5; Point-shaped phytoliths, Class 6. Classes 5 and 6 are from Sase and Kondo (1974) (adapted from Twiss 1992).

(e.g., ferns) (Blinnikov 2005; Lentfer 2003; Piperno 1988), gynosperms (e.g., conifers) (Blinnikov 2005; Bozarth 1993; Klein and Geis 1978; Norgren 1973), monocotyledons (e.g., sedges) (Ollendorf 1992), and eudicots (e.g., oaks) (Bozarth 1992). As a result of these studies, a number of diagnostic and characteristic morphotypes have been observed within the plant groups listed above, which allows for reconstructions of the non-grass vegetative context in a given site to various taxonomic levels.

Important gynosperms of North American forests include the Pinaceae family (e.g., pine trees), which have been extensively studied and appear to have a number of characteristic and diagnostic morphotypes (Blinnikov 2005; Bozarth 1993). Diagnostic forms have been identified in the needles of *Pinus ponderosa* (ponderosa pine), characterized by spiny or spiked irregular bodies (Figure 4.4) (Blinnikov 2005; Bozarth 1993; Norgren 1973). *Pseudotsuga menziesii* (Douglas-fir) also produces a large diagnostic form characterized as a branched asterosclereid type (Figure 4.5) (Blinnikov 2005; Brydon et al. 1963; Klein and Geis 1978; Norgren 1973). Bozarth (1993) describes a characteristic form produced by *Picea glauca* (white spruce), characterized by a thin epidermal plate with wavy margins on all four sides (Figure 4.6). Bozarth (1992, 1993) and Blinnikov (2005) both identify a number of characteristic phytolith forms that are produced in Pinaceae. These forms include blocky polyhedrals with smooth and grainy surfaces and at least eight non-parallel sides, which are characteristic of *Picea* (spruce), but also observed in *Abies* (fir) (Figure 4.6). *Larix occidentalis* (western larch) produces characteristic forms of epidermal phytoliths with unevenly thickened cell walls (Figure 4.7).

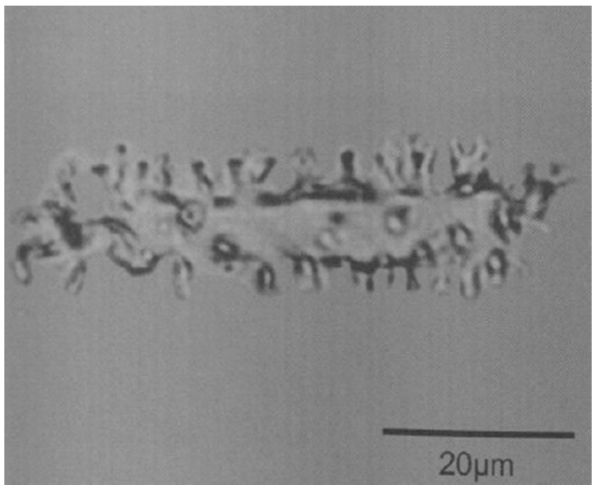

Figure 4.4 Diagnostic spiny phytolith from the Pinaceae (from Bozarth 1993).

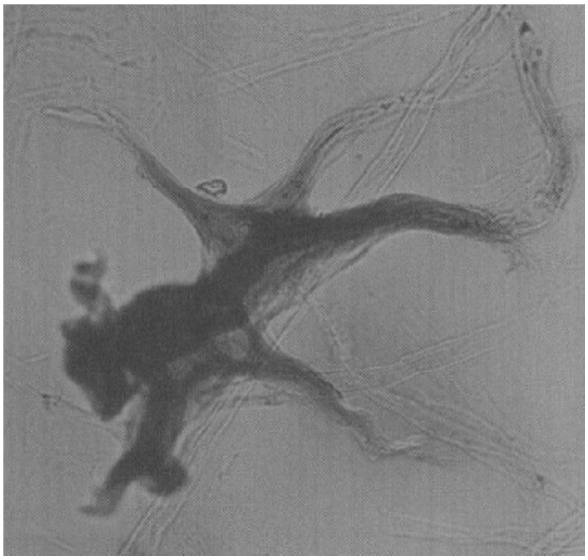

Figure 4.5 Diagnostic asterosclereid phytolith from *Pseudotsuga menziesii*. The phytolith is over 100 µm long (from Blinnikov 1999).

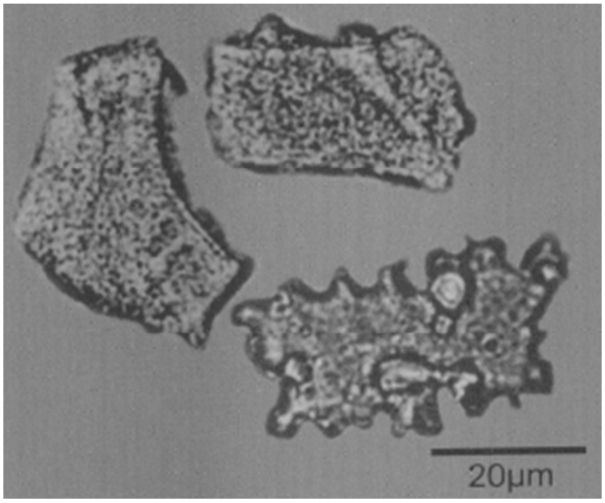

Figure 4.6 Characteristic epidermal phytolith with wavy margins from *Picea glauca*, bottom right, and blocky polyhedral endodermal forms from *Picea mariana*, top and left (adapted from Bozarth 1993).

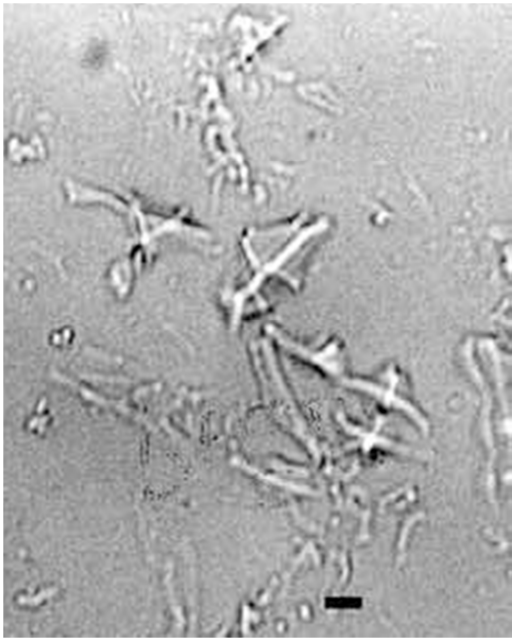

Figure 4.7 Characteristic phytoliths from *Larix occidentalis*. Scale bar equals 10µm (from Blinnikov 2005).

Eudicots is another major plant group of North America that includes a variety of woody (e.g., Fagaceae, Salicaceae, and Ulmaceae) and herbaceous (e.g., Asteraceae, Caesalpiniaceae, and Fabaceae) plant families (Piperno 2006). A variety of phytolith morphologies have been observed with this large group of plants. Bozarth (1992) provides a phytolith classification system for selected dicotyledons that are native to the Great Plains of North America that recognizes nine types of phytoliths unique to eudicots.

The most frequent forms observed by Bozarth (1992) were two types of silicified epidermal cells: epidermal polyhedral (Figure 4.8) and epidermal anticlinal (Figure 4.9) phytoliths are produced in the leaves of many wood and herbaceous eudicots. Epidermal polyhedral phytoliths are characterized as a flat polyhedrals with four to eight sides and parallel tops and bottoms; these forms have been observed in a number of woody (e.g., Aceraceae, Ulmaceae, and Salicaceae) and herbaceous (e.g., Asteraceae, Fabaceae, and Mimosaceae) eudicots (Bozarth 1992). Epidermal polyhedral forms have also been observed in some conifer and grass species (Klein and Geis 1978; Rovner 1971); however, these forms can be distinguished from the eudicot types. Conifers produce endodermal blocky phytolith forms that exhibit irregular morphologies with at least eight non-parallel sides, which can be used to separate them from the eudicot forms (Bozarth 1992). Grasses produce polyhedral phytoliths that typically have only four sides, allowing them to be distinguished from eudicot forms that typically have more than four sides. Epidermal anticlinal phytolith forms have also been identified in both woody (e.g., Aceraceae and Salicaceae) and herbaceous (e.g., Asteraceae and Fabaceae)

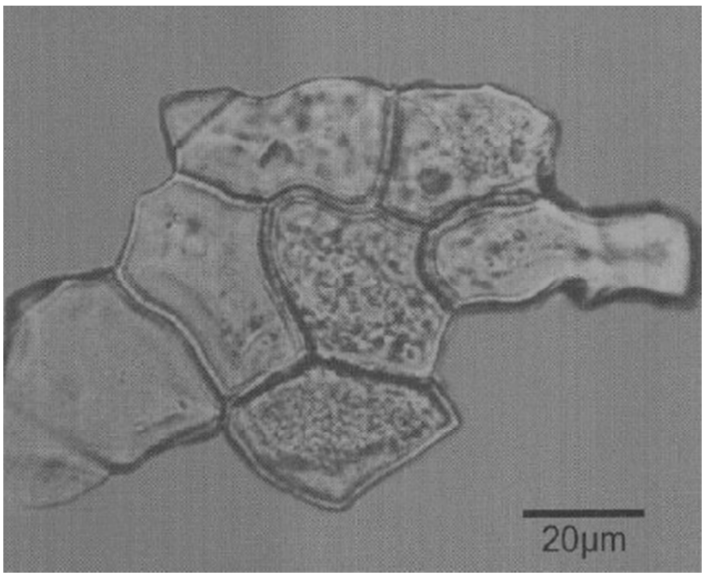

Figure 4.8 Epidermal polyhedral phytoliths from *Artemisia ludoviciana* (from Bozarth 1992).

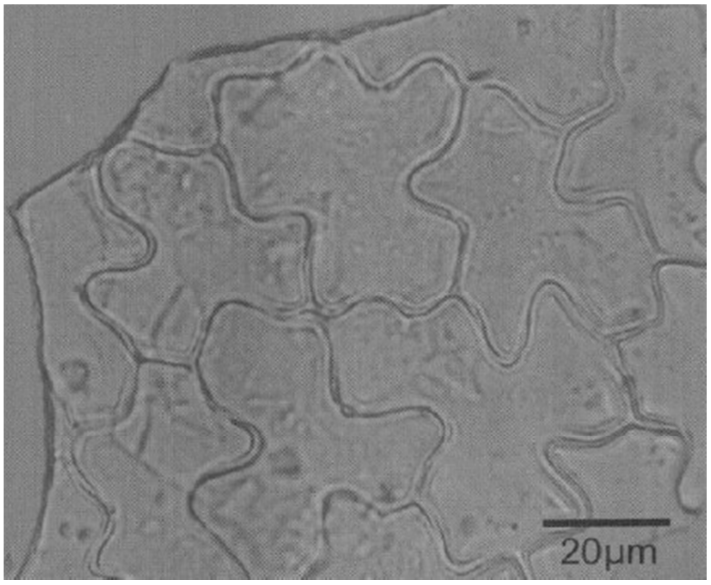

Figure 4.9 Epidermal anticlinal phytoliths from *Hedyosmum* (from Piperno 2006).

eudicots. These forms are sometimes referred to as jigsaw-puzzle pieces as they exhibit irregular shapes with wavy or sinuate margins (Bozarth 1992; Piperno 2006).

Another form observed in many woody (e.g., Aceraceae, Salicaceae, and Ulmaceae) and herbaceous (e.g., Asteraceae, Fabaceae, and Mimosaceae) eudicots is branched tracheary elements with spiral thickenings (Figure 4.10) (Bozarth 1992; Piperno 2006). These forms are produced by the silicification of vascular tissue (e.g., xylem and phloem), which are characterized as cylindrical structures with branched spiral thickenings (Piperno 2006). While considered characteristic of eudicots, these branched tracheary elements do not permit higher levels of taxonomic classification.

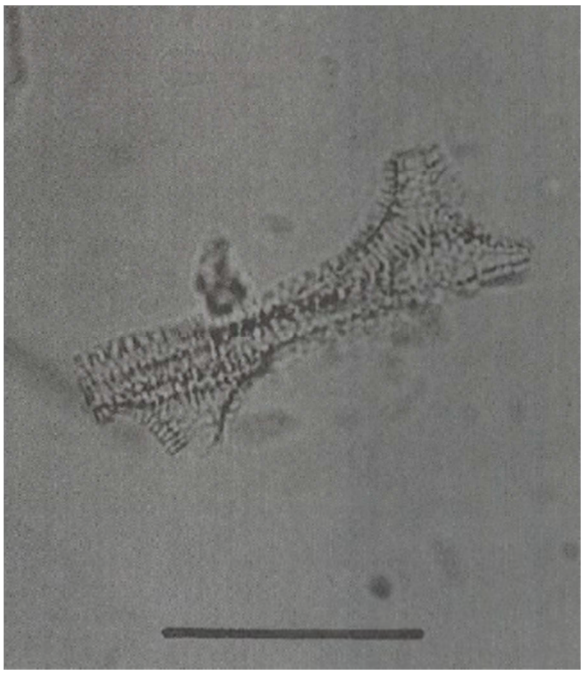

Figure 4.10 Branched tracheary elements with spiral thickenings in *Helianthus grosseserratus*. Scale bar equals 40μm (from Bozarth 1992).

Honeycomb assemblages were also observed in a number of woody (e.g., Aceraceae and Fagaceae) and herbaceous (e.g., Asteraceae and Fabaceae) eudicots. These forms are characterized by silicification of clusters of palisade mesophyll cells, which have been further subdivided into elongate and shallow honeycomb assemblages (Bozarth 1992). Elongate forms (Figure 4.11) have undergone complete silicification of the palisade mesophyll tissue, while shallow forms (Figure 4.12) have undergone partial silicification of the palisade mesophyll tissue end walls (Bozarth 1992; Piperno 2006). Similar phytolith forms have occasionally been observed in the Poaceae family; however, these can be distinguished from eudicot varieties because Poaceae forms occur in straight rows compared to the eudicot clusters (Bozarth 1992). These forms are considered to be characteristic of eudicots.

Two varieties of platelet phytoliths have been observed in some woody (e.g., Ulmaceae) and herbaceous (e.g., Asteraceae) eudicots; these varieties include opaque perforated platelets and echinate platelets (Bozarth 1992). The opaque perforated platelet forms (Figure 4.13) are large plates with irregular margins that exhibit systematic perforations across the surface, which are believed to be unique to limited species of the Asteraceae family (Bozarth 1992; Piperno 2006). Echinate platelet forms (Figure 4.14) have been observed in the Ulmaceae family and are characterized as small flat plates with irregular margins that exhibit echinate (spiny) sculpturing on one side while the other side is psilate (smooth) (Bozarth 1992). Echinate platelets are considered diagnostic of *Celtis occidentalis* (hackberry), while the perforated platelet forms are diagnostic of Asteraceae (Piperno 2006).

Verrucate (bumpy) phytolith forms are sometimes referred to as cystoliths (Piperno 2006), which are silica and/or calcium carbonate bodies that formed within specialized epidermal cells called lithocysts. These cystolith forms (Figures 4.15 and 4.16) are characterized as spherical shapes that exhibit various kinds of verrucate, echinate, or tuberculate surface sculpturing. Occasionally, they retain distinct stalks that are used to anchor these forms to the cell wall (Bozarth 1992; Piperno 2006). These forms can be used to identify selected members of the eudicot group, which includes woody varieties like *C. occidentalis* of the Ulmaceae family and herbaceous varieties of the Urticaceae family (Bozarth 1992).

Hair cell and hair base phytoliths have been observed in a number of woody (e.g., Ulmaceae and Moraceae) and herbaceous (e.g., Asteraceae, Boraginaceae, Cucurbitaceae, and Urticaceae) eudicots (Bozarth 1992; Piperno 2006). Hair cell forms (Figure 4.17) are typically lanceolate-shaped with a flat, spherical, or elliptical base and a pointed or rounded tip; these forms have been further subdivided into two groups: segmented and nonsegmented types (Piperno 2006). Nonsegmented hair cell phytoliths are unicellular and lack the distinct divisions observed in the multicellular, segmented variety, which may exhibit two to four segments (Bozarth 1992; Piperno 2006). Both varieties of hair cells originate from hair base cells that are located in the epidermal tissue of a given plant. These hair base forms (Figure 4.18) exhibit a wide range of morphological variability, which typically is observed as flattish spheres that may retain circular marks associated with the site of hair cell attachment (Piperno 2006). These forms can be used to identify a number of woody and herbaceous family members within the eudicot group.

Figure 4.11 Elongate honeycomb assemblage in *Platanus occidentalis.* Scale bar equals 40μm (from Bozarth 1992).

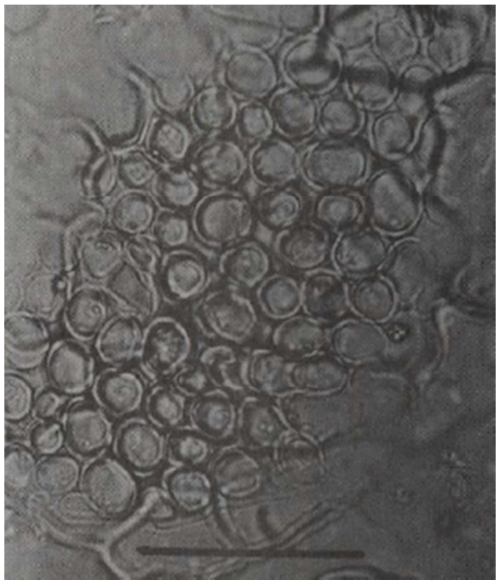

Figure 4.12 Shallow honeycomb assemblage in *P. occidentalis.* Scale bar equals 40μm (from Bozarth 1992).

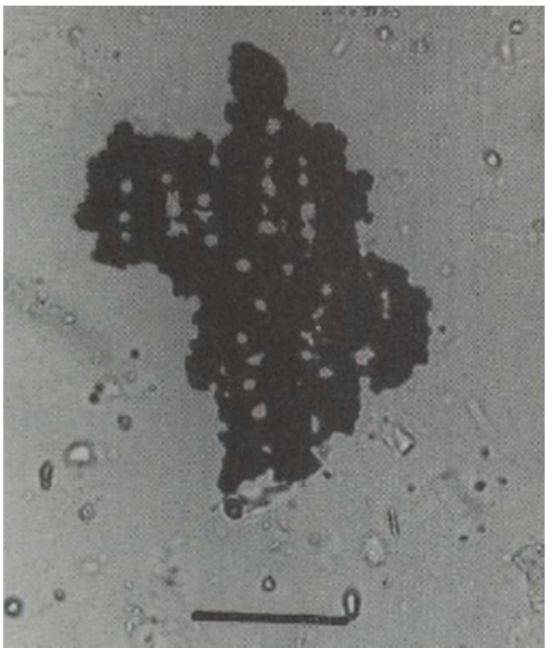

Figure 4.13 Opaque platelets with systematic perforations in *Ambrosia psilostachya*. Scale bar equals 40µm (from Bozarth 1992).

Figure 4.14 Echinate platelets in *Celtis occidentalis.* Scale bar equals 40µm (from Bozarth 1992).

Figure 4.15 Spherical cystolith with low verrucate sculpturing and stalk-like projection in *C. occidentalis.* Scale bar equals 40μm (from Bozarth 1992).

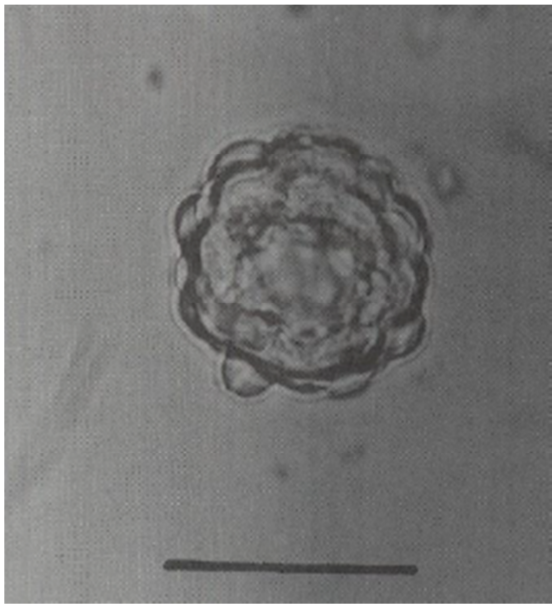

Figure 4.16 Spherical cystolith with high verrucate sculpturing in *Boehmeria cylindrical.* Scale bar equals 40μm (from Bozarth 1992).

Figure 4.17 Three segmented thick-walled hair in *Solidago rigida.* Scale bar equals 40μm (from Bozarth 1992).

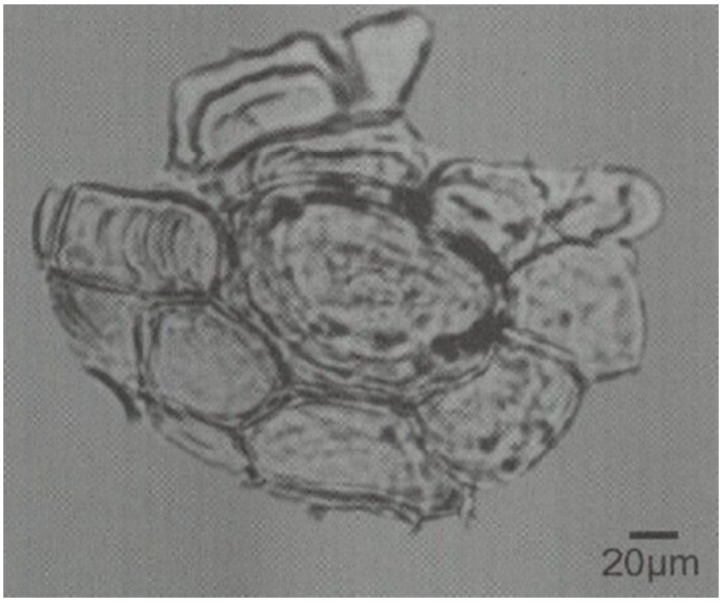

Figure 4.18 A hair base in *Cordia lutea.* (from Piperno 2006).

Bozarth (1992) identified a final phytolith form, which he characterized as scalloped phytoliths. These are spherical and elliptical forms (Figure 4.19) that exhibit distinctive surficial sculpturing, argued to be characteristic of arboreal vegetation (Piperno 2006). Bozarth (1992) reported a form that is argued to be diagnostic of herbaceous eudicots, specifically the Cucurbitaceae family.

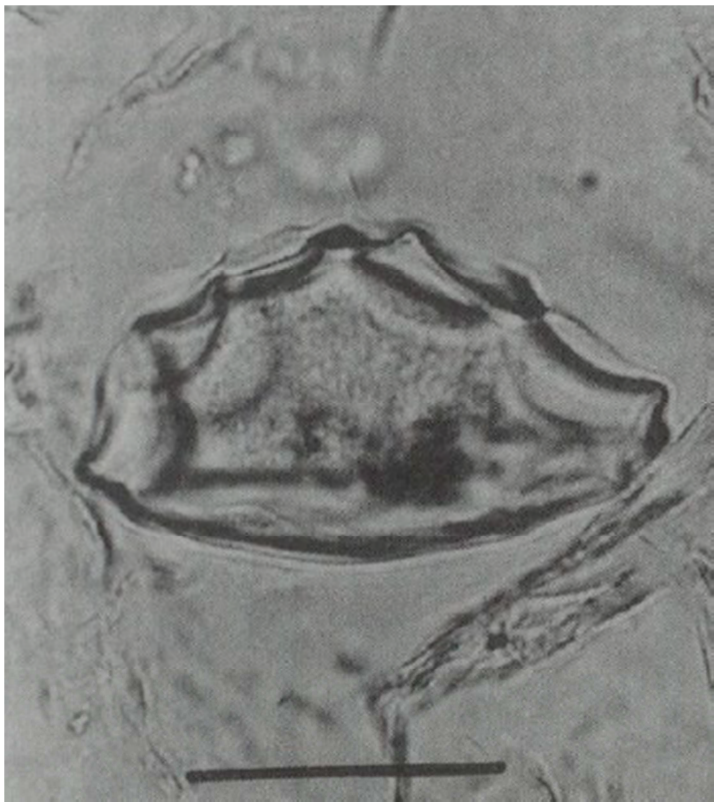

Figure 4.19 Phytolith with deeply scalloped surface in *Cucurbita foetidissima.* Scale bar equals 40μm (from Bozarth 1992).

The variety of characteristic and diagnostic phytolith morphologies observed within non-Poaceae plant communities has permitted researchers to construct a number of classification systems (Blinnikov 2005; Bozarth 1992, 1993; Piperno 2006). As a

result, it is possible to examine fossil phytolith assemblages and reconstruct aspects of arboreal vegetation (Blinnikov 2005; Blinnikov et al. 2001, 2002; Bozarth 1993; Piperno 2006).

Ecological Significance of Phytolith Assemblages

Researchers have demonstrated that phytolith analysis can be reliably used to inform and improve paleoenvironmental reconstructions within a variety of global contexts (Pearsall 2010; Piperno 2006). Since phytoliths can be used to identify a wide range of plants at various levels of taxonomic specificity, it is possible to reconstruct aspects of vegetative communities at various temporal and spatial scales. This is a powerful paleoenvironmental proxy tool given that certain plant taxa are restricted to various environmental contexts, which are largely controlled by climatic variables (e.g., temperature and precipitation) (Piperno 2006). The ability to reconstruct vegetation of a given site can, in turn, provide proxy data related to larger ecological and climatic conditions. When viewed diachronically, phytolith data can provide a history of ecological change at local and regional scales.

In some cases, phytolith analysis can achieve higher levels of taxonomic identification compared to other late Quaternary environmental records such as pollen (Pearsall 2010; Piperno 2006). Pollen does not permit subfamily identification within the Poaceae family; phytoliths, in contrast, can be readily identified to subfamily levels (Fredlund and Tieszen 1994; Piperno 2006; Twiss 1992; Twiss et al. 1969) and in some cases to the genus level (Blinnikov et al. 2001, 2002; Blinnikov 2005). Within the context of grasslands, the ability to identify subfamilies (e.g., Pooideae, Chloridoideae, and

Panicoideae) is ecologically significant given that each subfamily is restricted to certain environmental conditions (Fredlund and Tieszen 1994; Piperno 2006; Twiss 1992).

Phytolith production and morphology has been extensively studied within the Poaceae families of the North American Great Plains (Brown 1984; Fredlund and Tieszen 1994; Mulholland 1989; Twiss 1992; Twiss et al. 1969). These studies have validated the use of phytolith analysis to identify the presence and frequency of the three subfamilies that dominate North American grasslands: Pooideae, Chloridoideae, and Panicoideae. The distribution of these subfamilies is largely influenced by climatic factors, which is also reflected in the photosynthetic mechanisms used by these subfamilies (Fredlund and Tieszen 1994; Piperno 2006; Rovner 1983; Twiss 1992).

The two photosynthetic mechanisms used by plants are referred to as C_3 and C_4 photosynthetic pathways, and they are related to the different modes CO_2 fixation and subsequent sugar production utilized by a given plant (Fredlund and Tieszen 1994; Piperno 2006; Rovner 1983). During photosynthesis C_3 plants will actively discriminate against ^{13}C as they produce 3-carbon phosphoglyceric acid as the first stable product of photosynthesis (Rovner 1983). C_3 plant communities (e.g., Pooideae) are most prevalent in cooler climates found at high latitudes and/or elevations (Twiss 1992). Conversely, C_4 plant communities (e.g., Chloridoideae and some Panicoideae) do not discriminate against ^{13}C as actively as C_3 plants while they produce 4-carbon organic acid as the first stable product of photosynthesis (Rovner 1983). C_4 plant communities are prevalent in hot dry climates (Twiss 1992).

The ability to distinguish C_3 plants from C_4 plants significantly informs paleoenvironmental reconstructions and interpretations at-large. Within the context of North American grasslands, it is possible to identify C_3 Pooideae grasses (e.g., *Poa*, *Festuca*, and *Agropyron)*, C_4 Chloridoideae grasses (e.g., *Bouteloua*), and C_4 Panicoideae grasses (e.g., *Andropogon*) from one another on the basis of phytolith assemblages. Twiss (1992) reviews the global distribution of these three Poaceae subfamilies, highlighting the influence of climate on the observed distribution. Within the context of the Pacific Northwest of North America, it is recognized that the dominate grass subfamily is Pooideae, which comprises over 80% of the total grass flora from the region (Twiss 1992). The subfamilies Panicoideae and Chloridoideae comprise the remaining grasses of the region with each contributing less than 10% to the total regional grass flora (Twiss 1992).

Phytolith Classification in the Columbia River Plateau

To date, phytolith analysis within the context of the Columbia River Plateau has been limited to a number of studies conducted by pedologists (Norgren 1973; Witty and Knox 1964), archaeologists (Davis and Collins 2009; Eccleston 1999; Somer 2003), and paleoecologists (Blinnikov 2005; Blinnikov et al. 2001, 2002). These studies have addressed a variety of issues related to phytolith production in modern plants and preservation in modern soils (Blinnikov 2005; Norgren 1973; Witty and Knox 1964), production in modern plants and preservation in archaeological sediments (Eccleston 1999), and the ecological interpretation of fossil assemblages sampled from geological and archaeological contexts (Blinnikov et al. 2001, 2002; Davis and Collins 2009; Somer

2003). The combined results of these studies have lead to the development of a regional classification system (Blinnikov 2005) that is based on observations from modern reference collections and fossil assemblages.

Recent paleoecological studies in the Columbia River Plateau have reconstructed the late Quaternary vegetative histories of the region (Blinnikov et al. 2001, 2002) on the basis of phytolith assemblages recovered from loess sections in area (e.g., KP-1 loess section). These phytolith assemblages were compared to additional paleoenvironmental data derived from the KP-1 loess section (e.g., stable isotopes and insect burrows) and the Carp Lake pollen sequence (see Chapter 2 for discussion on these additional records) in order to reconstruct a 100,000 year vegetative history of the Columbia Basin (Blinnikov et al. 2001, 2002).

The interpretations of the fossil phytolith assemblages presented by Blinnikov et al. (2001, 2002) are based on the classification system developed by Blinnikov (2005). Blinnikov (2005) examined phytolith production and morphology in 38 plant species that comprise the dominate trees, shrubs, grasses, and forbs of the modern Columbia Basin. Blinnikov (2005) compared the assemblages from modern plant tissue to those recovered from 58 modern soil samples in the region, and observed 20 different phytolith forms that could be used to distinguish eight different vegetation zones. The eight vegetation zones that are distinguished by phytolith assemblages are: *Artemisia*-dominated shrub steppe, *Stipa*-dominated grasslands, *Agropyron*-dominated grasslands, *Festuca*-dominated grasslands, *Elymus cinereus* grasslands, *Pinus ponderosa*-dominated forests, *Abies*

grandis-Pseudotsuga menziesii forests, and *Abies lasiocarpa-Picea engelmannii* forests (Blinnikov 2005:96).

It is argued that any environmental interpretation of fossil phytolith assemblages should be based on modern observations of phytolith production and preservation within plants and soils of the region to be studied (Pearsall 2010; Piperno 2006). In fact Blinnikov (2005:72) wrote:

> This study provides a modern analog dataset required for any paleoenvironmental reconstruction of the late Pleistocene and Holocene vegetation of the region, including previously published work (Blinnikov et al. 2001, 2002).

Blinnikov's (2005) classification system not only allows interpretation and reconstruction of fossil phytolith assemblages derived from the Columbia Basin, but it also presents a framework for distinguishing certain genera of Pooideae subfamily. The ability to distinguish members of the Pooideae subfamily (e.g., *Agropyron*, *Festuca*, *Poa*, and *Stipa*) is significant within the context of the Columbia Basin because of the overall lack of Chloridoideae and Panicoideae flora in the region; together these two subfamilies account for less than 10% of the regional grass flora (Blinnikov 2005:96). Despite limitations associated with redundancy and multiplicity, it was recognized that members of the Pooideae subfamily typically produced two to three morphotypes that composed roughly 75% of all phytoliths produced by said member (Blinnikov 2005:77).

The phytolith classification system developed by Blinnikov (2005) for the Columbia Basin region recognizes 20 individual morphotypes (Figure 4.20) that can be used to reconstruct late Quaternary vegetative patterns. Thirteen morphotypes were

identified within the dominate grasses of the region, including a variety of short cell and long cell phytoliths. The short cell forms are subdivided into four groups: rectangular plates with straight edges (morphotype 1), plates with wavy margins (morphotypes 2 and 3, also referred to as “crenates”) (Fredlund and Tieszen 1994), rondels (morphotypes 9-12), and bilobates of the *Stipa*-type (morphotype 13) (Fredlund and Teiszen 1994; Mulholland 1989). The long cell phytolith forms are also subdivided into four broad groups: rectangular long cells (morphotype 4), indented long cells (morphotype 5), deeply indented long cells (morphotype 6), and angular long cells (morphotype 7) (Blinnikov 2005:77). The final two forms observed in grasses are dendritic long cells (morphotype 8) and scutiform opal, both of which are formed within the seed epidermis. These two forms are grouped together as a single category of phytoliths (Blinnikov 2005:77).

Two additional morphotypes identified by Blinnikov (2005) include trichomes (morphotype 14) and silicified hairs and hair bases (morphotype 15). While trichomes have been observed primarily in grasses, they are also produced in members of the Asteraceae family (Bozarth 1992). Similarly, silicified hairs and hair bases have been observed in all of the dominate grass flora of the region in addition to a number of eudicots (Blinnikov 2005; Bozarth 1992).

The remaining morphotypes recognized in the classification system are derived from a variety of non-grass species in the region, which include dominate trees, shrubs, and forbs of the Columbia Basin. The Pinaceae family (conifer trees) produces a variety of diagnostic and characteristic phytolith morphologies. Polyhedral endodermal blocky

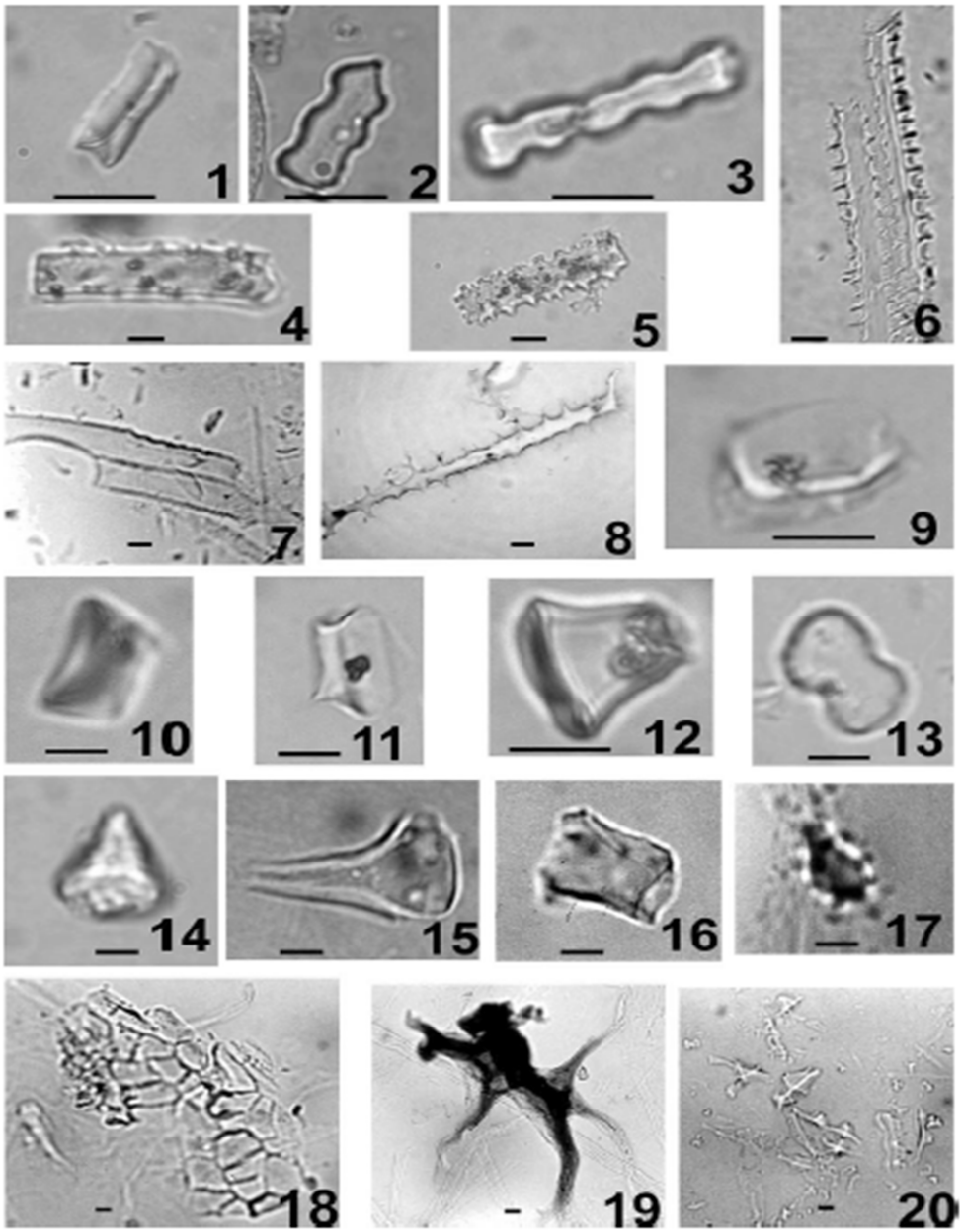

Figure 4.20 Phytolith morphotypes identified by Blinnikov (2005). Morphotypes 1-13 are from grasses, 14 and 15 are from grasses or non-grasses, and 16-20 are from non-grasses. Scale bar equals 10μm (adapted from Blinnikov 2005).

forms (morphotype 16) are considered characteristic of Pinaceae and Asteraceae families as they were observed in *Abies*, *Picea*, and *Artemisia*, which produce forms with smooth or granulate textures on many nonparallel surfaces (Blinnikov 2005; Bozarth 1993; Klein and Geis 1978). *Pinus ponderosa* produces diagnostic forms characterized as spiny irregular shaped bodies (morphotype 17) (Blinnikov 2005; Bozarth 1993; Norgren 1973). *Pseudotsuga menziesii* produces a large diagnostic asterosclereid phytolith (morphotype 19), which is characterized as a dark large branching body (Blinnikov 2005; Klein and Geis 1978; Norgren 1973). Two varieties of epidermal phytoliths were recognized and include a flat polygonal epidermal form (morphotype 18) and a flat anticlinal epidermal form, both of which are produced by *Abies*, *Picea*, and some members of the Asteraceae family (e.g., *Artemisia*) (Blinnikov 2005; Bozarth 1993). The final form observed in Blinnikov's (2005) system is characterized as epidermal phytoliths with unevenly thickened cell walls (morphotype 20) formed in the needles of *Larix occidentalis* (western larch).

Blinnikov used this morphological classification system to evaluate fossil phytolith assemblages derived from geologic exposures within the Columbia River Plateau and reconstructed the vegetative history of the region spanning a period of roughly the last 100,000 years (Blinnikov et al. 2001, 2002). Blinnikov et al. (2002) compared the phytolith data with local pollen records derived from Carp Lake, Washington and reconstructed the vegetative context of the Columbia River Plateau since the last glacial maximum (LGM) in which they identify conditions associated with four

periods; the LGM (ca. 21,000 yr BP), the Late Glacial (ca. 15,000-11,000 yr BP), early to mid-Holocene (ca. 11,000-6,000 yr BP), and the present day.

Assemblages associated with the LGM indicate that environmental conditions were much drier and colder than today. Phytolith assemblages recovered from KP-1 (410 masl) indicate extensive cover of *Artemisia* shrubs, and grasses consisting of *Stipa, Poa,* and *Festuca* (Blinnikov et al. 2001, 2002). The phytolith data is supported by pollen records recovered from Carp Lake (714 masl), which indicate high frequencies of *Artemisia*, grass, and *Picea* pollen during the LGM (Whitlock 1992; Whitlock and Bartlein 1997; Whitlock et al. 2000). The interpretation of the data is argued to reflect the presence of an extensive xeric *Artemisia*-dominated shrub steppe during the LGM, which is supported further by the presence of abundant cicada burrows identified within the Washtucna Soil (O'Geen and Busacca 2001). Analysis of stable isotopes recovered from pedogenic carbonate suggests that conditions were dry and cold (Stevenson 1997), favoring the expansion of shrub steppe vegetation.

Following the LGM, environmental conditions began to change as it became warmer and wetter; however, the conditions associated with the Late Glacial interval (ca. 15,000-11,000 yr BP) are still considered to be cooler and wetter than present day (Blinnikov et al. 2001, 2002). The phytolith assemblage recovered from KP-1 indicates a shift from the previous xeric *Artemisia*-dominated shrub steppe to mesic *Festuca*-dominated grassland, which is supported by the cooler and wetter conditions of the Late-Glacial (Blinnikov et al. 2001, 2002). The replacement of *Artemisia* by grassland components is supported further by the lack of cicada burrows in the Late Glacial-aged

sediments at KP-1 (O'Geen and Busacca 2001). Isotopic data associated with this period also suggests that conditions were gradually warming and becoming wetter compared to conditions during the LGM (Stevenson 1997). Pollen data from Carp Lake indicates that the site supported *Picea* parkland communities during this period of cooler and wetter climatic conditions (Whitlock 1992; Whitlock and Bartlein 1997; Whitlock et al. 2000).

The next period of environmental change occurs during the Early and Mid-Holocene (ca. 11,000-6,000 yr BP) when conditions became warmer and drier compared to those during the Late Glacial. During the early Holocene (ca. 11,000-7,000 yr BP) at KP-1, the phytolith record indicates a shift in grassland composition as xeric *Agropyron*-dominated communities replaced the mesic *Festuca*-dominated communities of the Late-Glacial period (Blinnikov et al. 2001, 2002). Conditions continued to become drier during the middle Holocene (ca. 7,000-5,000 yr BP), which is reflected in the phytolith assemblage by increased frequencies of *Artemisia* phytoliths (Blinnikov et al. 2001, 2002). The inferred middle Holocene drying trend is further supported by observed increases in cicada burrow activity within middle Holocene aged loess deposits of the Columbia River Plateau (O'Geen and Busacca 2001), which provides an indirect measure of *Artemisia* cover (O'Geen 1998). Isotopic records from KP-1 also reflect a gradual warming and drying during Holocene (Stevenson 1997). Pollen data from Carp Lake indicated warming and drying during early and middle Holocene as grassland communities replace *Picea* parkland communities during the early Holocene, which are then replaced by *Pinus*-*Quercus* woodlands (Whitlock 1992; Whitlock and Bartlein 1997; Whitlock et al. 2000).

Following the middle Holocene, modern conditions become established within the Columbia River Plateau as reflected in the phytolith assemblages from KP-1 and pollen data from Carp Lake (Blinnikov et al. 2001, 2002; Whitlock 1992; Whitlock and Bartlein 1997; Whitlock et al. 2000). The brief expansion of *Artemisia* during the middle Holocene was replaced by extensive *Agropyron-Festuca* grasslands during the late Holocene, and these have persisted to present day in the area of KP-1 (Blinnikov et al. 2001, 2002). Pollen data from Carp Lake also indicates the establishment of the modern *P. ponderosa-Pseudotsuga* forest during the late Holocene (ca. 4,000 yr BP) when climatic conditions became cooler and wetter compared to the early and middle Holocene conditions (Whitlock 1992; Whitlock and Bartlein 1997; Whitlock et al. 2000).

Phytolith Classification in the Lower Salmon River Canyon

To date, phytolith analysis and classification within the context of the lower Salomon River canyon (LSRC) has been limited to a few archaeological and paleoenvironmental studies (Davis and Collins 2009; Eccleston 1999; Somer 2003). While the number of phytolith studies in the LSRC remains small, these preliminary studies have shown that phytoliths are abundant within modern plants; recoverable from late Quaternary deposits in the LSRC; and that they can be used to reconstruct vegetative histories of the area. The following section will discuss the results of these previous phytolith studies in the LSRC.

Eccleston (1999) was one of the first researchers to explore the applicability of phytolith analysis in the Columbia River Plateau within the context of an archaeological research design. Eccleston (1999) examined phytolith production in modern plants of the

Columbia River Plateau by collecting over 100 plant species and processing a total of 171 samples. Eccleston (1999) identified and classified a variety of phytolith morphotypes from 80 plant species, which she used to develop a classification system for the region. The classification system was applied to interpret fossil phytolith assemblages recovered from the Cottonwood-Divide Creek site, an upland archaeological site located on the Joseph Plains (Eccleston 1999). The primary goal of her study was to use the classification system to "…identify root crop phytoliths in the soil samples" (Eccleston 1999:154). The identification of root crop phytoliths in archaeological sediments was applied to measure the intensity of floral exploitation in the Columbia River Plateau during the late Holocene occupation of the Cottonwood-Divide Creek site.

Eccleston (1999) identified a number of root crop phytolith forms that she considered to be characteristic of Liliaceae and Apiaceae (e.g., camas and cous). Soil samples obtained from the Cottonwood-Divide Creek site were processed and scanned for root crop forms. The frequency of root crop forms was low overall; however, three samples did contain large quantities of root crop forms (Eccleston 1999). These samples were associated with cultural features and ground stone tool technology that dated to the earliest occupations of the site (ca. 3,500 yr BP). Eccleston argued that the phytolith data suggests "…that intensive root crop processing occurred from the earliest periods of the site until the height of occupation" (1999:205).

Eccleston (1999) validated the applicability of phytolith analysis within the context of archaeological research in the Columbia River Plateau. Her work identified a number of characteristic phytolith forms produced by economically important plant

communities in the region, which could be used to reconstruct environmental contexts and prehistoric plant use patterns. However, the morphology of root crop phytoliths exhibited redundancy issues as there is overlap with some short-cell forms produced in Poaceae subfamilies (e.g., bilobate and polylobate forms). Eccleston (1999) was aware of these redundancy issues and suggested that further research could attempt to address these problems by increasing the comparative collection of modern plants and analyzing assemblage production and preservation in modern soils.

A second phytolith study conducted in the LSRC by Somer (2003) used the phytolith record as a means of testing the validity of the "Oasis effect" hypothesis proposed by Davis (2001a). Davis (2001a) argued that local vegetative conditions of the riparian zones in the LSRC were largely influenced by the phreatophytic effects of increased groundwater availability along the floodplain, which allowed these riparian vegetative communities to persist during episodes of climatic change. As a result of the "Oasis effect", Davis (2001a) argued that riparian zones along the canyon bottom supported higher densities of plants and animals compared to canyon slopes and upland sites, which were directly influenced by regional climatic change. The availability of a stable and productive riparian zone is argued to have influenced the cultural patterns of early and middle Holocene (c.a. 9,000-2,000 yr BP) occupations of the LSRC, which are preserved in the archaeological record of the canyon.

Somer (2003) conducted phytolith analysis of geologic exposures located at Hammer Creek (SR-23) and Lyons Bar (SR-26A and SR-26C), which contain sediments spanning a period of ca. 20,000 yr BP to present. Somer (2003) examined the reference

collection produced by Eccleston (1999) in addition to other published reference materials (Bozarth 1992; Fredlund and Tieszen 1993; Klein and Geis 1978; Twiss et al. 1969) to develop a morphologically based classification system that could measure vegetative composition and change through time. Somer (2003) argued that phytolith records could be used to reconstruct late Quaternary vegetative histories of the LSRC and this, in turn, could then be used to test the validity of the "Oasis effect". The vegetative stability associated with the "Oasis effect" should, arguably, create largely homogenous phytolith assemblages from a period of roughly 9,000 to 2,000 yr BP because that riparian vegetative composition is expected to have experienced little to no change during this period (Somer 2003:2).

The results of Somer's (2003) phytolith study in the LSRC provided a record of vegetative composition since the end of the LGM, which contains six episodes of vegetative fluctuation. The phytolith assemblages derived from the Lyons Bar sections SR-26A and SR-26C provided a record of late Pleistocene (ca. 21,000-17,600 yr BP and 15,400-9,600 yr BP) vegetative conditions (Somer 2003). The Lyons Bar assemblages exhibit little variation through time, which Somer discusses in the following manner: "Since no trends in phytolith composition are discernible one must assume that there was stable vegetation cover at this site…" (2003:109). The phytolith data suggests that during the late Pleistocene, the Lyons Bar local supported mixed grasslands composed largely of Pooideae grasses, which accounted for 55-70% of the total assemblage (Somer 2003). Other grassland components include the Panicoideae and Chloridoideae subfamilies, both of which accounted for between 2-10% of the total assemblage. Additional vegetative

cover is thought to include members of the Pinaceae family, such as *Picea* and *Pinus,* which account for <5-9% of the total assemblage (Somer 2003).

Phytolith assemblages derived from the Hammer Creek section SR-23 provide a record of late Pleistocene and Holocene vegetative conditions that have been divided into six different phytolith zones on the basis of assemblage composition (Somer 2003). Section SR-23 also contained sterile zones between 190-140 cm, and again at 120cm, in which phytoliths frequencies were inadequate for analysis. The phytolith zones are characterized by Somer (2003:101-104) in the following manner:

Zone I (400-300 cm) (ca. 17,000-14,900 yr BP) is characterized by abundant Pooideae phytolith forms, which account for over 70% of the total assemblage, while Panicoideae and Chloridoideae forms both account for <3-7% of the assemblage. Non-grass phytolith forms considered characteristic of *Picea/Pinus ponderosa* (<6%) and *Picea/Pinus monticola* (<5%) are present within this zone as well.

Zone II (290-190 cm) (ca. 14,900-12,700 yr BP) is characterized by a decline in Pooideae phytoliths, which account for <70% of the total assemblage. During this time, the frequency of Panicoideae forms increases slightly accounting for 7-10% of the assemblage, while Chloridoideae forms account for <4%. Non-grass phytolith forms include a diagnostic *Pinus ponderosa* type, which accounts for 3-10% of the assemblage. Additional non-grass forms include characteristic *Picea/Pinus ponderosa* forms, which account for 3-10% of the total assemblage.

Zone III (130-100 cm) (7,200-5,500 yr BP) is characterized by an increase in Pooideae forms, which account for ca. 75% of the total assemblage. Panicoideae and

Chloridoideae forms both decline with the former, accounting for ca. 3% and the latter <1% of the total assemblage. Non-grass phytolith forms are limited within this zone; however, characteristic *Picea/Pinus ponderosa* forms account for ca. 4% of the total assemblage while diagnostic *Pinus ponderosa* forms are virtually absent.

Zone IV (90-50 cm) (5,500-2,400 yr BP) is characterized by a continued increase in Pooideae forms, which account for ≥80% of the total assemblage. Panicoideae forms increase slightly as they account for 3-5% of the total assemblage, while Chloridoideae forms are virtually absent. Non-grass phytolith forms are limited within this zone with characteristic *Picea/Pinus ponderosa* forms accounting for ca. 2% of the total assemblage.

Zone V (40-10 cm) (2,400-500 yr BP) is characterized by continued dominance of Pooideae forms, which account for ca. 75% of the total assemblage. Chloridoideae forms increase within this zone and account for ca. 5% of the assemblage, while Panicoideae forms decline to <5%. Non-grass phytolith forms are limited within this zone with characteristic *Picea/Pinus ponderosa* forms accounting for <5% of the total assemblage and diagnostic *Pinus ponderosa* forms accounting for <3%.

Zone VI (0 cm) (modern assemblage) is characterized by a continued dominance of Pooideae forms, which account for ca. 70% of the total assemblage. Panicoideae and Chloridoideae forms each account for ca. 5% of the assemblage. Non-grass phytolith forms are rare within this zone with all diagnostic and characteristic *Picea* and *Pinus* forms accounting for ≤4% of the total assemblage.

Somer (2003) used the phytolith records from Lyons Bar (SR-26A and SR-26C) and Hammer Creek (SR-23) to summarize the late Quaternary paleoenvironmental conditions of the LSRC. These records suggest that since the LGM, the LSRC has supported a predominantly Pooideae grassland with limited arboreal species consisting of *Picea/Pinus ponderosa.* Following the LGM, the phytolith records indicate a decline in the frequencies of arboreal species while grassland communities expanded (Somer 2003). Somer (2003:119) argues that the phytolith records do not fully support the "Oasis effect" because the data suggests a steady shift in vegetative composition to a more restricted arboreal component during the late Pleistocene and Holocene. However, the data indicates that the LSRC supported C_3 Pooideae grasses (e.g. *Agropyron, Festuca, and Poa*) throughout the Holocene, which may have influenced cultural use of the canyon bottom (Somer 2003).

While Somer (2003) is unable to fully address the validity of the "Oasis effect", his research does provide a framework for understanding late Quaternary paleoenvironmental context and change within the LSRC through the use of phytolith analysis. There are some potential issues with the dataset created by Somer (2003), one of which is related to errors in the stratigraphy of SR-26 at the Lyons Bar section (Davis and Collins 2009). Additionally, Somer (2003) attempts to test the "Oasis effect" hypothesis with the phytolith records; however, none of the samples were recovered from riparian floodplain deposits that would have experienced the phreatophytic benefits associated with increase groundwater availability. Rather, Somer's (2003) data provides a record of

vegetative change associated with the non-phreatophytic zones associated with the lower elevation canyon slopes adjacent to the floodplain of the LSRC.

Finally, the morphological classification scheme utilized in Somer's (2003) study was developed largely from observations made in modern plant tissue, which is a valid approach to understanding phytolith production and morphology of a given species. However, no attempts were made to examine assemblage production and preservation within modern sediments and soils, which can be used to characterize ecologically specific assemblage compositions (e.g., grassland assemblages versus forest assemblages) of the region. Meaningful interpretations of fossil phytolith assemblages should, arguably, integrate knowledge regarding assemblage production and preservation in plants, soils, and sediments derived from modern phytolith studies within the region of interest (Blinnikov 2005; Bowdery 1998; Pearsall 2010; Piperno 2006).

A third phytolith study conducted within the LSRC examined the phytolith assemblages derived from 11 stratigraphic sections, which were used to develop an initial model of late Quaternary paleoenvironmental conditions and vegetative change (Davis and Collins 2009). The stratigraphic sections examined include Unit: A at the Cooper's Ferry site; Unit: B at the American Bar site; three profiles in the Slate Creek drainage; two profiles in the Alison Creek drainage; and four profiles in the Eagle Creek drainage. The dataset created spans a period of the last 17,000 yr BP and provides a record of local vegetation for low elevation sites in the canyon bottom, middle elevation sites in tributary side canyons, and higher elevation upland sites (Davis and Collins 2009). These phytolith records were integrated and compared with other relevant paleoenvironmental proxy

records, including stable isotope analysis (Davis and Muehlenbachs 2001; Davis et al. 2002), lithostratigraphic, pedostratigraphic and geomorphic analysis (Davis 2001a), and phytolith analysis (Eccleston 1999; Somer 2003).

The integration of these datasets helped to inform paleoenvironmental reconstructions of the LSRC. These paleoenvironmental reconstructions provide a basis for modeling landscape scale vegetative contexts and changes within the LSRC since the LGM (Davis and Collins 2009). The results of Davis and Collins (2009) phytolith study indicate that at all sections, there is a noticeable decline in the frequencies of arboreal species (e.g., *Picea* and *Pinus* spp.) in relation to Poaceae species (e.g., Pooideae grasses) since the LGM (Davis and Collins 2009).

At low elevation sites, including Cooper's Ferry and American Bar, the phytolith records indicate the presence of arboreal vegetation with a grassland component of predominately Pooideae grasses during the late Pleistocene, where arboreal phytoliths account for over 60% of the assemblages (Davis and Collins 2009). During the early and middle Holocene, these records indicate a shift in local vegetation as arboreal species decline at the expense of expanding Pooideae grasslands. Grass phytolith frequencies increase during the early and middle Holocene, accounting for 55-71% of the assemblages (Davis and Collins 2009). The assemblages derived from the profiles in the Eagle Creek drainage indicate the presence of stable Pooideae grasslands that have existed since the late Pleistocene. The grass phytolith frequencies associated the Eagle Creek profiles account for 80-100% of the assemblages (Davis and Collins 2009).

At higher elevation sites located within the Slate Creek and Allison Creek drainages, the phytolith records also reflect this broad trend of non-arboreal expansion following the terminal Pleistocene. The profiles examined within the Slate Creek drainage indicate the presence of an arboreal forest composed largely of *Picea, Pinus,* and *Larix* spp. with a limited grass component composed largely of Pooideae grass species (Davis and Collins 2009). This closed canopy arboreal forest slowly transitioned into an open forest-grassland vegetative composition as modern environmental conditions became established during the middle and late Holocene. This forest-grassland composition supports a forest component of *Pinus, Pseudotsuga,* and *Picea* spp., while the grassland component is predominately Pooideae spp. with very limited Panicoideae and Chloridoideae spp. (Davis and Collins 2009).

The profiles examined from the Allison Creek drainage indicate the presence of a relatively stable closed canopy arboreal forest with a limited grass understory, which has recently given way to grassland expansions. Both profiles contain abundant characteristic *Picea* and *Pinus* phytolith forms, which account for ≥68% of the assemblages obtained from buried sediments, while modern sediments contained ≤56% of these types (Davis and Collins 2009). Davis and Collins (2009:56) note that the modern samples from Allison Creek record a 30-63% decline in arboreal phytolith frequencies, which is argued to be a possible result of historic and modern logging practices within the area.

The phytolith study conducted by Davis and Collins (2009) once again confirms the applicability of phytolith analysis within the LSRC as they found recoverable quantities of phytoliths within a variety of stratigraphic samples. The vegetative records

inferred from the phytolith data can be used to model spatial and temporal vegetative contexts within the LSRC, which can then be used to inform our interpretations of the archaeological record in the LSRC. Davis and Collins (2009) study largely followed the morphological classification scheme developed by Eccleston (1999) and Somer (2003) and did not attempt to quantify assemblage production and preservation within modern vegetative contexts. Many phytolith analysts (Blinnikov 2005; Pearsall 2010; Piperno 2006) are recommending that research regarding assemblage production and preservation within modern environmental contexts (i.e., modern plant tissue, soils, and sediment) is needed to adequately interpret fossil assemblages. These modern studies should be conducted within the region of interest in order to develop regionally based classification systems that can adequately interpret fossil phytolith assemblages (Blinnikov 2005; Bowdery 1998; Pearsall 2010; Piperno 2006). Blinnikov (2005) provides a regional classification system for the dominate vegetation of the southern Columbia River Plateau that is based on modern and fossil assemblages.

Chapter 5. Field and Laboratory Sampling Procedures

As part of the present study three sediment profiles (SR-23, SR-27, and SR-34) and one archaeological site (10IH73) were sampled for phytolith analysis. While mapping the late Quaternary surficial deposits of the LSRC Davis (2001a) conducted the initial stratigraphic description of these sections. Davis (2001a) identified late Pleistocene and Holocene-aged sedimentary deposits within these sections, which may be sampled for paleoenvironmental proxy data. Sections SR-23 and 10IH73 have been previously sampled for isotope and grain size analysis (Davis et al. 2002), which was used to model paleoenvironmental conditions of the LSRC since the terminal Pleistocene. Initial phytolith research conducted at SR-23 (Somer 2003) and 10IH73 (Davis and Collins 2009) was used to model paleovegetative conditions of the LSRC, which was then compared to other paleoenvironmental data sets from the LSRC (Davis and Muehlenbachs 2001; Davis et al. 2002).

These sections were sampled in order to elaborate upon the previous phytolith research in efforts to establish contextualized reconstructions of late Quaternary paleoenvironmental conditions of the LSRC. Sections SR-23 and 10IH73 were sampled in order to compare the existing phytolith assemblage data (Somer 2003; Davis and Collins 2009) with the data produced from the present study, which will then be interpreted within a regional classification scheme developed for the Columbia basin and surrounding region (Blinnikov 2005).

Profile Descriptions

Profile SR-23 (Hammer Creek)

Section SR-23 or the Hammer Creek section (45° 45’ 47” N, 116° 19’ 30” E) is located near the Hammer Creek Recreation Site at an elevation of 480 masl (Figure 5.1). The section is an east-facing exposure located on the west side of the Salmon River that was exposed as a result of historic hydraulic placer mining within the LSRC. Davis et al. (2002) provided the initial stratigraphic descriptions of SR-23, which is characterized as a 4.2 m thick deposit of aeolian silt loam and sandy loam that overlies alluvial gravels.

At the base of SR-23 there are late Pleistocene-aged deposits of alluvium, which is comprised of rounded cobble and pebble gravels of basaltic lithology. Overlying the late Pleistocene alluvium are thick deposits of non-bedded carbonaceous silty and sandy loess, which were deposited during the late Pleistocene and Holocene (Davis 2001a; Davis et al. 2002). Loess deposition in the LSRC is believed to be the result of the redistribution of alluvial sediments by aeolian processes, which caused floodplain sediments to be redeposited upslope on adjacent landforms (Davis 2001a).

Davis (2001a) identified two paleosols that formed within the loess at SR-23. The lower paleosol observed is believed to be a weakly-developed expression of the China Gardens Soil. The China Gardens Soil formation occurred as pedogenic process altered relatively stable loess deposits within the LSRC between ca. <25,000 and >15,000 yr BP (Davis 2001a:126). The China Gardens Soil at SR-23 is characterized by a weakly-developed cambic horizon in yellowish brown sandy loam (Davis 2001a). The upper paleosol observed is believed to be a weakly-developed expression of a Rock Creek Soil.

The Rock Creek Soil formation occurred as pedogenic processes altered relatively stable loess deposits within the LSRC between ca. 13,000 and 10,740 yr BP (Davis 2001a:126).

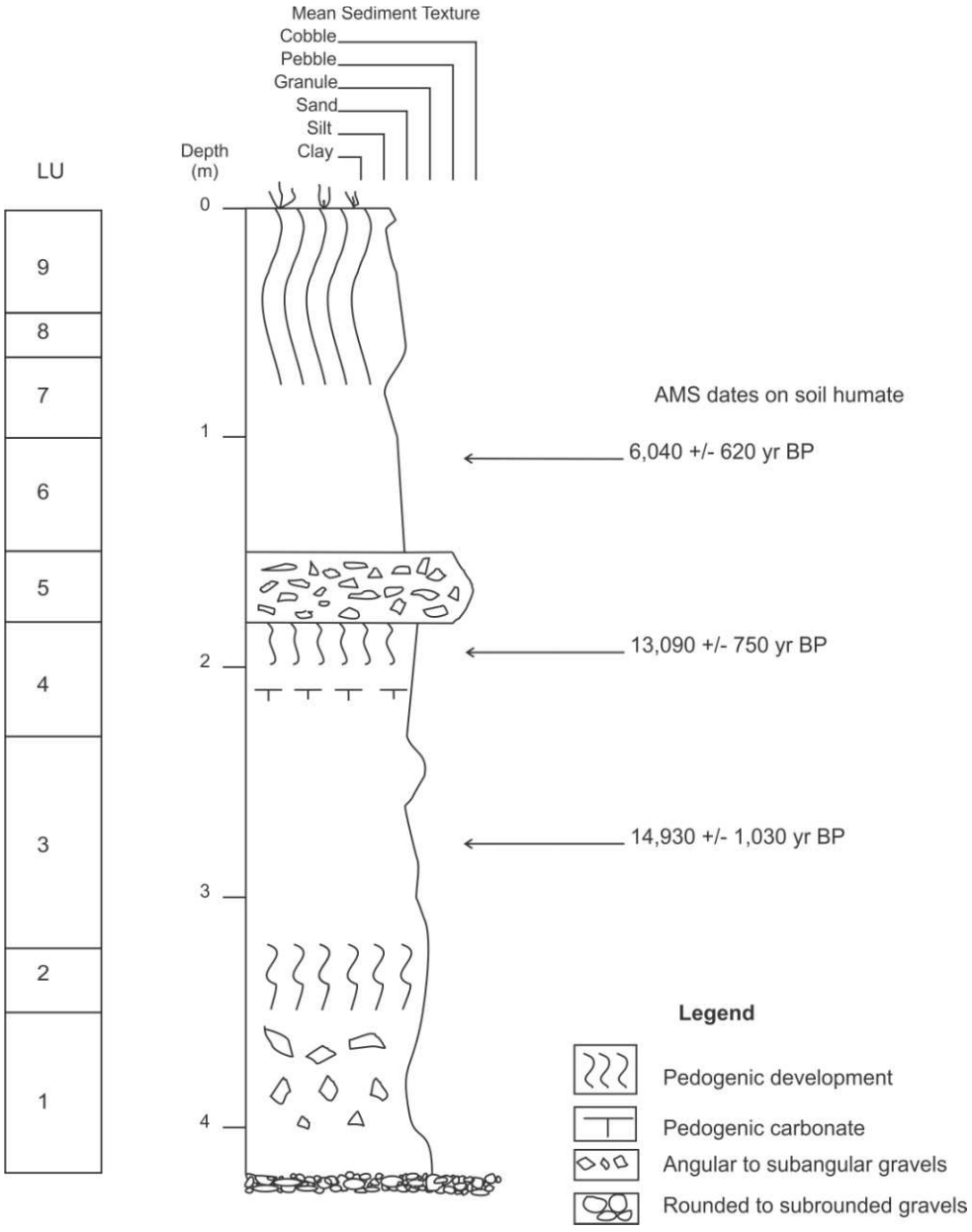

Figure 5.1 SR-23 (Hammer Creek) stratigraphic profile. LU= lithostratigraphic unit (adapted from Davis 2001a).

The Rock Creek Soil at SR-23 is characterized by a weakly-developed calcic horizon in light yellowish brown to yellowish brown sandy loam (Davis 2001a)

The chronology of SR-23 is established from three soil humate AMS dates, which returned the following dates; 6,040±620 yr BP (TO-7816) at 100-110 cm below the surface, 13,090±750 yr BP (TO-7817) at 190-200 cm below the surface and 14,930±1030 yr BP (TO-7818) at 280-290 cm below the surface (Davis 2001a; Davis et al. 2002). Davis (2001) identified an erosional unconformity in the middle of the profile at 190 cm below the surface, which is immediately above the soil humate date of 13,090±750 yr BP (TO-7817).

For sampling purposes the section was cleaned using a shovel and trowel in order to remove modern contamination and expose the stratigraphy. The original position of the section sampled by Davis (2001a) and Somer (2003) could still be observed and sampled directly for the purpose of the present study. Bulk sediment samples were collected with a trowel and placed into a clean plastic bag, which was sealed and labeled with the appropriate provenience information. A column sample provided bulk sediment samples (≥200 g) for every 10 cm interval. Following the collection of each sample the trowel was wiped clean in order to avoid any mixing of sediment samples (Pearsall 2010; Piperno 2006).

Profile SR-27

Section SR-27 (45° 48’ 46” N, 116° 18’ 40” E) is located ca. 5 km downriver from the Hammer Creek Recreation Site at an elevation of 432 masl (Figure 5.2). The section is an east facing exposure located on the west side of the Salmon River that was

exposed as a result of historic hydraulic placer mining in the LSRC. Davis (2001a) provided the initial stratigraphic descriptions of SR-27, which is characterized as a 3.2 m thick deposit of aeolian silt loam, sandy loam and loamy sand.

At the base of SR-27 there are deposits of late Pleistocene-early Holocene-aged loess, which are comprised of non-bedded carbonaceous pale brown silt loams (Davis 2001a). Overlying the LP/EH aged loess are thick deposits of middle and late Holocene-aged loess, which are comprised of non-bedded carbonaceous brown to light yellowish brown sandy loams (Davis 2001a). The loess deposits formed as alluvial floodplain deposits were mobilized and re-deposited upslope by aeolian processes (Davis 2001a).

Davis (2001a) identified one paleosol that formed within the LP/EH aged loess, which is referred to as the Rock Creek Soil. The Rock Creek Soil formation occurred as pedogenic processes altered relatively stable loess deposits within the LSRC between ca. 13,000 and 10,740 yr BP (Davis 2001a:130). The Rock Creek Soil at SR-27 is characterized by a weakly-developed calcic horizon in brown sandy loam with common calcium carbonate accumulations (Davis 2001a).

The relative chronology of SR-27 is established from a single soil humate AMS date recovered from the surface of the Rock Creek Soil at 200-210 cm below the surface, which returned an age of 12,220±310 yr BP (TO-7819) (Davis 2001a). Correlation of identified stratigraphic units at SR-27 with those from other dated stratigraphic sections in the LSRC study area permitted Davis (2001a) to establish this initial chronological framework.

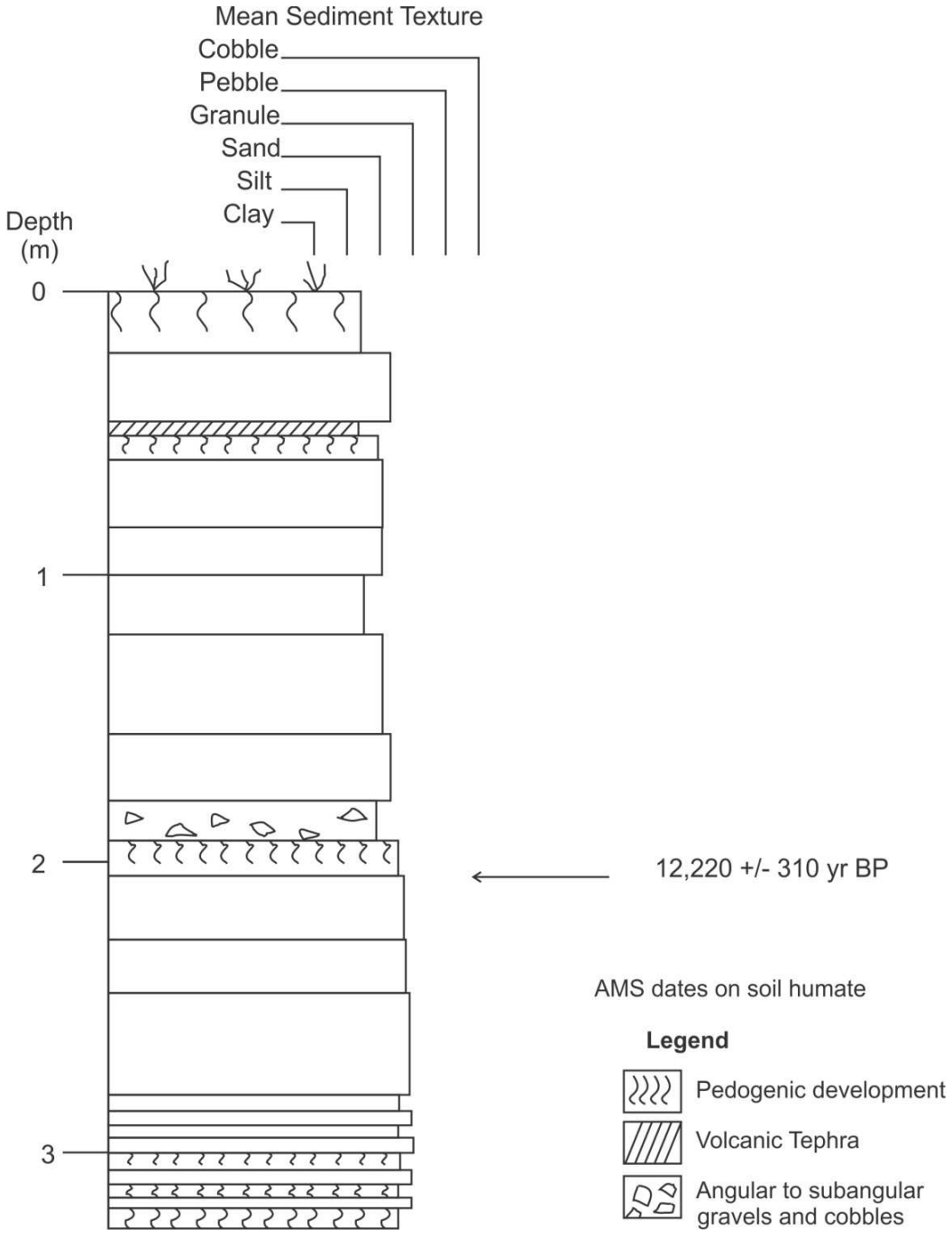

Figure 5.2 SR-27 stratigraphic profile (adapted from Davis 2001a).

The original position of section sample by Davis (2001a) could be identified; however, the section had been disturbed by modern burrowing activity of owls. Due the disturbance, the current project sampled an area directly adjacent to the area sampled by Davis (2001a). For sampling purposes the section was cleaned with shovel and trowel in order to remove modern contamination and expose the stratigraphy. The section was reevaluated and described in the field following guidelines set forth by the Natural Resources Conservation Service (NRCS) (Schoeneberger 2012) and Birkeland (1999) in efforts to expand upon the initial descriptions made by Davis (2001a). This data will be presented in the following chapter. Bulk sediment samples were collected with a trowel and placed into a clean plastic bag, which was sealed and labeled with the appropriate provenience information. A column sample provided bulk sediment samples (≥200 g) for every 10 cm interval. Following the collection of each sample the trowel was wiped clean in order to avoid any mixing of sediment samples (Pearsall 2010; Piperno 2006). Additional sediment samples were collected for the purpose AMS dating of soil humates in order to refine the chronology of SR-27.

Profile SR-34

Section SR-34 (45° 48’ 46” N, 116° 18’ 40” E) is located ca. 75 m north of SR-27 on the same terrace at an elevation of 430 masl (Figure 5.3). The section is an east facing exposure located on the west side of the Salmon River that was exposed as a result of historic hydraulic placer mining in the LSRC. Davis (2001a) provided the initial stratigraphic descriptions of SR-34, which is characterized as a 5.5 m thick deposit of aeolian silt loam, sandy loam and loamy sand that overlies alluvial fan gravels.

At the base of SR-34 there is a deposit of late Pleistocene alluvial fan gravels, which are comprised of poorly sorted clast-supported subangular to angular cobble and pebble gravels of basaltic and mixed lithology (Davis 2001a). Overlying the alluvial fan deposit are thick deposits of late Pleistocene and Holocene-aged loess, which are comprised of non-bedded carbonaceous brown to light yellowish brown silt and sandy loams (Davis 2001a). Loess deposition in the LSRC is believed to be the result of the redistribution of alluvial sediments by aeolian processes, which caused floodplain sediments to be re-deposited upslope on adjacent landforms (Davis 2001a).

Davis (2001a) identified one paleosol that formed within the LP/EH aged loess, which is referred to as the Rock Creek Soil. The Rock Creek Soil formation occurred as pedogenic processes altered relatively stable loess deposits within the LSRC between ca. 13,000 and 10,740 yr BP (Davis 2001:130). The Rock Creek Soil at SR-34 is characterized by a weakly-developed calcic horizon in yellowish brown sandy loam with common calcium carbonate accumulations (Davis 2001a).

The relative chronology of SR-34 is largely incomplete given that no dates have been directly obtained from the profile. Correlation of identified stratigraphic units at SR-34 with those from other dated stratigraphic sections in the LSRC study area permitted Davis (2001a) to establish this initial chronological framework.

The original position of the section sampled by Davis (2001a) could still be observed and sampled directly for the purpose of the present study. For sampling purposes the section was cleaned using a shovel and trowel in order to remove modern contamination and expose the stratigraphy. The section was reevaluated and described in

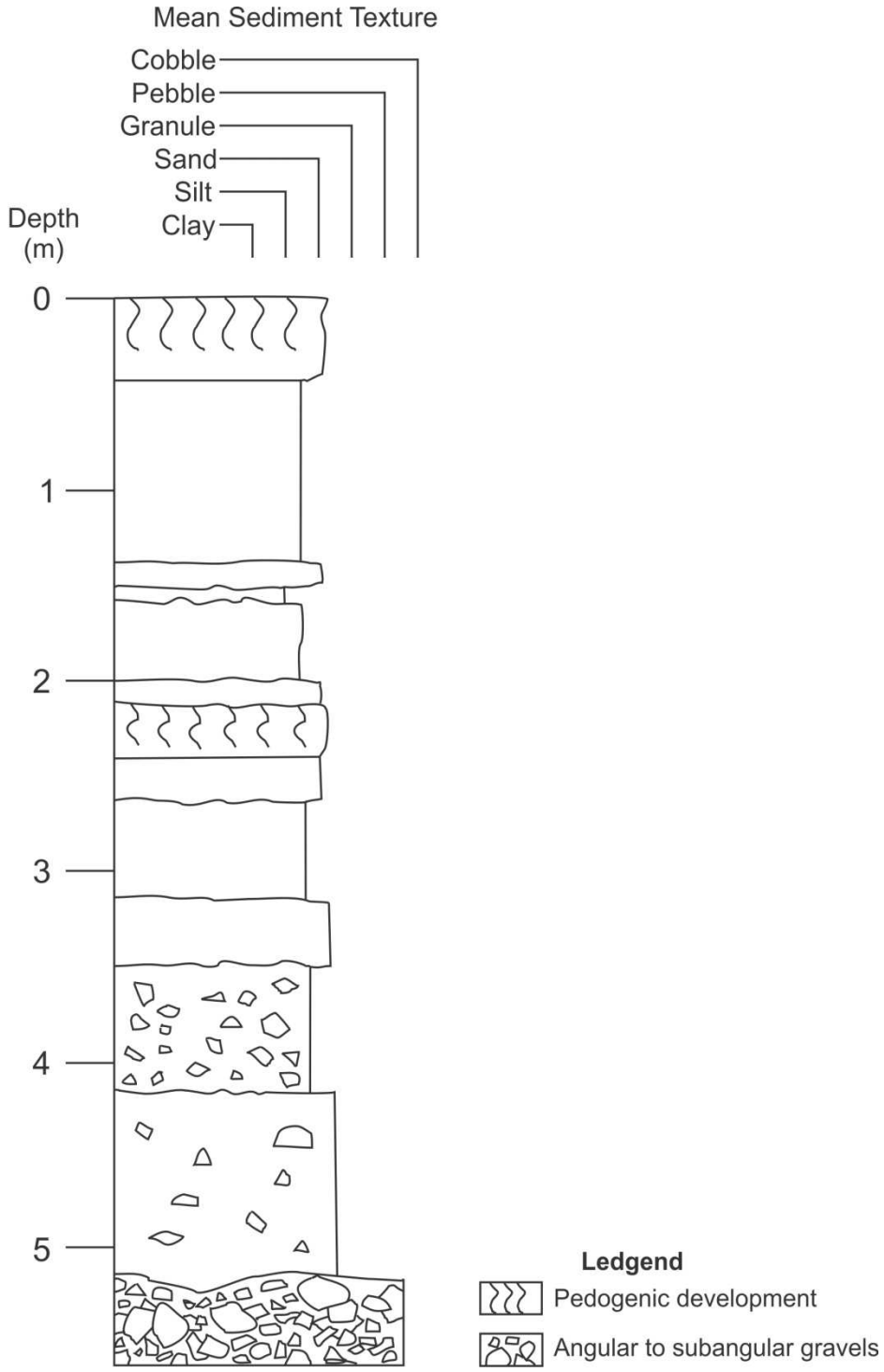

Figure 5.3 SR-34 stratigraphic profile (adapted from Davis 2001a).

the field following guidelines set forth by the Natural Resources Conservation Service (NRCS) (Schoeneberger 2012) and Birkeland (1999) in efforts to expand upon the initial descriptions made by Davis (2001a). This data will be presented in the following chapter. Bulk sediment samples were collected with a trowel and placed into a clean plastic bag, which was sealed and labeled with the appropriate provenience information. A column sample provided bulk sediment samples (≥200 g) for every 10 cm interval. Following the collection of each sample the trowel was wiped clean in order to avoid any mixing of sediment samples (Pearsall 2010; Piperno 2006). Additional sediment samples were collected for the purpose AMS dating of soil humates in order to refine the chronology of SR-34.

Cooper's Ferry Site (10IH73): Unit A Profile

The Cooper's Ferry Site (45° 54' 20" N, 116° 23' 46" E) is located on a small terrace near the confluence of Rock Creek and the Salmon River at an elevation of 413.7 masl, which is ca. 16 km downstream from the Hammer Creek Recreation site (Figure 5.4). The site is contains the earliest record of human occupation in the LSRC spanning a period from 11,410 to after 8,430 yr BP (Davis and Schweger 2004). Davis and Schweger (2004) provided the initial stratigraphic descriptions of the Unit A profile, which was the north wall of a 2x2 m test unit excavated in 1997. The profile observed in Unit A is characterized as a 3.2 m thick deposit of alternating alluvial and aeolian sand, loamy sand, and sandy loams (Davis and Schweger 2004).

Davis and Schweger (2004) identified nine lithostratigraphic units beneath the modern surface fill at the Cooper's Ferry site. The results of their initial stratigraphic descriptions are closely paraphrased here (Davis and Schweger 2004:694).

At the base of 10IH73 there is a deposit of late Pleistocene alluvium designated as lithostratigraphic unit 1 (LU1), which is comprised of a relatively poorly sorted deposit of clast-supported, round to subrounded basalt clasts of fine pebble to medium cobble size. Carbonate coats the surfaces of basalt clasts and cements some clasts together. Overlying LU1 is another deposit of late Pleistocene alluvium designated as LU2, which is comprised of yellowish brown, moderately well-sorted, carbonaceous sand. These late Pleistocene deposits of alluvium reflect different depositional environments associated with the Salmon River. LU1 is interpreted as channel gravels associated with higher-energy alluvial depositional events of the Salmon River, while LU2 is associated with lower-energy alluvial deposition of sand (Davis 2001a).

Overlying the late Pleistocene alluvium (LU1 and LU2) there is a deposit of late Pleistocene-early Holocene loess designated as LU3, which is comprised of brown, well-sorted, fine sandy loam that contains common calcium carbonate filaments. Overlying LU3 is another deposit of late Pleistocene-early Holocene loess designated as LU4, which is comprised of yellowish brown, well-sorted, fine loamy sand that contains common calcium carbonate filaments. These late Pleistocene-early Holocene deposits of loess reflect a shift in the depositional processes from alluvial deposition to aeolian deposition. It is argued that aeolian processes reworked alluvial deposits (e.g., LU1 and LU2), which then blanketed the landforms adjacent to the river with loess (Davis 2001a).

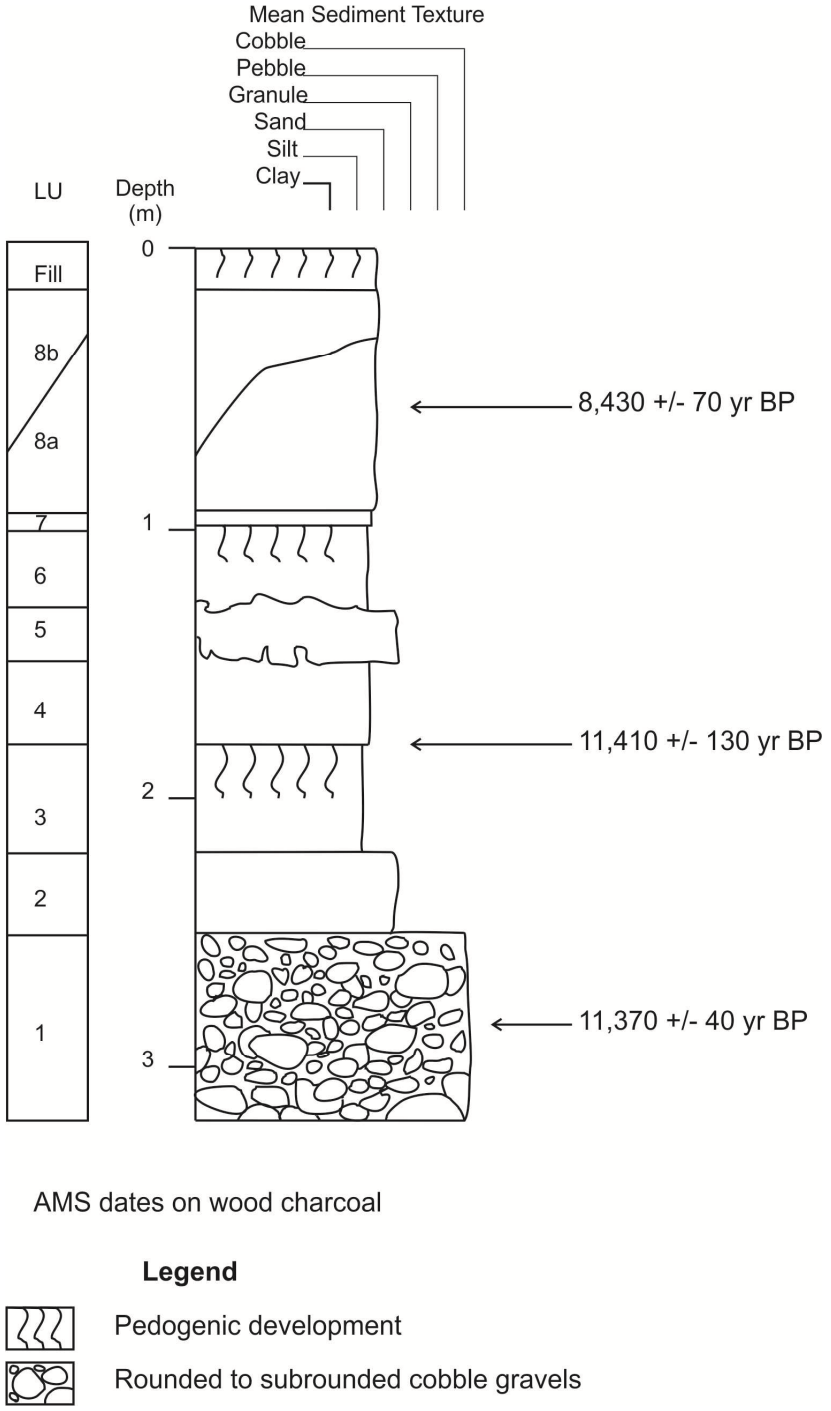

Figure 5.4 10IH73 (Cooper's Ferry) Unit A stratigraphic profile. LU= lithostratigraphic unit (adapted from Davis 2001a).

Overlying the late Pleistocene-early Holocene loess (LU3 and LU4) there is a deposit of late Pleistocene-Holocene alluvium designated as LU5, which is comprised of brown, moderately well-sorted sand that contains abundant mica and biotite flakes. Overlying LU5 is another deposit of late Pleistocene-Holocene alluvium designated as LU6, which is comprised of brown, moderately well-sorted loamy sand. Overlying LU6 is another deposit of late Pleistocene-Holocene alluvium designated as LU7, which is comprised of a thin deposit of dark grayish-brown fine loamy sand that dips slightly to the west. Overlying LU7 is another deposit of late Pleistocene-Holocene alluvium designated as LU8, which has been further subdivided into two units (LU8a and LU8b) on the basis of an observed erosional unconformity. LU8b directly overlies LU7 and is comprised of grayish-brown, well-sorted, medium sand. A sharp, wavy bedding line composed of fine silt with some carbonate accumulation represents the erosional unconformity that separates the overlying LU8a deposit, which is identical to LU8b. These deposits of late Pleistocene-Holocene alluvium reflect a shift from aeolian depositional processes (LU3 and LU4) back to alluvial processes, which deposited LU5-LU8a during different episodes of overbank sedimentation within the low-energy floodplain of the LSRC (Davis 2001a).

Overlying the late Pleistocene-Holocene alluvium of LU8a there is a deposit of fill associated with historic road-building activities that occurred during the 20th century. The fill is composed of a dark brown, moderately sorted, medium to fine loamy sand that contains occasional gravels.

Davis and Schweger (2004) identified two weakly developed paleosols (S1 and S2) at 10IH73 that developed with late Pleistocene-early Holocene loess (LU3) and late Pleistocene-Holocene alluvium (LU6). The first incipient paleosol (S1) developed within the surface of LU3 and characterized as a brown, fine sandy loam with a massive to weakly granular structure and common carbonate filaments. Slight increases in carbonate content and organic matter were observed within the S1 profile. Due to the pedologic characteristics of the paleosol and its associated development within the late-Pleistocene-early Holocene loess S1 is designated as an expression of the Rock Creek Soil (Davis 2001a; Davis and Schweger 2004). The second incipient paleosol (S2) developed within the surface of LU6 and is characterized as a brown, loamy sand with a massive structure and common carbonate filaments. Increases in carbonate content and organic matter were observed within the S2 profile. The S2 paleosol has not been observed elsewhere in the LSRC at this time and as a result there is no regional identifier (e.g., Rock Creek Soil or China Gardens Soil) (Davis 2001a; Davis and Schweger 2004).

The chronology of 10IH73 was established by a series eight radiocarbon dates obtained from wood-charcoal and bone-collagen samples that were collected during the 1997 excavations of Unit A (Davis and Schweger 2004). Of the eight radiocarbon dates sampled only three are considered to accurately reflect the antiquity of the site, while the other five are considered suspect as a result of bone contamination and sample displacement due to faunalturbation (Davis and Schweger 2004). The three radiocarbon dates considered valid provided the following ages. A Wood charcoal sample obtained from the surface of LU3 and associated with the Rock Creek Soil returned an age of

11,410±130 yr BP (TO-7349), while another wood charcoal sample obtained from the contents of Pit fFeature 2 returned an age of 11,370±40 yr BP (Beta-114949) (Davis and Schweger 2004). The remaining wood charcoal sample was obtained from the upper portion of LU8a and returned an age of 8,430±70 yr BP (Beta-114952) (Davis and Schweger 2004). Based upon these radiocarbon ages Davis and Schweger (2004:702) established a site chronology that spans a period from ca. 11,410 yr BP to ca. 8,430 yr BP.

For sampling purposes the profile of Unit A was cleaned with a trowel in order to remove any modern contamination associated with ongoing excavations as well as expose the stratigraphy. Due to the previous stratigraphic descriptions of Unit A provided by Davis and Schweger (2004) sampling for the present study was limited to phytoliths only. A sediment sample was collected from each lithostratigraphic unit, except for the thin LU7 deposit, with a trowel and placed into a clean plastic bag, which was sealed and labeled with the appropriate provenience information. Care was taken to sample areas of intact deposits that have not been disturbed by faunalturbation, which may cause mixing of different depositional units and associated phytolith assemblages. Following the collection of each sample the trowel was wiped clean in order to avoid any mixing of sediment samples (Pearsall 2000; Piperno 2006).

Sediment Processing and Phytolith Extraction Procedure

While there is no single and standardized method of phytolith extraction from sediment and soil samples there are basic laboratory procedures that permit the separation of phytoliths from these types of samples. A review of the literature provides researchers

with a variety of extraction methods (see Perry and Smithson 1958; Twiss et al. 1969; Rovner 1971; Carbone 1977; Zhao and Pearsall 1998; Lentfer and Boyd 1998, 1999, 2000; Pearsall 2000; Coil et al. 2003; Piperno 2006). Despite the variations in each method the basics of the extraction procedure are the same, which includes removal of clays, carbonate, and organic matter prior to the heavy liquid separation for the phytoliths.

The present study followed a modified version of the extraction procedure developed by Piperno (2006:89-93) to process the sediment samples collected from sections SR-23, SR-27, SR-34 and 10IH73 (Cooper's Ferry Site) in Dr. Noller's pedology laboratory. The modifications include the removal of carbonate and organic matter prior to the separation of clays and coarse sand. The procedure is summarized below.

Step 1) Bulk sediment samples were air dried overnight and sieved through a 2.0 mm geologic sieve to remove any coarse materials such as gravels and roots. 20 grams of the sieved sediment sample was weighed out for further processing and placed into a clean 150 ml plastic container. Disaggregation of mineral and organic particles was achieved by mixing the sample in a dispersion agent comprised of a 5% solution of Calgon or sodium hexametaphosphate $(NaPO_3)_6$. The sample was then placed in an automatic shaker for 24 hours, then removed and allowed to settle overnight for 12 hours. Once the sample had settled out of suspension the supernatant was carefully decanted. The sample was transferred into clean 50 ml centrifuge tube. The sample and tube were weighed to the nearest one hundredth of a gram and distilled water was added to the 50

ml mark. Paired samples of equal weight were placed opposite of one another in a centrifuge and run for three minutes at 3,000 rpm to wash the sample. The supernatant was carefully poured off and the distilled water wash was repeated. Following the final wash the sample was transferred into a 300 ml glass beaker.

Step 2) Under a fume hood, 20 ml of a 10% solution of hydrochloric acid (HCl) was carefully poured into the glass beaker containing the sediment sample and mixed thoroughly with a glass stirring rod. A reaction was observed if carbonates were present in the sample. The sample was left in the fume hood until the reaction had ceased after (ca. two hours). The sample was then transferred back into the appropriate 50 ml centrifuge tube and centrifuged for three minutes at 3,000 rpm after which the supernatant was carefully poured off. The sample was transferred back into the 300 ml glass beaker and step two was repeated until no reaction was observed following the addition of fresh HCl to the sample. The sample was transferred back into the appropriate 50 ml centrifuge tube and washed with distilled water for three minutes at 3,000 rpm after which the supernatant was carefully poured off. The distilled water wash was repeated once more. Following the final wash the sample was transferred back into a 300 ml glass beaker.

Step 3) Under a fume hood, 10 ml of a 30% solution of hydrogen peroxide was carefully poured into the glass beaker containing the sediment sample and mixed thoroughly with a glass stirring rod. A reaction was observed if organic materials were present within the sample. The sample was left in the fume hood until the reaction ceased (ca. one hour) and the supernatant turned a yellowish color. The sample was then

transferred into the appropriate 50 ml centrifuge tube and centrifuged for three minutes at 3,000 rpm after which the supernatant was carefully poured off. The sample was transferred back into the 300 ml glass beaker and step three was repeated once to ensure that all organic materials are removed. The sample was transferred back into the appropriate 50 ml centrifuge tube and washed with distilled water for three minutes at 3,000 rpm after which the supernatant was carefully poured off. The distilled water wash was repeated once more.

Step 4) The sample was wet-sieved through a 250-micron wire mesh sieve with distilled water in order to separate the medium and coarse sand fraction of the sediment sample from the smaller fine sand, silt and clay fraction. The fine sand-to-clay fraction of the sample was transferred into a 1,000 ml graduated cylinder and filled with distilled water to a height of 30 cm. The sample was vigorously stirred and allowed to stand for three hours, which allowed the fine sand to silt fraction to settle out of solution. After three hours the supernatant containing the clay sized fraction of the sample was carefully poured off. This process was repeated several times (three-five times) until the supernatant was relatively clear after the limiting time of three hours had been met. Once all or most of the clay sized particles were removed the sample was split into four 5 g samples and transferred into new 50 ml centrifuge tubes and washed once more with distilled water for three minutes at 3,000 rpm after which the supernatant was carefully poured off.

Up to this point the samples have undergone the removal of any coarse particle sizes (>250-microns) as well as any small clay sized particles (<5-microns) in order to

concentrate phytoliths, which are typically 5-200microns. All carbonates and organic materials have been oxidized and removed from the samples as well, which may cause binding of particles including phytoliths.

Step 5) Phytoliths were separated from the sediment sample through a process of heavy liquid floatation. Phytoliths have a specific gravity that ranges from 1.5 to 2.3 g/cm^3, while quartz has a specific gravity of 2.65 g/cm^3 (Piperno 2006). In order to isolate and separate the phytoliths from the remaining sediment, a solution of sodium polytungstate (SPT) was mixed to a specific gravity of 2.35 g/cm^3 and added to the 50 ml centrifuge tubes. The samples and tubes were weighed to the nearest one hundredth of a gram as the SPT solution was filled to the 40 ml mark. The sample and SPT solution was thoroughly mixed with a tube shaker and samples of equal weights were placed opposite of one another in the centrifuge and ran for 10 minutes at 3,000 rpm. This allowed heavier particles to settle out of solution while the lighter phytoliths floated at the very top of the tube. The floating phytolith fraction was removed carefully with a pasture pipette and transferred into a clean 15 ml centrifuge tube. The samples were thoroughly mixed again and sampled one additional time in efforts to ensure adequate phytolith recovery.

Following the final recovery of phytoliths from the samples the centrifuge tubes were filled with distilled water to the 50 ml line, mixed thoroughly and centrifuged for three minutes at 5,000 rpm after which the supernatant was carefully poured off and collected for recycling of the SPT. The used SPT solution was vacuum filtered through a 2-micron filter paper membrane and dehydrated in an oven (Pearsall 2000; Piperno

2006). Following filtration the dehydrated SPT can be mixed to the appropriate specific gravity and reused. This is significant because SPT is relatively non-toxic compared to other heavy liquids used in phytolith separation (e.g., cadmium iodide and potassium iodide mixture). However, SPT is very expensive compared to other heavy liquids and must be recycled in order to be cost effective.

Step 6) Distilled water was added to the 15 ml centrifuge tubes containing the recovered phytolith solution to a height of 15 ml, which effectively lowered the specific gravity of the solution to below 1.5 g/cm^3. The samples were then centrifuged for five minutes at 3,000 rpm, which caused the phytoliths to settle to the bottom of the tube. After five minutes the supernatant was carefully poured off. Step six was repeated twice more to ensure that all of the heavy liquid had been removed. Following the final distilled water wash the phytoliths were transferred onto a watch glass with acetone and allowed to dry under a fume hood. When dried the sample looked like a whitish powder on the watch glass, which was collected to prepare slide mounts.

Step 7) The final step in the phytolith extraction procedures was to mount a portion of the sample onto a microscope slide. This was accomplished by placing a small amount of the mounting medium benzyl benzoate onto a clean microscope slide. Using a metal scoop, a small portion of the phytolith sample was mixed into the mounting medium and spread out across the slide surface. A slide cover was placed over the sample and the slide was labeled with the appropriate provenience information. The slide samples were stored in horizontal slide folders.

Morphological Counting Procedure

Following the review of previously published phytolith studies relevant to the Pacific Northwest (Blinnikov 2005; Blinnikov et al. 2001, 2002; Norgren 1973; Witty and Knox 1964) and the Lower Salmon River Canyon, Idaho (Davis and Collins 2009; Eccleston 1999; Somer 2003) the present study will follow the morphological classification system developed by Blinnikov (2005). Blinnikov's phytolith classification system is based on "… a modern analog dataset required for any paleoenvironmental reconstruction of the late Pleistocene and Holocene vegetation of the region…" (2005:72).

Blinnikov's (2005) study of phytolith production and classification in both modern plants and soils builds upon the earlier works from the region (Norgren 1973; Witty and Knox 1964). In fact Blinnikov (2005) observed many of the morphotypes recognized by Norgren (1973), which allowed Blinnikov (2005) to reconcile Norgren's (1973) antiquated descriptive terminology with the current descriptive terminology. This is extremely useful given that Norgren's (1973) comparative collection is available at Oregon State University, which allowed direct observation and comparison of morphotypes used within Blinnikov's (2005) regional classification system.

Blinnikov (2005) uses a modified version of the Twiss et al. (1969) and Fredlund and Tieszen (1994) grass phytolith classification systems to describe the grass morphotypes, which accounts for both long and short cell grass phytolith forms. The inclusion of long and short cell grass phytolith forms permits genus level identification of different Pooideae grass communities (e.g., *Poa, Festuca,* and *Agropyron*) (Blinnikov

2005). Blinnikov's (2005) non-grass phytolith classification system largely follows Piperno (1988) and Bozarth (1993) in regards to the morphological description of phytolith forms. The counting methodology used for the present study can be found in Appendix A.

The slide samples were examined under a T490B Amscope optical microscope at high magnification (400X). Systematic scanning of the slides at high magnification permitted identification of all phytolith forms present within the sample. The three-dimensional shapes of the phytoliths were observed by applying slight pressure on the slide cover with a probe, which causes phytoliths to rotate within the benzyl benzoate, which aided the identification of phytolith forms (Pearsall 2010).

Each slide was systematically scanned by running transects across the sample until 200-300 phytolith forms were counted. The frequency of each form encountered was recorded on the count sheet. A minimum count of 200 is considered standard procedure in both pollen and phytolith analysis as it has been demonstrated to provide a representative assemblage of the sample (Pearsall 2010; Piperno 2006).

The phytolith frequency data for each stratigraphic section (SR-23, SR-27, SR-34, and 10IH73) will be presented as phytolith diagrams created in TILIA-GRAPH (Grimm 1993). TILIA-GRAPH was created as a means of generating pollen diagrams however it has been increasingly utilized in phytolith research to present data as well. TILIA-GRAPH also permits analysis and zonation of the phytolith data through the use of its cluster analysis (CONISS) function (Grimm 1993).

Chapter 6. Results: A Late Pleistocene and Holocene Phytolith Record of Vegetative History from the Lower Salmon River Canyon, Idaho

The results of the phytolith analysis of sediment samples obtained from stratigraphic profiles SR-23, SR-27, SR-34, and 10IH73 provides a record of vegetative change that extends from ca. 22,000 yr BP to present. The final results of each profile are presented in the form of phytolith diagrams created in the software program TILIA-GRAPH (Grimm 1993).

Phytolith zones were established for each diagram using the stratigraphically constrained incremental sum of squares cluster analysis (CONISS) program (Grimm 1993). The CONISS program is an agglomerative and hierarchical approach that "carries out stratigarphicaly constrained cluster analysis by the method of incremental sum of squares" which permits the phytolith frequency data from each sample to be clustered based on the minimum total within-cluster dispersion (Grimm 1987:14). The phytolith frequency data exhibits variability between individually adjacent samples from a particular stratigraphic section, which does not allow the clusters to exhibit minimum total dispersion. Therefore, the hierarchical nature of the clusters permit local determination of the of individual zone boundaries within the stratigraphic section (Grimm 1987).

The clustering algorithm uses a dissimilarity matrix of squared Euclidian distances to cluster the adjacent samples; however, the phytolith frequency data is transformed to produce dissimilarity coefficients other than the simple Euclidian distance (Grimm 1987). The transformation used in this study was a square-root transformation of the phytolith frequency data to produce the chord distance of Edwards and Cavalli-Sforza

(1964), which up-wieghts the rare phytolith forms relative to the abundant forms (Grimm 1987). The end result of the clusting creates a dendrogram that illustrates the hierarchical relationships of the stratigraphically adjacent phytolith assemblages. Individual zones can subsequently be defined by cutting a straight line across the dendrogram at a given height based on the total sum of squares. This approach will commonly produce individual zones similar to those that may have been identified by visual inspection of the structure of the frequency data, which has also been a common approach used by both pollen and phytolith analysists (Pearsall 2010; Piperno 2006).

Blinnikov's (2005) morphological classification system identified a number of characteristic and diagnostic phytolith forms that permit vegetative reconstruction of fossil phytolith assemblages (see chapter 4). Blinnikov et al. (2001:38-40, 2002) interpreted the fossil phytolith forms recognized by the classification system in the following manner: characteristic phytolith forms included short wavy crenates (with 3-4 undulations) of *Poa* or *Koeleria*, long wavy crenates (> 5 undulations) of *Calamagrostis* and *Stipa*, elongated rondels and deeply indented long cells of *Agropyron spicatum*, horned rondels of *Festuca* and *Stipa*, pyramidal rondels of *Agropyron* or *Stipa*, indented long cells of *Festuca*, blocky forms of *Artemisia, Abies*, and *Picea*, unevenly thickened cell walls and thin elongate grainy forms of *Larix*, flat epidermal forms with sinuous margins on all four sides of *Picea*, and silicified tracheids of Pinaceae. Diagnostic phytolith forms included *Stipa*-type bilobates and bilobates of *Stipa*, spiny irregular shaped forms of *Pinus ponderosa*, large asterosclereids of *Pseudotsuga menziesii*, and conical forms of *Carex*.

The taxonomic affiliation of epidermal polygonal forms are more ambiguous and could have come from *Artemisia*; however, they have also been observed in other eudicots and some members of Pinaceae (Blinnikov 2005). Similarly epidermal anticlinal forms are argued to represent Asteraceae herbs and they have also been observed in other eudicots (Bozarth 1992; Blinnikov 2005).

Additional phytolith forms including rectangular plates, smooth rectangular long cells, angular long cells, keeled rondels, dendritic and scutiform types, tricomes, and hairs are not considered to be diagnostic of any particular species and are argued to be characteristic to the family level (e.g., rectangular plates, long cells, keeled rondels, and tricomes of the Poaceae family) (Blinnikov et al. 2001, 2002).

While Blinnikov (2005:77) identifies four different types of rondel phytolith forms (e.g., elongate or oval, horned, pyramidal, and keeled types) he states that the "classification system should be approached with caution" due to the observance of transitional forms. As such the total sum of all rondel phytoliths are reported to minimize risks associated with misidentification of rondel variants; the sum of all rondels are interpreted as a measure of *Festuca* spp. Similarly the total sum of all long cell forms (e.g., rectangular, indented, deeply indented, and angular types) are interpreted as a measure of *Agropyron spicatum* or a combination of *A. spicatum* and *Festuca idahoensis* (Blinnikov 2005; Blinnikov et al. 2001, 2002).

SR-23 (Hammer Creek) Phytolith Profile

A total of forty-two sediment samples were processed from the SR-23 stratigraphic profile. Thirty-eight of theses samples produced sufficient quantities of well

preserved phytoliths that permitted counting, classification, and identification of five phytolith zones. Four samples did not contain sufficient quantities of phytoliths to permit counting and classification. These samples were observed from 120-160 cm below the surface and separate phytolith zones III and IV.

Five phytolith zones (Figure 6.1) were established using the CONISS function in TILIA-GRAPH (Grimm 1993), which clustered stratigraphically adjacent smaples based on the changes in the frequencies of twenty distinct morphotypes. The five zones will now be discussed in ascending order.

Phytolith Zone I (420-320 cm)

Results: Phytolith zone I contains 10 samples with an estimated age of >14,930±1,030 yr BP (Davis et al. 2002). Poaceae phytolith forms comprised 48-73% of the total assemblages and non-Poaceae phytoliths comprised 27-52%. The Poaceae phytoliths are all derived from the Pooideae subfamily of C_3 grasses. The most common characteristic Pooideae forms were rondels (7-23%) of *Agropyron* and *Festuca*, short wavy crenates (8-16%) of *Poa* and *Koeleria*, long wavy crenates (1-3%) of *Calamagrostis* and *Stipa*, and long cells (5-14%) of *Agropyron* and *Festuca*. Diagnostic *Stipa*-type bilobates were limited to (<1-4%) within the lower portion of the zone.

The most common characteristic non-Poaceae phytoliths consisted of blocky forms (13-26%) of *Artemisia*, *Abies*, and *Picea*, epidermal polygonal (8-17%) of *Artemisia*, *Abies*, and Asteraceae, epidermal anticlinal (1-7%) of Asteraceae, and other conifer forms (<1-3%) of *Pinus*, *Abies*, *Picea*, or *Larix*. Diagnostic non-Poaceae forms were limited to *P. ponderosa* type representing (<1-3%) within the zone.

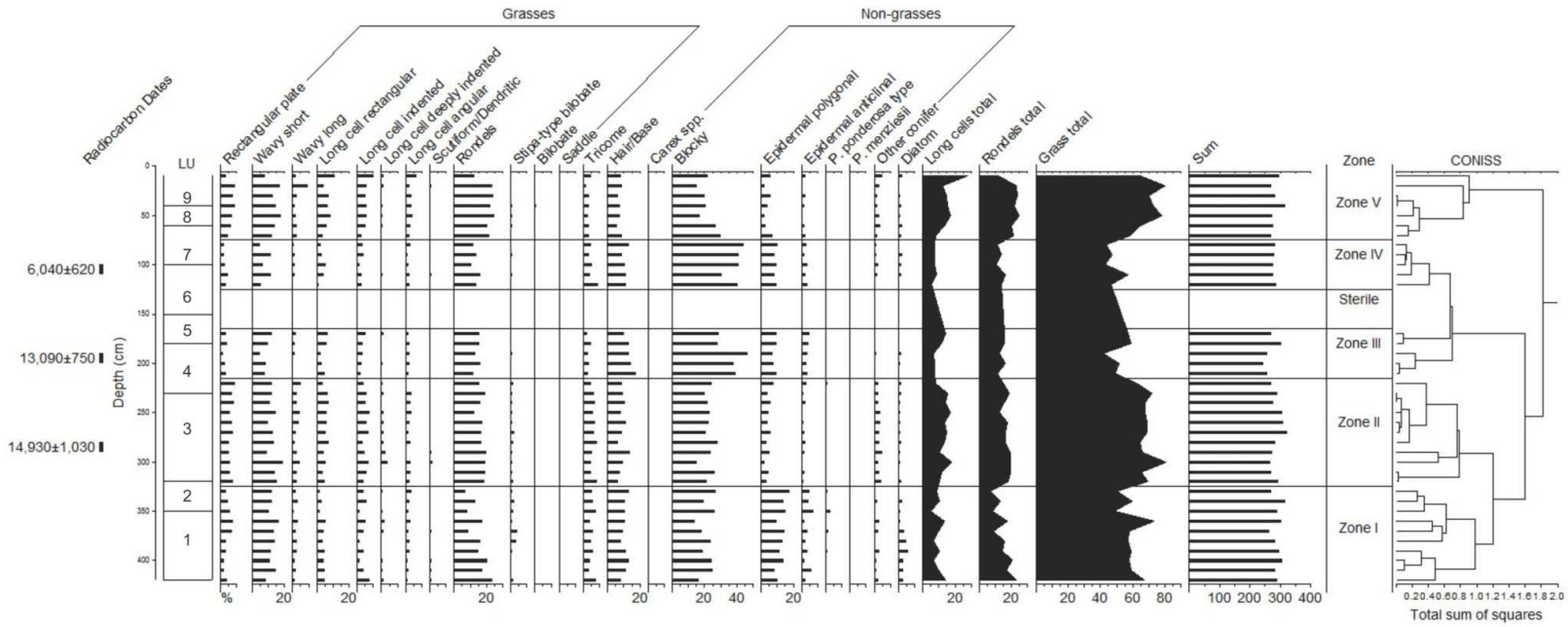

Figure 6.1 SR-23 phytolith profile. LU= lithostratigraphic unit.

Interpretation: Zone I (>14,930±1,030 yr BP) comprised the basal portion of SR-23 and its assemblages contained fluctuating proportions of both grass (48-73%) and non-grass (27-52%) phytolith forms. The assemblages of grass phytoliths suggest that a mix of C_3 Pooideae grasses existed at the site. This grass cover was predominately composed of *Agropyron, Festuca,* and *Poa* indicated by the frequencies of rondels, short wavy crenates, and long cell forms. A secondary and minor component of the grass cover consisted of *Stipa* indicated by long wavy crenates and *Stipa*-type forms. The assemblages of non-grass forms suggest that a mix of arboreal and shrub species existed at the site. The arboreal and shrub cover was composed of members of the Asteraceae and Pinaceae Families indicated by the frequencies of blocky, epidermal, and both characteristic and diagnostic conifer forms. The identification of species composition of the arboreal and shrub communities is limited due to the observed redundancy in blocky and epidermal polygonal phytolith forms from the two families represented. However, the higher proportion of blocky (13-26%) and epidermal polygonal (8-17%) forms relative to other conifer forms (<1-3%) and diagnostic *P. ponderosa* types (<1-3%) would suggest that *Artemisia* and other Asteraceae species were the predominate contributors of the blocky and epidermal polygonal forms.

Zone I also contains portions of a truncated paleosol, between 320 and 350 cm, believed to be an expression of the China Gardens Soil, whiched formed within the LSRC between ca. >15,000 and <25,000 yr BP (Davis 2001a). The period of relative landscape stability and soil formation associated with this cambic horizon observed at SR-23 could have provided an opportunity for the phtyolith assemblages associated with different vegetative conditions to become mixed together if conditions changed

significantly during the period of stability. Fredlund and Tieszen (1994:331) refer to this process of mixing as “inheritance”, which acknowledges the potential of long-term (hundreds of years or more) mix of phytolith assemblages with soils. Therefore, assemblages associated with the paleosol should be interpreted as representation of the long-term average of vegetative conditions at the site. With regards to Zone I at SR-23, the samples recovered from the China Gardens Soil horizon likely reflect the mixture of grass and shrub stepp communities during this period.

Collectively, the assemblages from Zone I suggest the existence of a shrub steppe community. The inferred vegetation consisted of *Artemisia* and other Asteraceae shrubs and/or herbs with associations of Pooideae grasses. Fluctuations within the rondel and long cell assemblages suggest that *Agropyron* and *Festuca* were unstable, which may represent fluctuations in local moisture availability with a higher frequency of *Festuca* during relatively wetter periods and *Agropyron* during drier periods. The low frequencies of other conifer forms and diagnostic *P. ponderosa* types suggest that these species did not comprise a substantial portion of the non-grass cover that would be more suggestive of a closed canopy arboreal forest.

Phytolith Zone II (320-210cm)

Results: Phytolith zone II contains eleven samples with an estimated age range between 13,090±750 to >14,930±1,030 yr BP (Davis et al. 2002). Poaceae phytolith forms comprised 63-81% of the total assemblages and non-Poaceae phytolith forms comprised 19-37%. The Poaceae phytoliths are predominately derived from the Pooideae subfamily of C_3 grasses with an extremely limited presence of the Chloridoideae subfamily of C_4 grasses. The most common characteristic Pooideae forms were rondels

(12-19%) of *Agropyron* and *Festuca*, short wavy crenates (8-18%) of *Poa* and *Koeleria*, long wavy crenates (1-5%) of *Calamagrostis* and *Stipa*, and long cells (8-18%) of *Agropyron* and *Festuca*. Saddle shaped phytoliths of the Chloridoideae subfamily were limited to (<1%) within the zone. Diagnostic *Stipa*-type bilobates were limited to (<1-2%) within the zone. The most common characteristic non-Poaceae phytoliths consisted of blocky forms (15-28%) of *Artemisia*, *Abies*, and *Picea*, epidermal polygonal (1-7%) of *Artemisia*, *Abies*, and Asteraceae, epidermal anticlinal (<1-3%) of Asteraceae, and other conifer forms (2-4%) of *Pinus*, *Abies*, *Picea*, or *Larix*. Diagnostic non-Poaceae forms were limited to *P. ponderosa* type representing (<1%) within the zone.

Interpretation: Zone II (13,090±750 to >14,930±1,030 yr BP) contained fluctuating proportions of both grass (63-81%) and non-grass (19-37%) phytolith forms. However, the zone contains a relatively higher proportion of grass forms compared to Zone I. The assemblages of grass phytoliths suggest that a mix of C_3 Pooideae grasses existed at the site. This grass cover was predominately composed of *Agropyron*, *Festuca*, and *Poa* indicated by the frequencies of rondels, short wavy crenates, and long cell forms. A secondary and minor component of the grass cover consisted of *Stipa* indicated by long wavy crenates and *Stipa*-type forms. Additionally it is noted that a single saddle shaped phytolith form of the Chloridoideae subfamily was observed. The assemblages of non-grass forms suggest that a mix of arboreal and shrub species existed at the site. The arboreal and shrub cover was composed of members of the Asteraceae and Pinaceae Families indicated by the frequencies of blocky, epidermal, and both characteristic and diagnostic conifer forms. The identification of species composition of the arboreal and shrub communities is limited due to the observed redundancy in blocky and epidermal

polygonal phytolith forms from the two families represented. However, the higher proportion of blocky (15-28%) and epidermal polygonal (1-7%) forms relative to other conifer forms (2-4%) and diagnostic *P. ponderosa* types (<1%) would suggest that *Artemisia* and other Asteraceae species were the predominate contributors of the blocky and epidermal polygonal forms.

Collectively, the assemblages from Zone II suggest the existence of a transitional environment shifting from a shrub steppe community to a grass steppe community indicated by the overall increase in grass phytoliths relative to Zone I. The inferred vegetation consisted of Pooideae grasses with associations of *Artemisia* and Asteraceae shrubs and/or herbs. Both rondel and long cell assemblages are relatively stable compared to those of Zone I suggesting that fluctuations in local moisture availability were not as pronounced, which permitted relative stability of *Agropyron* and *Festuca*. Lower proportions of both epidermal polygonal and anticlinal forms relative to Zone I suggest that *Artemisia* and/or Asteraceae species declined during this period. Higher frequency of other conifer forms relative to Zone I suggest that Pinaceae species increased slightly during this period, however, the assemblages do not suggest a closed canopy arboreal forest.

Phytolith Zone III (210-160cm)

Results: Phytolith zone III contains five samples with an estimated age range between >6,040±620 to 13,090±750 yr BP (Davis et al. 2002). Poaceae phytolith forms comprised 42-59% of the total assemblages and non-Poaceae phytolith forms comprised 41-58%. The Poaceae phytoliths are all derived from the Pooideae subfamily of C_3 grasses. The most common characteristic Pooideae forms were rondels (11-16%) of

Agropyron and *Festuca*, short wavy crenates (4-12%) of *Poa* and *Koeleria*, long wavy crenates (1-2%) of *Calamagrostis* and *Stipa*, and long cells (7-14%) of *Agropyron* and *Festuca*. Diagnostic *Stipa*-type bilobates were limited to (<1%) within the zone. The most common characteristic non-Poaceae phytoliths consisted of blocky forms (28-46%) of *Artemisia*, *Abies*, and *Picea*, epidermal polygonal (7-9%) of *Artemisia*, *Abies*, and Asteraceae, epidermal anticlinal (3-4%) of Asteraceae, and other conifer forms (<1-1%) of *Pinus*, *Abies*, *Picea*, or *Larix*. Diagnostic non-Poaceae forms were limited to *Carex* type representing (<1%) within the zone.

Interpretation: Zone III (>6,040±620 to 13,090±750 yr BP) contained fluctuating proportions of both grass (42-59%) and non-grass (41-58%) phytolith forms. However, the zone contains a relatively higher proportion of non-grass forms compared to Zone II. The assemblages grass phytoliths suggest that a mix of C_3 Pooideae grasses existed at the site. The grass cover was predominately composed of *Agropyron*, *Festuca*, and *Poa* indicated by the frequencies of rondels, short wavy crenates, and long cell forms. A secondary and very minor component of the grass cover consisted of *Stipa* indicated by long wavy crenates and *Stipa*-type forms. The assemblages of non-grass forms suggest that a mix of arboreal and shrub species existed at the site. The arboreal and shrub cover was composed of members of the Asteraceae and Pinaceae Families indicated by the frequencies of blocky, epidermal, and characteristic conifer forms. The identification of species composition of the arboreal and shrub communities is limited due to the observed redundancy in blocky and epidermal polygonal phytolith forms from the two families represented. However, the higher proportion of blocky (28-46%) and epidermal polygonal (7-9%) forms relative to other conifer forms (<1-1%) would suggest that

Artemisia and other Asteraceae species were the predominate contributors of the blocky and epidermal polygonal forms.

Zone III also contains portions of a truncated paleosol, between 180 and 230 cm, believed to be an expression of the Rock Creek Soil, whiched formed within the LSRC between ca. 10,740 and 13,000 yr BP (Davis 2001a). The period of relative landscape stability and soil formation associated with this calcic horizon observed at SR-23 could have provided an opportunity for the phtyolith assemblages associated with different vegetative conditions to become mixed together if conditions changed significantly during the period of stability. Fredlund and Tieszen (1994:331) refer to this process of mixing as “inheritance”, which acknowledges the potential of long-term (hundreds of years or more) mix of phytolith assemblages with soils. Therefore, assemblages associated with the paleosol should be interpreted as representation of the long-term average of vegetative conditions at the site. With regards to Zone III at SR-23, the samples recovered from the China Gardens Soil horizon likely reflect the mixture of grass and shrub stepp communities during this period.

Collectively, the assemblages from Zone III suggest a return to conditions that supported a shrub steppe community indicated by the decline in grass phytoliths relative to Zone II. The inferred vegetation consisted of *Artemisia* and other Asteraceae shrubs and/or herbs with associations of Pooideae grasses. Fluctuations within the rondel and long cell assemblages suggest that *Agropyron* and *Festuca* were unstable, which may represent fluctuations in local moisture availability. Specifically, a decline in long cell forms within the lower portion of the zone suggests that slightly wetter conditions favored *Festuca* over *Agropyron.* A single *Carex* type was also observed within the lower

portion of the zone, which also suggests wetter conditions. Long cell forms increase within the upper portion of the zone, which suggests that conditions became slightly drier allowing for an increase in *Agropyron* grasses at the site. The increase in long cell forms occurs at the same time that blocky forms decrease, suggesting that shrub communities became reduced as grass communities expanded. The very low frequency of other conifer forms and lack of diagnostic *P. ponderosa* types suggests a reduction in Pinaceae communities near the site.

Phytolith Zone IV (120-70cm)

Results: Phytolith zone IV contains five samples with an estimated age range between ca. 6,040±620 yr BP to >2,000 (Davis 2001). Poaceae phytolith forms comprised 43-57% of the total assemblages and non-Poaceae phytolith forms comprised 43-57%. The Poaceae phytoliths are all derived from the Pooideae subfamily of C_3 grasses. The most common characteristic Pooideae forms were rondels (11-16%) of *Agropyron* and *Festuca*, short wavy crenates (5-11%) of *Poa* and *Koeleria*, long wavy crenates (1%) of *Calamagrostis* and *Stipa*, and long cells (5-8%) of *Agropyron* and *Festuca*. Diagnostic *Stipa*-type bilobates were limited to (<1%) within the zone. The most common characteristic non-Poaceae phytoliths consisted of blocky forms (30-44%) of *Artemisia*, *Abies*, and *Picea*, epidermal polygonal (8-10%) of *Artemisia*, *Abies*, and Asteraceae, epidermal anticlinal (1-4%) of Asteraceae, and other conifer forms (<1-2%) of *Pinus*, *Abies*, *Picea*, or *Larix*. No diagnostic non-Poaceae forms were observed within the zone.

Interpretation: Zone IV (ca. 6,040±620 to >2,000 yr BP) contained fluctuating proportions of both grass (43-57%) and non-grass (43-57%) phytolith forms. The

assemblages from the zone are similar to those of Zone III. The assemblages of grass phytoliths suggest that a mix of C_3 Pooideae grasses existed at the site. This grass cover was predominately composed of *Agropyron, Festuca,* and *Poa* indicated by the frequencies of rondels, short wavy crenates, and long cell forms. A secondary and very minor component of the grass cover consisted of *Stipa* indicated by long wavy crenates and *Stipa*-type forms. The assemblages of non-grass forms suggest that a mix of arboreal and shrub species existed at the site. The arboreal and shrub cover was composed of members of the Asteraceae and Pinaceae Families indicated by the frequencies of blocky, epidermal, and characteristic conifer forms. The identification of species composition of the arboreal and shrub communities is limited due to the observed redundancy in blocky and epidermal polygonal phytolith forms from the two families represented. However, the higher proportion of blocky (30-44%) and epidermal polygonal (8-10%) forms relative to other conifer forms (<1-2%) would suggest that *Artemisia* and other Asteraceae species were the predominate contributors of the blocky and epidermal polygonal forms.

Collectively, the assemblages from Zone IV suggest the continued existence of a shrub steppe community similar to Zone III. The inferred vegetation consisted of *Artemisia* and other Asteraceae shrubs and/or herbs with associations of Pooideae grasses. Long cell forms remain relatively stable within the zone suggesting stability of *Agropyron* grasses compared to *Festuca.* Rondels fluctuate slightly within the zone, suggesting minor fluctuations in the local moisture availability with wetter conditions supporting higher frequency of *Festuca* relative to drier conditions. The higher frequency of other conifer forms relative to Zone III suggests that Pinaceae species increased

slightly during this period however, the assemblages do not suggest a closed canopy arboreal forest.

Phytolith Zone V (70-0cm)

Results: Phytolith zone IV contains seven samples with an estimated age range of >2,000 yr BP to present (Davis 2001). Poaceae phytolith forms comprised 58-80% of the total assemblages and non-Poaceae phytolith forms comprised 20-42%. The Poaceae phytoliths are predominately derived from the Pooideae subfamily of C_3 grasses with an extremely limited presence of the Panicoideae subfamily of C_4 grasses. The most common characteristic Pooideae forms were rondels (12-25%) of *Agropyron* and *Festuca*, short wavy crenates (8-17%) of *Poa* and *Koeleria*, long wavy crenates (1-9%) of *Calamagrostis* and *Stipa*, and long cells (8-28%) of *Agropyron* and *Festuca*. Bilobate shaped phytoliths of the Panicoideae subfamily were limited to (<1%) within the zone. Diagnostic *Stipa*-type bilobates were limited to (<1%) within the zone. The most common characteristic non-Poaceae phytoliths consisted of blocky forms (15-30%) of *Artemisia*, *Abies*, and *Picea*, epidermal polygonal (2-7%) of *Artemisia*, *Abies*, and Asteraceae, epidermal anticlinal (1-2%) of Asteraceae, and other conifer forms (1-4%) of *Pinus*, *Abies*, *Picea*, or *Larix*. No diagnostic non-Poaceae forms were observed within the zone.

Interpretation: Zone V (>2,000 yr BP to Present) contained fluctuating proportions of both grass (58-80%) and non-grass (20-42%) phytolith forms. However, the zone contains a relatively higher proportion of grass forms compared to Zone IV. The assemblages of grass phytoliths suggest that a mix of C_3 Pooideae grasses existed at the site. The grass cover was predominately composed of *Agropyron*, *Festuca*, and *Poa*

indicated by the frequencies of rondels, short wavy crenates, and long cell forms. A secondary and very minor component of the grass cover consisted of *Stipa* indicated by long wavy crenates and *Stipa*-type forms. Additionally, it is noted that a single bilobate shaped phytolith form of the Panicoideae subfamily was observed. The assemblages of non-grass forms suggest that a mix of arboreal and shrub species existed at the site. The arboreal and shrub cover was composed of members of the Asteraceae and Pinaceae Families indicated by the frequencies of blocky, epidermal, and characteristic conifer forms. The identification of species composition of the arboreal and shrub communities is limited due to the observed redundancy in blocky and epidermal polygonal phytolith forms from the two families represented. However, the higher proportion of blocky (15-30%) and epidermal polygonal (2-7%) forms relative to other conifer forms (1-4%) would suggest that *Artemisia* and other Asteraceae species were the predominate contributors of the blocky and epidermal polygonal forms.

Collectively, the assemblages from Zone V suggest a transition from a shrub steppe community to a grass steppe community indicated by the increase in grass phytoliths relative to Zone IV. The inferred vegetations consisted of Pooideae grasses with associations of *Artemisia* and other Asteraceae shrubs and/or herbs. Fluctuations within the rondel and long cell assemblages suggest that *Agropyron* and *Festuca* were unstable, which may represent fluctuations in local moisture availability. Specifically, an overall increase in rondels relative to the other zones from SR-23 suggests that conditions of increased moisture availability favored the expansion of *Festuca* relative to *Agropyron.* However, at the top of the zone there is a marked decrease in the frequencies of rondels and an increase in long cell forms, which suggests that conditions became

relatively drier allowing for an increase in *Agropyron* grasses at the site. The higher frequency of other conifer forms relative to Zone IV suggests that Pinaceae species increased slightly during this period however, the assemblages do not suggest a closed canopy arboreal forest. Zone V assemblages suggest the transition to the grass steppe community that reflects the modern vegetation at the site.

SR-27 Phytolith Profile

SR-27 was redescribed and sampled in order to elaborate upon the initial section descriptions and chronology developed by Davis (2001a). The updated profile descriptions that were conducted as part of this study identified nine lithostratigraphic units within the 3.2 m thick section at SR-27, which are characterized by late Pleistocene and Holocene-aged deposits of aeolian loess overlying a late Pleistocene-aged alluvial fan deposit (Figure 6.2).

At the base of SR-27 is a deposit of clast supported alluvial fan debris (LU1) comprised of angular to subangular gravels and cobbles of mixed lithologies with light yellowish brown interstitial sands. Overlying the alluvial fan debris are thick deposits of late Pleistocene-early Holocene loess (LU2-LU7), which are comprised of non-bedded carbonaceous brown to very pale brown loamy sands, sandy loams, and sands. These older loess deposits are overlain by deposits of middle and late Holocene-aged sandy loess (LU8 and LU9), which are comprised of non-bedded carbonaceous brown to pale brown sandy loams. These late Pleistocene and Holocene loess deposits formed as alluvial sediments deposited on the floodplain were mobilized and redeposited upslope by aeolian processes, draping the adjacent landforms (Davis 2001a).

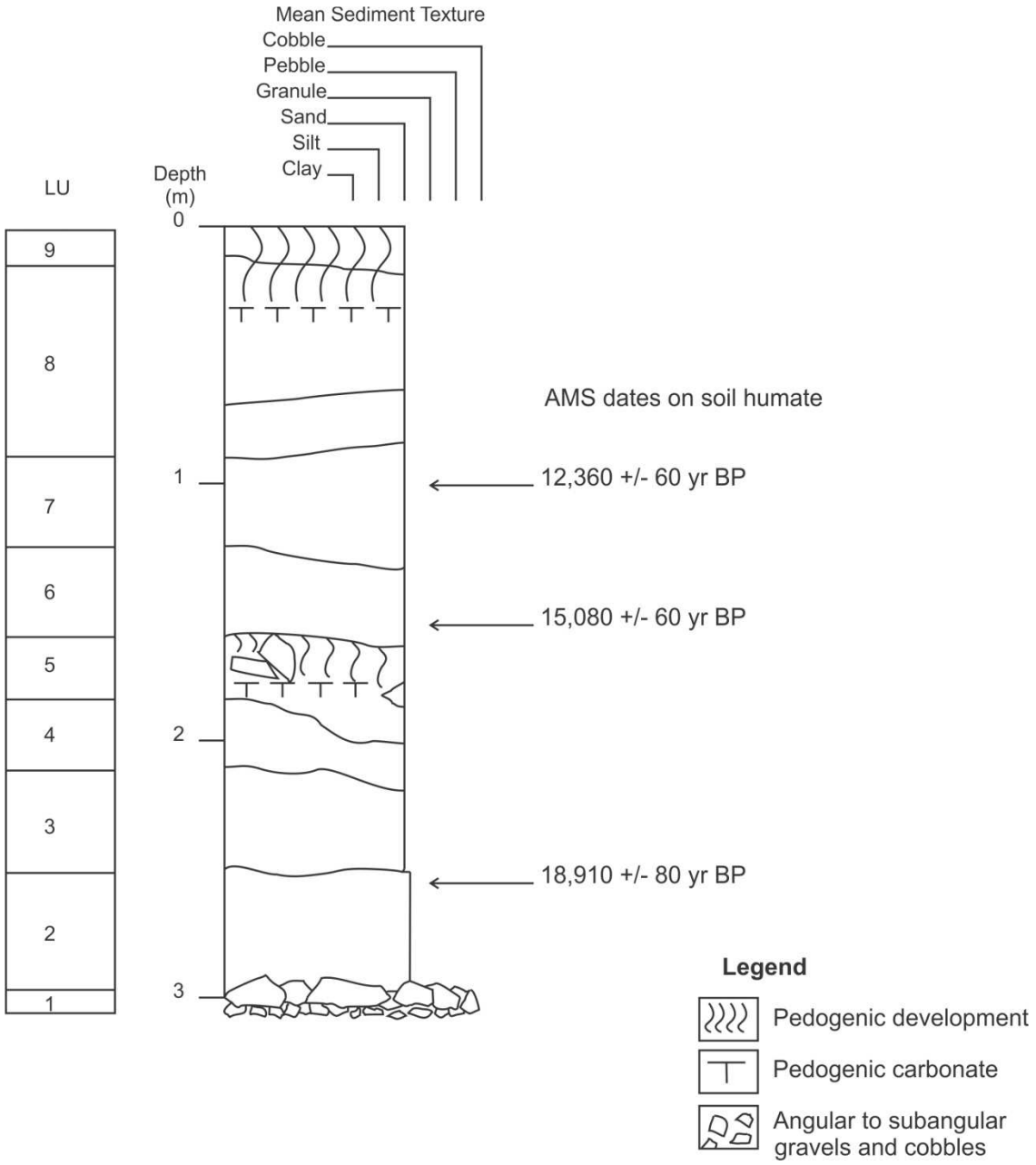

Figure 6.2 SR-27 stratigraphic profile. LU= lithostratigraphic unit.

A series of three new radiocarbon ages were obtained from AMS dates recovered from soil humate samples recovered from the section, which allowed for the refinement of the initial chronology proposed by Davis (2001a). The first sample recovered from the

upper part of LU2 (250-260 cm below the surface) returned an age of 18,910 ± 80 yr BP. The second sample recovered from the basal portion of LU6 (150-160 cm below the surface) returned an age of 15,080 ± 60 yr BP. The third sample recovered from the upper part of LU7 (100-110 cm below the surface) returned an age of 12,360 ± 60 yr BP.

A single paleosol was identified within the late Pleistocene loess associated with LU5. This corresponds with the paleosol originally identified by Davis (2001a), which was believed to represent an expression of the Rock Creek Soil that formed within late Pleistocene-early Holocene loess deposits in the LSRC between ca. 13,000 to 10,740 yr BP. However, based on the new AMS date of 15,080 ± 60 yr BP obtained directly above the paleosol from LU6 it is believed that the paleosol represents an expression of the China Gardens Soil. The China Gardens Soil developed within late Pleistocene loess in the LSRC between ca. <25,000 to >15,000 yr BP and is characterized at SR-27 by a weakly-developed yellowish brown sandy loam calcic horizon with common calcium carbonate accumulations.

A total of thirty sediment samples were processed from the SR-27 stratigraphic profile. Twenty-two of these samples produced sufficient quantities of well preserved phytoliths that permitted counting, classification, and identification of four phytolith zones. Eight samples did not contain sufficient quantities of phytoliths to permit counting and classification. These samples were observed from 50-80, 170-200, and 260-280 cm below the surface and separate zones I and II, zones II and III, and zones III and IV.

Four phytolith zones (Figure 6.3) were established using the CONISS function in TILIA-GRAPH (Grimm 1993), which clustered stratigraphically adjacent samples based

on changes in the frequencies of eighteen distinct morphotypes. The four zones will now be discussed in ascending order.

Phytolith Zone I (300-280 cm)

Results: Phytolith zone I contains two samples with an estimated age of >18,910±80 yr BP. Poaceae phytoliths comprised 56-61% of the total assemblage and non-Poaceae phytoliths comprised 39-44%. The Poaceae phytoliths are all derived from the Pooideae subfamily of C_3 grasses. The most common characteristic Pooideae forms were rondels (12-21%) of *Agropyron* and *Festuca*, short wavy crenates (11-12%) of *Poa* and *Koeleria*, long wavy crenates (1%) of *Calamagrostis* and *Stipa*, and long cells (10-11%) of *Agropyron* and *Festuca.* A single diagnostic *Stipa*-type bilobate was identified within the upper portion of the zone. The most common characteristic non-Poaceae phytoliths consisted of blocky forms (29-32%) of *Artemisia, Abies,* and *Picea*, epidermal polygonal (6-7%) of *Artemisia, Abies*, and Asteraceae, epidermal anticlinal (1%) of Asteraceae, and other conifer forms (2%) of *Pinus, Abies, Picea,* or *Larix.* Diagnostic non-Poaceae forms were limited to *P. ponderosa* type representing (<1%) of the zone.

Interpretation: Zone I (>18,910±80 yr BP) comprised the basal portion of SR-27 and its assemblages contained fluctuating proportions of both grass (56-61%) and non-grass (39-44%) phytolith forms. The assemblages of grass phytoliths suggest that a mix of C_3 Pooideae grasses existed at the site. The grass cover was predominately composed of *Agropyron, Festuca,* and *Poa* indicated by the frequencies of rondels, short wavy crenates, and long cell forms. A secondary and very minor component of the grass cover consisted of *Stipa* indicated by long wavy crenates and *Stipa*-type forms. The assemblages of non-grass forms suggest that a mix of arboreal and shrub species existed

at the site. The arboreal and shrub cover was composed of members of the Asteraceae and Pinaceae Families indicated by the frequencies of blocky, epidermal, and both characteristic and diagnostic conifer forms. The identification of species composition of the arboreal and shrub communities is limited due to the observed redundancy in blocky and epidermal polygonal phytolith forms from the two families represented. However, the higher proportion of blocky (29-32%) and epidermal polygonal (6-7%) forms relative to other conifer forms (2%) and diagnostic *P. ponderosa* types (<1%) would suggest that *Artemisia* and other Asteraceae species were the predominate contributors of the blocky and epidermal polygonal forms.

Collectively, the assemblages from Zone I suggest the existence of a shrub steppe community. The inferred vegetation consisted of *Artemisia* and other Asteraceae shrubs and/or herbs with associations of Pooideae grasses. Fluctuations within the rondel assemblages suggest that *Festuca* were unstable, which may represent fluctuations in local moisture availability with a higher frequency of *Festuca* during wetter periods. Specifically, rondel frequencies decline in the upper portion of the zone, suggesting that conditions became relatively drier. Long cell assemblages remain stable within the zone, suggesting stability within *Agropyron.* The low frequencies of other conifer forms and diagnostic *P. ponderosa* types suggest that these species did not comprise a substantial portion of the non-grass cover suggestive of a closed canopy arboreal forest.

Phytolith Zone II (260-200 cm)

Results: Phytolith zone II contains six samples with an estimated age range of >15,080±60 to ≥18,910±80 yr BP. Poaceae phytoliths comprised 53-63% of the total assemblage and non-Poaceae phytoliths comprised 37-47%. The Poaceae phytoliths are

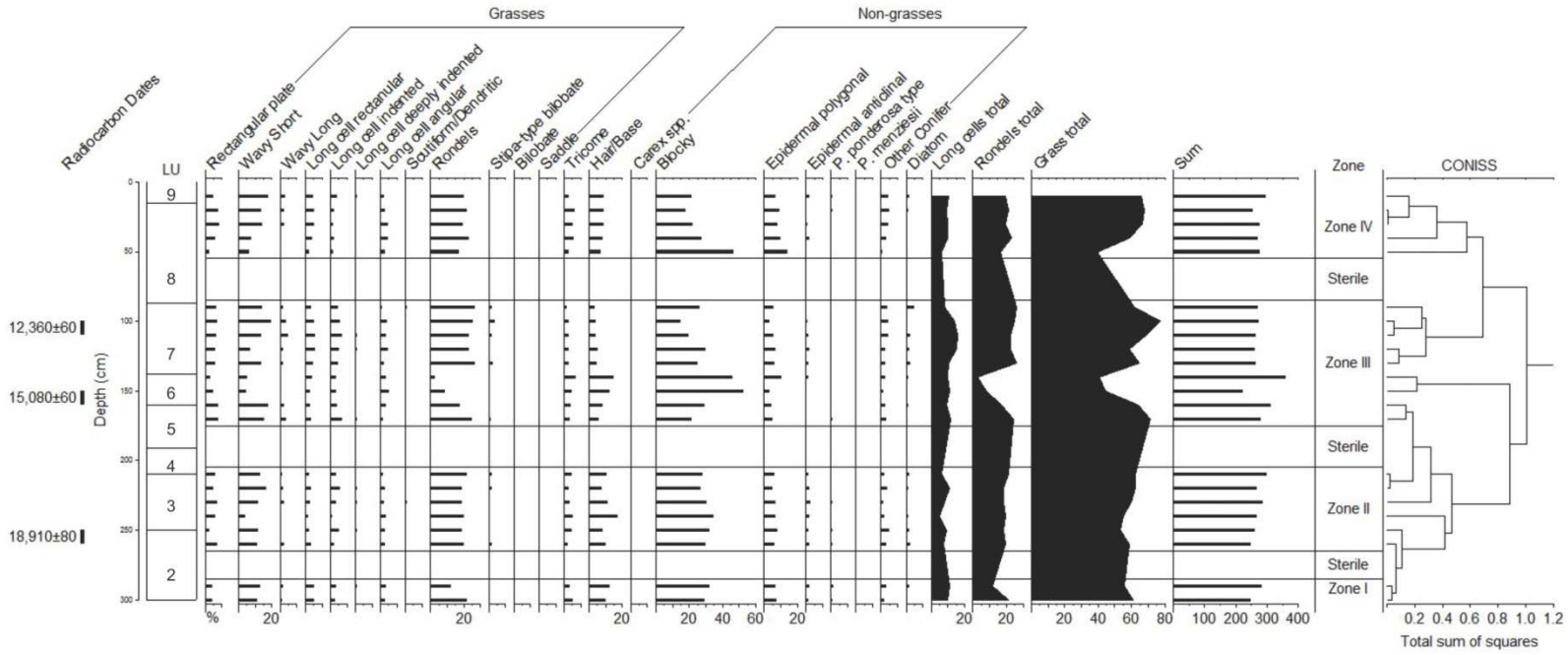

Figure 6.3 SR-27 phytolith profile. LU= lithostratigraphic unit.

all derived from the Pooideae subfamily of C_3 grasses. The most common characteristic Pooideae forms were rondels (18-21%) of *Agropyron* and *Festuca*, short wavy crenates (3-16%) of *Poa* and *Koeleria*, long wavy crenates (<1-2%) of *Calamagrostis* and *Stipa*, and long cells (5-11%) of *Agropyron* and *Festuca*. Diagnostic *Stipa*-type bilobates were limited to (<1-2%) within the zone. The most common characteristic non-Poaceae phytoliths consisted of blocky forms (27-34%) of *Artemisia*, *Abies*, and *Picea*, epidermal polygonal (5-7%) of *Artemisia, Abies,* and Asteraceae, epidermal anticlinal (1-2%) of Asteraceae, and other conifer forms (1-5%) of *Pinus, Abies, Picea,* or *Larix.* Diagnostic non-Poaceae forms were limited to *P. ponderosa* type representing (<1-1%) within the zone.

Interpretation: Phytolith zone II (>15,080±60 to ≥18,910±80 yr BP) contained fluctuating proportions of both grass (53-63%) and non-grass (37-47%) phytolith forms. The assemblages from the zone are relatively similar to those of Zone I. The assemblages of grass phytoliths suggest that a mix of C_3 Pooideae grasses existed at the site. The grass cover was predominately composed of *Agropyron, Festuca,* and *Poa* indicated by the frequencies of rondels, short wavy crenates, and long cell forms. A secondary and very minor component of the grass cover consisted of *Stipa* indicated by long wavy crenates and *Stipa*-type forms. The assemblages of non-grass forms suggest that a mix of arboreal and shrub species existed at the site. The arboreal and shrub cover was composed of members of the Asteraceae and Pinaceae Families indicated by the frequencies of blocky, epidermal, and both characteristic and diagnostic conifer forms. The identification of species composition of the arboreal and shrub communities is limited due to the observed redundancy in blocky and epidermal polygonal phytolith forms from the two families

represented. However, the higher proportion of blocky (27-34%) and epidermal polygonal (5-7%) forms relative to other conifer forms (1-5%) and diagnostic *P. ponderosa* types (<1-1%) would suggest that *Artemisia* and other Asteraceae species were the predominate contributors of the blocky and epidermal polygonal forms.

Collectively, the assemblages from Zone II suggest the continued existence of a shrub steppe community similar to Zone I. The inferred vegetation consisted of *Artemisia* and Asteraceae shrubs and/or herbs with associations of Pooideae grasses. However, an overall increase in grass phytolith forms is observed within the upper half of the zone, which suggests that conditions permitted the expansion of grass communities at the site. Rondels remain relatively stable within the zone suggesting that *Festuca* persisted compared to *Agropyron* and *Poa*. Both short wavy crenates and long cell forms fluctuate within the zone, suggesting that local environmental conditions caused instability within the *Agropyron* and *Poa* of the grass community. The frequencies of other conifer forms and *P. ponderosa* types are similar to Zone I, which suggests that these species continued to exist near the site as minor components of the local vegetation. These Pinaceae assemblages still do not suggest a closed canopy arboreal forest.

Phytolith Zone III (170-80 cm)

Results: Phytolith zone III contains nine samples with an estimated age range of >2,000 to ≥15,080±60 yr BP (Davis 2001). Poaceae phytoliths comprised 40-77% of the total assemblage and non-Poaceae phytoliths comprised 23-60%. The Poaceae phytoliths are all derived from the Pooideae subfamily of C_3 grasses. The most common characteristic Pooideae forms were rondels (3-26%) of *Agropyron* and *Festuca*, short wavy crenates (5-19%) of *Poa* and *Koeleria*, long wavy crenates (1-5%) of

Calamagrostis and *Stipa*, and long cells (9-16%) of *Agropyron* and *Festuca*. No diagnostic *Stipa*-type bilobates were identified within the zone. The most common characteristic non-Poaceae phytoliths consisted of blocky forms (15-52%) of *Artemisia, Abies*, and *Picea*, epidermal polygonal (3-10%) of *Artemisia, Abies*, and Asteraceae, epidermal anticlinal (1-2%) of Asteraceae, and other conifer forms (1-4%) of *Pinus*, *Abies, Picea*, or *Larix.* Diagnostic non-Poaceae forms were limited to *P. ponderosa* type representing (<1%) within the zone.

Interpretation: Zone III (>2,000 to ≥15,080±60 yr BP) exhibits considerable fluctuation within the proportions of both grass (40-77%) and non-grass (23-60%) phytolith forms. The zone suggests considerable environmental instability compared to Zone II. The assemblages of grass phytoliths suggest that a mix of C_3 Pooideae grasses existed at the site. The grass cover was predominately composed of *Agropyron, Festuca,* and *Poa* indicated by the frequencies of rondels, short wavy crenates, and long cell forms. A secondary and minor component of the grass cover consisted of *Stipa* indicated by long wavy crenates and *Stipa*-type forms. The assemblages of non-grass forms suggest that a mix of arboreal and shrub species existed at the site. The arboreal and shrub cover was composed of members of the Asteraceae and Pinaceae Families indicated by the frequencies of blocky, epidermal, and both characteristic and diagnostic conifer forms. The identification of species composition of the arboreal and shrub communities is limited due to the observed redundancy in blocky and epidermal polygonal phytolith forms from the two families represented. However, the higher proportion of blocky (15-52%) and epidermal polygonal (3-10%) forms relative to other conifer forms (1-4%) and

diagnostic *P. ponderosa* types (<1%) would suggest that *Artemisia* and other Asteraceae species were the predominate contributors of the blocky and epidermal polygonal forms.

The basal portion of Zone III also contains a sample from a portion of a truncated paleosol, between 160 and 191 cm, believed to be an expression of the China Gardens Soil, whiched formed within the LSRC between ca. >15,000 and <25,000 yr BP (Davis 2001a). The period of relative landscape stability and soil formation associated with this calcic horizon observed at SR-27 could have provided an opportunity for the phtyolith assemblages associated with different vegetative conditions to become mixed together if conditions changed significantly during the period of stability. Fredlund and Tieszen (1994:331) refer to this process of mixing as “inheritance”, which acknowledges the potential of long-term (hundreds of years or more) mix of phytolith assemblages with soils. Therefore, assemblages associated with the paleosol should be interpreted as representation of the long-term average of vegetative conditions at the site; however, with regards to Zone III at SR-27, the samples recovered from most of the China Gardens Soil horizon (sterile zone between 170 and 200 cm) lacked adequate quantaties of phytoliths to permit analysis. The single sample from the top of the paleosol at 160 cm likely reflects the mixture of grass and shrub stepp communities during this period.

Collectively, the assemblages from Zone III suggest the existence of an unstable environment which transitioned between grass and shrub steppe communities. The inferred vegetation associated with the lower portion of the zone consisted of Pooideae grasses with associations of *Artemisia* and Asteraceae shrubs and/or herbs. However, within the middle portion of the zone there is a pronounced reduction in grass phytolith forms suggesting a transition back to a shrub steppe community. Additionally, as grass

forms decline overall within this middle portion of the zone rondels decline to the lowest frequencies observed within SR-27. This decrease in grass forms at large and rondels specifically would suggest that conditions of increase aridity occurred, which supported an expansion of *Artemisia* coverage and associated *Agropyron* grasses. Following this period of increased aridity grass assemblages rebound and attain frequencies similar to and higher than those of the lower portion of the zone, suggesting a transition back to a grass steppe community. Decreased aridity and increased local moisture availability is inferred for the upper portion of the zone relative to the middle portion of the zone. This increase in moisture availability is inferred by the increase in rondel frequencies, which suggests an expansion of *Festuca* at the site. At the top of the zone grass phytoliths decrease once again, suggesting a transition back to a shrub steppe community. Interestingly, rondel frequencies remain stable while long cell and short wavy crenates declined. This would suggest that conditions remained relatively moist, which permitted stability within the *Festuca* grasses, however, expansion of *Artemisia* and other Asteraceae species is inferred by overall grass reduction. The frequencies of other conifer forms and *P. ponderosa* types are similar to Zone I, which suggests that these species continued to exist near the site as minor components of the local vegetation. These Pinaceae assemblages still do not suggest a closed canopy arboreal forest.

Phytolith Zone IV (50-0 cm)

Results: Phytolith zone V contains five samples with an estimated age range of >6,000 yr BP to present (Davis 2001). Poaceae phytoliths comprised 39-68% of the total assemblage and non-Poaceae phytoliths comprised 32-61%. The Poaceae phytoliths are all derived from the Pooideae subfamily of C_3 grasses. The most common characteristic

Pooideae forms were rondels (17-23%) of *Agropyron* and *Festuca*, short wavy crenates (6-17%) of *Poa* and *Koeleria*, long wavy crenates (2-3%) of *Calamagrostis* and *Stipa*, and long cells (6-11%) of *Agropyron* and *Festuca*. Diagnostic *Stipa*-type bilobates were limited to (<1%) within the zone. The most common characteristic non-Poaceae phytoliths consisted of blocky forms (17-46%) of *Artemisia*, *Abies*, and *Picea*, epidermal polygonal (6-14%) of *Artemisia, Abies*, and Asteraceae, epidermal anticlinal (<1-2%) of Asteraceae, and other conifer forms (<1-5%) of *Pinus, Abies, Picea,* or *Larix.* Diagnostic non-Poaceae forms were limited to *P. ponderosa* type representing (<1%) and *Carex* type representing (<1%) within the zone.

Interpretation: Zone IV (>6,000 yr BP to Present) contained fluctuating proportions of both grass (39-68%) and non-grass (32-61%) phytolith forms. The zone suggests another episode of environmental change similar to those observed in Zone III. The assemblages of grass phytoliths suggest that a mix of C_3 Pooideae grasses existed at the site. The grass cover was predominately composted of *Agropyron, Festuca*, and *Poa* indicated by the frequencies of rondels, short wavy crenates, and long cell forms. A secondary and very minor component of the grass cover consisted of *Stipa* indicated by long wavy crenates and *Stipa*-type forms. The assemblages of non-grass forms suggest that a mix of arboreal and shrub species existed at the site. The arboreal and shrub cover was composed of members of the Asteraceae and Pinaceae Families indicated by the frequencies of blocky, epidermal, and both characteristic and diagnostic conifer forms. The identification of species composition of the arboreal and shrub communities is limited due to the observed redundancy in blocky and epidermal polygonal phytolith forms from the two families represented. However, the higher proportion of blocky (17-

46%) and epidermal polygonal (6-14%) forms relative to other conifer forms (<1-5%) and diagnostic *P. ponderosa* types (<1%) would suggest that *Artemisia* and other Asteraceae species were the predominate contributors of the blocky and epidermal polygonal forms.

Collectively, the assemblages from Zone IV suggest that conditions transitioned from a shrub steppe to a grass steppe community. The inferred vegetation associated with the bottom of the zone consisted of *Artemisia* and Asteraceae shrubs and/or herbs with associations of Pooideae grasses. However, grass phytolith frequencies increase substantially within the remaining upper portion of the zone, suggesting the transition to a grassland community. The inferred vegetation associated with the upper portion of the zone consisted of Pooideae grasses with associations of *Artemisia* and Asteraceae shrubs and/or herbs. The frequencies of rondels and long cell forms remain relatively stable within the upper portion of the zone, suggesting stability of the expanding *Agropyron* and *Festuca* grass communities. The frequencies of other conifer forms and *P. ponderosa* types are similar to Zone III, which suggests that these species continued to exist near the site. Zone IV assemblages suggest the transition to the grass steppe community that reflects the modern vegetation at the site.

SR-34 Phytolith Profile

SR-34 was redescribed and sampled in order to elaborate upon the initial section descriptions and chronology developed by Davis (2001a). The updated profile descriptions that were conducted as part of this study identified eleven lithostratigraphic units within the 5 m thick section at SR-34, which are characterized by late Pleistocene

and Holocene aged deposits of aeolian loess and sandy loess overlying a late Pleistocene alluvial fan deposit (Figure 6.4).

At the base of SR-34 is a deposit of clast-supported alluvial fan debris (LU 1) comprised of angular to subangular gravels and cobbles of mixed lithologies with pale brown loamy sand in the matrix of the gravels and cobbles. Overlying the alluvial fan debris are thick deposits of late Pleistocene and late Pleistocene-early Holocene loess (LU2-LU8), which are comprised of non-bedded carbonaceous yellowish brown to pale brown loamy sands and sandy loams. These older loess deposits are overlain by deposits of middle and late Holocene sandy loess (LU9-LU11), which are comprised of non-bedded carbonaceous brown to yellowish brown sandy loams, loams, and loamy sands. These late Pleistocene and Holocene loess deposits formed as alluvial sediments deposited on the floodplain were mobilized and redeposited upslope by aeolian processes, draping the adjacent landforms (Davis 2001a).

A series of four new radiocarbon ages were obtained from AMS dates recovered from soil humate samples recovered from the section, which allowed for the refinement of the initial chronology proposed by Davis (2001a). The first sample recovered from the middle part of LU3 (400-410 cm below the surface) returned an age of 22,130 ± 110 yr BP. The second sample recovered from the upper portion of LU3 (350-360 cm below the surface) returned an age of 18,870 ± 80 yr BP. The third sample recovered from the lower part of LU5 (300-310 cm below the surface) returned an age of 18,080 ± 80 yr BP. The fourth sample recovered from the lower part of LU10 (100-110 cm below the surface) returned an age of 5,890 ± 40 yr BP.

Two paleosol were identified within the late Pleistocene loess associated with

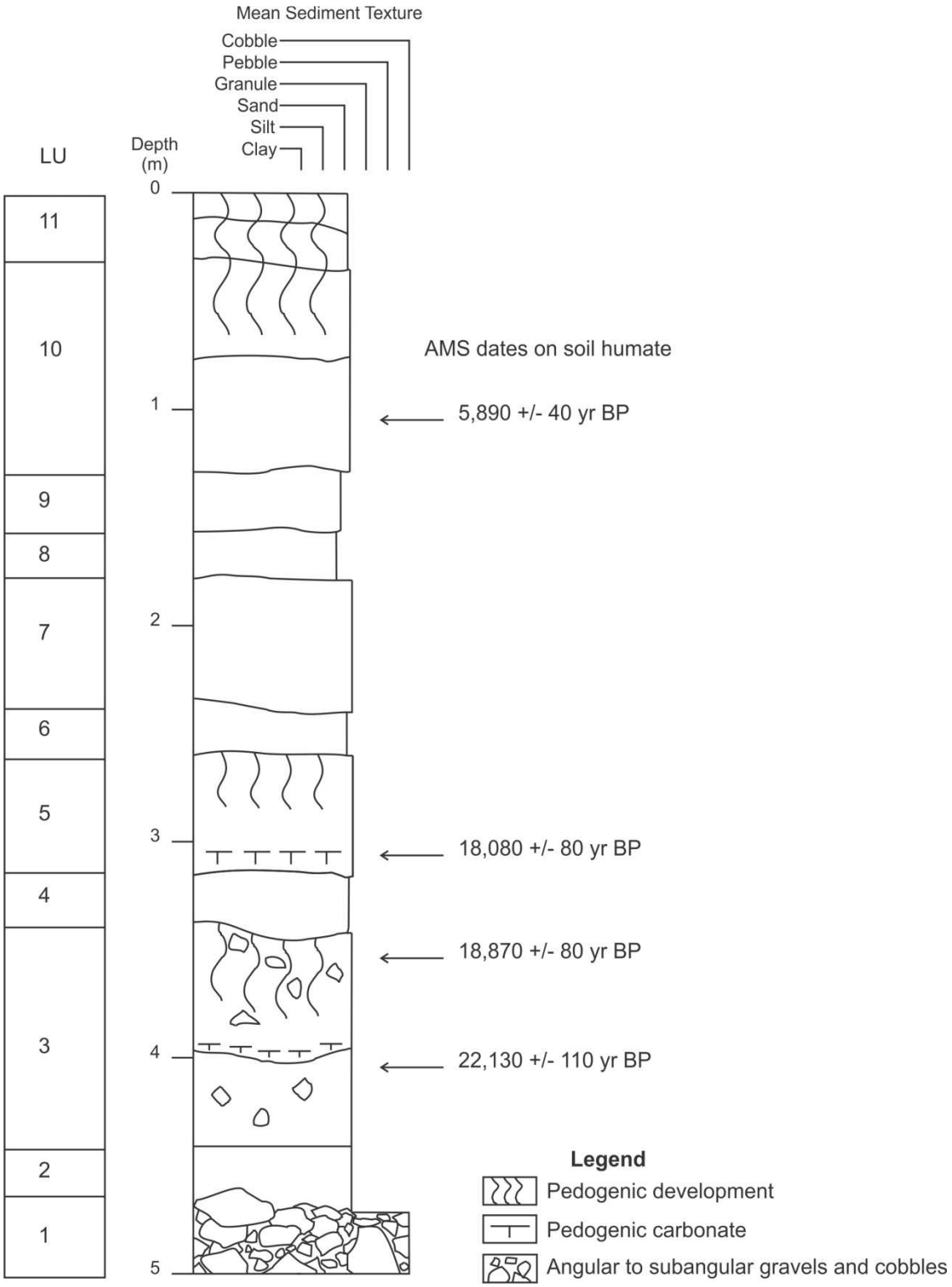

Figure 6.4 SR-34 stratigraphic profile. LU= lithostratigraphic unit.

LU3 and LU5. The stratigraphic positions of these two paleosols do not correspond with the single paleosol originally identified by Davis (2001a), which was believed to represent an expression of the late Pleistocene-early Holocene-aged Rock Creek Soil. However, based on the new AMS date of 18,080 ± 80 yr BP obtained below the paleosol from LU6 and 18,870 ± 80 yr BP obtained from the upper part of the paleosol in LU3 it is believed that the paleosols represent expressions of the late Pleistocene-aged China Gardens Soil. The China Gardens Soil developed within late Pleistocene loess deposits LU5 and LU3 at SR-34 and is characterized by weakly-developed light yellowish brown and yellowish brown sandy loam and loamy sand calcic horizons with common calcium carbonate accumulations.

A total of fifty sediment samples were processed from the SR-34 stratigraphic profile. Forty-eight of these samples produced sufficient quantities of well preserved phytoliths that permitted counting, classification, and identification of six phytolith zones. Two samples did not contain sufficient quantities of phytoliths to permit counting and classification. These samples were observed from 160-180 cm below the surface and separate phytolith zones III and IV.

Six phytolith zones (Figure 6.5) were established using the CONISS function in TILIA-GRAPH (Grimm 1993), which clustered stratigraphically adjacent samples based on the changes in the frequencies of twenty-one distinct morphotypes. The six zones will now be discussed in ascending order.

Phytolith Zone I (500-410 cm)

Results: Phytolith zone I contains nine samples with an estimated age of >22,130±110 yr BP. Poaceae phytolith forms comprised 24-40% of the total assemblage

and non-Poaceae phytolith forms comprised 60-76%. The Poaceae phytoliths are predominately derived from the Pooideae subfamily of C_3 grasses with an extremely limited presence of the Panicoideae subfamily of C_4 grasses. The most common characteristic Pooideae forms were rondels (2-9%) of *Agropyron* and *Festuca*, short wavy crenates (2-11%) of *Poa* and *Koeleria*, long wavy crenates (<1-2%) of *Calamagrostis* and *Stipa*, and long cells (2-8%) of *Agropyron* and *Festuca*. Bilobate shaped phytoliths of the Panicoideae subfamily were limited to (<1%) within the zone. Diagnostic *Stipa*-type bilobates were limited to (<1%) within the zone. The most common characteristic non-Poaceae phytoliths consisted of blocky forms (28-46%) of *Artemisia*, *Abies*, and *Picea*, epidermal polygonal (19-30%) of *Artemisia*, *Abies*, and Asteraceae, epidermal anticlinal (2-5%) of Asteraceae, and other conifer forms (1-3%) of *Pinus*, *Abies, Picea*, or *Larix*. Diagnostic non-Poaceae forms were limited to *P. ponderosa* type representing (<1%) and *Carex* type representing (<1-1%) within the zone.

Interpretation: Zone I (>22,130±110 yr BP) comprised the basal portion of SR-34 and its assemblages contained fluctuating proportions of both grass (24-40%) and non-grass (60-76%) phytolith forms. The assemblages of grass phytoliths suggest that a mix of C_3 Pooideae grasses existed at the site. This grass cover was predominately composed of *Agropyron, Festuca,* and *Poa* indicated by the frequencies of rondels, short wavy crenates, and long cell forms. A secondary and very minor component of the grass cover consisted of *Stipa* indicated by long wavy crenates and *Stipa*-type forms. Additionally, it is noted that a very low frequency (<1%) of bilobate shaped phytoliths of the Panicoideae subfamily were observed. The assemblages of non-grass forms suggest that a mix of

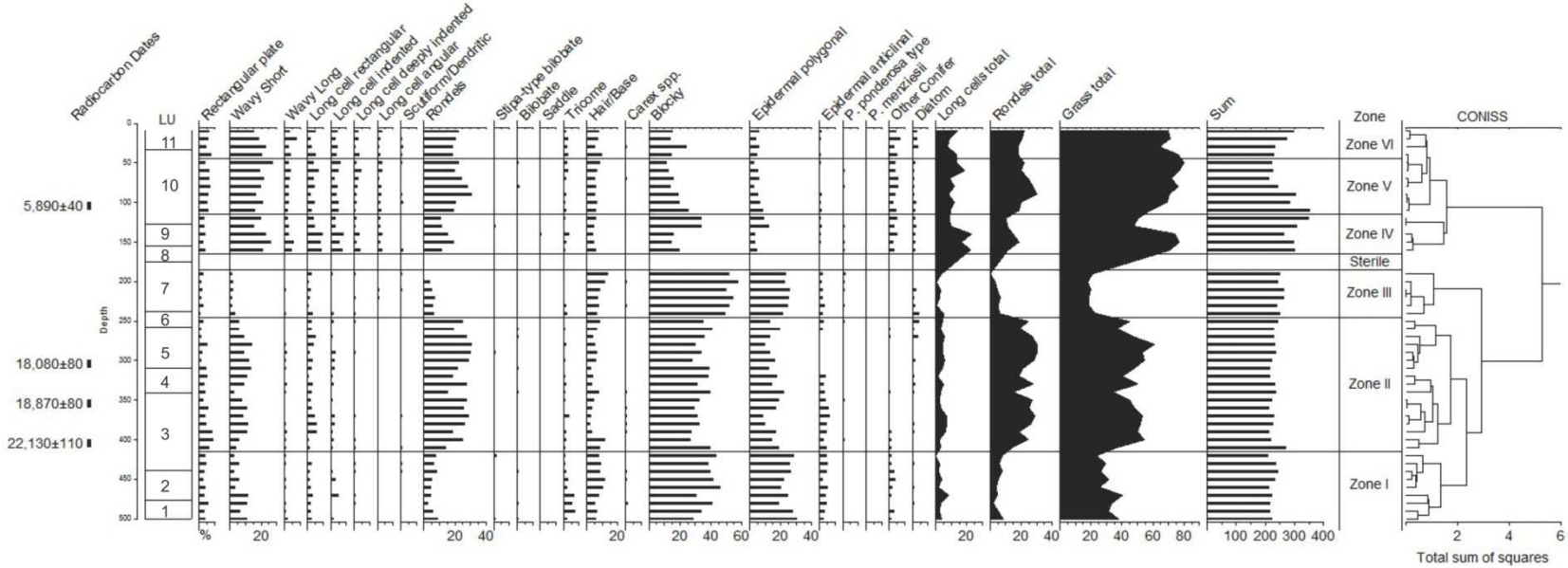

Figure 6.5 SR-34 phytolith profile. LU= lithostratigraphic unit.

arboreal and shrub species existed at the site. The arboreal and shrub cover was composed of members of the Asteraceae and Pinaceae Families indicated by the frequencies of blocky, epidermal, and both characteristic and diagnostic conifer forms. The identification of species composition of the arboreal and shrub communities is limited due to the observed redundancy in blocky and epidermal polygonal phytolith forms from the two families represented. However, the higher proportion of blocky (28-46%) and epidermal polygonal (19-30%) forms relative to other conifer forms (1-3%) and diagnostic *P. ponderosa* types (<1%) would suggest that *Artemisia* and other Asteraceae species were the predominate contributors of the blocky and epidermal polygonal forms.

Collectively, the assemblages from Zone I suggest the existence of a shrub steppe community. The inferred vegetation consisted of *Artemisia* and other Asteraceae shrubs and/or herbs with associations of Pooideae grasses. Fluctuations within the rondel, long cell, and short wavy crenate assemblages suggest that *Agropyron, Festuca,* and *Poa* were relatively unstable, which may represent fluctuations in local moisture availability. Overall, the grass assemblages suggest that these Pooideae species were relatively sparse at the site during this time. The low frequencies of other conifer forms and diagnostic *P. ponderosa* types suggest that these species did not comprise a substantial portion of the non-grass cover suggestive of a closed canopy arboreal forest.

Phytolith Zone II (410-240 cm)

Results: Phytolith zone II contains seventeen samples with an estimated age of >15,000 to ≥22,130±110 yr BP (Davis 2001). Poaceae phytolith forms comprised 34-61% of the total assemblages and non-Poaceae phytolith forms comprised 39-66%. The

Poaceae phytoliths are predominately derived from the Pooideae subfamily of C_3 grasses with an extremely limited presence of the Panicoideae subfamily of C_4 grasses. The most common characteristic Pooideae forms were rondels (14-31%) of *Agropyron* and *Festuca*, short wavy crenates (2-14%) of *Poa* and *Koeleria,* long wavy crenates (<1-1%) of *Calamagrostis* and *Stipa,* and long cells (1-7%) of *Agropyron* and *Festuca*. Bilobate shaped phytoliths of the Panicoideae subfamily were limited to (<1%) within the zone. Diagnostic *Stipa*-type bilobates were limited to (<1-1%) within the zone. The most common characteristic non-Poaceae phytoliths consisted of blocky forms (26-40%) of *Artemisia*, *Abies*, and *Picea*, epidermal polygonal (8-22%) of *Artemisia*, *Abies*, and Asteraceae, epidermal anticlinal (2-7%) of Asteraceae, and other conifer forms (<1-1%) of *Pinus*, *Abies*, *Picea*, or *Larix*. Diagnostic non-Poaceae forms were limited to *P. ponderosa* representing (<1-1%) and *Carex* type representing (<1%) within the zone.

Interpretation: Phytolith zone II (>15,000 to ≥22,130±110 yr BP) contained fluctuating proportions of both grass (34-61%) and non-grass (39-66%) phytolith forms. However, the zone contains a relatively higher proportion of grass forms compared to Zone I. The assemblages of grass phytoliths suggest that mix of C_3 Pooideae grasses existed at the site. The grass cover was predominately composed of *Agropyron, Festuca,* and *Poa* indicated by the frequencies of rondels, short wavy crenates, and long cell forms. A secondary and very minor component of the grass cover consisted of *Stipa* indicated by long wavy crenates and *Stipa*-type forms. Again, a very low frequency (<1%) of bilobate shaped phytoliths of the Panicoideae subfamily were observed. The assemblages of non-grass forms suggest that a mix of arboreal and shrub species existed at the site. The arboreal and shrub cover was composed of members of the Asteraceae

and Pinaceae Families indicated by the frequencies of blocky, epidermal, and both characteristic and diagnostic conifer forms. The identification of species composition of the arboreal and shrub communities is limited due to the observed redundancy in blocky and epidermal polygonal phytolith forms from the two families represented. However, the higher proportion of blocky (26-40%) and epidermal polygonal (8-22%) forms relative to other conifer forms (<1-1%) and diagnostic *P. ponderosa* types (<1-1%) would suggest that *Artemisia* and other Asteraceae species were the predominate contributors of the blocky and epidermal polygonal forms.

Zone II also contains portions of two truncated paleosols believed to be expressions of the China Gardens Soil, whiched formed within the LSRC between ca. >15,000 and <25,000 yr BP (Davis 2001a). The lower paleosol is characterized by a truncated calcic horizon observed within LU3 between 341 and 398 cm. The upper paleosol is characterized by a truncated calcic horizon observed within LU5 between 258 and 310 cm. The periods of relative landscape stability and soil formation associated with these calcic horizons observed at SR-34 could have provided an opportunity for the phtyolith assemblages associated with different vegetative conditions to become mixed together if conditions changed significantly during the period of stability. Fredlund and Tieszen (1994:331) refer to this process of mixing as “inheritance”, which acknowledges the potential of long-term (hundreds of years or more) mix of phytolith assemblages with soils. Therefore, assemblages associated with the paleosols should be interpreted as representation of the long-term average of vegetative conditions at the site. With regards to Zone II at SR-34, the samples recovered from the China Gardens Soil horizons likely reflect the mixture of grass and shrub stepp communities during this period.

Collectively, the assemblages from Zone II suggest the continued existence of a shrub steppe community similar to Zone I. However, grass communities expanded during this time relative to Zone I. The inferred vegetation consisted of *Artemisia* and Asteraceae shrubs and/or herbs with associations of Pooideae grasses. A pronounced increase in the frequency of rondels suggests that *Festuca* expanded during this time, which may indicate an overall increase in local moisture availability. However, rondel frequencies fluctuate, suggesting that conditions fluctuated between periods of increased moisture and those of increased aridity. Lower frequencies of other conifer forms and *P. ponderosa* types suggest that Pinaceae communities declined during this period relative to zone I.

Phytolith Zone III (240-180 cm)

Results: Phytolith zone III contains six samples with an estimated age of ≥8,400 to >15,000 yr BP (Davis 2001). Poaceae phytolith forms comprised 18-23% of the total assemblages and non-Poaceae phytolith forms comprised 77-82%. The Poaceae phytoliths are all derived from the Pooideae subfamily of C_3 grasses. The most common characteristic Pooideae forms were rondels (3-7%) of *Agropyron* and *Festuca*, short wavy crenates (1-3%) of *Poa* and *Koeleria,* long wavy crenates (<1%) of *Calamagrostis* and *Stipa,* and long cells (<1-5%) of *Agropyron* and *Festuca*. Diagnostic *Stipa*-type bilobates were limited to (<1%) within the zone. The most common characteristic non-Poaceae phytoliths consisted of blocky forms (49-57%) of *Artemisia*, *Abies*, and *Picea*, epidermal polygonal (21-26%) of *Artemisia*, *Abies*, and Asteraceae, and epidermal anticlinal (1-3%) of Asteraceae. Other conifer forms of *Pinus*, *Abies*, *Picea*, or *Larix* were not identified

within the zone. Diagnostic non-Poaceae forms were limited to *P. ponderosa* type representing (<1-2%), and *Carex* type representing (<1%) within the zone.

Interpretation: Zone III (≥8,400 to >15,000 yr BP) contained fluctuating proportions of grass (18-23%) and non-grass (77-82%) phytolith forms. However, the zone contains a relatively lower proportion of grass forms compared to Zone II. The assemblages of grass phytoliths suggest that a mix of C_3 Pooideae grasses existed at the site. The grass cover was predominately composed of *Agropyron, Festuca,* and *Poa* indicated by the frequencies of rondels, short wavy crenates, and long cell forms. A secondary and very minor component of the grass cover consisted of *Stipa* indicated by long wavy crenates and *Stipa*-type forms. The assemblages of non-grass forms suggest that a mix of arboreal and shrub species existed at the site. The arboreal and shrub cover was composed of members of the Asteraceae and Pinaceae Families indicated by the frequencies of blocky, epidermal, and both characteristic and diagnostic conifer forms. The identification of species composition of the arboreal and shrub communities is limited due to the observed redundancy in blocky and epidermal polygonal phytolith forms from the two families represented. However, the higher proportion of blocky (49-57%) and epidermal polygonal (21-26%) forms relative to the lack other conifer forms and low frequency of diagnostic *P. ponderosa* types (<1%) would suggest that *Artemisia* and other Asteraceae species were the predominate contributors of the blocky and epidermal polygonal forms.

Collectively, the assemblages from Zone III suggest the continued existence of a shrub steppe community. However, shrub communities expanded significantly as grass communities declined during this period with assemblages more similar to Zone I than

Zone II. The inferred vegetation consisted of *Artemisia* and Asteraceae shrubs and/or herbs with associations of Pooideae grasses. The pronounced decrease in the frequencies of all characteristic grass forms suggests that *Agropyron, Festuca,* and *Poa* declined, possibly in response to a reduction in locally available moisture at the site. These conditions favored the expansion of *Artemisia* and other Asteraceae shrubs and/or herbs indicated by the increased frequencies of blocky and epidermal forms. Additionally, there is a relative increase in the frequency of diagnostic *P. ponderosa* types relative to the previous zones, suggesting an expansion of the species. However, other conifer forms were absent from the zone, suggesting that *P. ponderosa* was the only predominate Pinaceae species near the site.

Phytolith Zone IV (160-110 cm)

Results: Phytolith zone IV contains five samples with an estimated age of >5,890±40 to <8,400 yr BP (Davis 2001). Poaceae phytolith forms comprised 47-77% of the total assemblages and non-Poaceae phytolith forms comprised 23-53%. The Poaceae phytoliths are predominately derived from the Pooideae subfamily of C_3 grasses with an extremely limited presence of the Panicoideae and Chloridoideae subfamilies of C_4 grasses. The most common characteristic Pooideae forms were rondels (10-19%) of *Agropyron* and *Festuca,* short wavy crenates (15-26%) of *Poa* and *Koeleria*, long wavy crenates (2-6%) of *Calamagrostis* and *Stipa*, and long cells (7-23%) of *Agropyron* and *Festuca*. Bilobate shaped phytoliths of the Panicoideae subfamily and saddle shaped phytoliths of the Chloridoideae subfamily were both limited to (<1%) within the zone. Diagnostic *Stipa*-type bilobates were limited to (<1-1%) within the zone. The most common characteristic non-Poaceae phytoliths consisted of blocky forms (14-34%) of

Artemisia, *Abies*, and *Picea*, epidermal polygonal (3-12%) of *Artemisia*, *Abies*, and Asteraceae, epidermal anticlinal (<1-1%) of Asteraceae, and other conifer forms (2-5%) of *Pinus*, *Abies*, *Picea*, or *Larix*. Diagnostic non-Poaceae forms were limited to *P. ponderosa* type representing (<1-1%) of the zone.

Interpretation: Zone IV (>5,890±40 to <8,400 yr BP) contained fluctuating proportion of grass (47-77%) and non-grass (23-53%) phytolith forms. However, the zone contains a relatively higher proportion of grass forms compared to Zone III. The assemblages of grass phytoliths suggest that a mix of C_3 Pooideae grasses existed at the site. The grass cover was predominately composed of *Agropyron, Festuca,* and *Poa* indicated by the frequencies of rondels, short wavy crenates, and long cell forms. A secondary and minor component of the grass cover consisted of *Stipa* indicated by long wavy crenates and *Stipa*-type forms. Additionally, a very low frequency of bilobate (<1%) and saddle (<1%) shaped phytoliths of the Panicoideae and Chloridoideae subfamilies were observed. The assemblages of non-grass forms suggest that a mix of arboreal and shrub species existed at the site. The arboreal and shrub cover was composed of members of the Asteraceae and Pinaceae Families indicated by the frequencies of blocky, epidermal, and both characteristic and diagnostic conifer forms. The identification of species composition of the arboreal and shrub communities is limited due to the observed redundancy in blocky and epidermal polygonal phytolith forms from the two families represented. However, the higher proportion of blocky (14-34%) and epidermal polygonal (3-12%) forms relative to other conifer forms (2-5%) and diagnostic *P. ponderosa* types (<1-1%) would suggest that *Artemisia* and other

Asteraceae species were the predominate contributors of the blocky and epidermal polygonal forms.

Collectively, the assemblages from the lower half Zone IV suggests that conditions permitted the transition from a shrub steppe community to a grass steppe community relative to Zone III. However, these conditions were unstable and a transition back to a shrub steppe community is inferred from the upper half of the zone. Within the lower half of the zone the inferred vegetation consisted of Pooideae grasses with associations of *Artemisia* and other Asteraceae shrubs and/or herbs. Fluctuations in the frequencies of rondels and long cell forms suggest that *Agropyron* and *Festuca* cover fluctuated, which my represent changes in locally available moisture at the site with expansions of *Festuca* during wetter conditions. Within the upper half of the zone the inferred vegetation consisted of *Artemisia* and other Asteraceae shrubs and/or herbs with associations of Pooideae grasses. This shift is inferred by a decrease in the frequency of grass phytolith forms while blocky and epidermal polygonal forms increase. Additionally, there is an increase in the frequencies of other conifer forms while *P. ponderosa* types decrease slightly relative to Zone III. The frequency of Pinaceae types suggests that these species were present near the site.

Phytolith Zone V (110-40 cm)

Results: Phytolith zone V contains seven samples with an estimated age of ≥2,000 to ≥5,890±40 yr BP (Davis 2001). Poaceae phytolith forms comprised 58-80% of the total assemblages and non-Poaceae phytolith forms comprised 20-42%. The Poaceae phytoliths are predominately derived from the Pooideae subfamily of C_3 grasses with an extremely limited presence of the Panicoideae subfamily of C_4 grasses. The most

common characteristic Pooideae forms were rondels (19-30%) of *Agropyron* and *Festuca*, short wavy crenates (16-27%) of *Poa* and *Koeleria*, long wavy crenates (2-4%) of *Calamagrostis* and *Stipa*, and long cells (8-18%) of *Agropyron* and *Festuca*. Bilobate shaped phytoliths of the Panicoideae subfamily were limited to (<1-1%) within the zone. No diagnostic *Stipa*-type bilobates were identified within the zone. The most common characteristic non-Poaceae phytoliths consisted of blocky forms (11-26%) of *Artemisia*, *Abies*, and *Picea*, epidermal polygonal (3-9%) of *Artemisia*, *Abies*, and Asteraceae, and epidermal anticlinal (1%) of Asteraceae, and other conifer forms (2-6%) of *Pinus*, *Abies*, *Picea*, or *Larix*. Diagnostic non-Poaceae forms were limited to *P. ponderosa* type representing (1%) and *Carex* type representing (<1%) within the zone.

Interpretation: Zone V (≥2,000 to ≥5,890±40 yr BP) contained fluctuating proportions of grass (58-80%) and non-grass (20-42%) phytolith forms. However, the zone contains a relatively higher proportion of grass forms compared to Zone IV. The assemblages of grass phytoliths suggest that a mix of C_3 Pooideae grasses existed at the site. The grass cover was predominately composed of *Agropyron*, *Festuca*, and *Poa* indicated by the frequencies of rondels, short wavy crenates, and long cell forms. A secondary and minor component of the grass cover consisted of bilobate (≤1%) shaped phytoliths of the Panicoideae subfamily. The assemblages of non-grass forms suggests that a mix of arboreal and shrub species existed at the site. The arboreal and shrub cover was composed of members of the Asteraceae and Pinaceae Families indicated by the frequencies of blocky, epidermal, and both characteristic and diagnostic conifer forms. The identification of species composition of the arboreal and shrub communities is limited due to the observed redundancy in blocky and epidermal polygonal forms from

the two families. However, the higher proportion of blocky (11-26%) and epidermal polygonal (3-9%) forms relative to other conifer (2-6%) forms and diagnostic *P. ponderosa* types (1%) would suggest that *Atremisia* and other Asteraceae species were the predominate contributors of the blocky and epidermal polygonal forms.

Collectively, the assemblages from Zone V suggest that conditions transitioned back to a grass steppe community relative to the upper portion of Zone IV. The inferred vegetation consisted of Pooideae grasses with associations of *Artemisia* and other Asteraceae shrubs and/or herbs. The frequency of rondels steadily increases throughout the lower half of the zone, suggesting an increase in local moisture availability and expansion of *Festuca*. This trend is contrasted by a decrease in the frequency of rondels within the upper half of the zone while long cell frequencies increase. This would suggest a reduction in local moisture availability causing a reduction in *Festuca* while *Agropyron* expanded. Additionally, there is an overall decrease in the frequency of grass phytolith forms within the top of the zone, suggesting a reduction in grass cover at the site. The frequencies of other conifer forms and *P. ponderosa* types are similar to Zone IV suggesting that Pinaceae species were present near the site.

Phytolith Zone VI (40-0 cm)

Results: Phytolith zone VI contains four samples with an estimated age of ≤2,000 yr BP to present (Davis 2001). Poaceae phytolith forms comprised 64-76% of the total assemblages and non-Poaceae phytolith forms comprised 24-36%. The Poaceae phytoliths are predominately derived from the Pooideae subfamily of C_3 grasses with an extremely limited presence of the Panicoideae subfamily of C_4 grasses. The most common characteristic Pooideae forms were rondels (18-22%) of *Agropyron* and

Festuca, short wavy crenates (15-23%) of *Poa* and *Koeleria*, long wavy crenates (2-8%) of *Calamagrostis* and *Stipa*, and long cells (7-14%) of *Agropyron* and *Festuca*. Bilobate shaped phytoliths of the Panicoideae subfamily were limited to (<1%) within the zone. Diagnostic *Stipa*-type bilobates were limited to (<1%) within the zone. The most common characteristic non-Poaceae phytoliths consisted of blocky forms (14-24%) of *Artemisia*, *Abies*, and *Picea*, epidermal polygonal (4-6%) of *Artemisia*, *Abies*, and Asteraceae, epidermal anticlinal (<1-1%) of Asteraceae, and other conifer forms (3-7%) of *Pinus*, *Abies*, *Picea*, or *Larix*. Diagnostic non-Poaceae forms were limited to *P. ponderosa* type representing (<1%) and *Carex* type representing (<1%) within the zone.

Interpretation: Zone VI (≤2,000 yr BP to present) contained fluctuating proportions of grass (64-76%) and non-grass (24-36%) phytolith forms. The assemblages of grass phytoliths suggest that a mix of C_3 Pooideae grasses existed at the site. The grass cover was predominately composed of *Agropyron*, *Festuca*, and *Poa* indicated by the frequencies of rondels, short wavy crenates, and long cell forms. A secondary and very minor component of the grass cover consisted of *Stipa* indicated by long wavy crenates and *Stipa*-type forms. The assemblages of non-grass forms suggest that a mix of arboreal and shrub species existed at the site. The arboreal and shrub cover was composed of members of the Asteraceae and Pinaceae Families indicated by the frequencies of blocky, epidermal, and both characteristic and diagnostic conifer forms. The identification of species composition of the arboreal and shrub communities is limited due to the observed redundancy in blocky and epidermal polygonal phytolith forms from the two families represented. However, the higher proportion of blocky (14-24%) and epidermal polygonal (4-6%) forms relative to other conifer (3-7%) forms and diagnostic *P.*

ponderosa types (<1%) would suggest that *Artemisia* and other Asteraceae species were the predominate contributors of the blocky and epidermal polygonal forms.

Collectively, the assemblages from Zone VI suggest that conditions continued to support a grass steppe community similar to Zone V. The frequencies of grass forms are relatively lower within the bottom of the Zone, indicating a continued decline in grass cover at the site that was observed within the top of Zone V, however. Grass cover expanded within the top of the Zone. The inferred vegetation consisted of Pooideae grasses with associations of *Artemisia* and other Asteraceae shrubs and/or herbs. The frequencies of long cells and rondels steadily increase towards the top of the zone, suggesting that *Agropyron* and *Festuca* expanded. The frequencies of other conifer forms and *P. ponderosa* types are similar to Zone V suggesting that Pinaceae species were present near the site. Zone VI assemblages suggest the continued existence of a grassland community that reflects the modern vegetation at the site.

Profile 10IH73 (Cooper's Ferry Site Unit A)

A total of seven sediment samples were processed from the stratigraphic profile of the north wall of 10IH73 Unit: A. Six of the samples produced sufficient quantities of well preserved phytoliths that permitted counting, classification, and identification of four phytolith zones. One sample recovered from LU2 did not contain sufficient quantities of phytoliths to permit counting and classification. This sample was recovered from 230-240 cm below the surface and underlies phytolith zone I.

The four phytolith zones (Figure 6.6) were established using the CONISS function in TILIA-GRAPH (Grimm 1993), which clustered stratigraphically adjacent

samples based on the changes in the frequencies of twenty distinct morphotypes. The four zones will now be discussed in ascending order.

*Phytolith Zone I (220-180 cm***)**

Results: Phytolith Zone I contained a single sample recovered from LU3 at a depth of 200-210 cm. The sample has an estimated age of >11,410±130 yr BP (Davis and Schweger 2004). Poaceae phytolith forms comprised 64% of the total assemblage and non-Poaceae phytolith forms comprised 36%. The Poaceae phytoliths are predominantly derived from the Pooideae subfamily of C_3 grasses with an extremely limited presence of both the Panicoideae and Chloridoideae subfamilies of C_4 grasses. The most common characteristic Pooideae forms were rondels (17%) of *Agropyron* and *Festuca,* short wavy crenates (17%) of *Poa* and *Koeleria*, long wavy crenates (3%) of *Calamagrostis* and *Stipa,* and long cells (4%) of *Agropyron* and *Festuca*. Bilobate shaped phytoliths of the Panicoideae subfamily were limited to (1%) and saddle shaped phytoliths of the Chloridoideae subfamily were limited to (<1%) within the zone. Diagnostic *Stipa*-type bilobates were limited to (2%) within the zone. The most common characteristic non-Poaceae phytoliths consisted of blocky forms (13%) of *Artemisia, Abies,* and *Picea,* epidermal polygonal (13%) of *Artemisia*, *Abies,* and Asteraceae, epidermal anticlinal (3%) of Asteraceae, and other conifer forms (5%) of *Pinus, Abies*, *Picea*, or *Larix*. Diagnostic non-Poaceae forms were limited to *P. ponderosa* type representing (<1%) and *Carex* type representing (<1%) within the zone.

Interpretation: Zone I (>11,410±130 yr BP) represents the single assemblage recovered from LU3 at the Cooper's Ferry Site. The assemblage contains a high proportion of grass (64%) phytolith forms relative to non-grass (36%) phytolith forms.

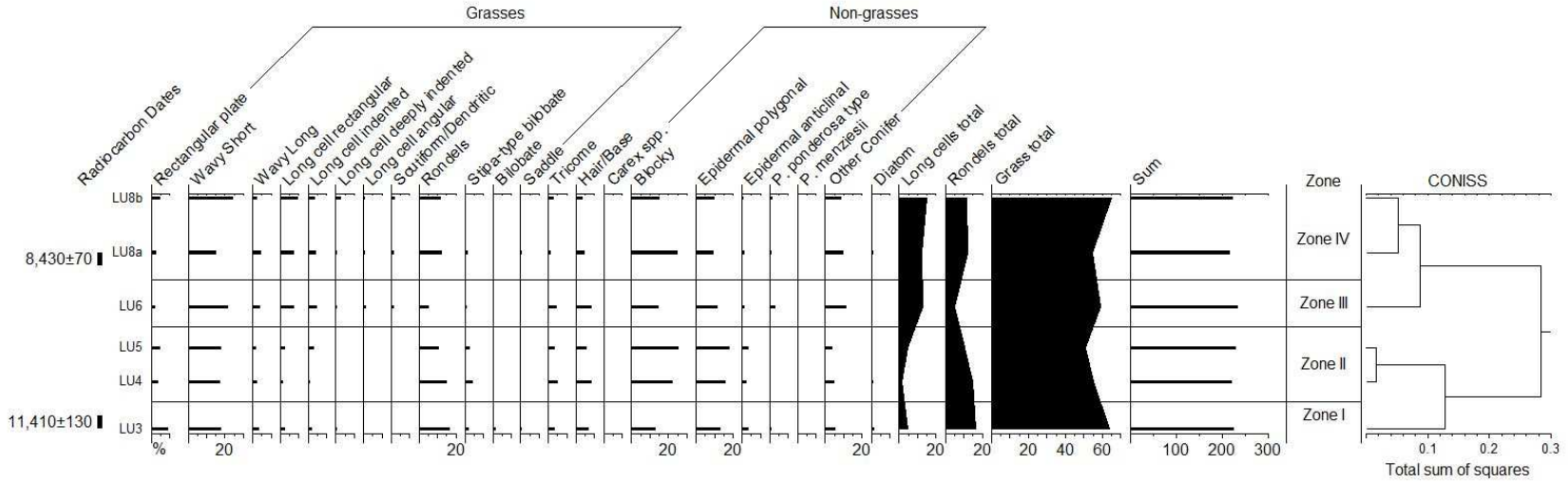

Figure 6.6 10IH73 phytolith profile. LU= lithostratigraphic unit.

The assemblage of grass phytolith forms suggest that a mix of C_3 Pooideae grasses existed at the site. The grass cover was predominately composed of *Agropyron*, *Festuca*, and *Poa* indicated by the frequencies of rondels, short wavy crenates, and long cell forms. A secondary and minor component of the grass cover consisted of *Stipa* indicated by the long wavy crenates and *Stipa*-type forms. Additionally, it is noted that a very low frequency of bilobate (1%) and saddle (<1%) shaped phytoliths of the Panicoideae and Chloridoideae subfamilies. The assemblages of non-grass forms suggest that a mix of arboreal and shrub species existed at the site. The arboreal and shrub cover was composed of members of the Asteraceae and Pinaceae Families indicated by the frequencies of blocky, epidermal, and both characteristic and diagnostic conifer forms. The identification of species composition of the arboreal and shrub communities is limited due to the observed redundancy in blocky and epidermal polygonal phytolith forms from the two families represented. However, the higher proportion of blocky (13%) and epidermal polygonal (13%) forms relative to other conifer forms (5%) and diagnostic *P. ponderosa* types (<1%) would suggest that *Artemisia* and other Asteraceae species were the predominate contributors of the blocky and epidermal polygonal forms.

The Zone I phytolith assemblage recovered from LU3 is associated with the Rock Creek Soil, whiched formed within the LSRC between ca. 10,740 and 13,000 yr BP (Davis 2001a). The period of relative landscape stability and soil formation associated with this cambic horizon observed at 10IH73 could have provided an opportunity for the phtyolith assemblages associated with different vegetative conditions to become mixed together if conditions changed significantly during the period of stability. Fredlund and Tieszen (1994:331) refer to this process of mixing as “inheritance”, which acknowledges

the potential of long-term (hundreds of years or more) mix of phytolith assemblages with soils. Therefore, the assemblage associated with the paleosol should be interpreted as a representation of the long-term average of vegetative conditions at the site. With regards to Zone I at 10IH73, the sample recovered from the Rock Creek Soil horizon likely reflects the mixture of grass and shrub steppe communities within the riparian zone.

Collectively, the assemblage from Zone I suggest the existence of a grass steppe community. The inferred vegetation consisted of Pooideae grasses with associations of *Artemisia* and other Asteraceae shrubs and/or herbs. The high frequencies of rondels and short wavy crenates suggest that *Festuca* and *Poa* were the predominate component of the grass cover at the site. The low frequencies of other conifer forms and diagnostic *P. ponderosa* types suggest that Pinaceae species were present near the site.

Phytolith Zone II (180-130 cm)

Results: Phytolith Zone II contains two samples recovered from LU4 at a depth of 160-170 cm and LU5 at a depth of 130-140 cm. The samples have an estimated age of >8,430±70 to <11,410±130 yr BP (Davis and Schweger 2004). Poaceae phytolith forms comprised 51-55% of the total assemblage and non-Poaceae phytolith forms comprised 45-49%. The Poaceae phytoliths are predominantly derived from the Pooideae subfamily of C_3 grasses with an extremely limited presence of the Panicoideae subfamily of C_4 grasses. The most common characteristic Pooideae forms were rondels (11-15%) of *Agropyron* and *Festuca*, short wavy crenates (17-18%) of *Poa* and *Koeleria*, long wavy crenates (2%) of *Calamagrostis* and *Stipa*, and long cells (1-5%) of *Agropyron* and *Festuca*.

Bilobate shaped phytoliths of the Panicoideae subfamily were limited to (<1%) within the zone. Diagnostic *Stipa*-type bilobates were limited to (2-4%) within the zone. The most common characteristic non-Poaceae phytoliths consisted of blocky forms (22-25%) of *Artemisia*, *Abies*, and *Picea*, epidermal polygonal (16-18%) of *Artemisia*, *Abies*, and Asteraceae, epidermal anticlinal (2-3%) of Asteraceae, and other conifer forms (4-5%) of *Pinus*, *Abies*, *Picea*, or *Larix*. No diagnostic non-Poaceae forms were identified within the zone.

Interpretation: Zone II (>8,430±70 to <11,410±130 yr BP) represents two samples recovered from LU4 and LU5 at the site. The assemblages contain fluctuating proportions of grass (51-55%) and non-grass (45-49%) phytolith forms. However, the zone contains a relatively lower proportion of grass forms compared to Zone I. The assemblages of grass phytoliths suggest that a mix of C_3 Pooideae grasses existed at the site. The grass cover was predominately composed of *Agropyron, Festuca,* and *Poa* indicated by the frequencies of rondels, short wavy crenates, and long cell forms. A secondary and minor component of the grass cover consisted of *Stipa* indicated by the long wavy crenates and *Stipa*-type forms. Additionally, it is noted that a very low frequency of bilobate (<1%) shaped phytoliths of the Panicoideae subfamily were observed in the sample from LU5. The assemblages of non-grass forms suggest that a mix of arboreal and shrub species existed at the site. The arboreal and shrub cover was composed of members of the Asteraceae and Pinaceae Families indicated by the frequencies of blocky, epidermal, and both characteristic and diagnostic conifer forms. The identification of species composition of the arboreal and shrub communities is limited due to the observed redundancy in blocky and epidermal polygonal phytolith

forms from the two families represented. However, the higher proportion of blocky (22-25%) and epidermal polygonal (16-18%) forms relative to other conifer forms (4-5%) and lack of diagnostic Pinaceae forms would suggest that *Artemisia* and other Asteraceae species were the predominate contributors of the blocky and epidermal polygonal forms.

Collectively, the assemblages from Zone II suggest that conditions transitioned into a shrub steppe community. The inferred vegetation consisted of *Artemisia* and other Asteraceae shrubs and/or herbs with associations of Pooideae grasses. The frequencies of rondels and short wavy crenates associated with the sample from LU4 suggest that *Festuca* and *Poa* were the predominate components of the grass community. The sample from LU5 indicates a decline in rondel frequencies while long cell frequencies increase. This would suggest that conditions became drier as local moisture availability declined at the site, which allowed *Agropyron* to expand. The low frequency of other conifer forms and lack diagnostic *P. ponderosa* types suggest that Pinaceae species were still present near the site.

Phytolith Zone III (130-100 cm)

Results: Phytolith Zone III contains a single sample recovered from LU6 at a depth of 110-120 cm. The sample has an estimated age of >8,430±70 to <11,410±130 yr BP (Davis and Schweger 2004). Poaceae phytolith forms comprised 59% of the total assemblage and non-Poaceae phytolith forms comprised 41%. The Poaceae phytoliths are all derived from the Pooideae subfamily of C_3 grasses. The most common characteristic Pooideae forms were rondels (5%) of *Agropyron* and *Festuca*, short wavy crenates (22%) of *Poa* and *Koeleria*, long wavy crenates (4%) of *Calamagrostis* and *Stipa*, and long cells (13%) of *Agropyron* and *Festuca*. Diagnostic *Stipa*-type bilobates were limited to (1%)

within the zone. The most common characteristic non-Poaceae phytoliths consisted of blocky forms (14%) of *Artemisia, Abies,* and *Picea,* epidermal polygonal (11%) of *Artemisia, Abies,* and Asteraceae, epidermal anticlinal (1%) of Asteraceae, and other conifer forms (11%) of *Pinus, Abies, Picea,* or *Larix*. Diagnostic non-Poaceae forms were limited to *P. ponderosa* type representing (3%) and *Carex* type representing (<1%) within the zone.

Interpretation: Zone III (>8,430±70 to <11,410±130 yr BP) represents a single sample recovered from LU6 at the site. The assemblage contains a high proportion of grass (59%) phytolith forms relative to non-grass (41%) phytolith forms. However, the zone contains a relatively higher proportion of grass forms compared to Zone II. The assemblage of grass phytoliths suggest that a mix of C_3 Pooideae grasses existed at the site. The grass cover was predominately composed of *Agropyron, Festuca,* and *Poa* indicated by the frequencies of rondels, short wavy crenates, and long cell forms. A secondary and minor component of the grass cover consisted of *Stipa* indicated by the long wavy crenates and *Stipa*-type forms. The assemblages of non-grass forms suggest that a mix of arboreal and shrub species existed at the site. The arboreal and shrub cover was composed of members of the Asteraceae and Pinaceae Families indicated by the frequencies of blocky, epidermal, and both characteristic and diagnostic conifer forms. The identification of species composition of the arboreal and shrub communities is limited due to the observed redundancy in blocky and epidermal polygonal phytolith forms from the two families represented. However, the higher proportion of blocky (14%) and epidermal polygonal (11%) forms relative to other conifer forms (11%) and

diagnostic *P. ponderosa* types (3%) would suggest that *Artemisia* and other Asteraceae species were the predominate contributors of the blocky and epidermal polygonal forms.

The Zone III phytolith assemblage recovered from LU6 is associated with an unnamed incipient paleosol identified by Davis and Schweger (2004). The incipient paleosol fromed within the LU6 alluvium between ca. 8,430 and 11,410 yr BP and reflects a period of relative landscape stability and soil formation along the floodplain of the LSRC. The phytolith assemblage associated with this cambic horizon observed at 10IH73 could have provided an opportunity for the phtyolith assemblages associated with different vegetative conditions to become mixed together if conditions changed significantly during the period of stability. Fredlund and Tieszen (1994:331) refer to this process of mixing as “inheritance”, which acknowledges the potential of long-term (hundreds of years or more) mix of phytolith assemblages with soils. Therefore, the assemblage associated with the paleosol should be interpreted as a representation of the long-term average of vegetative conditions at the site. With regards to Zone III at 10IH73, the sample recovered from the paleosol likely reflects the mixture of grass and shrub steppe communities within the riparian zone.

Collectively, the assemblage from Zone III suggests the continued existence of a shrub steppe community; however, the increase in grass phytolith forms suggests that these communities were expanding relative to Zone II. The inferred vegetation consisted of *Artemisia* and other Asteraceae shrubs and/or herbs with associations of Pooideae grasses. The frequency of rondels declined while long cells increased suggesting that *Agropyron* expanded. This may reflect a continued reduction in local moisture availability at the site, which promoted the decline of *Festuca*. The frequency of other

conifer forms and diagnostic *P. ponderosa* types increased relative to Zone II, which suggests an expansion of Pinaceae species near the site.

Phytolith Zone IV (100-20 cm)

Results: Phytolith zone IV contains two samples recovered from LU8a at a depth of 70-80 cm and LU8b at a depth of 30-40 cm. The samples have an estimated age of >8,430±70 to <11,410±130 yr BP (Davis and Schweger 2004). Poaceae phytolith forms comprised 55-65% of the total assemblage and non-Poaceae phytolith forms comprised 35-45%. The Poaceae phytoliths are predominantly derived from the Pooideae subfamily of C_3 grasses with an extremely limited presence of both the Panicoideae and Chloridoideae subfamilies of C_4 grasses. The most common characteristic Pooideae forms were rondels (12%) of *Agropyron* and *Festuca,* short wavy crenates (15-24%) of *Poa* and *Koeleria,* long wavy crenates (2-4%) of *Calamagrostis* and *Stipa,* and long cells (12-15%) of *Agropyron* and *Festuca*. Bilobate shaped phytoliths of the Panicoideae subfamily were limited to (<1%) and saddle shaped phytoliths of the Chloridoideae subfamily were limited to (<1%) within the zone. Diagnostic *Stipa*-type bilobates were limited to (1%) within the zone. The most common characteristic non-Poaceae phytoliths consisted of blocky forms (15-25%) of *Artemisia, Abies,* and *Picea,* epidermal polygonal (9-10%) of *Artemisia, Abies,* and Asteraceae, epidermal anticlinal (<1-1%) of Asteraceae, and other conifer forms (9%) of *Pinus, Abies, Picea,* or *Larix*. Diagnostic non-Poaceae forms were limited to *P. ponderosa* type representing (<1-1%) within the zone.

Interpretation: Zone IV (>8,430±70 to <11,410±130 yr BP) represents two samples recovered from LU8a and LU8b at the site. The assemblages contain fluctuating proportions of grass (55-65%) and non-grass (35-45%) phytolith forms. The assemblages

of grass phytoliths suggest that a mix of C_3 Pooideae grasses existed at the site. The grass cover was predominately composed of *Agropyron, Festuca,* and *Poa* indicated by the frequencies of rondels, short wavy crenates, and long cell forms. A secondary and minor component of the grass cover consisted of *Stipa* indicated by the long wavy crenates and *Stipa*-type forms. Additionally, it is noted that a very low frequency of bilobate (<1%) and saddle (<1%) shaped phytoliths of the Panicoideae and Chloridoideae subfamilies were observed in the sample from LU8a. The assemblages of non-grass forms suggest that a mix of arboreal and shrub species existed at the site. The arboreal and shrub cover was composed of members of the Asteraceae and Pinaceae Families indicated by the frequencies of blocky, epidermal, and both characteristic and diagnostic conifer forms. The identification of species composition of the arboreal and shrub communities is limited due to the observed redundancy in blocky and epidermal polygonal phytolith forms from the two families represented. However, the higher proportion of blocky (15-25%) and epidermal polygonal (9-10%) forms relative to other conifer forms (9%) and diagnostic *P. ponderosa* types (<1-1%) would suggest that *Artemisia* and other Asteraceae species were the predominate contributors of the blocky and epidermal polygonal forms.

Collectively, the assemblages from Zone IV suggest the continued existence of a shrub steppe community, however. The sample from LU8b contains a higher frequency of grass phytolith forms, which suggests that conditions were transitioning towards a grass steppe community relative to the sample from lithostratigraphic unit 8a as well as Zone III. The inferred vegetation consisted of *Artemisia* and other Asteraceae shrubs and/or herbs with associations of Pooideae grasses. The frequencies of rondels increased

relative to Zone III, which suggests an increase in local moisture availability and expansion of *Festuca*. Both long cell and rondel forms remain stable throughout Zone IV. The frequency of other conifer forms and diagnostic *P. ponderosa* types were similar to Zone III, which suggests that Pinaceae species persisted near the site.

Chapter 7: Discussion

Late Quaternary Paleoenvironments and Human Ecology of the Lower Salmon River Canyon

The phytolith records obtained from SR-23, SR-27, and SR-34 characterize the late Quaternary vegetation patterns associated with lower elevation canyon slopes adjacent to the riparian zones of the LSRC. The phytolith record from 10IH73 characterizes the vegetative patterns of the riparian zone during the late Pleistocene and early Holocene. Comparisons of the phytolith records obtained from this study with previous phytolith studies in the LSRC (Davis and Collins 2009; Somer 2003) and other locally derived paleoenvironmental data sets (Davis 2001a; Davis and Muehlenbachs 2001; Davis et al. 2002; Davis and Schweger 2004) aid in the reconstruction of paleoecological conditions of the LSRC. Discussion of the autecologies (i.e., ecological study of an individual organism or species) of local faunal communities of the Columbia River Plateau (Chatters 1998), Idaho (Scott et al. 2002), and the LSRC (Davis 2001a) provides information regarding the ecological requirements of species that may have been utilized by prehistoric hunter-gatherers for subsistence purposes. Together, these data sets contribute to the development of a human ecological framework which aims to contextualize the biophysical environment that prehistoric hunter-gatherer socioeconomic systems were adapted.

The late Quaternary paleoenvironmental conditions represented by the phytolith assemblages from SR-23, SR-27, SR-34, and 10IH73 suggest that fluctuating environmental conditions supported shrub and grass steppe environments within the LSRC for the last ca. 22,000 yr BP. Comparisons made here between phytolith records

and local and paleoclimate proxy records indicate that shifts in the LSRC vegetation were driven by changes in local temperature and moisture availability. Locally derived stable isotope records obtained from river mussel shell carbonate (Davis and Muehlenbachs 2001) and pedogenic carbonate (Davis et al. 2002) provide paleoenvironmental proxy records from which comparisons to the phytolith assemblage data can be made. Pedogenic carbonates provided a measure of $\delta^{18}O$ and $\delta^{13}C$ spanning a period of ca. 24,000-21,000 yr BP and ca. 18,000-2,000 yr BP. Increased concentrations of $\delta^{18}O$ and $\delta^{13}C$ are associated with arid conditions and expansions of C_4 plants, while decreases in the concentrations of these isotopes are associated with more temperate conditions and expansions of C_3 plant communities (Davis et al. 2002). Measures of $\delta^{18}O$ concentrations derived from river mussel shells provide a proxy record of precipitation spanning a period of ca. 12,000-8,000 yr BP and ca. 5,000 yr BP to present. Relative to the modern concentration value of $\delta^{18}O$ (13.6‰) increased concentrations from archaeological samples indicate periods of decreased precipitation, while decreased concentrations indicate periods of increased precipitation (Davis and Muehlenbachs 2001).

It should be noted that Blinnikov's (2005) phytolith classification system for the region acknowledges redundancy of blocky forms in *Artemisia, Picea,* and *Abies*. However, there was an observed correlation in the frequency of blocky forms, *Artemisia,* and presence of cicada burrows in the loess sections from the Columbia Basin (Blinnikov et al. 2001). Cicada burrow activity has been observed in many of the late Pleistocene and Holocene-aged loess sections within the LSRC (Loren Davis, personal communication 2014), suggesting the presence of *Artemisia* communities during these periods. While O'Geen (1998) demonstrated the correlation between per volume cicada

burrow activity with presence of *Artemisia*, no attempt has been made to quantify the per volume abundance of cicada burrow activity within the stratigraphic sections discussed in this study. However, the current study does argues that blocky forms identified within the phytolith assemblages from the stratigraphic sections from the LSRC reflect *Artemisia* communities based on the relative lack in the frequency of other diagnostic and characteristic conifer forms associated with subalpine *Picea* forest assemblages reported by Blinnikov (2005). This interpretation of blocky forms from the LSRC will be used to re-evaluate the inferred vegetation proposed by previous phytolith studies from low elevation localities in the LSRC (Davis and Collins 2009; and Somer 2003) within the discussions of late Pleistocene, late Pleistocene-early Holocene, middle Holocene, and late Holocene periods.

Late Pleistocene Human Ecology of the LSRC ca. 24,000-12,000 yr BP

Paleoclimate

During the late Pleistocene, $\delta^{18}O$ and $\delta^{13}C$ records from pedogenic carbonate samples dating between ca. 24,000-21,000 yr BP indicate cold temperatures within the LSRC, with the coldest temperatures recorded ca. 21,000 yr BP; during this period $\delta^{13}C$ concentrations indicate fluctuations between dry and wet conditions, with the wettest period recorded ca. 21,000 yr BP (Davis et al. 2002). There is a gap in the $\delta^{18}O$ and $\delta^{13}C$ pedogenic carbonate between ca. 21,000-18,000 yr BP. Following the period associated with this gap in the pedogenic isotope data the $\delta^{18}O$ and $\delta^{13}C$ records indicate that conditions became relatively warmer, drier, and stable compared to the >18,000 yr BP data (Davis et al. 2002).

Paleovegetation

The late Pleistocene vegetation of low elevation canyon slopes adjacent to the Salmon River is inferred from the phytolith assemblages obtained from SR-23 Zones I-III (this study) and Zones I-II (Somer 2003), SR-26C and lower portion of SR-26A (Somer 2003), SR-27 Zones I-IV, SR-34 Zones I-III, and the LU14a assemblage from American Bar (10IH395) (Davis and Collins 2009). Collectively, these phytolith assemblages are interpreted primarily as indicators of Poaceae, Asteraceae, and limited Pinaceae vegetative communities respectively. These communities reflect the presence of shrub steppe vegetation along the lower elevation canyon slopes during this period.

Assemblages from SR-34 Zones I-II (>22,000 to >15,000 yr BP) indicate the presence of *Artemisia* with primary associations of Pooideae grasses, secondary associations of unidentified Asteraceae shrubs/herbs, and limited arboreal Pinaceae cover. Fluctuations in the grass assemblages suggest that prior to 22,000 yr BP that conditions were relatively dry, favoring *Agropyron* and *Poa*. Sometime after 22,000 yr BP the grass assemblage data suggests conditions became relatively wetter favoring expansion of *Festuca,* which appears to correlate with a wet interval observed in the $\delta^{13}C$ data just after ca. 21,000 yr BP (Davis et al. 2002). Pinaceae phytolith forms from these zones are very limited suggesting that these species were present in the LSRC possibly as isolated or scattered stands in the vicinity of SR-34.

The gap in the $\delta^{18}O$ and $\delta^{13}C$ records from pedogenic carbonate between 21,000-18,000 yr BP corresponds with the assemblages from SR-34 Zone II and SR-27 Zone I. Both of these assemblages indicate the continued presence of *Artemisia* with primary associations of Pooideae grasses, secondary associations of unidentified Asteraceae

shrubs/herbs, and limited arboreal Pinaceae cover. Grass assemblages indicate that wet conditions persisted, supporting *Festuca* communities. However, fluctuations observed in the frequencies of the grass assemblages from SR-34 Zone II suggest that brief intervals of increased aridity occurred between 19,000-18,000 yr BP, causing *Festuca* communities and grass coverage at large to decline. Pinaceae phytolith frequencies remained low during this period.

The assemblages from SR-26C (Somer 2003) and LU14a from American Bar (Davis and Collins 2009) also correspond with this period of 21,000-18,000 yr BP. While Davis and Collins (2009) acknowledge errors related to Somer's (2003) stratigraphy of SR-26, Somer observed little variation in the phytolith assemblages from SR-26C (ca. 21,000-18,000) and SR-26A (ca. 15,400-9,600 yr BP) and argued vegetative stability in the vicinity of the Lyons Bar locality, which allows for some discussion and comparisons with the data sets from this study. The SR-26C assemblage was interpreted as reflecting a Pooideae grassland community with limited *Picea* and/or *Pinus* in the vicinity (Somer 2003). The LU14a assemblage was interpreted as reflecting the presence of arboreal vegetation consisting of *Pinus, Picea,* and limited *Pseudotsuga menziesii* with associations of Pooideae grasses (Davis and Collins 2009). Both the SR-26C and LU14a assemblages interpreted blocky phytolith forms as characteristic indicators of *Pinus* and *Picea.* Given the higher frequencies of blocky forms relative to other characteristic and diagnostic Pinaceae forms identified, this study argues that these assemblages reflect the presence of *Artemisia* and Poaceae communities during this period rather than a *Pinus* and *Picea* forest community.

The assemblages from SR-23 Zones I-III (this study) and Zones I-II (Somer 2003), SR-26A, SR-27 Zones II-IV, and SR-34 Zones II-III correspond with the remaining late Pleistocene period ca. 18,000-12,000 yr BP. Collectively, these assemblages indicate the continued presence of *Artemisia* with primary associations of Pooideae grasses, secondary associations of unidentified Asteraceae shrubs/herbs, and limited arboreal Pinaceae cover. Grass assemblages from these zones fluctuate during this period, suggesting relative climatic instability as conditions fluctuated between wetter and drier intervals respectively. Pooideae grasses appear to track these fluctuations as *Festuca* communities expand during relatively wette periods and contract during relatively drier intervals. Again, the low frequencies of blocky forms observed by Somer (2003) are argued to represent *Artemisia* rather than *Picea* and *Pinus* by this study. Diagnostic and characteristic Pinaceae phytoliths frequencies remain limited during the rest of this period, suggesting these species were present in the LSRC as isolated or scattered stands in the vicinity of the sections sampled.

Human Ecology

Despite the lack of archaeological evidence within the LSRC during this period it is possible to discuss the generalized economic opportunities that may have existed in the canyon during this time. The shrub steppe vegetative communities inferred from the phytolith assemblages derived from the low elevation canyon slopes would have supported a variety of faunal communities (Table 7.1). Density and distribution of faunal resources is primarly dependent upon the local environmental productivity of a given area. The relatively sparse shrub steppe vegetative cover on the canyon slopes may have supported lower densities of faunal resources while the riparian zone may have

Table 7.1 Faunal resources within the LSRC may have included, but were not limited to the following species (adapted from Chatters 1998; Davis 2001a; Scott et al. 2002).

Avian Species	
Common Name	Scientific Name
Grouse	e.g., *Centrocercus urophasianus, Tympanuchus phasianellus, Bonasa umbellus*
Quail	e.g., *Oreortyx pictus, Callipepla californica*
Prairie Falcon	*Falco mexcanus*
Eagles	e.g., *Haliaeetus leucocephalus, Aquila chrysateos*
Hawks	e.g., *Accipiter straitus, Buteo jamaicensis*
Sage Sparrows	*Amphispiza belli*
Sage Thrasher	*Oreoscoples montanus*
Ducks	e.g., *Aix sponsa, Anas platyrhynchos, Mergus merganser*
Owls	e.g., *Bubo virginianus, Otus kennicotti*
Wild Turkey	*Meleagris gallopavo*
Geese	e.g., *Branta canadensis*
Small Mammalian Species	
Badger	*Taxidea taxus*
Rabbits	e.g., *Lepus californicus, L. townsendii, Sylvilagus idahoensis, Brachylagus idahoensis*
Mink	*Mustela vison*
Ground Squirrel	*Spermophilus beldingi*
Gopher	*Thomamys idahoensis*
Wood Rat	*Neotoma cinerea*
Raccoon	*Procyon lotor*
Porcupine	*Erethizon dorsatum*
Coyote	*Canus latrans*
Bobcat	*Lynx rufus*
Large Ungulate Mammalian Species	
Elk	*Cervus elaphus*
Deer	e.g., *Odocoileus hemionus, O. virginianus*
Bighorn Sheep	*Ovis canadensis*
Pronghorn	*Antilocapra americana*
Bison	e.g., *Bison antiquus, B. bison*
Aquatic Species	
River Mussels	e.g., *Margaritifera falcata, Gonidea angulata*
Salmon	e.g., *Oncorhynchus tschawytsha, O. kisutch*
Steelhead Trout	*O. mykiss*
Cutthroat Trout	*O. clarki*
Dolly Varden Trout	*Salvelinus malma*
Northern Pikeminnow	*Ptychocheilus oregonensis*
Chiselmouth	*Acrocheilus alutaceus*
Mountain Whitefish	*Prosopium williamsoni*

experienced greater vegetative productivity and in turn higher densities of these resources (Chatters 1998; Davis 2001a; Scott et al. 2002).

The larger ungulate species occupy a variety of different habitats; however, they all share the basic requirements of water, adequate forage, and vegetative cover for protection from predators and the elements respectively. Drawing on the autecologies associated with these ungulate species (Chatters 1998, Davis 2001a; Scott et al. 2002) it is possible to make some generalized statements regarding their occurrence within the LSRC during this period relative to the composition of associated vegetative communities.

Elk and deer will typically inhabit areas that transition between arboreal and non-arboreal vegetation, which provides them both with access to food and cover (Chatters 1998; Davis 2001a). The relatively sparse arboreal vegetative cover inferred from the phytolith assemblages suggest that elk and deer population densities may have been relatively low during this period; these species may have been found in areas with scattered or isolated stands of conifers located along the canyon slopes and tributary drainages. Bighorn sheep have similar requirements as elk and deer; however, they are less concerned with cover as they typically inhabit grassy areas adjacent to steep slopes that provide easy escape from predators (Chatters 1998; Davis 2001a). The shrub steppe vegetation and associated grasses may have supported higher densities of bighorn relative to elk and deer during this period. Bison and pronghorn share similar habitat requirements consisting of open grasslands typically associated with open plains or prairies, both of which would provide adequate forage and open spaces for escape from potential predators (Chatters 1998; Davis 2001a). While the shrub steppe vegetation and

associated grasses may have provided adequate forage for bison and pronghorn, the relatively narrow and steep canyons may have limited these species to the upland prairies adjacent to the canyon. Therefore, bison and pronghorn population densities were likely very low or non-existent within the lower elevation of the canyon.

Late Pleistocene-Early Holocene Human Ecology of the LSRC ca. 12,000-9,000 yr BP

Paleoclimate

During the late Pleistocene-early Holocene transition (ca. 12,000-9,000 yr BP), $\delta^{18}O$ and $\delta^{13}C$ records from pedogenic carbonate samples and $\delta^{18}O$ records obtained from river mussel shell indicate unstable climatic conditions during this relatively brief period (Davis and Muehlenbachs 2001; Davis et al. 2002). The isotope concentrations recovered from these data sets fluctuate widely as reflecting relatively warmer and drier conditions ca. 12,000 yr BP, which is immediately followed by a pronounced shift to cooler and wetter conditions. By 11,000 yr BP warm and dry conditions returned in the LSRC. This is followed by multiple, less pronounced eposides of warm/dry and cool/wet conditions between 11,000-9,000 yr BP (Davis and Muehlenbachs 2001; Davis et al. 2002).

Paleovegetation

The late Pleistocene-early Holocene transition vegetation of the LSRC riparian zone is inferred from the phytolith assemblages obtained from Cooper's Ferry 10IH73 Zones I-II (this study) and LU3-LU5 (Davis and Collins 2009). Collectively, these phytolith assemblages are interpreted primarily as indicators of Poaceae, Asteraceae, and limited Pinaceae vegetative communities respectively. These communities reflect the presence of a grass steppe during the terminal Pleistocene, which appears to transition towards a shrub steppe during the early Holocene as Poaceae frequencies decline.

The assemblage recovered from Zone I of this study is associated with a sample from LU3 and indicates the presence of Pooideae grasses with primary associations of *Artemisia,* other unidentified Asteraceae shrubs/herbs, and limited arboreal Pinaceae cover. Grass assemblages suggest that conditions were relatively wet, which supported *Festuca* at the site. These relatively wet conditions appear to correlate with the pronounced cool/wet interval observed in the isotope data sets (Davis and Muehlenbachs 2001; Davis et al. 2002). Interestingly, the LU3 assemblage reported by Davis and Collins (2009) indicates a higher frequency of *Pinus* and *Picea* phytoliths relative to Poaceae forms, which does not correlate well with the Zone I data from this study.

The two assemblages from Zone II of this study are associated with LU4 and LU5 and reflect a decline in Pooideae grasses relative to *Artemisia,* other unidentified Asteraceae shrubs/herbs, and Pinaceae suggesting a transition from grass steppe to a shrub steppe community. The LU4 and LU5 assemblages reported by Davis and Collins (2009) reflect an overall increase in Poaceae forms relative to their LU3 assemblage suggesting expansion of the Pooideae grasses at the site. However, the relative frequency of Poaceae forms overall from their LU4 and LU 5 assemblages are similar to the Zone II assemblages from this study. The Zone II grass assemblages suggest that conditions became relatively warmer and drier causing *Festuca* to decline as *Agropyron* expanded. This period of increased temperatures and aridity appears to correlate with the onset of a relatively warm/dry period observed in the isotope data that occurred ca. 11,000 yr BP (Davis and Muehlenbachs 2001; Davis et al. 2002).

Again, this study argues that the blocky phytolith forms reported by Davis and Collins (2009) reflect the presence of *Artemisia* rather than Pinaceae species due to the

very limited frequencies characteristic and diagnostic Pinaceae types observed from both studies. Pinaceae phytolith forms from these zones are very limited suggesting that these species were present in the LSRC possibly as isolated or scattered stands in the vicinity of Cooper's Ferry.

Human Ecology

The late Pleistocene-early Holocene transition is associated with the earliest archaeological evidence of prehistoric hunter-gatherers in the LSRC. This evidence comes from Cooper's Ferry and is associated with the Cooper's Ferry Phase I (11,500-11,000 yr BP) and Phase II (11,000-8,400 yr BP) (Davis 2001b). Cooper's Ferry Phase I is characterized by the presence of WST lithic technologies in association with a pit cache that contained four stemmed projectile points, two cores, two blades, one uniface, and a hammer stone. Other artifacts included bifaces, unifaces, multidirectional flake cores, and modified flakes (Davis 2001b). The faunal assemblages consisted of unidentified ungulate bones bearing cut marks, river mussel shell, and land snail shell (Davis 2001a). Cooper's Ferry Phase II is characterized by the continued manufacture and use of WST lithic technologies observed in Phase I assemblages in addition to lanceolate projectile points, larger scrapers, and unlined hearth features. Faunal assemblages are also similar to Cooper's Ferry Phase I; however, increased fish exploitation is inferred from the faunal remains (Davis 2001b).

The grass steppe and shrub steppe vegetation inferred from the phytolith assemblages derived from Cooper's Ferry may have continued to support similar faunal communities associated with the late Pleistocene assemblages (Table 7.1). Small mammal and bird communities would have likely continued to occur in higher densities

within the LSRC lusher riparian zones compared to adjacent canyon slopes (Chatters 1998; Davis 2001a; Scott et al. 2002). The inferred vegetation still suggests relatively spares arboreal cover in the LSRC, which may have continued to support relatively low densities of elk and deer. Bighorn sheep densities may have remained relatively higher compared to elk and deer during this period of grass and shrub steppe vegetation. Pronghorn and bison could have been supported by the inferred vegetation; however, as previously discussed, the narrow and steep canyon may have limited these species to the upland prairies adjacent to the canyon.

Additionally, the river itself provided a number of economically important aquatic resources that appear in the archaeological record associated with this period. These resources are not tied to the terrestrial productivity of the LSRC and therefore would have provided a relatively stable and reliable subsistence sources for prehistoric hunter-gatherer groups during this period (Chatters 1998). The continued and increased use of these resources is seen within the faunal assemblages associated with Cooper's Ferry Phases I and II (Davis 2001b).

Middle Holocene Human Ecology of the LSRC ca. 9,000-5,000 yr BP

Paleoclimate

During the middle Holocene (ca. 9,000-5,000 yr BP), $\delta^{18}O$ records from pedogenic carbonate samples continued to exhibit fluctuations in local temperatures; however, these fluctuations are not as pronounced as the variability observed during the late Pleistocene-early Holocene transition with conditions characterized as warmer and drier. The $\delta^{13}C$ records from pedogenic carbonate samples indicate more stability between ca. 8,500-6,000 yr BP with relatively drier conditions compared to the late

Pleistocene-early Holocene transition; however, between ca. 6,000-5,000 yr BP the record indicates a brief period of relatively wetter conditions followed by the return to arid conditions (Davis et al. 2002). The $\delta^{18}O$ records from river mussel shell samples are largely absent from the period with only four data points indicating arid conditions ca. 9,000 yr BP followed by wet conditions though ca. 8,000 yr BP after which arid conditions returned (Davis and Muehlenbachs 2001). Following the data point immediately after 8,000 yr BP there is a gap in the record until just after 5,000 yr BP.

Paleovegetation

The middle Holocene vegetation of the LSRC is inferred from phytolith assemblages recovered from low elevation canyon slopes at SR-23 Zones III-IV (this study) and Zone III (Somer 2003), SR-27 top of Zone III, SR-34 Zone IV, and the LU14b assemblage from American Bar (10IH395) (Davis and Collins 2009). Riparian vegetation is inferred from the assemblages recovered from Cooper's Ferry Zone IV (this study) and the LU8a assemblage (Davis and Collins 2009). Collectively, these phytolith assemblages are interpreted primarily as indicators of Poaceae, Asteraceae, and limited Pinaceae vegetative communities respectively. These communities reflect the presence of transitionary grass steppe/shrub steppe vegetation along the lower elevation canyon slopes and riparian zones along the LSRC during this period.

The assemblages recovered from SR-23 Zones III-IV (this study) indicate the presence of *Artemisia* with primary associations of Pooideae grasses, secondary associations of unidentified Asteraceae shrubs/herbs, and limited arboreal Pinaceae cover. Grass assemblages suggest that conditions were relatively wet, supporting *Festuca* during this period; however, some fluctuations are observed suggesting arid periods

occurred, causing decline in *Festuca* relative to *Agropyron* and *Poa.* Somer's (2003) Zone III indicates a greater presence of Pooideae grasses relative to Zones III-IV from this study; however, both grass assemblages suggest relatively wet conditions at SR-23. The assemblage from the top of Zone III at SR-27 exhibits a similar trend of relatively wet conditions supporting *Festuca.* The isotope data from SR-23 indicates that conditions were relatively warm and dry between ca. 8,000-5,500 yr BP (Davis et al. 2002); this does not correlate very well with the associated phytolith assemblages suggesting a possible disconnect may exist between the two data sets.

The assemblages from lower portion of SR-34 Zone IV contain higher frequencies of grass phytoliths, suggesting that a grass steppe composed of Pooideae grasses with primary associations of *Artemisia,* secondary associations of unidentified Asteraceae shrubs/herbs, and limited arboreal Pinaceae cover existed at SR-34 prior to ca. 6,000 yr BP. The grass assemblages suggest that wet conditions supported *Festuca* at this time, which also does not correlate very well with the isotope data from this period. However, there is a pronounced decline in Pooideae communities at the site around 6,000 yr BP, suggesting that period of warm and dry conditions occurred causing a decline in grass cover in the area which does appear to correlate with the pedogenic isotope data sets from the LSRC (Davis et al. 2002).

The assemblages from Cooper's Ferry Zone IV from this study are associated with samples from LU8a and LU8b. The LU8a assemblage indicates the presence of *Artemisia* with primary associations of Pooideae grasses, secondary associations of unidentified Asteraceae shrubs/herbs, and limited arboreal Pinaceae cover. The grass assemblage from LU8a suggests conditions were relatively wet, which supported a stable

community of *Agropyron* and *Festuca* grasses. LU8b continues to exhibit the same trend, however, Pooideae frequencies increase overall indicating expansion of the grass component at Cooper's Ferry. Assemblage data from LU8a reported by Davis and Collins (2009) is similar to that reported from this study. The two assemblages from LU14b at American Bar are bracketed between radiocarbon ages of 8,360 ± 80 to 6,680 ± 48 yr BP and also indicate the presence of a Pooideae dominated grass steppe at the site (Davis and Collins 2009). The pedogenic isotope data suggests that conditions fluctuated slightly between relatively warmer and cooler temperatures, while relatively drier conditions persisted during this period. The presence of relatively stable *Festuca* grasses at Cooper's Ferry and Pooideae grasses at American Bar may represent conditions associated with "Oasis effect", which permitted the more drought intolerant adapted grasses to persist during warmer and drier periods due to the presence of elevated ground water within the riparian zone.

Again, this study argues that the blocky phytolith forms reported by the other studies (Davis and Collins 2009; Somer 2003)) reflect the presence of *Artemisia* rather than Pinaceae species due to the very limited frequencies characteristic and diagnostic Pinaceae types observed from both studies. Pinaceae phytolith forms from these zones are very limited suggesting that these species were present in the LSRC possibly as isolated or scattered stands in the vicinity of Cooper's Ferry.

Human Ecology

This middle Holocene period (ca. 9,000-5,000 yr BP) is associated with the end of the Cooper's Ferry Phase II (11,000-8,400 yr BP) and the Craig Mountain Phase (8,400-3,500 yr BP) (Davis 2001b). Archaeological assemblages from both Cooper's Ferry and

American Bar indicate that during the Craig Mountain Phase the LSRC experienced intensified settlement and increased resource exploitation of the surrounding areas. Leaf or foliate shaped projectile point forms appear in the lithic assemblages immediately before the beginning of the Craig Mountain Phase and persist through the entire phase. Additional artifact types included Cold Springs Side-Notched projectile points, antler wedges, and edge-ground cobbles in addition the assemblages associated with Cooper's Ferry Phase II (Davis 2001b). The records associated with the Craig Mountain Phase assemblages recovered from Weis Rockshelter, Cooper's Ferry, and American Bar provide evidence for cultural continuity in the LSRC between ca. 8,400-3,500 yr BP (Butler 1968; Davis 2001b). Faunal records indicate increased exploitation of river mussel species, deer, and bison; however, it is unclear if bison were exploited within the context of the lower elevation canyons associated with the Rock Creek drainage or if the faunal remains recovered from Weis Rockshelter were transported from upland praire settings (Butler 1962).

The warmer and drier conditions associated with the middle Holocene climatic records suggest that vegetative productivity of the LSRC would have been relatively reduced overall. However, areas that permitted access to available ground water associated with elevated water tables within the riparian zones would have likely supported more productive patches of vegetation for exploitation by hunter-gatherer groups. The vegetation associated with the transitionary grass steppe/shrub steppe communities would have likely continued to support similar faunal communities inferred for the late Pleistocene and early Holocene period (Table 7.1). Higer densities of small mammals and birds would have likely been restricted to the relativley lusher riparian

zones compared to the drier slopes of the LSRC during this period (Chatters 1998; Davis 2001a; Scott et al. 2002).

The inferred vegetation still suggests relatively spares arboreal cover in the LSRC, which might have continued to support relatively low densities of elk and deer. These species may have been restricted to the riparian zones during this period. Intensified exploitation of deer is reflected in the archaeological record during this period, suggesting local environments supported higher population densities relative to the late Pleistocene and early Holocene (Davis 2001a). Bighorn sheep densities may have remained relatively higher during this period of grass and shrub steppe vegetation. While pronghorn and bison could have been supported by the inferred vegetation, it is still believed that the narrow and steep canyon may have limited these species to the upland prairies adjacent to the canyon. As discussed above, bison remains were recovered from Weis Rockshelter; however the limited nature of remains (e.g., tooth fragments representing two individuals) makes it difficult to determine if they reflect hunting in the canyon or transport from the adjacent uplands (Butler 1968).

The Salmon River continued to support a varity of aquatic resources during the middle Holocene. These resources continued to make up an important part of the subsistence base for hunter-gatherer groups in the LSRC as they continue to be recovered in greater quantities from the archaeological records of the LSRC and the region at large (Chatters 1998; Davis 2001a).

Late Holocene Human Ecology of the LSRC ca. 5,000 yr BP to Present

Paleoclimate

Late Holocene $\delta^{18}O$ and $\delta^{13}C$ records from pedogenic carbonate samples from the LSRC are available for the period between ca. 5,000-2,000 yr BP and indicate relatively cooler and wetter conditions overall compared to the middle Holocene records (Davis et al. 2002). The $\delta^{18}O$ data derived from river mussel shell is also reestablished during this period from ca. 5,000 yr BP to present (Davis and Muehlenbachs 2001). Both of these data sets identify an abrupt shift at ca. 2,000 yr BP; this abrupt shift is associated with extremely wet conditions reflected in the mussel shell data. This period of increased precipitation is argued to have triggered a geomorphic event characterized by channel incision of the existing Salmon River floodplain as the river attained its modern gradient and associated freestone structure (Davis et al. 2002). Following this episode of channel incision the $\delta^{18}O$ values obtained from river mussel shell trend towards modern levels.

Paleovegetation

The late Holocene vegetation of the LSRC is inferred from the phytolith assemblages recovered from low elevation canyon slopes at SR-23 Zone V (this study) and Zones IV-VI (Somer 2003), SR-27 Zone IV, and SR-34 Zones V-VI. Collectively, the phytolith assemblages recovered from these zones are interpreted primarily as indicators of Poaceae, Asteraceae, and limited Pinaceae vegetative communities respectively. These communities reflect the presence of transitionary shrub steppe/grass steppe and the development of the grass steppe vegetation along the lower elevation canyon slopes that characterize the modern LSRC.

The assemblages recovered from SR-23 Zone V (this study) indicate the presence of Pooideae grasses with primary associations *Artemisia,* secondary associations of unidentified Asteraceae shrubs/herbs, and limited arboreal Pinaceae cover. Grass assemblages suggest that conditions were relatively wet at the section during most of the late Holocene (ca. 5,000-present), supporting some of the highest frequencies of *Festuca* observed in the section; however, the very top of the profile exhibits a sharp decrease in *Festuca* and a pronounced increase in *Agropyron* in the vicinity as the modern vegetation is established. Zones IV-V reported by Somer (2003) indicate similar trends, with Pooideae grass communities inferred from assemblages dating ca. 5,500-550 yr BP. This is followed by a slight decline in grass assemblages associated with the modern surface sample of Zone VI. The isotope data from pedogenic carbonates indicates that conditions were relatively wetter and warmer between ca. 5,000-2,000 yr BP compared to the middle Holocene records (Davis et al. 2002), which correlates with expansion of *Festuca*.

The assemblages form SR-27 and SR-34 also indicate the same trends of Pooideae expansion on the lower elevation canyon slopes with primary associations *Artemisia,* secondary associations of unidentified Asteraceae shrubs/herbs, and limited Pinaceae cover. Both sections contain grass assemblages that suggest relatively wet conditions supported stable communities of *Festuca* similar to those observed at SR-23; however the modern assemblages indicate that *Festuca* either remained stable (SR-27) or increased slightly (SR-34). This would suggest that the local conditions in the vicinity of SR-27 and SR-34 have relatively greater moisture availability compared to SR-23, which is likely a product of the local drainage patterns associated with canyon slopes adjacent to these sections.

Again, this study argues that the blocky phytolith forms reported by the other studies (Somer 2003)) reflect the presence of *Artemisia* rather than Pinaceae species given that Pinaceae forms are very limited in these zones. Presently, Pinaceae these species are limited to north and east facing slopes and drainages that contain greater amounts of available moisture.

Human Ecology

This late Holocene period (ca. 5,000 yr BP to present) is associated with end of the Craig Mountain Phase (8,400-3,500 yr BP), the Grave Creek Phase (3,500-2,000 yr BP), the Rocky Canyon Phase (2,000-600 yr BP), and the Camas Prairie Phase (600-150 yr BP) (Davis 2001b). Archaeological assemblages associated with the Grave Creek Phase increase frequencies of Bitterroot Side-Notched projectile point forms, which replace the leaf or foliate shaped forms associated with the earlier Craig Mountain Phase. Ground stone tool technology also appears during the Grave Creek Phase, reflecting intensification of plant resource extraction possibly associate with edible root crops (i.e., *Camassia quamash*). Overall occupation and resource extraction along the floodplain and alluvial fans within the LSRC intensifies during the Grave Creek Phase, although formal residential structures (i.e., pit houses) and food storage pits are absent (Davis 2001b). Similar subsistence bases utilized during the Craig Mountain Phase continued to be exploited along with expansion of hunter-gatherer diet breadth indicated by integration of additional plant resources associated with ground stone technologies.

The following Rocky Canyon Phase is associated with some dramatic changes in the archaeological record of the LSRC. Notably, formal pit house structures appear as site occupation intensifies in the canyon. These sites and structures are associated with dense

accumulations of cultural materials (e.g., lithic artifacts and faunal remains) and food storage pits. The geomorphic event associated with channel incision of the existing floodplain is argued to have improved the local fishery as the freestone river became a much more hospitable environment for anadromous fish species; this increased abundance and reliability of this resource allowed prehistoric groups to adopt new socioeconomic and settlement strategies (Davis 2001b, 2007). Evidence of tool technology also reflects this shift as fishing gear (e.g., net weights) appears in the archaeological record of the LSRC (Davis 2007) in addition to smaller corner-notched projectile point forms. Exploitation of other established river (e.g., river mussels) and terrestrial (e.g., elk, deer, and mountain sheep) resources continued throughout this period (Davis 2001b).

The Camas Prairie Phase reflects the establishments of the ethnographic patterns of the Nez Perce as groups continue to utilize pit houses and storage features at occupation sites situated along the riparian zones of the LSRC. Resource extraction continues to utilize a wide variety of riverine and terrestrial resources found within the LSRC and adjacent upland prairies. Projectile point forms undergo further changes as small basal- and corner-notched varieties appear in the record. Inclusion of hopper and mortar bases are observed within the ground stone technologies of this phase. Trade goods also appear as contact between Europeans and the Nez Perce occurs (Davis 2001b).

The relatively cooler and wetter conditions associated with the late Holocene climatic records suggest that vegetative productivity of the LSRC would have increased relative to the middle Holocene period. Riparian zone areas would have likely continued

to support more productive patches of vegetation as well as some of the locally wetter areas along the low elevation canyon slopes. The grass steppe vegetation inferred from the phytolith assemblages would have likely continued to support similar faunal communities (Table 7.1) inferred for the middle Holocene (Chatters 1998; Davis 2001a; Scott et al. 2002).

Communities of small mammals and birds may have continued to occur in higher densities along the riparian zones relative to the adjacent canyon slopes. The inferred vegetation still suggests relatively spares arboreal cover in the LSRC, which may have continued to support relatively low densities of elk and deer; however intensified exploitation of deer is reflected in the archaeological record continues to suggest the local environments supported higher populations during this period (Chatters 1998; Davis 2001a). Bighorn sheep densities and populations might have remained relatively higher during this period of grass steppe vegetation. Pronghorn and bison could have been supported by the inferred vegetation; however, as previously discussed, the narrow and steep canyon may have limited these species to the upland prairies adjacent to the canyon. Additionally, bison would have only been available until ca. 250 yr BP after which they disappear from the Plateau (Davis 2001a).

As discussed above, aquatic resources continued to play an important role within the subsistence systems of hunter-gatherer groups within the LSRC. The reorganization of socioeconomic systems and settlement strategies that are reflected in the archaeological record of the LSRC support this fact as aquatic resource extraction intensifies during the late Holocene (Davis 2001b, 2007)

Chapter 8: Conclusion

Current and ongoing research at the Cooper's Ferry site in the LSRC, Idaho aims to expand our understanding of the adaptive strategies employed by earliest peoples of the southern Columbia River Plateau. The development of a human ecological model of the LSRC provides a suitable framework for understanding the behaviors and adaptive strategies represented by the archaeological record of Cooper's Ferry and region during the late Pleistocene and Holocene epochs. Development of a human ecological model requires a contextually based understanding of the biophysical environment that would have provided a variety of socioeconomic opportunities and constraints to prehistoric hunter-gatherer in the region.

Locally derived paleoenvironmental data sets derived from geoarchaeological studies (Davis 2001a; Davis and Schweger 2004), stable isotope geochemistry (Davis and Muehlenbachs 2001; Davis et al. 2002), and phytolith analysis (Davis and Collins 2009; Eccleston 1999; Somer 2003) provide a means of generating the type data to allow development of a human ecological model of the LSRC. This study contributes to these necessary data sets by expanding upon the relatively small number of phytolith analyses conducted within the lower elevation context of the canyon (Davis and Collins 2009; Somer 2003). Phytolith assemblages derived from four stratigraphic sections at SR-23, SR-27, SR-34, and the north wall of Unit A at the Cooper's Ferry were analyzed using a regionally based morphological classification applicable to the southern Columbia River Plateau (Blinnikov 2005). The results of this study provide a record of paleovegetative patterns spanning the last ca. 22,000 yr BP, which further demonstrates the applicability of phytolith analysis within the context of archaeological research.

Analysis of fossil phytolith assemblages from both archaeological and geological contexts have been shown to provide useful records of paleovegetative communities. These data sets can be compared with other locally derived paleoenvironmental proxy records to further contextualize upon the nature of past environments and their evolution through time, which provides to an appropriate framework to understand co-evolutionary patterns of the environment and cultural systems. Phytolith assemblage data provides a powerful tool in that it complements traditional data sets such as pollen and in some cases permits higher levels of taxonomic identification (e.g., subfamily and genus level identification of the Poaceae family).

This study permitted identification and reconstruction of grass and shrub steppe vegetative communities that existed in the LSRC since the last glacial maximum. The identification of different genera of the Pooideae subfamily of grasses, the Asteraceae family, and the Pinaceae family associated with the grass and shrub steppe communities provided a proxy measure of possible associations of economically important faunal communities might have been available to prehistoric hunter-gatherers occupying the LSRC.

The phytolith assemblages generated by this study and comparisons with other studies in the canyon (Davis and Collins 2009; Somer 2003) indicate that predominantly C_3 vegetative communities have existed within the LSRC for the last 22,000 yr BP. The communities inferred from the phytolith data consisted of C_3 Pooideae grasses, *Artemisia* and other unidentified Asteraceae species, and limited numbers of Pinaceae species. While the associations of these species exhibited some fluctuations during this period, the assemblage data suggests that environmental change in the LSRC was relatively limited

as communities transitioned between shrub steppe and grass steppe. In other words, the assemblage data does not reflect significant shifts between disparate vegetative communities.

There are some questions regarding the assemblage data that warrant further research to fully evaluate in order to further refine the interpretative powers of these data sets. One issue discussed in this study is related to the redundancy of phytolith forms between different plant taxa. For example, it has been reported that blocky phytolith forms occur in *Artemisia, Abies,* and *Picea* species which requires consideration of the entire phytolith assemblage to differentiate subalpine forests from sagebrush steppes. Another issue is that while phytolith analysis has been a firmly established field since the 1970s with proven methodological approaches to paleoecological and archaeological research. There are still many questions to be answered regarding phytolith production among various taxa, assemblage formation and preservation, and level of taxonomic reconstructions. Answers to these questions may be obtained through the continued study of phytolith production, preservation, and assemblage formation associated with individual plants as well as specific vegetation types of the regions being studied.

Continued phytolith analysis within the context of the Columbia River Plateau and the LSRC should embrace these types of questions and seek the answers through additional research of phytolith production and preservation in modern plants, modern soils, archaeological contexts, and geological contexts. These efforts should allow refinement of local classification systems, which may permit higher levels of environmental reconstructions to develop more detailed to human ecological models of the region.

BIBLIOGRAPHY

Adovasio, James M., and David R. Pedler
2013 The Ones that Still Won't Go Away. Paper presented at the Paleoamerican Odyssey Conference, Santa Fe.

Aikens, C. Melvin, Thomas J. Connolly, and Dennis L. Jenkins
2011 *Oregon Archaeology.* Oregon State University Press, Corvallis.

Alt, David D. and Donald W. Hyndman
1989 *Roadside Geology of Idaho.* Mountain Press Publishing Company, Missoula.

Ames, Kenneth M., Don E. Dumond, Jerry R. Galm, and Rick Minor
1998 Prehistory of the Southern Plateau. In *Handbook of North American Indians, Vol. 12: Plateau,* edited by D.E. Walker, Jr., pp. 103-119. Smithsonian Institution, Washington D.C.

Ames, Kenneth M., J. P. Green, and M. Pfoertner
1981 Hatwai (10NP143): Interim Report. *Archaeological Reports No.9.* Boise State University, Boise.

Ames, Kenneth M., and Alan G. Marshall
1980 Villages, Demography and Subsistence Intensification on the Southern Columbia Plateau. *North American Archaeologist* 2(1):25-52.

Amundson, Ronald G., Oliver A. Chadwick, Janet M. Sowers, and Harvey E. Doner
1988 Relationship between Climate and Vegetation and the Stable Isotope Chemistry of Soils in the Eastern Mojave Desert, Nevada. *Quaternary Research* 29(3):245-254.

Atwell, Ricky G.
1989 *Subsistence Variability on the Columbia Plateau.* Unpublished Master's thesis, Portland State University, Portland.

Baker,
1959 Opal Phytoliths in Some Victorian Soils and "Red Rain" Residues. *Australian Journal of Botany* 7(1):64-87.

Barnosky, Cathy W.
1985 Late Quaternary Vegetation in the Southwestern Columbia Basin, Washington. *Quaternary Research* 23:109-122

Barnosky, Cathy, Patricia Anderson, and Patrick Bartlein
1987 The Northwestern U.S. During Deglaciation: Vegetation History and Paleoclimatic Implications. In *The Geology of North America,* edited by W.F. Ruddiman and H. E. Wright Jr., pp. 289-321. The Geological Society of America.

Beaudoin, Alwynne B.
1993 A Compendium and Evaluation of Postglacial Pollen Records in Alberta. *Canadian Journal of Archaeology* 17:92-112.

1999 What They Saw: The Climatic and Environmental context for Euro-Canadian Settlement in Alberta. *Prairie Forum* 24:1-40.

Beavers, A. H., and I. Stephen
1958 Some Features of the Distribution of Plant Opal in Illinois Soils. *Soil Science* 86(1):1-5.

Berger, Glenn W., and Alan J. Busacca
1995 Thermoluminescence dating of late Pleistocene loess and tephra from eastern Washington and southern Oregon and implications for the eruptive history of Mount St. Helens. *Journal of Geophysical Research: Solid Earth (1978-2012)* 100(B11):22361-22374.

Birkeland, P. W.
1999 *Soils and Geomorphology:* 3rd ed. Oxford University Press, New York.

Blinnikov, Mikhail S.
1999 *Late Pleistocene History of the Columbia Basin Grassland Based on Phytolith Records in Loess.* Unpublished Ph.D dissertation, University of Oregon, Eugene.

2005 Phytoliths in plants and soils of the interior Pacific Northwest, USA. *Review of Palaeobotany and Palynology* 135(1):71-98.

Blinnikov, Mikhail S., Alan Busacca, and Cathy Whitlock
2001 A New 100,000-Year Phytolith Record From The Columbia Basin, Washington, U.S.A. In *Phytoliths: Applications in Earth Sciences and Human History,* edited by Jean Dominique Meunier and Fabrice Colin, pp. 27-55. A.A. Balkema Publishers, Lisse.

2002 Reconstruction of the late Pleistocene grassland of the Columbia basin, Washington, USA, based on phytolith records in loess. *Palaeogeography, Palaeoclimatology, Palaeoecology* 177(1):77-101.

Bonnichsen, Bill, and Roy M. Breckenridge
1982 *Cenozoic Geology of Idaho*. Idaho Bureau of Mines and Geology, Moscow.

Bowdery,
1998 *Phytolith Analysis Applied to Pleistocene-Holocene Archaeological Sites in the Australian Arid Zone. BAR International Series* 695. British Archaeological Reports, Oxford.

Bozarth, Steven R.
1992 Classification of Opal Phytoliths Formed in Selected Dicotyledons Native to the Great Plains. In *Phytolith Systematics: Emerging Issues*, edited by George Rapp Jr. and Susan C. Mulholland, pp. 193-214. Plenum Press, New York.

1993 Biosilicate Assemblages of Boreal Forests and Aspen Parklands. In *Current Research in Phytolith Analysis: Applications in Archaeology and Paleoecology*, edited by Deborah M. Pearsall and Dolores R. Piperno, pp. 95-105. MASCA Research Papers in Science and Archaeology Vol. 10. MASCA, The University of Museum of Archaeology and Anthropology, University of Pennsylvania, Philadelphia.

Brauner, David R.
1975 Archaeological Salvage of the Scorpion Knoll Site, 45AS41, Southeastern Washington. *Archaeological Research Center, Project Report* 23. Washington State University, Pullman.

1976 *Alpowai: The Culture History of the Alpowa Locality.* Unpublished Ph.D. dissertation, Washington State University, Pullman.

1985 *Early Human Occupation in the Uplands of the Southern Plateau: Archaeological Excavations at the Pilcher Creek Site (35UN147), Union County, Oregon.* Department of Anthropology, Oregon State University, Corvallis. Submitted to USDA Soil Conservation Service and the National Geographic Society, Washington.

Brauner, David R., and Nahani Stricker
1990 *Archaeological Test Excavations and Evaluation of the Proposed Clearwater Fish Hatchery site (10CW4), Clearwater County, Idaho: Phase II.* Department of Anthropology, Oregon State University, Corvallis. Submitted to the Walla Walla District, Army Corps of Engineers, Walla Walla.

Breckenridge, Roy M.
1989 Pleistocene Ice Dams and Glacial Lake Missoula Floods in Northern Idaho and Adjacent Areas. In *Guidebook to the Geology of Northern and Western Idaho and Surrounding Area*, edited by V. E. Chamberlain, R. M. Breckenridge, and B. Bonnichsen, pp. 5-16. Idaho Geological Survey Bulletin 28.

Bretz, J. Harlen
1929 Valley Deposits East of the Channeled Scablands. *Journal of Geology* 37: 393-427, 505-541.

Brown, Dwight A.
1984 Prospects and Limits of a Phytolith Key for Grasses in the Central United States. *Journal of Archaeological Science* 11(4):345-368.

Bryan, Alan L.
1980 The Stemmed Point Tradition: An Early Technological Tradition in Western North America. In *Anthropological Papers in Memory of Earl H. Swanson, Jr.*, edited by L. Harten, C. Warren, and D. Tuohy, pp. 77-107. Special Publication of the Idaho State University Museum of Natural History, Pocatello.

1988 The Relationship of the Stemmed Point and Fluted Point Traditions in the Great Basin. In *Early Human Occupation in Far Western North America: The Clovis-Archaic Interface*, edited by J. Willig, C. Aikens, and J. Fagan, pp. 53-74. Nevada State Museum Anthropological Papers No. 21, Carson City.

Brydon, James E., William G. Dore, and John S. Clark
1963 Silicified Plant Asterosclereids Preserved in Soil. *Soil Science Society of America Journal* 27(4):476-477.

Busacca, Alan J., Kevin T. Nelstead, Eric V. McDonald, and Michael D. Purser
1992 Correlation of Distal Tephra Layers in Loess in the Channeled Scabland and Palouse of Washington State. *Quaternary Research* 37(3):281-303.

Butler, B. Robert
1968 *A Guide to Understanding Idaho Archaeology.* A Special Publication of the Idaho State Museum, Pocatello.

1969 The Earlier Cultural Remains at Cooper's Ferry. *Tebiwa* 12(2):35-50.

Butzer, Karl W.
1982 *Archaeology as Human Ecology: Method and Theory for a Contextual Approach.* Cambridge University Press, Cambridge.

Carbone, Victor A.
1977 Phytoliths as Paleoecological Indicators. *Annals of the New York Academy of Sciences* 288:194-204.

Cerling, Thure E.
1984 The Stable Isotopic Composition of Modern Soil Carbonate and its Relationship to Climate. *Earth and Planetary Sciences Letters* 71(2):229-240.

1992 Development of Grasslands and Savannas in East Africa During the Neogene. *Palaeogeography, Palaeoclimatology, Palaeoecology* 97(3):241-247.

1999 Paleorecords of C_4 Plants and Ecosystems. In *C_4 Plant Biology*, edited by Rowan F. Sage and Russell K. Monson, pp. 445-469. Academic Press, San Diego.

Cerling, Thure E., and Jay Quade
1993 Stable Carbon and Oxygen Isotopes in Soil Carbonates. *Geophysical Monograph Series* 78:217-231.

Chadwick, Oliver A., Robert D. Hall, and Fred M. Phillips
1997 Chronology of Pleistocene Glacial Advances in the Central Rocky Mountains. *Geological Society of America Bulletin* 109(11):1443-1452.

Chambers, Richard L.
1984 Sedimentary Evidence for Multiple Glacial Lakes Missoula. In *Northwest Montana and Adjacent Canada,* edited by J.D. McBane and P.B. Garrison, pp. 189-199. Montana Geological Society, Billings.

Chance, David H., J. V. Chance, E. Anderson, N. Bowers, B. Cochran, M. L. Falen, M. A. Fosberg, D. L. Olson, E. Paul, R. Schalk, R. K. Steinhorst, N. A. Stenholm, S. Valastro Jr., and S. B. Whitwer
1989 *Archaeology of the Hatiuhpuh village.* Alfred W. Bowers Laboratory of Anthropology, University of Idaho, Moscow. Submitted to the Walla Wall District, Army Corps of Engineers, Walla Walla.

Chatters, James C.
1989 Resource Intensification and Sedentism on the Southern Plateau. *Archaeology in Washington* 1:3-19.

1998 Environment. In *Handbook of North American Indians, Vol. 12: Plateau*, edited by D.E. Walker, Jr. pp. 29-48. Smithsonian Institution, Washington D.C.

Chatters, James C., and Karin A. Hoover
1992 Response of the Columbia River fluvial System to Holocene Climatic Change. *Quaternary Research* 37(1):42-59.

Chatters, James C., and David L. Pokotylo
1998 Prehistory: Introduction. In *Handbook of North American Indians, Vol. 12: Plateau,* edited by D.E. Walker, Jr., pp. 73-80. Smithsonian Institution, Washington D.C.

Clark, James S., Eric C. Grimm, Jason Lynch, and Pietra G. Mueller
2001 Effects of Holocene Climate Change on the C_4 Grassland/Woodland Boundary in the Northern Plains, USA. *Ecology* 82:620-636.

Cleveland, Gregory C. (editor)
1976 Preliminary Archaeological Investigations at the Miller Site, Strawberry Island, 1976: A Late Prehistoric Village Near Burbank, Franklin County, Washington. *Washington Archaeological Research Center. Project Report* 46. Washington State University, Pullman.

Coil, James M., Alejandra Korstanje, Steven Archer, and Christine A. Hastorf
2003 Laboratory Goals and Considerations for Multiple Microfossil Extraction in Archaeology. *Journal of Archaeological Science* 30(8):991-1008.

Collins, Michael B., Dennis J. Stanford, and Darrin L. Lowery
2013 North America before Clovis: Variance in Temporal/Spatial Cultural Patterns, 24,000 to 13,000 BP. Paper presented at the Paleoamerican Odyssey Conference, Santa Fe.

Crandell, D. R., D.R. Mullineaux, M. Rubin, E. Soiker, and M. L. Kelly
1981 *Radiocarbon Dates from Volcanic Deposits at Mount St. Helens, Washington.* US Department of the Interior, Geological Survey, Denver.

Cummings, Linda Scott
1992 Illustrated Phytoliths from Assorted Food Plants. In *Phytolith Systematics: Emerging Issues*, edited by George Rapp Jr. and Susan C. Mulholland, pp. 175-192. Advances in Archaeological and Museum Science Vol. 1, Plenum Press, New York.

Daubenmire, Rexford F., and Jean B. Daubenmire
1968 Forest Vegetation of Eastern Washington and Northern Idaho. *Technical Bulletin of the Agricultural Experiment Station,* Vol. 60, College of Agriculture, Washington State University, Pullman.

Daubenmire, Rexford F.
1970 Steppe Vegetation of Washington. *Technical Bulletin of the Agricultural Experiment Station,* Vol. 62, College of Agriculture, Washington State University, Pullman.

Daugherty, Richard D.
1956 Archaeology of the Lind Coulee Site, Washington. *Proceedings of the American Philosophical Society* 100(3):223-278. Philadelphia.

Davis, Loren G.
2001a *The Coevolution of Early Hunter-Gatherer Culture and Riparian Ecosystems in the Southern Columbia River Plateau.* Unpublished Ph.D. dissertation, University of Alberta, Edmonton.

2001b Lower Salmon River Cultural Chronology: A Revised and Expanded Model. *Northwest Anthropological Research Notes* 35:229-248.

2007 Paleoseismicity, Ecological Change, and Prehistoric Exploitation of Anadromous Fishes in the Lower Salmon River Basin, Western Idaho, USA. *North American Archaeologist* 28(3):233-263.

2009 Past and Future Research at the Cooper's Ferry Site, Lower Salmon River Canyon, Idaho. Paper presented at the 62nd Northwest Anthropological Conference, Newport.

Davis, Loren G., and Karlis Muehlenbachs
2001 A Late Pleistocene to Holocene Record of Precipitation Reflected in *Margaritifera falcata* Shell $\delta^{18}O$ From Three Archaeological Sites in the Lower Salmon River Canyon, Idaho. *Journal of Archaeological Science* 28(3):291-303.

Davis, Loren G., Karlis Muehlenbachs, Charles E. Schweger, and Nathaniel W. Rutter
2002 Differential response of vegetation to postglacial climate in the Lower Salmon River Canyon, Idaho. *Palaeogeography, Palaeoclimatology, Palaeoecology* 185(3):339-354.

Davis, Loren G., and Shawn K. Collins
2009 *Late Pleistocene to Holocene Phytolith Records from the Lower Salmon River Canyon, Idaho.* Submitted to Bureau of Land Management, Cottonwood Field Office, Cottonwood, Idaho, as part of Challenge Cost Share Agreement HAA003D00, Task Order No. HAF043F15.

Davis, Loren G., and Charles E. Schweger
2004 Geoarchaeological context of Late Pleistocene and Early Holocene Occupation at the Cooper's Ferry Site, Western Idaho, USA. *Geoarchaeology* 19(7):685-704.

Dickerson, Kenneth R.
1997 *Soils of the Gill Gulch Site (10IH1308) Idaho County, Idaho.* Report on file, Bureau of Land Management, Upper Columbia and Salmon Clearwater Districts, Cottonwood Resource Area, Cottonwood, Idaho.

Dillehay, Tom D. (editor)
1989 *Monte Verde: A Late Pleistocene Settlement in Chile, Vol. 1.* Smithsonian Institution Press, Washington, D.C.

2013 Late Pleistocene Economic and Cultural Diversity in North Peru. Paper presented at the Paleoamerican Odyssey Conference, Santa Fe.

Dort, Wakfield Jr.
1965 Glaciation in Idaho: A Summary of Present Knowledge. *Tebiwa* 11:31-37.

Eccleston, Kendall
1999 *The Applicability of Phytolith Analysis to the Columbia Plateau: The Cottonwood Divide Creek Site, A Test Model.* Unpublished Master's thesis, University of Idaho, Moscow.

Edwards, A. W. F., and L. L. Cavalli-Sforza
1964 Reconstruction of Evolutionary Trees. In *Phenetic and Phylogenetic Classification: Systematics Association Publication* 6:67-76.

Ehrenberg, C. G.
1841 Über Verbreitung und Einfluss des Mikroskopischen Lebens in Süd- und Nordamerika. *Monatsberichte der Könglich Preussischen Akademie der Wissenschaften zu Berlin,* pp. 139-144.

1854 *Mikrogeologie: Das Erden und Felsen Schaffende Wirken das Unsichtbar Kleinen Selbständigen Lebens Auf der Erde.* Vol. 1 Leopold Voss, Leipzig.

Franklin, Jerry F., C. T. Dyrness
1988 *Natural Vegetation of Oregon and Washington.* Oregon State University Press, Corvallis.

Fredlund, Glen G.
1986 A 620,000 Year Opal Phytolith Record from Central Nebraska Loess. In *Plant Opal Phytolith Analysis in Archaeology and Paleoecology*, edited by Irwin Rovner, pp. 12-23.

Fredlund, Glen G., C. Britt Bousman, and Douglas K. Boyd
1998 The Holocene Phytolith Record from Morgan Playa in the Rolling Plains of Texas. *Plains Anthropologist* 43:187-200. Occasional Papers No. 1 of The Phytolitharien, North Carolina State University, Raleigh.

Fredlund, Glen G., and Larry T. Tieszen
1994 Modern Phytolith Assemblages from the North American Plains. *Journal of Biogeography* 21:321-335.

1997 Calibrating Grass Phytolith Assemblages in Climatic Terms: Application to Late Pleistocene Assemblages from Kansas and Nebraska. *Palaeogeography, Palaeoclimatology, Palaecology* 136(1):199-211.

Freeman, Otis W., J. D. Forrester, and R. L. Lupher
1945 Physiographic Divisions of the Columbia Intermontane Province. *Annals of the Association of American Geographers* 25:53-75.

Geis, James W.
1973 Biogenic Silica in Selected Species of Deciduous Angiosperms. *Soil Science* 116(2):113-130.

1978 Biogenic Opal in Three Species of Poaceae. *Annals of Botany* 42:1119-1129.

Gilbert, M. Thomas P., Dennis L. Jenkins, Anders Gotherstrom, Nuria Naveran, Juan J. Sanchez, Michael Hofreiter, Philip Francis Thomsen, Jonas Binladen, Thomas F. G. Higham, Robert M. Yohe II, Robert Parr, Linda Scott Cummings, Eske Willerslev
2008 DNA from Pre-Clovis Human Coprolites in Oregon, North America. *Science* 320(5877):786-789.

Gosse, John C., E. B. Evenson, J. Klein, and R. Middleton
1995 Precise cosmogenic ^{10}Be measurement in western North America: Support for a global Younger Dryas cooling event. *Geology* 23(10):877-880.

Gould, Frank W., and Robert B. Shaw
1983 *Grass Systematics.* 2nd ed. Texas A&M University Press, College Station.

GPWG (Grass Phylogeny Working Group
2001 Phylogeny and Subfamilial Classification of the Grasses (Poaceae). *Annals of the Missouri Botanical Garden* 88:373-457.

Graham, Russel W., and Eric C. Grimm
1990 Effects of Global Climate Change on the Patterns of Terrestrial Biological Communities. *Trends in Ecology and Evolution* 5(9):289-292.

Grimm, Eric C.
1987 CONISS: A Fortran 77 Program for Stratigraphically Constrained Cluster Analysis by the Method of Incremental Sum of Squares. *Computers & Geosciences* 13(1):13-35.

1992 TILIAGRAPH Version 1.7.16. Illinois State Museum Research and collection Center, Springfield.

Hicks, Brent A. (editor)
2004 *Marmes Rockshelter: A Final Report on 11,000 Years of Cultural Use.* Washington University Press, Pullman.

Holden, Gregory S.
1974 *Chemical and Petrographic Stratigraphy of the Columbia River Basalt in the Lower Salmon River Canyon, Idaho*. Unpublished Master's thesis, Washington State University, Pullman.

Horrocks, Mark
2005 A Combined Procedure for Recovering Phytoliths and Starch Residues from Soils, Sedimentary Deposits and Similar Materials. *Journal of Archaeological Science* 32(8):1169-1175.

Irwin, Ann M., and Ula L. Moody
1978 The Lind Coulee Site (45GR97). *Washington Archaeological Research Center Project Report 56.* Washington State University, Pullman.

Jenkins, Dennis L.
2007 Distribution and Dating of Cultural and Paleontological Remains at the Paisley Five Mile Point Caves in the Northern Great Basing: An Early Assessment. In *Paleoindian or Paleoarchaic? Great Basin Human Ecology at the Pleistocene-Holocene Transition*, edited by Kelly E. Graf and Dave N. Schmitt, pp. 57-81. University of Utah Press, Salt Lake City.

2013 Paisley Caves: 14,500 Years of Human Occupations in the Northern Great Basin. Paper presented at the Paleoamerican Odyssey Conference, Santa Fe.

Jenkins, Denis L., Paula Campos, Edwards Davis, Loren G. Davis, Bryan Hockett, Thomas W. Stafford, Jr., Mark E. Swisher, and Eske Willerslev
2010 Chrono-Stratigraphic Analysis of Late Pleistocene to Middle Holocene Deposits in the Paisley Caves of South-Central Oregon. Paper presented at the 32nd Great Basin Anthropological Conference, Layton.

Jenkins, Dennis L., Loren G. Davis, Thomas W. Stafford Jr., Paula F. Campos, Bryan Hockett, George T. Jones, Linda Scott Cummings, Chad Yost, Thomas J. Connolly, Robert M. Yohe II, Summer C. Gibbons, Maanasa Raghavan, Morten Rasmussen, Johanna L. A. Paijmans, Michael Hofreiter, Brian M. Kemp, Jodi Lynn Barta, Cara Monroe, M. Thomas P. Gilbert, Eske Willerslev.
2012 Clovis Age Western Stemmed Projectile Points and Human Coprolites at the Paisley Caves. *Science* 337(6091):223-228.

Jones, Robert L.
1964 Note on Occurrence of Opal Phytoliths in Some Cenozoic Sedimentary Rocks. *Journal of Paleontology* 38:773-775.

Jones, Robert L., and A. H. Beavers
1964 Variation of Opal Phytolith Content Among Some Great Soil Groups in Illinois. *Soil Science Society of America Journal* 28(5):711-712.

Jones, Robert L., W. W. Hay, and A. H. Beavers
1963 Microfossils in Wisconsin Loess and Till from Western Illinois and Eastern Iowa. *Science* 140(3572):1222-1224.

Kirk, Ruth, and Richard D. Daugherty
2007 *Archaeology in Washington.* University of Washington Press, Seattle.

Klein, Robert L., and James W. Geis
1978 Biogenic Silica in the Pinaceae. *Soil Science* 126(3):145-156.

Kondo, Renzo, Cyril Walter Childs, Ian Athol Edwards Atkinson, and Tony Pritchard
1994 *Opal Phytoliths of New Zealand.* Manaaki Whenua Press, Lincoln.

Kuchler, August Wilhelm
1964 *Potential Natural Vegetation of the Conterminous United States.* American Geographical Society, New York.

Kurmann, Marie H.
1985 An Opal Phytolith and Palynomorph Study of Extant and Fossil Soils in Kansas (USA). *Palaeogeography, Palaeoclimatology, and Palaeoecology* 49(3):217-235.

Lentfer, Carol J.
2003 *Plants, People, and Landscapes in Prehistoric Papua New Guinea: A Compendium of Phytolith (and Starch) Analyses.* Unpublished Ph.D. dissertation, Southern Cross University, Lismore.

Lentfer, Carol J., and William E. Boyd
1998 A Comparison of Three Methods for the Extraction of Phytoliths from Sediments. *Journal of Archaeological Science* 25(12):1159-1183

1999 An Assessment of Techniques for the Deflocculation and Removal of Clays from Sediments Used in Phytolith Analysis. *Journal of Archaeological Science* 26(1):31-44.

2000 Simultaneous Extraction of Phytoliths, Pollen and Spores from Sediments. *Journal of Archaeological Science* 27(5):363-372.

Lentfer, Carol J., Maria M. Cotter, and William E. Boyd
2003 Particle Settling Times for Gravity Sedimentation and Centrifugation: A Practical Guide for Palynologists. *Journal of Archaeological Science* 30(2):149-168.

Leonhardy, Frank C., and David G. Rice
1970 A Proposed Cultural Typology for the Lower Snake River Region, Southeastern Washington. *Northwest Anthropological Research Notes* 4(1):1-29.

Licciardi, Joseph M., Peter U. Clark, Edward J. Brook, Kenneth L. Pierce, Mark D. Kurz, David Elmore, and Pankaj Sharma
2001 Cosmogenic ^{3}He and ^{10}Be Chronologies of the late Pinedale northern Yellowstone ice cap, Montana, USA. *Geology* 29(12):1095-1098.

Licciardi, Joseph M., Peter U. Clark, Edward J. Brook, David Elmore, and Pankaj Sharma
2004 Variable responses of western U.S. glaciers during the last deglaciation. *Geology* 32(1):81-84.

Loshe, E. S., and Roderick Sprague
1998 History of Research. In *Handbook of North American Indians, Vol. 12: Plateau,* edited by D.E. Walker, Jr., pp. 8-28. Smithsonian Institution, Washington D.C.

Mack, Richard N., N. W. Rutter, Vaughn M. Bryant, and S. Valastro
1978a Late Quaternary Pollen Record from Big Meadow, Pend Oreille County, Washington. *Ecology* 59:956-966.

1978b Reexamination of Postglacial Vegetation History in Northern Idaho: Hager Pond, Bonner County. *Quaternary Environments* 10:241-255.

Mack, Richard N., N. W. Rutter, and S. Valastro
1979 Holocene Vegetation History of the Okanogan Valley, Washington. *Quaternary Research* 12:212-225.

1983 Holocene Vegetation of the Kootenai river Valley, Montana. *Quaternary Research* 20:177-193.

Madella, Marco, Alix H. Powers-Jones, and Martin K. Jones
1998 A Simple Method of Extraction of Opal Phytoliths from Sediments Using a Non-Toxic Heavy Liquid. *Journal of Archaeological Science* 25(8):801-803.

Maley, Terry S.
1987 *Exploring Idaho Geology.* Mineral Land Publications, Boise.

Madesn, David B. (editor)
2004 *Entering America: Northeast Asia and Beringia Befor the Last Glacial Maximum.* University of Utah Press, Salt Lake City.

McDonald, Eric V., and Alan J. Busacca
1992 Late Quaternary stratigraphy of loess in the Channeled Scabland and Palouse regions of Washington State. *Quaternary Research* 38(2):141-156.

McKee, Bates
1972 *Cascadia: The Geologic Evolution of the Pacific Northwest.* McGraw Hill, New York.

Meatte, Daniel S.
1986 Evidence for the Historic Occurrence and Aboriginal Utilization of Caribou in Southern Idaho. *Idaho Archaeologist* 9:41-42.

Mehringer, Peter J. Jr., Stephen F. Arno, and Kenneth L. Petersen
1977 Postglacial History of Lost Trail Pass Bog, Bitterroot Mountains, Montana. *Arctic and Alpine Research* 9:345-368.

Mehringer, Peter J. Jr., and Franklin F. Foit
1990 Volcanic Ash Dating of the Clovis Cache at East Wenatchee, Washington. *National Geographic Research* 6(4):495-503.

Metcalfe, Charles R.
1960 *Anatomy of the Monocotyledons. I. Gramineae.* Oxford University Press, London.

Mulholland, Susan C.
1989 Phytolith Shape Frequencies in North Dakota Grasses: A Comparison to General Patterns. *Journal of Archaeological Science* 16(5):489-511.

1993 A Test of Phytolith Analysis at Big Hidatsa, North Dakota. In *Current Research in Phytolith Analysis: Applications in Archaeology and Paleoecology,* edited by Deborah M. Pearsall and Dolores R. Piperno, pp. 131-145. MASCA Research Papers in Science and Archaeology Vol. 10. MASCA, The University of Museum of Archaeology and Anthropology, University of Pennsylvania, Philadelphia.

Mulholland, Susan C., and George Rapp Jr.
1992a Phytolith Systematics: An Introduction. In *Phytolith Systematics: Emerging Issues,* edited by George Rapp Jr. and Susan C. Mulholland, pp. 1-13. Advances in Archaeological and Museum Science Vol. 1, Plenum Press, New York.

1992b A Morphological Classification of Grass Silica-Bodies. In *Phytolith Systematics: Emerging Issues,* edited by George Rapp Jr. and Susan C. Mulholland, pp. 65-89. Advances in Archaeological and Museum Science Vol. 1, Plenum Press, New York.

Nelson, Charles M.
1966 A Preliminary Report on 45CO1, a Stratified Open Site in the Southern Columbia Plateau. *Laboratory of Anthropology, Report of Investigations* 39. Washington State University, Pullman.

Norgen, Joel A.
1973 *Distribution, Form and Significance of Plan Opal in Oregon Soils.* Unpublished Ph.D. dissertation, Oregon State University, Corvallis.

O'Connor, Jim E.
1993 Hydrology, Hydraulics, and Geomorphology of the Bonneville Flood. *Geologic Society of America Special Paper* 274.

O'Geen, Anthony T.
1998 *Faunal Paleoecology of Late Quaternary Paleosols on the Columbia Plateau.* Unpublished Ph.D. dissertation, Washington State University, Pullman.

O'Geen, Anthony T., and Alan J. Busacca
2001 Late Quaternary Paleoenvironments of the Columbia Plateau, PNW U.S., from Faunal Burrows in Paleosols. *Palaeogeography, Palaeoclimatology, Palaeoecology* 169(1):23-37.

Ollendorf, Amy L.
1992 Toward a Classification Scheme of Sedge (Cyperaceae) Phytoliths. In *Phytolith Systematics: Emerging Issues,* edited by George Rapp Jr. and Susan C. Mulholland, pp. 91-111. Advances in Archaeological and Museum Science Vol. 1, Plenum Press, New York.

Omernik, James M.
1987 Map Supplement: Ecoregions of the Conterminous United States. *Annals of the Association of American Geographers* 77(1):118-125.

Parry D. Wynn, and Frank Smithson
1958a Silicification of Bulliform Cells in Grasses. *Nature* 181:1549-1550.

1958b Techniques for Studying Opaline Silica in Grass Leaves. *Annals of Botany* 22:543-550.

1964 Types of Opaline Silica Depositions in the Leaves of British Grasses. *Annals of Botany* 28:169-185.

1966 Opaline Silica in the Inflorescences of Some British Grasses and Cereals. *Annals of Botany* 30:525-538.

Pavesic, Max G.
1986 Descriptive Archaeology of Hells Canyon Creek Village. *Boise State University Archaeological Reports* 14. Boise.

Pearsall, Deborah M.
1978 Phytolith Analysis of Archaeological Soils: Evidence for Maize Cultivation in Formative Ecuador. *Science* 199(4325):177-178.

1982 Phytolith Analysis: Applications of a New Paleoethnobotanical Technique in Archaeology. *American Anthropologist* 84(4):862-871.

2010 *Paleoethnobotany: A Handbook of Procedures.* 2nd ed. Left Coast Press, Walnut Creek.

Piperno, Dolores R.
1984 A Comparison and Differentiation of Phytoliths from Maize and Wild Grasses: Use of Morphological Criteria. *American Antiquity* 49:361-383.

1985a Phytolithic Analysis of Geological Sediments from Panama. *Antiquity* 59(225):13-19.

1985b Phytolith Analysis and tropical Paleo-Ecology: Production and Taxonomic Significance of Siliceous Forms in New World Plant Domesticates and Wild Species. *Review of Palaeobotany and Palynology* 45(3):185-228.

1985c Phytolith Taphonomy and Dirstributions in Archaeological Sediments from Panama. *Journal of Archaeological Science* 12(4):247-267.

1988 *Phytolith Analysis: An Archaeological and Geological Perspective.* Academic Press, New York.

1989 The Occurrence of Phytoliths in the Reproductive Structures of Selected Tropical Angiosperms and Their Significance in Tropical Paleoecology, Paleoethnobotany, and Systematics. *Review of Palaeobotany and Palynology* 61(1):147-173.

1995 Plant Microfossils and Their Application in the New world Tropics. In *Archaeology in the Lowland American Tropics: Current Analytical Methods and Recent Applications*, edited by Peter W. Stahl, pp. 130-153. Cambridge University Press, Cambridge.

1998 Paleoethnobotany in the Neotropics from Microfossils: New Insights into Ancient Plant Use and Agricultural Origins in the Tropical Forest. *Journal of World Prehistory* 12(4):393-449.

2001 On Maize and Sunflower. *Science* 292(5525):2260-2261.

2006 *Phytoliths: A Comprehensive Guide for Archaeologists and Paleoecologists.* AltaMira Press, Lanham.

Piperno, Dolores R., Karen H. Clary, Richard G. Cooke, Anthony K. Ranere, and Doris Weiland

1985 Preceramic Maize in Central Panama: Phytolith and Pollen Evidence. *American Anthropologist* 87(4):871-878.

Piperno, Dolores R., and Deborah M. Pearsall

1993 Phytoliths in the Reproductive Structures of Maize and Teosinte: Implications for the Study of Maize Evolution. *Journal of Archaeological Science* 20(3):337-362.

1998 The Silica Bodies of Tropical American Grasses: Morphology, Taxonomy, and Implications for Grass Systematics and Fossil Phytolith Identification. *Smithsonian Contributions to Botany* No. 85. Smithsonian Institution Press, Washington D.C.

Powers, Alix H.

1992 Great Expectations: A Short Historical Review of European Phytolith Systematics. In *Phytolith Systematics: Emerging Issues*, edited by George Rapp

Jr. and Susan C. Mulholland, pp. 15-35. Advances in Archaeological and Museum Science Vol. 1, Plenum Press, New York.

Powers, A. H., and D. D. Gilberston
1987 A Simple Preparation Technique for the Study of Opal Phytoliths from Archaeological and Quaternary Sediments. *Journal of Archaeological Science* 14(5):529-535.

Reidel, Stephen P.
1978 *The Stratigraphy and Petrogenesis of the Grande Ronde Basalt in the Lower Salmon and Adjacent Snake River Canyons*. Unpublished Ph.D. dissertation, Washington State University, Pullman.

Rice, David G.
1972 *The Windust Phase in Lower Snake River Region Prehistory.* Unpublished Ph.D. dissertation, Washington State University, Pullman.

Rice, Harvey S.
1965 *The Cultural Sequence at Windust Caves.* Unpublished Master's thesis, Washington State University, Pullman.

Richardson, C. A., E. V. McDonald, and A. J. Busacca
1997 Luminescence Dating of Loess from the Northwest United States. *Quaternary Science Reviews* 16(3):403-415.

Roll, Tom E., and Steven Hackenberger
1998 Prehistory of the Eastern Plateau. In *Handbook of North American Indians, Vol. 12: Plateau,* edited by D.E. Walker, Jr., pp. 120-137. Smithsonian Institution, Washington D.C.

Rovner, Irwin
1971 Potential of Opal Phytoliths for Use in Paleoecological Reconstruction. *Quaternary Research* 1(3):343-359.

1986 Downward Percolation of Phytoliths in Stable Soils: A Non-Issue. In *Plant Opal Phytolith Analysis in Archaeology and Paleoecology,* edited by Irwin Rovner, pp. 23-30. Occasional Papers No. 1 of the Phytolitharien. North Carolina State University, Raleigh.

Rovner, Irwin, and John C. Russ
1992 Darwin and Design in Phytolith Systematics: Morphometric Methods for Mitigating Redundancy. In *Phytolith Systematics: Emerging Issues,* edited by George Rapp Jr. and Susan C. Mulholland, pp. 253-276. Advances in Archaeological and Museum Science Vol. 1, Plenum Press, New York.

Sanders, Paul
1982 *A Lithic Analysis of the Windust Phase Compoent, Hatwai Site (10NP143), Nez Perce County, Idaho.* Unpublished Master's thesis, University of Wyoming, Laramie.

Sangster, A. G., M. J. Hodson, and H. J. Tubb
2001 Silicon Deposition in Higher Plants. In *Silicon in Agriculture,* edited by Lawrence E. Datnoff, George H. Snyder, and Gaspar H. Korndörfer, pp. 85-113. Elsevier Science, Amsterdam.

Sappington, Robert Lee
1988 Archaeological Test Excavations and Evaluations of the Proposed Clearwater Fish Hatchery Site (10CW4), on the North Fork of the Clearwater River, North Central Idaho. *Alfred W. Bowers Laboratory of Anthropology. Anthropological Reports* 88. University of Idaho, Moscow.

Sase, Taakashi, and Renzo Kondo
1974 The Study of Opal Phytoliths in the Humus Horizon of Buried Volcanic Ash Soils in Hokkaido. *Research Bulletin of Obihiro Zootechnical University,Series 1* 8(3):465-483.

Schoeneberger, Philip J.
2012 *Field Book for Describing and Sampling Soils, Version 3.0.* Natural Resources Conservation Service, National Soil Survey Center, Lincoln, Nebraska.

Scott, J. M., C. R. Peterson, J. W. Karl, E. Strand, L. K. Svancara, and N. M. Wright
2002 A Gap Analysis of Idaho: Final Report. Idaho Cooperative Fish and Wildlife Research Unit. Moscow, Idaho.

Sea, Debra S., and Cathy Whitlock
1995 Postglacial Vegetation and Climate of the Cascade Range, Central Oregon. *Quaternary Research* 43:370-381.

Schalk, Randall F.
1983 The 1978 and 1979 Excavations at Strawberry Island in the McNary Reservoir. *Laboratory of Archaeology and History. Project Report* 1. Washington State University, Pullman.

Sherard, C.
2006 *Timing of early Holocene Glacial Advances in Idaho and Washington.* Unpublished Master's thesis, University of Washington, Seattle.

Smith, Craig S.
1983 *A 4,300 Year History of Vegetation, Climate, and Fire from Blue Lake, Nez Perce County, Idaho.* Unpublished Master's thesis, Washington State University, Pullman.

Somer, Bradley F.
2003 *A Late Pleistocene and Holocene Phytolith Record, Lower Salmon River Canyon, Idaho.* Unpublished Master's thesis, University of Alberta, Edmonton.

Stevenson, Bryan A.
1997 *Stable Carbon and Oxygen Isotopes in Soils and Paleosols of the Palouse Loess, Eastern Washington State: Modern Relationships and Applications for Paleoclimatic Reconstruction.* Unpublished Ph.D. dissertation, Colorado State University, Fort Collins.

Struve, G. A.
1835 *De Silica in Plantis Nonnullis.* Unpublished Ph.D. dissertation, Berlin.

Swanson, Earl H. Jr.
1962 The Emergence of Plateau Culture. *Occasional Papers of the Idaho State College Museum* 8. Pocatello.

Thackray, Glenn D.
2001 Extensive Early and Middle Wisconsin Glaciation on the Western Olympic Peninsula, Washington, and the Variability of Pacific Moisture Delivery to the Northwestern United States. *Quaternary Research* 55(3):257-270.

Thackray, Glenn D., Kari A. Lundeen, and Jennifer A. Borgert
2004 Pleistocene Alpine Glacier Advances in the Sawtooth Mountains, Idaho, USA: Reflections of Midlatitude Moisture Transport at the Close of the Last Glaciation. *Geology* 32(3):225-228.

Twiss, Page C.
1992 Predicted World Distribution of C_3 and C_4 Grass Phytoliths. In *Phytolith Systematics: Emerging Issues,* edited by George Rapp Jr. and Susan C. Mulholland, pp. 113-128. Advances in Archaeological and Museum Science Vol. 1, Plenum Press, New York.

Twiss, Page C., Erwin Suess, and Robert M. Smith
1969 Morphological Classification of Grass Phytoliths. *Soil Science Society of America Journal* 33(1):109-115.

U.S. Environmental Protection Agency (USEPA)
2003 *Level III Ecoregions of the Continental United States (Revison of Omernick, 1987).* National Health and Environmental Effects Research Laboratory, Corvallis, various scales.

Waitt, Jr., Richard B., and Robert M. Thorson
1983 The Cordilleran Ice Sheet in Washington, Idaho, and Montana. In *Late Quaternary Environments of the United States, Volume* 1, edited by Stephen C. Porter, pp. 53-70. University of Minnesota Press, Minneapolis.

Waters, Michael R.
2013 In Search of the First Americans—What the Friedkin Site, Texas, Manis Site, Washington, and Others Tell us About the First Americans. Paper presented at the Paleoamerican Odyssey Conference, Santa Fe.

Waters, Michael R., and Thomas W. Stafford
2007 Redefining the Age of Clovis: Implications for the Peopling of the Americas. *Science* 315(5815):1122-1126.

Webster, Gary D., Mary J. Pankratz-Kuhns, and Gail L. Waggoner
1982 Late Cenozoic Gravels in Hells Canyon and the Lewiston Basin, Washington and Idaho. In *Cenozoic Geology of Idaho,* edited by Bill Bonnichsen and Roy M. Breckenridge, pp. 669-683. Idaho Bureau of Mines and Geology, Moscow.

Western Region Climate Center
2012 *Idaho Climate Summaries.* http://www.wrcc.dri.edu/summary/climsmid.html Accessed on September 5, 2012.

Whitlock, Cathy
1992 Vegetational and Climatic History of the Pacific Northwest During the Last 20,000 Years: Implications for Understanding Present-day Biodiversity. *The Northwest Environmental Journal* 8(5):5-28.

Whitlock, Cathy, and Patrick J. Bartlein
1997 Vegetation and Climate Change in Northwest America During the past 125kyr. *Nature* 388:57-60.

Whitlock, Cathy, Andrei M. Sarna-Wojcicki, Patrick J. Bartlein, and Rudy J. Nickmann
2000 Environmental History and Tephrostratigraphy at Carp Lake, Southwestern Columbia Basin, Washington, USA. *Palaeogeography, Palaeoclimatology, Palaeoecology* 155(1):7-29.

Witty, John E., and Ellis G. Knox
1964 Grass Opal in Some Chestnut and Forested Soils in North Central Oregon. *Soil Science Society of America Journal* 28(5):685-688.

Zhao, Zhijun
1998 The Middle Yangtze Region in China Is One Place Where Rice Was Domesticated: Phytolith Evidence from Diaotonghuan Cave, Northern Jiangxi. *Antiquity* 72(278):885-897.

Zhao, Zhijun, and Dolores R. Piperno
2000 Late Pleistocene/Holocene Environments in the Middle Yangtze River Valley, China and Rice (*Oryza sativa* L.) Domestication: The Phytolith Evidence. *Geoarchaeology* 15(2):203-222.

APPENDICES

Appendix A: Phytolith Scanning Sheet

Phytolith Scanning Sheet				
Site/Locality:				
Provenience:				
Morphotype			**Counts**	**Percent**
Descriptions				
Poaceae Morphotypes				
Rectangular Plate	**pr**			
Short Wavy <4 Lobes	**ws**			
Long Wavy >4 Lobes	**wl**			
Long Rectangular Parallel Sides	**lc**			
Long Indented	**li**			
Long Deeply Indented	**ld**			
Long Angular Non-Parallel	**la**			
Scutiform and Dendritic	**sd**			
Rondel Oval	**ro**			
Rondel Keeled	**rk**			
Rondel Horned	**rh**			
Rondel Pyramidal	**rp**			
Stipa-type Bilobate	**bs**			
Bilobate	**bi**			
Saddle	**sa**			
Tricome	**ht**			
Hair/Base	**hh**			
Non-Poaceae Morphotypes				
Blocky Grainy	**bg**			
Blocky Smooth	**bl**			
Epidermal Polygonal	**ep**			
Epidermal anticlinal	**ea**			
P. ponderosa Type	**pp**			
P. menziesii Type	**co**			
Larix Type	**co**			
Carex Type	**cx**			
Thin Plate W/Wavy Margins All Sides	**wp**			
Elongate Grainy	**el**			
Diatoms	**di**			
		Total:		

Appendix B: Pedological Descriptions and Results of Granulometric Analyses

SR-27 Pedological Descriptions

0-15cm (A)—dark brown (10YR 3/3) sandy loam, brown (10YR 5/3) dry; moderate coarse granular structure; slightly hard, very friable, slightly sticky and non-plastic; many fine and medium roots throughout; common fine dendritic tubular and common medium tubular pores; clear wavy boundary.

15-64cm (Bk1)—brown (10YR 4/3) sandy loam, pale brown (10YR 6/3) dry; moderate coarse subangular blocky structure; slightly hard, friable, slightly sticky and non-plastic; many fine and few coarse roots throughout; many fine and medium tubular and dendritic tubular pores; common medium clear white carbonate threads throughout; few distinct white carbonate coats on all faces of peds; gradual wavy boundary.

64-87cm (Ck1)—brown (10YR 4/3) sandy loam, pale brown (10YR 6/3) dry; massive structure; soft, very friable, slightly sticky and non-plastic; few fine roots throughout; common medium dendritic tubular and tubular pores; few medium clear white carbonate threads throughout; few distinct white carbonate coats on all faces of peds; clear wavy boundary.

87-138cm (Ck2)—brown (10YR 4/3) sandy loam, light yellowish brown (10YR 6/4) dry; massive structure; slightly hard, friable, non-sticky and non-plastic; common fine and medium tubular pores; few fine clear white carbonate threads throughout; clear smooth boundary.

138-160cm (Ck3)—brown (10YR 4/3) loamy sand, brown (10YR 5/3) dry; massive structure; slightly hard, very friable, non-sticky and non-plastic; few very fine roots throughout; few medium tubular pores; common fine clear white carbonate threads throughout; few distinct white carbonate coats on all faces of peds; few angular pebbles with carbonate coats on all surfaces clear smooth boundary.

160-191cm (Bkb)—dark yellowish brown (10YR 4/4) sandy loam, yellowish brown (10YR 5/4) dry; moderate coarse subangular blocky structure; hard, friable, slightly sticky and slightly plastic; common fine roots throughout; many fine dendritic tubular and tubular pores; common clear white carbonate threads and irregular masses throughout; few distinct white carbonate coats on surfaces along pores; few subangular pebbles and cobbles with carbonate coats on all surfaces; clear wavy boundary.

191-210cm (Ck1b)—brown (10YR 5/3) loamy sand, very pale brown (10YR 7/3) dry; massive structure; slightly hard, friable, slightly sticky and non-plastic; common fine and medium tubular pores; common clear white carbonate threads throughout; few subangular pebbles with carbonate coats on all surfaces; clear wavy boundary.

210-250cm (Ck2b)—dark yellowish brown (10YR 4/4) loamy sand, light yellowish brown (10YR 6/4) dry; massive structure; soft, very friable, non-sticky and non-plastic; finely disseminated carbonates throughout; gradual smooth boundary.

250-300cm (Cb)—dark yellowish brown (10YR 4/4) sand, light yellowish brown (10YR 6/4) dry; massive structure; loose; non-sticky and non-plastic; abrupt wavy boundary.

SR-34 Pedological Descriptions

0-10cm (A)—very dark brown (10YR 2/2) loamy sand, very dark grayish brown (10YR 3/2) dry; weak medium and coarse structure granular structure; soft, very friable, non-sticky and non-plastic; many very fine and fine roots throughout; many fine dendritic tubular and irregular pores; clear smooth boundary.

10-33cm (Bk1)—very dark brown (10YR 2/2) loamy sand, brown (10YR 4/3) dry; weak medium subangular blocky structure; slightly hard, very friable, non-sticky and non-plastic;

many very fine and fine roots throughout; few fine and medium tubular and dendritic pores; clear wavy boundary.

33-80cm (Bk2)—very dark grayish brown (10YR 3/2) loam, brown (10YR 5/3) dry; weak medium and coarse subangular blocky structure; moderately hard, friable, slightly sticky and non-plastic; few very fine and fine roots throughout; common medium and coarse tubular pores; clear wavy boundary.

80-128cm (Ck1)—brown (10YR4/3) loam, brown (10YR 5/3) dry; massive structure; slightly hard, friable, slightly sticky and slightly plastic; common very fine roots throughout; few fine tubular pores; common medium clear white irregular carbonate nodules and threads throughout; few distinct white carbonate coats on all faces of peds; clear smooth boundary.

128-155cm (Ck2)—brown (10YR 4/3) sandy loam, yellowish brown (10YR 5/4) dry; massive structure; slightly hard, friable, non-sticky and non-plastic; few very fine roots throughout; common fine tubular pores; common fine and medium clear white irregular carbonate masses and threads throughout; few distinct white carbonate coats on all faces of peds; clear smooth boundary.

155-175cm (Ck3)— brown (10YR 4/3) sandy loam, pale brown (10YR 6/3) dry; massive structure; slightly hard, friable, non-sticky and non-plastic; few very fine roots throughout; many very fine tubular pores; many fine and medium clear white irregular carbonate nodules and threads throughout; few distinct white carbonate coats on all faces of peds; abrupt smooth boundary.

175-238cm (Ck4)—brown (10YR 4/3) loamy sand, pale brown (10YR 6/3) dry; massive structure; soft, loose, non-sticky and non-plastic; few fine tubular pores; common fine clear

white carbonate threads throughout; few distinct white carbonate coats on all faces of peds; clear wavy boundary.

238-258cm (Ck5)—brown (10YR 4/3) sandy loam, pale brown (10YR 6/3) dry; massive structure; slightly hard, very friable, slightly sticky and non-plastic; few fine roots throughout; common fine and medium tubular pores; common fine clear white irregular carbonate nodules and threads throughout; few distinct white carbonate coats on surfaces along pores and on all faces of peds; clear wavy boundary.

258-310cm (Bkb1)—brown (10YR 4/3) sandy loam, light pale brown (10YR 6/4) dry; weak medium subangular blocky structure; slightly hard, very friable, slightly sticky and non-plastic; few fine tubular pores; few fine clear white carbonate threads throughout; few distinct white carbonate coats on all faces of peds; clear wavy boundary.

310-341cm (Ckb1)—brown (10YR 4/3) sandy loam, yellowish brown (10YR 5/4) dry; massive structure; slightly hard, very friable, slightly sticky and non-plastic; few very fine roots; many fine tubular and few coarse vesicular pores; few fine clear white irregular carbonate masses and threads throughout; few distinct white carbonate coats on all faces of peds; abrupt wavy boundary.

341-398cm (Bkb2)—dark yellowish brown (10YR 3/4) loamy sand, yellowish brown (10YR 5/4) dry; moderate medium subangular blocky structure; very hard, firm, slightly sticky and moderately plastic; few fine roots throughout; many very fine and fine tubular pores; few very coarse cylindrical insect casts; many fine and medium clear white irregular carbonate masses and threads throughout; common distinct white carbonate coats on all faces of peds and on surfaces along pores; common subangular pebbles and cobbles with carbonate coats on all surfaces; clear wavy boundary.

398-439cm (Ck1b2)—dark yellowish brown (10YR 3/4) loamy sand, light yellowish brown (10YR 6/4) dry; moderate medium subangular blocky structure; hard, very firm, non-sticky and non-plastic; common fine tubular pores; common fine clear white irregular carbonate masses and threads throughout; few distinct white carbonate coats on all faces of peds; common subangular pebbles with carbonate coats on all surfaces throughout; clear smooth boundary.

439-477cm (Ck2b2)—brown (10YR 4/3) loamy sand, pale brown (10YR 6/3) dry; moderate medium subangular blocky structure; very hard, firm, non-sticky and non-plastic; common very fine tubular pores; common fine clear white carbonate threads throughout; few distinct white carbonate coats on all faces of peds; common subangular pebbles with carbonate coats on all surfaces throughout; gradual wavy boundary.

477-500cm (Ck3b2)—brown (10YR 4/3), pale brown (10YR 6/3) dry, subangular and angular cobble clast-supported matrix with interstitial loamy sand; weak medium subangular blocky structure; slightly hard, very friable, slightly sticky and non-plastic; common fine tubular pores; few fine clear white carbonate threads throughout; many angular and subangular pebbles and cobbles with carbonate coats on all surfaces throughout; lower boundary not observed.

SR-27 GRANULOMETRY DATA WITH HORIZONS, ORGANIC MATTER AND CARBONATE CONTENT

SR-27												
	10	18	35	60	120	230	PAN		TEXTURE	Horizons	%OM	%CaCO3
LU	GR	VCS	CS	MS	FS	VFS	S+C			A	1.96	2.195467
9	0.2	0.4	0.2	9.3	29	35.7	24.6	99.4	Sandy loam	Bk	0.94	1.538462
8	0.6	0.3	0.6	2.2	29.1	42.7	24.2	99.7	Sandy loam	Ck1	0.8	1.180556
7	0.9	0	0.3	1.4	18.2	40.2	38.8	99.8	Sandy loam	Ck2	1.13	1.408451
6	0.7	0	0.1	1.2	30.8	46.7	20	99.5	Loamy sand	Ck3	1.06	1.632653
5	0.4	0.8	1.5	6.9	27.6	33	29.5	99.7	Sandy loam	Bkb	1.08	1.253298
4	0.2	0.2	1.1	13.8	36.5	27.9	19.8	99.5	Loamy sand	Ck1b	0.82	2.011923
3	0.6	0.1	0.9	13.3	33.2	32.1	19.6	99.8	Loamy sand	Ck2b	0.58	0.951734
2	0.1	0.8	1.6	18.7	42.4	24.2	12.1	99.9	Sand	Cb	1.56	1.7507

SR-34 GRANULOMETRY DATA WITH HORIZIONS, ORGANIC MATTER AND CARBONATE CONTENT

SR-34												
LU	GR	VCS	CS	MS	FS	VFS	S+C		TEXTURE	Horizons	%OM	%CaCO3
11	0.3	0.2	0.6	7.1	42.4	32.1	16.9	99.6	Loamy sand	A	1.57	1.802962
	0.6	0.6	1.1	6.2	38.2	32.9	20.2	99.8	Loamy sand	Bk1	0.92	1.417434
10	0.1	0.2	1.4	2.1	18.3	28.3	49.3	99.7	Loam	Bk2	1.47	2.027972
	0.5	0	0	4.1	13.2	29.3	52.4	99.5	Loam	Ck1	0.97	1.523546
9	0.2	0	0.2	4.7	22.2	34.2	38.1	99.6	Sandy loam	Ck2	0.77	1.266714
8	0.8	0.1	0.1	2	18.1	35.1	43.6	99.8	Sandy loam	Ck3	0.75	1.360544
7	0.4	0	0	2.3	32.4	45.4	18.7	99.2	Loamy sand	Ck4	0.66	1.318392
6	0.2	0.1	0.1	1	16.5	39.8	42.1	99.8	Sandy loam	Ck5	0.75	1.492537
5	0.7	0.1	0.3	1.3	16.9	41.2	39.2	99.7	Sandy loam	Bkb1	1.09	1.564626
4	0.2	0.1	0.2	2.2	26.7	42.8	27.3	99.5	Sandy loam	Ckb1	0.77	1.192146
3	0.1	1.6	2.1	12.6	30.6	27.6	25.2	99.8	Loamy sand	Bkb2	1.22	1.93299
	0.5	0.4	1	12.8	34.2	29.6	21.4	99.9	Loamy sand	Ck1b2	0.66	0.986842
2	0.9	1.8	2.2	12.5	32.1	27.9	22.2	99.6	Loamy sand	Ck2b2	0.74	1.348618
1	0.3	1.1	1.9	14.5	33.7	27.7	20.6	99.8	Loamy sand	Ck3b2	0.66	1.385224

Appendix C: Phytolith Counts from SR-23, SR-27, SR-34, and 10IH73 Unit A

Site/Locality: **SR23**			
Provenience: **0-10cm**			
Morphotype Descriptions			**Counts**
Poaceae Morphotypes			
Rectangular Plate	**pr**		10
Short Wavy <4 Lobes	**ws**		23
Long Wavy >4 Lobes	**wl**		5
Long Rectangular Parallel Sides	**lc**		32
Long Indented	**li**		28
Long Deeply Indented	**ld**		3
Long Angular Non-Parallel	**la**		19
Scutiform and Dendritic	**sd**		0
Rondel Oval	**ro**		35
Rondel Keeled	**rk**		0
Rondel Horned	**rh**		0
Rondel Pyramidal	**rp**		0
Stipa-type Bilobate	**bs**		0
Bilobate	**bi**		0
Saddle	**sa**		0
Tricome	**ht**		13
Hair/Base	**hh**		23
Non-Poaceae Morphotypes			
Blocky Grainy	**bg**		31
Blocky Smooth	**bl**		32
Epidermal Polygonal	**ep**		16
Epidermal anticlinal	**ea**		7
P. ponderosa Type	**pp**		0
P. menziesii Type	**co**		0
Larix Type	**co**		0
Carex Type	**cx**		0
Thin Plate W/Wavy Margins	**wp**		0
Elongate Grainy	**el**		13
Diatoms	**di**		5
		Total:	**295**

Site/Locality: **SR23**			
Provenience: **10-20cm**			
Morphotype Descriptions			**Counts**
Poaceae Morphotypes			
Rectangular Plate	**pr**		24
Short Wavy <4 Lobes	**ws**		44
Long Wavy >4 Lobes	**wl**		24
Long Rectangular Parallel Sides	**lc**		11
Long Indented	**li**		14
Long Deeply Indented	**ld**		2
Long Angular Non-Parallel	**la**		5
Scutiform and Dendritic	**sd**		1
Rondel Oval	**ro**		55
Rondel Keeled	**rk**		7
Rondel Horned	**rh**		0
Rondel Pyramidal	**rp**		0
Stipa-type Bilobate	**bs**		0
Bilobate	**bi**		0
Saddle	**sa**		0
Tricome	**ht**		4
Hair/Base	**hh**		23
Non-Poaceae Morphotypes			
Blocky Grainy	**bg**		25
Blocky Smooth	**bl**		15
Epidermal Polygonal	**ep**		4
Epidermal anticlinal	**ea**		0
P. ponderosa Type	**pp**		0
P. menziesii Type	**co**		0
Larix Type	**co**		0
Carex Type	**cx**		0
Thin Plate W/Wavy Margins	**wp**		0
Elongate Grainy	**el**		8
Diatoms	**di**		1
		Total:	**267**

Site/Locality: **SR23**			
Provenience: **20-30cm**			
Morphotype Descriptions			**Counts**
Poaceae Morphotypes			
Rectangular Plate	**pr**		22
Short Wavy <4 Lobes	**ws**		35
Long Wavy >4 Lobes	**wl**		6
Long Rectangular Parallel Sides	**lc**		19
Long Indented	**li**		13
Long Deeply Indented	**ld**		0
Long Angular Non-Parallel	**la**		9
Scutiform and Dendritic	**sd**		0
Rondel Oval	**ro**		60
Rondel Keeled	**rk**		4
Rondel Horned	**rh**		0
Rondel Pyramidal	**rp**		3
Stipa-type Bilobate	**bs**		0
Bilobate	**bi**		0
Saddle	**sa**		0
Tricome	**ht**		9
Hair/Base	**hh**		17
Non-Poaceae Morphotypes			
Blocky Grainy	**bg**		23
Blocky Smooth	**bl**		33
Epidermal Polygonal	**ep**		16
Epidermal anticlinal	**ea**		6
P. ponderosa Type	**pp**		0
P. menziesii Type	**co**		0
Larix Type	**co**		0
Carex Type	**cx**		0
Thin Plate W/Wavy Margins	**wp**		0
Elongate Grainy	**el**		5
Diatoms	**di**		2
		Total:	**282**

Site/Locality: **SR23**			
Provenience: **30-40cm**			
Morphotype Descriptions			**Counts**
Poaceae Morphotypes			
Rectangular Plate	**pr**		27
Short Wavy <4 Lobes	**ws**		44
Long Wavy >4 Lobes	**wl**		4
Long Rectangular Parallel Sides	**lc**		20
Long Indented	**li**		17
Long Deeply Indented	**ld**		1
Long Angular Non-Parallel	**la**		11
Scutiform and Dendritic	**sd**		0
Rondel Oval	**ro**		56
Rondel Keeled	**rk**		8
Rondel Horned	**rh**		0
Rondel Pyramidal	**rp**		5
Stipa-type Bilobate	**bs**		1
Bilobate	**bi**		1
Saddle	**sa**		0
Tricome	**ht**		10
Hair/Base	**hh**		22
Non-Poaceae Morphotypes			
Blocky Grainy	**bg**		37
Blocky Smooth	**bl**		26
Epidermal Polygonal	**ep**		11
Epidermal anticlinal	**ea**		4
P. ponderosa Type	**pp**		0
P. menziesii Type	**co**		0
Larix Type	**co**		0
Carex Type	**cx**		0
Thin Plate W/Wavy Margins	**wp**		0
Elongate Grainy	**el**		5
Diatoms	**di**		4
		Total:	**314**

Site/Locality: **SR23**			
Provenience: **40-50cm**			
Morphotype Descriptions			**Counts**
Poaceae Morphotypes			
Rectangular Plate	**pr**		19
Short Wavy <4 Lobes	**ws**		47
Long Wavy >4 Lobes	**wl**		5
Long Rectangular Parallel Sides	**lc**		22
Long Indented	**li**		14
Long Deeply Indented	**ld**		1
Long Angular Non-Parallel	**la**		10
Scutiform and Dendritic	**sd**		0
Rondel Oval	**ro**		60
Rondel Keeled	**rk**		5
Rondel Horned	**rh**		0
Rondel Pyramidal	**rp**		2
Stipa-type Bilobate	**bs**		1
Bilobate	**bi**		0
Saddle	**sa**		0
Tricome	**ht**		6
Hair/Base	**hh**		19
Non-Poaceae Morphotypes			
Blocky Grainy	**bg**		30
Blocky Smooth	**bl**		15
Epidermal Polygonal	**ep**		5
Epidermal anticlinal	**ea**		0
P. ponderosa Type	**pp**		0
P. menziesii Type	**co**		0
Larix Type	**co**		0
Carex Type	**cx**		0
Thin Plate W/Wavy Margins	**wp**		0
Elongate Grainy	**el**		8
Diatoms	**di**		2
		Total:	**271**

Site/Locality: **SR23**			
Provenience: **50-60cm**			
Morphotype Descriptions			**Counts**
Poaceae Morphotypes			
Rectangular Plate	**pr**		17
Short Wavy <4 Lobes	**ws**		37
Long Wavy >4 Lobes	**wl**		6
Long Rectangular Parallel Sides	**lc**		16
Long Indented	**li**		13
Long Deeply Indented	**ld**		1
Long Angular Non-Parallel	**la**		7
Scutiform and Dendritic	**sd**		0
Rondel Oval	**ro**		45
Rondel Keeled	**rk**		6
Rondel Horned	**rh**		0
Rondel Pyramidal	**rp**		4
Stipa-type Bilobate	**bs**		1
Bilobate	**bi**		0
Saddle	**sa**		0
Tricome	**ht**		8
Hair/Base	**hh**		15
Non-Poaceae Morphotypes			
Blocky Grainy	**bg**		28
Blocky Smooth	**bl**		45
Epidermal Polygonal	**ep**		7
Epidermal anticlinal	**ea**		4
P. ponderosa Type	**pp**		0
P. menziesii Type	**co**		0
Larix Type	**co**		0
Carex Type	**cx**		0
Thin Plate W/Wavy Margins	**wp**		0
Elongate Grainy	**el**		9
Diatoms	**di**		5
		Total:	**274**

Site/Locality: **SR23**			
Provenience: **60-70cm**			
Morphotype Descriptions			**Counts**
Poaceae Morphotypes			
Rectangular Plate	**pr**		12
Short Wavy <4 Lobes	**ws**		31
Long Wavy >4 Lobes	**wl**		6
Long Rectangular Parallel Sides	**lc**		9
Long Indented	**li**		7
Long Deeply Indented	**ld**		0
Long Angular Non-Parallel	**la**		5
Scutiform and Dendritic	**sd**		0
Rondel Oval	**ro**		50
Rondel Keeled	**rk**		7
Rondel Horned	**rh**		0
Rondel Pyramidal	**rp**		0
Stipa-type Bilobate	**bs**		0
Bilobate	**bi**		0
Saddle	**sa**		0
Tricome	**ht**		8
Hair/Base	**hh**		22
Non-Poaceae Morphotypes			
Blocky Grainy	**bg**		43
Blocky Smooth	**bl**		37
Epidermal Polygonal	**ep**		18
Epidermal anticlinal	**ea**		6
P. ponderosa Type	**pp**		0
P. menziesii Type	**co**		0
Larix Type	**co**		0
Carex Type	**cx**		0
Thin Plate W/Wavy Margins	**wp**		0
Elongate Grainy	**el**		4
Diatoms	**di**		4
		Total:	**269**

Site/Locality: **SR23**			
Provenience: **70-80cm**			
Morphotype Descriptions			**Counts**
Poaceae Morphotypes			
Rectangular Plate	**pr**		6
Short Wavy <4 Lobes	**ws**		13
Long Wavy >4 Lobes	**wl**		2
Long Rectangular Parallel Sides	**lc**		5
Long Indented	**li**		8
Long Deeply Indented	**ld**		0
Long Angular Non-Parallel	**la**		7
Scutiform and Dendritic	**sd**		0
Rondel Oval	**ro**		30
Rondel Keeled	**rk**		2
Rondel Horned	**rh**		0
Rondel Pyramidal	**rp**		0
Stipa-type Bilobate	**bs**		0
Bilobate	**bi**		0
Saddle	**sa**		0
Tricome	**ht**		13
Hair/Base	**hh**		36
Non-Poaceae Morphotypes			
Blocky Grainy	**bg**		59
Blocky Smooth	**bl**		63
Epidermal Polygonal	**ep**		27
Epidermal anticlinal	**ea**		7
P. ponderosa Type	**pp**		0
P. menziesii Type	**co**		0
Larix Type	**co**		0
Carex Type	**cx**		0
Thin Plate W/Wavy Margins	**wp**		0
Elongate Grainy	**el**		2
Diatoms	**di**		0
		Total:	**280**

Site/Locality: **SR23**			
Provenience: **80-90cm**			
Morphotype Descriptions			**Counts**
Poaceae Morphotypes			
Rectangular Plate	**pr**		6
Short Wavy <4 Lobes	**ws**		32
Long Wavy >4 Lobes	**wl**		3
Long Rectangular Parallel Sides	**lc**		7
Long Indented	**li**		10
Long Deeply Indented	**ld**		0
Long Angular Non-Parallel	**la**		3
Scutiform and Dendritic	**sd**		0
Rondel Oval	**ro**		30
Rondel Keeled	**rk**		8
Rondel Horned	**rh**		0
Rondel Pyramidal	**rp**		0
Stipa-type Bilobate	**bs**		1
Bilobate	**bi**		0
Saddle	**sa**		0
Tricome	**ht**		8
Hair/Base	**hh**		23
Non-Poaceae Morphotypes			
Blocky Grainy	**bg**		64
Blocky Smooth	**bl**		49
Epidermal Polygonal	**ep**		23
Epidermal anticlinal	**ea**		4
P. ponderosa Type	**pp**		0
P. menziesii Type	**co**		0
Larix Type	**co**		0
Carex Type	**cx**		0
Thin Plate W/Wavy Margins	**wp**		0
Elongate Grainy	**el**		3
Diatoms	**di**		5
		Total:	**279**

Site/Locality: **SR23**			
Provenience: **90-100cm**			
Morphotype Descriptions			**Counts**
Poaceae Morphotypes			
Rectangular Plate	**pr**		8
Short Wavy <4 Lobes	**ws**		17
Long Wavy >4 Lobes	**wl**		2
Long Rectangular Parallel Sides	**lc**		14
Long Indented	**li**		4
Long Deeply Indented	**ld**		0
Long Angular Non-Parallel	**la**		3
Scutiform and Dendritic	**sd**		0
Rondel Oval	**ro**		25
Rondel Keeled	**rk**		4
Rondel Horned	**rh**		0
Rondel Pyramidal	**rp**		0
Stipa-type Bilobate	**bs**		0
Bilobate	**bi**		0
Saddle	**sa**		0
Tricome	**ht**		14
Hair/Base	**hh**		28
Non-Poaceae Morphotypes			
Blocky Grainy	**bg**		53
Blocky Smooth	**bl**		60
Epidermal Polygonal	**ep**		26
Epidermal anticlinal	**ea**		9
P. ponderosa Type	**pp**		0
P. menziesii Type	**co**		0
Larix Type	**co**		0
Carex Type	**cx**		0
Thin Plate W/Wavy Margins	**wp**		0
Elongate Grainy	**el**		6
Diatoms	**di**		3
		Total:	**276**

Site/Locality: **SR23**			
Provenience: **100-110cm**			
Morphotype Descriptions			**Counts**
Poaceae Morphotypes			
Rectangular Plate	**pr**		12
Short Wavy <4 Lobes	**ws**		31
Long Wavy >4 Lobes	**wl**		3
Long Rectangular Parallel Sides	**lc**		10
Long Indented	**li**		7
Long Deeply Indented	**ld**		1
Long Angular Non-Parallel	**la**		5
Scutiform and Dendritic	**sd**		1
Rondel Oval	**ro**		36
Rondel Keeled	**rk**		8
Rondel Horned	**rh**		0
Rondel Pyramidal	**rp**		0
Stipa-type Bilobate	**bs**		1
Bilobate	**bi**		0
Saddle	**sa**		0
Tricome	**ht**		11
Hair/Base	**hh**		30
Non-Poaceae Morphotypes			
Blocky Grainy	**bg**		33
Blocky Smooth	**bl**		50
Epidermal Polygonal	**ep**		22
Epidermal anticlinal	**ea**		6
P. ponderosa Type	**pp**		0
P. menziesii Type	**co**		0
Larix Type	**co**		0
Carex Type	**cx**		0
Thin Plate W/Wavy Margins	**wp**		0
Elongate Grainy	**el**		4
Diatoms	**di**		3
		Total:	**274**

Site/Locality: **SR23**			
Provenience: **110-120cm**			
Morphotype Descriptions			**Counts**
Poaceae Morphotypes			
Rectangular Plate	**pr**		10
Short Wavy <4 Lobes	**ws**		14
Long Wavy >4 Lobes	**wl**		0
Long Rectangular Parallel Sides	**lc**		3
Long Indented	**li**		7
Long Deeply Indented	**ld**		0
Long Angular Non-Parallel	**la**		5
Scutiform and Dendritic	**sd**		0
Rondel Oval	**ro**		35
Rondel Keeled	**rk**		4
Rondel Horned	**rh**		0
Rondel Pyramidal	**rp**		0
Stipa-type Bilobate	**bs**		0
Bilobate	**bi**		0
Saddle	**sa**		0
Tricome	**ht**		24
Hair/Base	**hh**		32
Non-Poaceae Morphotypes			
Blocky Grainy	**bg**		52
Blocky Smooth	**bl**		63
Epidermal Polygonal	**ep**		27
Epidermal anticlinal	**ea**		10
P. ponderosa Type	**pp**		0
P. menziesii Type	**co**		0
Larix Type	**co**		0
Carex Type	**cx**		0
Thin Plate W/Wavy Margins	**wp**		0
Elongate Grainy	**el**		0
Diatoms	**di**		0
		Total:	**286**

Site/Locality: **SR23**			
Provenience: **160-170cm**			
Morphotype Descriptions			**Counts**
Poaceae Morphotypes			
Rectangular Plate	**pr**		8
Short Wavy <4 Lobes	**ws**		32
Long Wavy >4 Lobes	**wl**		4
Long Rectangular Parallel Sides	**lc**		17
Long Indented	**li**		13
Long Deeply Indented	**ld**		3
Long Angular Non-Parallel	**la**		4
Scutiform and Dendritic	**sd**		0
Rondel Oval	**ro**		33
Rondel Keeled	**rk**		7
Rondel Horned	**rh**		1
Rondel Pyramidal	**rp**		0
Stipa-type Bilobate	**bs**		0
Bilobate	**bi**		0
Saddle	**sa**		0
Tricome	**ht**		5
Hair/Base	**hh**		26
Non-Poaceae Morphotypes			
Blocky Grainy	**bg**		37
Blocky Smooth	**bl**		39
Epidermal Polygonal	**ep**		24
Epidermal anticlinal	**ea**		12
P. ponderosa Type	**pp**		0
P. menziesii Type	**co**		0
Larix Type	**co**		0
Carex Type	**cx**		0
Thin Plate W/Wavy Margins	**wp**		0
Elongate Grainy	**el**		1
Diatoms	**di**		1
		Total:	**267**

Site/Locality: **SR23**			
Provenience: **170-180cm**			
Morphotype Descriptions			**Counts**
Poaceae Morphotypes			
Rectangular Plate	**pr**		12
Short Wavy <4 Lobes	**ws**		29
Long Wavy >4 Lobes	**wl**		4
Long Rectangular Parallel Sides	**lc**		18
Long Indented	**li**		10
Long Deeply Indented	**ld**		0
Long Angular Non-Parallel	**la**		7
Scutiform and Dendritic	**sd**		0
Rondel Oval	**ro**		45
Rondel Keeled	**rk**		2
Rondel Horned	**rh**		0
Rondel Pyramidal	**rp**		0
Stipa-type Bilobate	**bs**		0
Bilobate	**bi**		0
Saddle	**sa**		0
Tricome	**ht**		13
Hair/Base	**hh**		39
Non-Poaceae Morphotypes			
Blocky Grainy	**bg**		32
Blocky Smooth	**bl**		53
Epidermal Polygonal	**ep**		28
Epidermal anticlinal	**ea**		11
P. ponderosa Type	**pp**		0
P. menziesii Type	**co**		0
Larix Type	**co**		0
Carex Type	**cx**		0
Thin Plate W/Wavy Margins	**wp**		0
Elongate Grainy	**el**		0
Diatoms	**di**		0
		Total:	**303**

Site/Locality: **SR23**			
Provenience: **180-190cm**			
Morphotype Descriptions			**Counts**
Poaceae Morphotypes			
Rectangular Plate	**pr**		3
Short Wavy <4 Lobes	**ws**		11
Long Wavy >4 Lobes	**wl**		2
Long Rectangular Parallel Sides	**lc**		5
Long Indented	**li**		7
Long Deeply Indented	**ld**		0
Long Angular Non-Parallel	**la**		5
Scutiform and Dendritic	**sd**		0
Rondel Oval	**ro**		30
Rondel Keeled	**rk**		2
Rondel Horned	**rh**		0
Rondel Pyramidal	**rp**		0
Stipa-type Bilobate	**bs**		1
Bilobate	**bi**		0
Saddle	**sa**		0
Tricome	**ht**		7
Hair/Base	**hh**		33
Non-Poaceae Morphotypes			
Blocky Grainy	**bg**		74
Blocky Smooth	**bl**		44
Epidermal Polygonal	**ep**		17
Epidermal anticlinal	**ea**		8
P. ponderosa Type	**pp**		0
P. menziesii Type	**co**		0
Larix Type	**co**		0
Carex Type	**cx**		0
Thin Plate W/Wavy Margins	**wp**		0
Elongate Grainy	**el**		2
Diatoms	**di**		4
		Total:	**255**

Site/Locality: **SR23**			
Provenience: **190-200cm**			
Morphotype Descriptions			**Counts**
Poaceae Morphotypes			
Rectangular Plate	**pr**		6
Short Wavy <4 Lobes	**ws**		19
Long Wavy >4 Lobes	**wl**		0
Long Rectangular Parallel Sides	**lc**		7
Long Indented	**li**		5
Long Deeply Indented	**ld**		1
Long Angular Non-Parallel	**la**		5
Scutiform and Dendritic	**sd**		0
Rondel Oval	**ro**		39
Rondel Keeled	**rk**		0
Rondel Horned	**rh**		0
Rondel Pyramidal	**rp**		0
Stipa-type Bilobate	**bs**		0
Bilobate	**bi**		0
Saddle	**sa**		0
Tricome	**ht**		8
Hair/Base	**hh**		34
Non-Poaceae Morphotypes			
Blocky Grainy	**bg**		29
Blocky Smooth	**bl**		62
Epidermal Polygonal	**ep**		18
Epidermal anticlinal	**ea**		7
P. ponderosa Type	**pp**		0
P. menziesii Type	**co**		0
Larix Type	**co**		0
Carex Type	**cx**		1
Thin Plate W/Wavy Margins	**wp**		0
Elongate Grainy	**el**		0
Diatoms	**di**		1
		Total:	**242**

Site/Locality: **SR23**			
Provenience: **200-210cm**			
Morphotype Descriptions			**Counts**
Poaceae Morphotypes			
Rectangular Plate	**pr**		8
Short Wavy <4 Lobes	**ws**		19
Long Wavy >4 Lobes	**wl**		0
Long Rectangular Parallel Sides	**lc**		11
Long Indented	**li**		4
Long Deeply Indented	**ld**		0
Long Angular Non-Parallel	**la**		4
Scutiform and Dendritic	**sd**		0
Rondel Oval	**ro**		25
Rondel Keeled	**rk**		4
Rondel Horned	**rh**		0
Rondel Pyramidal	**rp**		0
Stipa-type Bilobate	**bs**		0
Bilobate	**bi**		0
Saddle	**sa**		0
Tricome	**ht**		6
Hair/Base	**hh**		43
Non-Poaceae Morphotypes			
Blocky Grainy	**bg**		44
Blocky Smooth	**bl**		54
Epidermal Polygonal	**ep**		23
Epidermal anticlinal	**ea**		8
P. ponderosa Type	**pp**		0
P. menziesii Type	**co**		0
Larix Type	**co**		0
Carex Type	**cx**		0
Thin Plate W/Wavy Margins	**wp**		0
Elongate Grainy	**el**		1
Diatoms	**di**		0
		Total:	**254**

Site/Locality: **SR23**			
Provenience: **210-220cm**			
Morphotype Descriptions			**Counts**
Poaceae Morphotypes			
Rectangular Plate	**pr**		24
Short Wavy <4 Lobes	**ws**		32
Long Wavy >4 Lobes	**wl**		13
Long Rectangular Parallel Sides	**lc**		9
Long Indented	**li**		10
Long Deeply Indented	**ld**		1
Long Angular Non-Parallel	**la**		1
Scutiform and Dendritic	**sd**		0
Rondel Oval	**ro**		40
Rondel Keeled	**rk**		0
Rondel Horned	**rh**		0
Rondel Pyramidal	**rp**		0
Stipa-type Bilobate	**bs**		4
Bilobate	**bi**		0
Saddle	**sa**		0
Tricome	**ht**		11
Hair/Base	**hh**		23
Non-Poaceae Morphotypes			
Blocky Grainy	**bg**		38
Blocky Smooth	**bl**		26
Epidermal Polygonal	**ep**		19
Epidermal anticlinal	**ea**		7
P. ponderosa Type	**pp**		1
P. menziesii Type	**co**		0
Larix Type	**co**		0
Carex Type	**cx**		0
Thin Plate W/Wavy Margins	**wp**		0
Elongate Grainy	**el**		5
Diatoms	**di**		3
		Total:	**267**

Site/Locality: **SR23**			
Provenience: **220-230m**			
Morphotype Descriptions			**Counts**
Poaceae Morphotypes			
Rectangular Plate	**pr**		20
Short Wavy <4 Lobes	**ws**		34
Long Wavy >4 Lobes	**wl**		7
Long Rectangular Parallel Sides	**lc**		18
Long Indented	**li**		16
Long Deeply Indented	**ld**		2
Long Angular Non-Parallel	**la**		9
Scutiform and Dendritic	**sd**		0
Rondel Oval	**ro**		45
Rondel Keeled	**rk**		9
Rondel Horned	**rh**		0
Rondel Pyramidal	**rp**		0
Stipa-type Bilobate	**bs**		2
Bilobate	**bi**		0
Saddle	**sa**		0
Tricome	**ht**		18
Hair/Base	**hh**		27
Non-Poaceae Morphotypes			
Blocky Grainy	**bg**		39
Blocky Smooth	**bl**		18
Epidermal Polygonal	**ep**		11
Epidermal anticlinal	**ea**		3
P. ponderosa Type	**pp**		0
P. menziesii Type	**co**		0
Larix Type	**co**		0
Carex Type	**cx**		0
Thin Plate W/Wavy Margins	**wp**		0
Elongate Grainy	**el**		6
Diatoms	**di**		4
		Total:	**288**

Site/Locality: **SR23**			
Provenience: **230-240m**			
Morphotype Descriptions			**Counts**
Poaceae Morphotypes			
Rectangular Plate	**pr**		22
Short Wavy <4 Lobes	**ws**		29
Long Wavy >4 Lobes	**wl**		6
Long Rectangular Parallel Sides	**lc**		19
Long Indented	**li**		13
Long Deeply Indented	**ld**		0
Long Angular Non-Parallel	**la**		7
Scutiform and Dendritic	**sd**		0
Rondel Oval	**ro**		40
Rondel Keeled	**rk**		3
Rondel Horned	**rh**		0
Rondel Pyramidal	**rp**		0
Stipa-type Bilobate	**bs**		1
Bilobate	**bi**		0
Saddle	**sa**		0
Tricome	**ht**		19
Hair/Base	**hh**		28
Non-Poaceae Morphotypes			
Blocky Grainy	**bg**		34
Blocky Smooth	**bl**		26
Epidermal Polygonal	**ep**		15
Epidermal anticlinal	**ea**		6
P. ponderosa Type	**pp**		0
P. menziesii Type	**co**		0
Larix Type	**co**		0
Carex Type	**cx**		0
Thin Plate W/Wavy Margins	**wp**		0
Elongate Grainy	**el**		6
Diatoms	**di**		2
		Total:	**276**

Site/Locality: **SR23**			
Provenience: **240-250cm**			
Morphotype Descriptions			**Counts**
Poaceae Morphotypes			
Rectangular Plate	**pr**		17
Short Wavy <4 Lobes	**ws**		44
Long Wavy >4 Lobes	**wl**		12
Long Rectangular Parallel Sides	**lc**		18
Long Indented	**li**		23
Long Deeply Indented	**ld**		3
Long Angular Non-Parallel	**la**		9
Scutiform and Dendritic	**sd**		0
Rondel Oval	**ro**		32
Rondel Keeled	**rk**		5
Rondel Horned	**rh**		0
Rondel Pyramidal	**rp**		0
Stipa-type Bilobate	**bs**		2
Bilobate	**bi**		0
Saddle	**sa**		0
Tricome	**ht**		17
Hair/Base	**hh**		24
Non-Poaceae Morphotypes			
Blocky Grainy	**bg**		47
Blocky Smooth	**bl**		22
Epidermal Polygonal	**ep**		13
Epidermal anticlinal	**ea**		1
P. ponderosa Type	**pp**		1
P. menziesii Type	**co**		0
Larix Type	**co**		0
Carex Type	**cx**		0
Thin Plate W/Wavy Margins	**wp**		0
Elongate Grainy	**el**		11
Diatoms	**di**		3
		Total:	**304**

Site/Locality: **SR23**			
Provenience: **250-260cm**			
Morphotype Descriptions			**Counts**
Poaceae Morphotypes			
Rectangular Plate	**pr**		21
Short Wavy <4 Lobes	**ws**		29
Long Wavy >4 Lobes	**wl**		11
Long Rectangular Parallel Sides	**lc**		17
Long Indented	**li**		16
Long Deeply Indented	**ld**		2
Long Angular Non-Parallel	**la**		7
Scutiform and Dendritic	**sd**		0
Rondel Oval	**ro**		50
Rondel Keeled	**rk**		3
Rondel Horned	**rh**		0
Rondel Pyramidal	**rp**		0
Stipa-type Bilobate	**bs**		1
Bilobate	**bi**		0
Saddle	**sa**		0
Tricome	**ht**		22
Hair/Base	**hh**		34
Non-Poaceae Morphotypes			
Blocky Grainy	**bg**		43
Blocky Smooth	**bl**		26
Epidermal Polygonal	**ep**		11
Epidermal anticlinal	**ea**		3
P. ponderosa Type	**pp**		0
P. menziesii Type	**co**		0
Larix Type	**co**		0
Carex Type	**cx**		0
Thin Plate W/Wavy Margins	**wp**		0
Elongate Grainy	**el**		11
Diatoms	**di**		2
		Total:	**309**

Site/Locality: **SR23**			
Provenience: **260-270cm**			
Morphotype Descriptions			**Counts**
Poaceae Morphotypes			
Rectangular Plate	**pr**		24
Short Wavy <4 Lobes	**ws**		40
Long Wavy >4 Lobes	**wl**		5
Long Rectangular Parallel Sides	**lc**		16
Long Indented	**li**		22
Long Deeply Indented	**ld**		4
Long Angular Non-Parallel	**la**		5
Scutiform and Dendritic	**sd**		0
Rondel Oval	**ro**		52
Rondel Keeled	**rk**		0
Rondel Horned	**rh**		0
Rondel Pyramidal	**rp**		0
Stipa-type Bilobate	**bs**		5
Bilobate	**bi**		0
Saddle	**sa**		1
Tricome	**ht**		19
Hair/Base	**hh**		28
Non-Poaceae Morphotypes			
Blocky Grainy	**bg**		44
Blocky Smooth	**bl**		22
Epidermal Polygonal	**ep**		18
Epidermal anticlinal	**ea**		4
P. ponderosa Type	**pp**		0
P. menziesii Type	**co**		0
Larix Type	**co**		0
Carex Type	**cx**		0
Thin Plate W/Wavy Margins	**wp**		0
Elongate Grainy	**el**		8
Diatoms	**di**		3
		Total:	**320**

Site/Locality: **SR23**			
Provenience: **270-280cm**			
Morphotype Descriptions			**Counts**
Poaceae Morphotypes			
Rectangular Plate	**pr**		15
Short Wavy <4 Lobes	**ws**		36
Long Wavy >4 Lobes	**wl**		3
Long Rectangular Parallel Sides	**lc**		20
Long Indented	**li**		9
Long Deeply Indented	**ld**		2
Long Angular Non-Parallel	**la**		7
Scutiform and Dendritic	**sd**		0
Rondel Oval	**ro**		38
Rondel Keeled	**rk**		8
Rondel Horned	**rh**		0
Rondel Pyramidal	**rp**		0
Stipa-type Bilobate	**bs**		3
Bilobate	**bi**		0
Saddle	**sa**		0
Tricome	**ht**		22
Hair/Base	**hh**		17
Non-Poaceae Morphotypes			
Blocky Grainy	**bg**		43
Blocky Smooth	**bl**		34
Epidermal Polygonal	**ep**		8
Epidermal anticlinal	**ea**		5
P. ponderosa Type	**pp**		0
P. menziesii Type	**co**		0
Larix Type	**co**		0
Carex Type	**cx**		0
Thin Plate W/Wavy Margins	**wp**		0
Elongate Grainy	**el**		7
Diatoms	**di**		3
		Total:	**280**

Site/Locality: **SR23**			
Provenience: **280-290cm**			
Morphotype Descriptions			**Counts**
Poaceae Morphotypes			
Rectangular Plate	**pr**		14
Short Wavy <4 Lobes	**ws**		23
Long Wavy >4 Lobes	**wl**		6
Long Rectangular Parallel Sides	**lc**		10
Long Indented	**li**		12
Long Deeply Indented	**ld**		6
Long Angular Non-Parallel	**la**		0
Scutiform and Dendritic	**sd**		2
Rondel Oval	**ro**		52
Rondel Keeled	**rk**		0
Rondel Horned	**rh**		1
Rondel Pyramidal	**rp**		0
Stipa-type Bilobate	**bs**		2
Bilobate	**bi**		0
Saddle	**sa**		0
Tricome	**ht**		14
Hair/Base	**hh**		36
Non-Poaceae Morphotypes			
Blocky Grainy	**bg**		37
Blocky Smooth	**bl**		26
Epidermal Polygonal	**ep**		13
Epidermal anticlinal	**ea**		4
P. ponderosa Type	**pp**		0
P. menziesii Type	**co**		0
Larix Type	**co**		0
Carex Type	**cx**		0
Thin Plate W/Wavy Margins	**wp**		0
Elongate Grainy	**el**		12
Diatoms	**di**		2
		Total:	**272**

Site/Locality: **SR23**			
Provenience: **290-300cm**			
Morphotype Descriptions			**Counts**
Poaceae Morphotypes			
Rectangular Plate	**pr**		15
Short Wavy <4 Lobes	**ws**		49
Long Wavy >4 Lobes	**wl**		11
Long Rectangular Parallel Sides	**lc**		14
Long Indented	**li**		18
Long Deeply Indented	**ld**		9
Long Angular Non-Parallel	**la**		7
Scutiform and Dendritic	**sd**		4
Rondel Oval	**ro**		37
Rondel Keeled	**rk**		14
Rondel Horned	**rh**		0
Rondel Pyramidal	**rp**		0
Stipa-type Bilobate	**bs**		2
Bilobate	**bi**		0
Saddle	**sa**		0
Tricome	**ht**		11
Hair/Base	**hh**		24
Non-Poaceae Morphotypes			
Blocky Grainy	**bg**		28
Blocky Smooth	**bl**		11
Epidermal Polygonal	**ep**		4
Epidermal anticlinal	**ea**		1
P. ponderosa Type	**pp**		0
P. menziesii Type	**co**		0
Larix Type	**co**		0
Carex Type	**cx**		0
Thin Plate W/Wavy Margins	**wp**		0
Elongate Grainy	**el**		5
Diatoms	**di**		2
		Total:	**266**

Site/Locality: **SR23**			
Provenience: **300-310cm**			
Morphotype Descriptions			**Counts**
Poaceae Morphotypes			
Rectangular Plate	**pr**		16
Short Wavy <4 Lobes	**ws**		36
Long Wavy >4 Lobes	**wl**		6
Long Rectangular Parallel Sides	**lc**		9
Long Indented	**li**		15
Long Deeply Indented	**ld**		0
Long Angular Non-Parallel	**la**		7
Scutiform and Dendritic	**sd**		0
Rondel Oval	**ro**		31
Rondel Keeled	**rk**		16
Rondel Horned	**rh**		0
Rondel Pyramidal	**rp**		4
Stipa-type Bilobate	**bs**		2
Bilobate	**bi**		0
Saddle	**sa**		0
Tricome	**ht**		12
Hair/Base	**hh**		19
Non-Poaceae Morphotypes			
Blocky Grainy	**bg**		47
Blocky Smooth	**bl**		22
Epidermal Polygonal	**ep**		12
Epidermal anticlinal	**ea**		4
P. ponderosa Type	**pp**		0
P. menziesii Type	**co**		0
Larix Type	**co**		0
Carex Type	**cx**		0
Thin Plate W/Wavy Margins	**wp**		0
Elongate Grainy	**el**		8
Diatoms	**di**		1
		Total:	**267**

Site/Locality: **SR23**			
Provenience: **310-320cm**			
Morphotype Descriptions			**Counts**
Poaceae Morphotypes			
Rectangular Plate	**pr**		23
Short Wavy <4 Lobes	**ws**		44
Long Wavy >4 Lobes	**wl**		7
Long Rectangular Parallel Sides	**lc**		14
Long Indented	**li**		11
Long Deeply Indented	**ld**		0
Long Angular Non-Parallel	**la**		5
Scutiform and Dendritic	**sd**		0
Rondel Oval	**ro**		41
Rondel Keeled	**rk**		9
Rondel Horned	**rh**		0
Rondel Pyramidal	**rp**		3
Stipa-type Bilobate	**bs**		4
Bilobate	**bi**		0
Saddle	**sa**		0
Tricome	**ht**		24
Hair/Base	**hh**		18
Non-Poaceae Morphotypes			
Blocky Grainy	**bg**		39
Blocky Smooth	**bl**		22
Epidermal Polygonal	**ep**		9
Epidermal anticlinal	**ea**		3
P. ponderosa Type	**pp**		0
P. menziesii Type	**co**		0
Larix Type	**co**		0
Carex Type	**cx**		0
Thin Plate W/Wavy Margins	**wp**		0
Elongate Grainy	**el**		12
Diatoms	**di**		4
		Total:	**292**

Site/Locality: **SR23**			
Provenience: **320-330cm**			
Morphotype Descriptions			**Counts**
Poaceae Morphotypes			
Rectangular Plate	**pr**		8
Short Wavy <4 Lobes	**ws**		32
Long Wavy >4 Lobes	**wl**		5
Long Rectangular Parallel Sides	**lc**		4
Long Indented	**li**		9
Long Deeply Indented	**ld**		1
Long Angular Non-Parallel	**la**		9
Scutiform and Dendritic	**sd**		0
Rondel Oval	**ro**		13
Rondel Keeled	**rk**		0
Rondel Horned	**rh**		0
Rondel Pyramidal	**rp**		5
Stipa-type Bilobate	**bs**		1
Bilobate	**bi**		0
Saddle	**sa**		0
Tricome	**ht**		14
Hair/Base	**hh**		34
Non-Poaceae Morphotypes			
Blocky Grainy	**bg**		27
Blocky Smooth	**bl**		44
Epidermal Polygonal	**ep**		47
Epidermal anticlinal	**ea**		12
P. ponderosa Type	**pp**		2
P. menziesii Type	**co**		0
Larix Type	**co**		0
Carex Type	**cx**		0
Thin Plate W/Wavy Margins	**wp**		0
Elongate Grainy	**el**		1
Diatoms	**di**		1
		Total:	**269**

Site/Locality: **SR23**			
Provenience: **330-340cm**			
Morphotype Descriptions			**Counts**
Poaceae Morphotypes			
Rectangular Plate	**pr**		14
Short Wavy <4 Lobes	**ws**		37
Long Wavy >4 Lobes	**wl**		9
Long Rectangular Parallel Sides	**lc**		9
Long Indented	**li**		18
Long Deeply Indented	**ld**		0
Long Angular Non-Parallel	**la**		6
Scutiform and Dendritic	**sd**		0
Rondel Oval	**ro**		24
Rondel Keeled	**rk**		11
Rondel Horned	**rh**		1
Rondel Pyramidal	**rp**		5
Stipa-type Bilobate	**bs**		5
Bilobate	**bi**		0
Saddle	**sa**		0
Tricome	**ht**		17
Hair/Base	**hh**		32
Non-Poaceae Morphotypes			
Blocky Grainy	**bg**		24
Blocky Smooth	**bl**		37
Epidermal Polygonal	**ep**		43
Epidermal anticlinal	**ea**		12
P. ponderosa Type	**pp**		0
P. menziesii Type	**co**		0
Larix Type	**co**		0
Carex Type	**cx**		0
Thin Plate W/Wavy Margins	**wp**		0
Elongate Grainy	**el**		4
Diatoms	**di**		7
		Total:	**315**

Site/Locality: **SR23**			
Provenience: **340-350cm**			
Morphotype Descriptions			**Counts**
Poaceae Morphotypes			
Rectangular Plate	**pr**		17
Short Wavy <4 Lobes	**ws**		28
Long Wavy >4 Lobes	**wl**		2
Long Rectangular Parallel Sides	**lc**		5
Long Indented	**li**		4
Long Deeply Indented	**ld**		1
Long Angular Non-Parallel	**la**		4
Scutiform and Dendritic	**sd**		0
Rondel Oval	**ro**		19
Rondel Keeled	**rk**		3
Rondel Horned	**rh**		0
Rondel Pyramidal	**rp**		1
Stipa-type Bilobate	**bs**		3
Bilobate	**bi**		0
Saddle	**sa**		0
Tricome	**ht**		22
Hair/Base	**hh**		30
Non-Poaceae Morphotypes			
Blocky Grainy	**bg**		33
Blocky Smooth	**bl**		41
Epidermal Polygonal	**ep**		43
Epidermal anticlinal	**ea**		21
P. ponderosa Type	**pp**		8
P. menziesii Type	**co**		0
Larix Type	**co**		0
Carex Type	**cx**		0
Thin Plate W/Wavy Margins	**wp**		0
Elongate Grainy	**el**		1
Diatoms	**di**		2
		Total:	**288**

Site/Locality: **SR23**			
Provenience: **350-360cm**			
Morphotype Descriptions			**Counts**
Poaceae Morphotypes			
Rectangular Plate	**pr**		23
Short Wavy <4 Lobes	**ws**		49
Long Wavy >4 Lobes	**wl**		9
Long Rectangular Parallel Sides	**lc**		15
Long Indented	**li**		14
Long Deeply Indented	**ld**		5
Long Angular Non-Parallel	**la**		7
Scutiform and Dendritic	**sd**		0
Rondel Oval	**ro**		23
Rondel Keeled	**rk**		18
Rondel Horned	**rh**		0
Rondel Pyramidal	**rp**		11
Stipa-type Bilobate	**bs**		2
Bilobate	**bi**		0
Saddle	**sa**		0
Tricome	**ht**		12
Hair/Base	**hh**		32
Non-Poaceae Morphotypes			
Blocky Grainy	**bg**		18
Blocky Smooth	**bl**		22
Epidermal Polygonal	**ep**		27
Epidermal anticlinal	**ea**		4
P. ponderosa Type	**pp**		0
P. menziesii Type	**co**		0
Larix Type	**co**		0
Carex Type	**cx**		0
Thin Plate W/Wavy Margins	**wp**		0
Elongate Grainy	**el**		8
Diatoms	**di**		3
		Total:	**302**

Site/Locality: **SR23**			
Provenience: **360-370cm**			
Morphotype Descriptions			**Counts**
Poaceae Morphotypes			
Rectangular Plate	**pr**		18
Short Wavy <4 Lobes	**ws**		34
Long Wavy >4 Lobes	**wl**		4
Long Rectangular Parallel Sides	**lc**		10
Long Indented	**li**		9
Long Deeply Indented	**ld**		2
Long Angular Non-Parallel	**la**		4
Scutiform and Dendritic	**sd**		1
Rondel Oval	**ro**		14
Rondel Keeled	**rk**		3
Rondel Horned	**rh**		2
Rondel Pyramidal	**rp**		3
Stipa-type Bilobate	**bs**		10
Bilobate	**bi**		0
Saddle	**sa**		0
Tricome	**ht**		14
Hair/Base	**hh**		23
Non-Poaceae Morphotypes			
Blocky Grainy	**bg**		24
Blocky Smooth	**bl**		23
Epidermal Polygonal	**ep**		37
Epidermal anticlinal	**ea**		9
P. ponderosa Type	**pp**		4
P. menziesii Type	**co**		0
Larix Type	**co**		0
Carex Type	**cx**		0
Thin Plate W/Wavy Margins	**wp**		0
Elongate Grainy	**el**		5
Diatoms	**di**		8
		Total:	**261**

Site/Locality: **SR23**			
Provenience: **370-380cm**			
Morphotype Descriptions			**Counts**
Poaceae Morphotypes			
Rectangular Plate	**pr**		9
Short Wavy <4 Lobes	**ws**		38
Long Wavy >4 Lobes	**wl**		7
Long Rectangular Parallel Sides	**lc**		9
Long Indented	**li**		4
Long Deeply Indented	**ld**		0
Long Angular Non-Parallel	**la**		6
Scutiform and Dendritic	**sd**		0
Rondel Oval	**ro**		28
Rondel Keeled	**rk**		7
Rondel Horned	**rh**		5
Rondel Pyramidal	**rp**		4
Stipa-type Bilobate	**bs**		9
Bilobate	**bi**		0
Saddle	**sa**		0
Tricome	**ht**		13
Hair/Base	**hh**		23
Non-Poaceae Morphotypes			
Blocky Grainy	**bg**		37
Blocky Smooth	**bl**		29
Epidermal Polygonal	**ep**		37
Epidermal anticlinal	**ea**		6
P. ponderosa Type	**pp**		0
P. menziesii Type	**co**		0
Larix Type	**co**		0
Carex Type	**cx**		0
Thin Plate W/Wavy Margins	**wp**		0
Elongate Grainy	**el**		0
Diatoms	**di**		12
		Total:	**283**

Site/Locality: **SR23**			
Provenience: **380-390cm**			
Morphotype Descriptions			**Counts**
Poaceae Morphotypes			
Rectangular Plate	**pr**		9
Short Wavy <4 Lobes	**ws**		33
Long Wavy >4 Lobes	**wl**		6
Long Rectangular Parallel Sides	**lc**		14
Long Indented	**li**		11
Long Deeply Indented	**ld**		0
Long Angular Non-Parallel	**la**		6
Scutiform and Dendritic	**sd**		0
Rondel Oval	**ro**		27
Rondel Keeled	**rk**		5
Rondel Horned	**rh**		3
Rondel Pyramidal	**rp**		8
Stipa-type Bilobate	**bs**		1
Bilobate	**bi**		0
Saddle	**sa**		0
Tricome	**ht**		17
Hair/Base	**hh**		33
Non-Poaceae Morphotypes			
Blocky Grainy	**bg**		23
Blocky Smooth	**bl**		31
Epidermal Polygonal	**ep**		32
Epidermal anticlinal	**ea**		9
P. ponderosa Type	**pp**		2
P. menziesii Type	**co**		0
Larix Type	**co**		0
Carex Type	**cx**		0
Thin Plate W/Wavy Margins	**wp**		0
Elongate Grainy	**el**		9
Diatoms	**di**		16
		Total:	**295**

Site/Locality: **SR23**			
Provenience: **390-400cm**			
Morphotype Descriptions			**Counts**
Poaceae Morphotypes			
Rectangular Plate	**pr**		6
Short Wavy <4 Lobes	**ws**		32
Long Wavy >4 Lobes	**wl**		4
Long Rectangular Parallel Sides	**lc**		12
Long Indented	**li**		4
Long Deeply Indented	**ld**		1
Long Angular Non-Parallel	**la**		3
Scutiform and Dendritic	**sd**		2
Rondel Oval	**ro**		38
Rondel Keeled	**rk**		10
Rondel Horned	**rh**		2
Rondel Pyramidal	**rp**		12
Stipa-type Bilobate	**bs**		0
Bilobate	**bi**		0
Saddle	**sa**		0
Tricome	**ht**		11
Hair/Base	**hh**		39
Non-Poaceae Morphotypes			
Blocky Grainy	**bg**		51
Blocky Smooth	**bl**		22
Epidermal Polygonal	**ep**		42
Epidermal anticlinal	**ea**		4
P. ponderosa Type	**pp**		0
P. menziesii Type	**co**		0
Larix Type	**co**		0
Carex Type	**cx**		0
Thin Plate W/Wavy Margins	**wp**		0
Elongate Grainy	**el**		3
Diatoms	**di**		7
		Total:	**305**

Site/Locality: **SR23**			
Provenience: **400-410cm**			
Morphotype Descriptions			**Counts**
Poaceae Morphotypes			
Rectangular Plate	**pr**		5
Short Wavy <4 Lobes	**ws**		40
Long Wavy >4 Lobes	**wl**		4
Long Rectangular Parallel Sides	**lc**		12
Long Indented	**li**		10
Long Deeply Indented	**ld**		1
Long Angular Non-Parallel	**la**		4
Scutiform and Dendritic	**sd**		2
Rondel Oval	**ro**		31
Rondel Keeled	**rk**		7
Rondel Horned	**rh**		8
Rondel Pyramidal	**rp**		2
Stipa-type Bilobate	**bs**		0
Bilobate	**bi**		0
Saddle	**sa**		0
Tricome	**ht**		9
Hair/Base	**hh**		31
Non-Poaceae Morphotypes			
Blocky Grainy	**bg**		40
Blocky Smooth	**bl**		29
Epidermal Polygonal	**ep**		23
Epidermal anticlinal	**ea**		16
P. ponderosa Type	**pp**		0
P. menziesii Type	**co**		0
Larix Type	**co**		0
Carex Type	**cx**		0
Thin Plate W/Wavy Margins	**wp**		0
Elongate Grainy	**el**		2
Diatoms	**di**		7
		Total:	**283**

Site/Locality: **SR27**			
Provenience: **0-10cm**			
Morphotype Descriptions			**Counts**
Poaceae Morphotypes			
Rectangular Plate	**pr**		13
Short Wavy <4 Lobes	**ws**		51
Long Wavy >4 Lobes	**wl**		8
Long Rectangular Parallel Sides	**lc**		12
Long Indented	**li**		11
Long Deeply Indented	**ld**		2
Long Angular Non-Parallel	**la**		6
Scutiform and Dendritic	**sd**		0
Rondel Oval	**ro**		55
Rondel Keeled	**rk**		3
Rondel Horned	**rh**		0
Rondel Pyramidal	**rp**		0
Stipa-type Bilobate	**bs**		0
Bilobate	**bi**		0
Saddle	**sa**		0
Tricome	**ht**		8
Hair/Base	**hh**		24
Non-Poaceae Morphotypes			
Blocky Grainy	**bg**		39
Blocky Smooth	**bl**		23
Epidermal Polygonal	**ep**		19
Epidermal anticlinal	**ea**		4
P. ponderosa Type	**pp**		1
P. menziesii Type	**co**		0
Larix Type	**co**		0
Carex Type	**cx**		0
Thin Plate W/Wavy Margins	**wp**		0
Elongate Grainy	**el**		11
Diatoms	**di**		4
		Total:	**294**

Site/Locality: **SR27**			
Provenience: **10-20cm**			
Morphotype Descriptions			**Counts**
Poaceae Morphotypes			
Rectangular Plate	**pr**		18
Short Wavy <4 Lobes	**ws**		33
Long Wavy >4 Lobes	**wl**		5
Long Rectangular Parallel Sides	**lc**		12
Long Indented	**li**		5
Long Deeply Indented	**ld**		0
Long Angular Non-Parallel	**la**		6
Scutiform and Dendritic	**sd**		0
Rondel Oval	**ro**		48
Rondel Keeled	**rk**		6
Rondel Horned	**rh**		0
Rondel Pyramidal	**rp**		0
Stipa-type Bilobate	**bs**		1
Bilobate	**bi**		0
Saddle	**sa**		0
Tricome	**ht**		16
Hair/Base	**hh**		21
Non-Poaceae Morphotypes			
Blocky Grainy	**bg**		25
Blocky Smooth	**bl**		19
Epidermal Polygonal	**ep**		22
Epidermal anticlinal	**ea**		0
P. ponderosa Type	**pp**		1
P. menziesii Type	**co**		0
Larix Type	**co**		0
Carex Type	**cx**		1
Thin Plate W/Wavy Margins	**wp**		0
Elongate Grainy	**el**		12
Diatoms	**di**		2
		Total:	**253**

Site/Locality: **SR27**			
Provenience: **20-30cm**			
Morphotype Descriptions			**Counts**
Poaceae Morphotypes			
Rectangular Plate	**pr**		22
Short Wavy <4 Lobes	**ws**		38
Long Wavy >4 Lobes	**wl**		6
Long Rectangular Parallel Sides	**lc**		13
Long Indented	**li**		3
Long Deeply Indented	**ld**		0
Long Angular Non-Parallel	**la**		11
Scutiform and Dendritic	**sd**		0
Rondel Oval	**ro**		45
Rondel Keeled	**rk**		3
Rondel Horned	**rh**		0
Rondel Pyramidal	**rp**		5
Stipa-type Bilobate	**bs**		0
Bilobate	**bi**		0
Saddle	**sa**		0
Tricome	**ht**		13
Hair/Base	**hh**		23
Non-Poaceae Morphotypes			
Blocky Grainy	**bg**		34
Blocky Smooth	**bl**		25
Epidermal Polygonal	**ep**		21
Epidermal anticlinal	**ea**		1
P. ponderosa Type	**pp**		0
P. menziesii Type	**co**		0
Larix Type	**co**		0
Carex Type	**cx**		0
Thin Plate W/Wavy Margins	**wp**		0
Elongate Grainy	**el**		10
Diatoms	**di**		1
		Total:	**274**

Site/Locality: **SR27**			
Provenience: **30-40cm**			
Morphotype Descriptions			**Counts**
Poaceae Morphotypes			
Rectangular Plate	**pr**		14
Short Wavy <4 Lobes	**ws**		20
Long Wavy >4 Lobes	**wl**		0
Long Rectangular Parallel Sides	**lc**		10
Long Indented	**li**		5
Long Deeply Indented	**ld**		0
Long Angular Non-Parallel	**la**		11
Scutiform and Dendritic	**sd**		0
Rondel Oval	**ro**		48
Rondel Keeled	**rk**		10
Rondel Horned	**rh**		0
Rondel Pyramidal	**rp**		3
Stipa-type Bilobate	**bs**		0
Bilobate	**bi**		0
Saddle	**sa**		0
Tricome	**ht**		15
Hair/Base	**hh**		21
Non-Poaceae Morphotypes			
Blocky Grainy	**bg**		40
Blocky Smooth	**bl**		32
Epidermal Polygonal	**ep**		25
Epidermal anticlinal	**ea**		5
P. ponderosa Type	**pp**		0
P. menziesii Type	**co**		0
Larix Type	**co**		0
Carex Type	**cx**		0
Thin Plate W/Wavy Margins	**wp**		0
Elongate Grainy	**el**		7
Diatoms	**di**		1
		Total:	**267**

Site/Locality: **SR27**			
Provenience: **40-50cm**			
Morphotype Descriptions			**Counts**
Poaceae Morphotypes			
Rectangular Plate	**pr**		6
Short Wavy <4 Lobes	**ws**		16
Long Wavy >4 Lobes	**wl**		0
Long Rectangular Parallel Sides	**lc**		6
Long Indented	**li**		4
Long Deeply Indented	**ld**		0
Long Angular Non-Parallel	**la**		7
Scutiform and Dendritic	**sd**		0
Rondel Oval	**ro**		39
Rondel Keeled	**rk**		7
Rondel Horned	**rh**		0
Rondel Pyramidal	**rp**		0
Stipa-type Bilobate	**bs**		0
Bilobate	**bi**		0
Saddle	**sa**		0
Tricome	**ht**		6
Hair/Base	**hh**		18
Non-Poaceae Morphotypes			
Blocky Grainy	**bg**		59
Blocky Smooth	**bl**		69
Epidermal Polygonal	**ep**		38
Epidermal anticlinal	**ea**		0
P. ponderosa Type	**pp**		0
P. menziesii Type	**co**		0
Larix Type	**co**		0
Carex Type	**cx**		0
Thin Plate W/Wavy Margins	**wp**		0
Elongate Grainy	**el**		1
Diatoms	**di**		0
		Total:	**276**

Site/Locality: **SR27**			
Provenience: **80-90cm**			
Morphotype Descriptions			**Counts**
Poaceae Morphotypes			
Rectangular Plate	**pr**		16
Short Wavy <4 Lobes	**ws**		37
Long Wavy >4 Lobes	**wl**		3
Long Rectangular Parallel Sides	**lc**		9
Long Indented	**li**		12
Long Deeply Indented	**ld**		0
Long Angular Non-Parallel	**la**		2
Scutiform and Dendritic	**sd**		1
Rondel Oval	**ro**		51
Rondel Keeled	**rk**		9
Rondel Horned	**rh**		0
Rondel Pyramidal	**rp**		10
Stipa-type Bilobate	**bs**		3
Bilobate	**bi**		0
Saddle	**sa**		0
Tricome	**ht**		3
Hair/Base	**hh**		8
Non-Poaceae Morphotypes			
Blocky Grainy	**bg**		38
Blocky Smooth	**bl**		31
Epidermal Polygonal	**ep**		13
Epidermal anticlinal	**ea**		0
P. ponderosa Type	**pp**		0
P. menziesii Type	**co**		0
Larix Type	**co**		0
Carex Type	**cx**		0
Thin Plate W/Wavy Margins	**wp**		0
Elongate Grainy	**el**		9
Diatoms	**di**		12
		Total:	**267**

Site/Locality: **SR27**			
Provenience: **90-100cm**			
Morphotype Descriptions			**Counts**
Poaceae Morphotypes			
Rectangular Plate	**pr**		19
Short Wavy <4 Lobes	**ws**		52
Long Wavy >4 Lobes	**wl**		8
Long Rectangular Parallel Sides	**lc**		14
Long Indented	**li**		15
Long Deeply Indented	**ld**		0
Long Angular Non-Parallel	**la**		9
Scutiform and Dendritic	**sd**		0
Rondel Oval	**ro**		60
Rondel Keeled	**rk**		5
Rondel Horned	**rh**		0
Rondel Pyramidal	**rp**		3
Stipa-type Bilobate	**bs**		9
Bilobate	**bi**		0
Saddle	**sa**		0
Tricome	**ht**		6
Hair/Base	**hh**		10
Non-Poaceae Morphotypes			
Blocky Grainy	**bg**		23
Blocky Smooth	**bl**		17
Epidermal Polygonal	**ep**		8
Epidermal anticlinal	**ea**		2
P. ponderosa Type	**pp**		0
P. menziesii Type	**co**		0
Larix Type	**co**		0
Carex Type	**cx**		0
Thin Plate W/Wavy Margins	**wp**		0
Elongate Grainy	**el**		11
Diatoms	**di**		1
		Total:	**272**

Site/Locality: **SR27**			
Provenience: **100-110cm**			
Morphotype Descriptions			**Counts**
Poaceae Morphotypes			
Rectangular Plate	**pr**		16
Short Wavy <4 Lobes	**ws**		34
Long Wavy >4 Lobes	**wl**		12
Long Rectangular Parallel Sides	**lc**		14
Long Indented	**li**		17
Long Deeply Indented	**ld**		2
Long Angular Non-Parallel	**la**		8
Scutiform and Dendritic	**sd**		0
Rondel Oval	**ro**		47
Rondel Keeled	**rk**		7
Rondel Horned	**rh**		0
Rondel Pyramidal	**rp**		5
Stipa-type Bilobate	**bs**		3
Bilobate	**bi**		0
Saddle	**sa**		0
Tricome	**ht**		7
Hair/Base	**hh**		9
Non-Poaceae Morphotypes			
Blocky Grainy	**bg**		28
Blocky Smooth	**bl**		22
Epidermal Polygonal	**ep**		13
Epidermal anticlinal	**ea**		3
P. ponderosa Type	**pp**		0
P. menziesii Type	**co**		0
Larix Type	**co**		0
Carex Type	**cx**		0
Thin Plate W/Wavy Margins	**wp**		1
Elongate Grainy	**el**		9
Diatoms	**di**		6
		Total:	**263**

Site/Locality: **SR27**			
Provenience: **110-120cm**			
Morphotype Descriptions			**Counts**
Poaceae Morphotypes			
Rectangular Plate	**pr**		15
Short Wavy <4 Lobes	**ws**		17
Long Wavy >4 Lobes	**wl**		3
Long Rectangular Parallel Sides	**lc**		14
Long Indented	**li**		12
Long Deeply Indented	**ld**		2
Long Angular Non-Parallel	**la**		11
Scutiform and Dendritic	**sd**		0
Rondel Oval	**ro**		50
Rondel Keeled	**rk**		5
Rondel Horned	**rh**		0
Rondel Pyramidal	**rp**		4
Stipa-type Bilobate	**bs**		1
Bilobate	**bi**		0
Saddle	**sa**		0
Tricome	**ht**		6
Hair/Base	**hh**		12
Non-Poaceae Morphotypes			
Blocky Grainy	**bg**		37
Blocky Smooth	**bl**		40
Epidermal Polygonal	**ep**		16
Epidermal anticlinal	**ea**		5
P. ponderosa Type	**pp**		0
P. menziesii Type	**co**		0
Larix Type	**co**		0
Carex Type	**cx**		0
Thin Plate W/Wavy Margins	**wp**		0
Elongate Grainy	**el**		6
Diatoms	**di**		4
		Total:	**260**

Site/Locality: **SR27**			
Provenience: **120-130cm**			
Morphotype Descriptions			**Counts**
Poaceae Morphotypes			
Rectangular Plate	**pr**		14
Short Wavy <4 Lobes	**ws**		34
Long Wavy >4 Lobes	**wl**		3
Long Rectangular Parallel Sides	**lc**		12
Long Indented	**li**		11
Long Deeply Indented	**ld**		0
Long Angular Non-Parallel	**la**		4
Scutiform and Dendritic	**sd**		0
Rondel Oval	**ro**		57
Rondel Keeled	**rk**		8
Rondel Horned	**rh**		0
Rondel Pyramidal	**rp**		3
Stipa-type Bilobate	**bs**		6
Bilobate	**bi**		0
Saddle	**sa**		0
Tricome	**ht**		6
Hair/Base	**hh**		11
Non-Poaceae Morphotypes			
Blocky Grainy	**bg**		34
Blocky Smooth	**bl**		31
Epidermal Polygonal	**ep**		15
Epidermal anticlinal	**ea**		2
P. ponderosa Type	**pp**		0
P. menziesii Type	**co**		0
Larix Type	**co**		0
Carex Type	**cx**		0
Thin Plate W/Wavy Margins	**wp**		0
Elongate Grainy	**el**		5
Diatoms	**di**		6
		Total:	**262**

Site/Locality: **SR27**			
Provenience: **130-140cm**			
Morphotype Descriptions			**Counts**
Poaceae Morphotypes			
Rectangular Plate	**pr**		9
Short Wavy <4 Lobes	**ws**		17
Long Wavy >4 Lobes	**wl**		0
Long Rectangular Parallel Sides	**lc**		14
Long Indented	**li**		10
Long Deeply Indented	**ld**		0
Long Angular Non-Parallel	**la**		11
Scutiform and Dendritic	**sd**		0
Rondel Oval	**ro**		9
Rondel Keeled	**rk**		0
Rondel Horned	**rh**		0
Rondel Pyramidal	**rp**		0
Stipa-type Bilobate	**bs**		0
Bilobate	**bi**		0
Saddle	**sa**		0
Tricome	**ht**		23
Hair/Base	**hh**		52
Non-Poaceae Morphotypes			
Blocky Grainy	**bg**		105
Blocky Smooth	**bl**		58
Epidermal Polygonal	**ep**		35
Epidermal anticlinal	**ea**		4
P. ponderosa Type	**pp**		0
P. menziesii Type	**co**		0
Larix Type	**co**		0
Carex Type	**cx**		0
Thin Plate W/Wavy Margins	**wp**		0
Elongate Grainy	**el**		7
Diatoms	**di**		4
		Total:	**358**

Site/Locality: **SR27**			
Provenience: **140-150cm**			
Morphotype Descriptions			**Counts**
Poaceae Morphotypes			
Rectangular Plate	**pr**		9
Short Wavy <4 Lobes	**ws**		10
Long Wavy >4 Lobes	**wl**		0
Long Rectangular Parallel Sides	**lc**		6
Long Indented	**li**		7
Long Deeply Indented	**ld**		0
Long Angular Non-Parallel	**la**		11
Scutiform and Dendritic	**sd**		0
Rondel Oval	**ro**		18
Rondel Keeled	**rk**		0
Rondel Horned	**rh**		0
Rondel Pyramidal	**rp**		0
Stipa-type Bilobate	**bs**		0
Bilobate	**bi**		0
Saddle	**sa**		0
Tricome	**ht**		10
Hair/Base	**hh**		27
Non-Poaceae Morphotypes			
Blocky Grainy	**bg**		55
Blocky Smooth	**bl**		60
Epidermal Polygonal	**ep**		6
Epidermal anticlinal	**ea**		0
P. ponderosa Type	**pp**		0
P. menziesii Type	**co**		0
Larix Type	**co**		0
Carex Type	**cx**		0
Thin Plate W/Wavy Margins	**wp**		0
Elongate Grainy	**el**		2
Diatoms	**di**		0
		Total:	**221**

Site/Locality: **SR27**			
Provenience: **150-160cm**			
Morphotype Descriptions			**Counts**
Poaceae Morphotypes			
Rectangular Plate	**pr**		22
Short Wavy <4 Lobes	**ws**		54
Long Wavy >4 Lobes	**wl**		6
Long Rectangular Parallel Sides	**lc**		7
Long Indented	**li**		12
Long Deeply Indented	**ld**		0
Long Angular Non-Parallel	**la**		10
Scutiform and Dendritic	**sd**		0
Rondel Oval	**ro**		45
Rondel Keeled	**rk**		4
Rondel Horned	**rh**		0
Rondel Pyramidal	**rp**		5
Stipa-type Bilobate	**bs**		0
Bilobate	**bi**		0
Saddle	**sa**		0
Tricome	**ht**		11
Hair/Base	**hh**		24
Non-Poaceae Morphotypes			
Blocky Grainy	**bg**		51
Blocky Smooth	**bl**		39
Epidermal Polygonal	**ep**		12
Epidermal anticlinal	**ea**		0
P. ponderosa Type	**pp**		0
P. menziesii Type	**co**		0
Larix Type	**co**		0
Carex Type	**cx**		0
Thin Plate W/Wavy Margins	**wp**		0
Elongate Grainy	**el**		6
Diatoms	**di**		3
		Total:	**311**

Site/Locality: **SR27**			
Provenience: **160-170cm**			
Morphotype Descriptions			**Counts**
Poaceae Morphotypes			
Rectangular Plate	**pr**		21
Short Wavy <4 Lobes	**ws**		42
Long Wavy >4 Lobes	**wl**		8
Long Rectangular Parallel Sides	**lc**		8
Long Indented	**li**		18
Long Deeply Indented	**ld**		2
Long Angular Non-Parallel	**la**		4
Scutiform and Dendritic	**sd**		0
Rondel Oval	**ro**		53
Rondel Keeled	**rk**		9
Rondel Horned	**rh**		0
Rondel Pyramidal	**rp**		6
Stipa-type Bilobate	**bs**		3
Bilobate	**bi**		0
Saddle	**sa**		0
Tricome	**ht**		9
Hair/Base	**hh**		15
Non-Poaceae Morphotypes			
Blocky Grainy	**bg**		37
Blocky Smooth	**bl**		21
Epidermal Polygonal	**ep**		13
Epidermal anticlinal	**ea**		0
P. ponderosa Type	**pp**		1
P. menziesii Type	**co**		0
Larix Type	**co**		0
Carex Type	**cx**		0
Thin Plate W/Wavy Margins	**wp**		0
Elongate Grainy	**el**		8
Diatoms	**di**		1
		Total:	**279**

Site/Locality: **SR27**			
Provenience: **200-210cm**			
Morphotype Descriptions			**Counts**
Poaceae Morphotypes			
Rectangular Plate	**pr**		16
Short Wavy <4 Lobes	**ws**		38
Long Wavy >4 Lobes	**wl**		2
Long Rectangular Parallel Sides	**lc**		6
Long Indented	**li**		9
Long Deeply Indented	**ld**		0
Long Angular Non-Parallel	**la**		4
Scutiform and Dendritic	**sd**		0
Rondel Oval	**ro**		50
Rondel Keeled	**rk**		7
Rondel Horned	**rh**		0
Rondel Pyramidal	**rp**		6
Stipa-type Bilobate	**bs**		5
Bilobate	**bi**		0
Saddle	**sa**		0
Tricome	**ht**		12
Hair/Base	**hh**		30
Non-Poaceae Morphotypes			
Blocky Grainy	**bg**		45
Blocky Smooth	**bl**		37
Epidermal Polygonal	**ep**		16
Epidermal anticlinal	**ea**		3
P. ponderosa Type	**pp**		0
P. menziesii Type	**co**		0
Larix Type	**co**		0
Carex Type	**cx**		0
Thin Plate W/Wavy Margins	**wp**		0
Elongate Grainy	**el**		5
Diatoms	**di**		5
		Total:	**296**

Site/Locality: **SR27**			
Provenience: **210-220cm**			
Morphotype Descriptions			**Counts**
Poaceae Morphotypes			
Rectangular Plate	**pr**		12
Short Wavy <4 Lobes	**ws**		43
Long Wavy >4 Lobes	**wl**		4
Long Rectangular Parallel Sides	**lc**		9
Long Indented	**li**		14
Long Deeply Indented	**ld**		1
Long Angular Non-Parallel	**la**		6
Scutiform and Dendritic	**sd**		0
Rondel Oval	**ro**		45
Rondel Keeled	**rk**		4
Rondel Horned	**rh**		0
Rondel Pyramidal	**rp**		0
Stipa-type Bilobate	**bs**		3
Bilobate	**bi**		0
Saddle	**sa**		0
Tricome	**ht**		6
Hair/Base	**hh**		19
Non-Poaceae Morphotypes			
Blocky Grainy	**bg**		42
Blocky Smooth	**bl**		29
Epidermal Polygonal	**ep**		12
Epidermal anticlinal	**ea**		5
P. ponderosa Type	**pp**		0
P. menziesii Type	**co**		0
Larix Type	**co**		0
Carex Type	**cx**		0
Thin Plate W/Wavy Margins	**wp**		0
Elongate Grainy	**el**		9
Diatoms	**di**		3
		Total:	**266**

Site/Locality: **SR27**			
Provenience: **220-230cm**			
Morphotype Descriptions			**Counts**
Poaceae Morphotypes			
Rectangular Plate	**pr**		19
Short Wavy <4 Lobes	**ws**		32
Long Wavy >4 Lobes	**wl**		6
Long Rectangular Parallel Sides	**lc**		7
Long Indented	**li**		9
Long Deeply Indented	**ld**		1
Long Angular Non-Parallel	**la**		5
Scutiform and Dendritic	**sd**		2
Rondel Oval	**ro**		40
Rondel Keeled	**rk**		8
Rondel Horned	**rh**		0
Rondel Pyramidal	**rp**		4
Stipa-type Bilobate	**bs**		0
Bilobate	**bi**		0
Saddle	**sa**		0
Tricome	**ht**		8
Hair/Base	**hh**		30
Non-Poaceae Morphotypes			
Blocky Grainy	**bg**		49
Blocky Smooth	**bl**		37
Epidermal Polygonal	**ep**		18
Epidermal anticlinal	**ea**		6
P. ponderosa Type	**pp**		2
P. menziesii Type	**co**		0
Larix Type	**co**		0
Carex Type	**cx**		0
Thin Plate W/Wavy Margins	**wp**		0
Elongate Grainy	**el**		2
Diatoms	**di**		0
		Total:	**285**

Site/Locality: **SR27**			
Provenience: **230-240cm**			
Morphotype Descriptions			**Counts**
Poaceae Morphotypes			
Rectangular Plate	**pr**		14
Short Wavy <4 Lobes	**ws**		9
Long Wavy >4 Lobes	**wl**		0
Long Rectangular Parallel Sides	**lc**		3
Long Indented	**li**		2
Long Deeply Indented	**ld**		0
Long Angular Non-Parallel	**la**		8
Scutiform and Dendritic	**sd**		0
Rondel Oval	**ro**		45
Rondel Keeled	**rk**		3
Rondel Horned	**rh**		0
Rondel Pyramidal	**rp**		4
Stipa-type Bilobate	**bs**		1
Bilobate	**bi**		0
Saddle	**sa**		0
Tricome	**ht**		13
Hair/Base	**hh**		44
Non-Poaceae Morphotypes			
Blocky Grainy	**bg**		53
Blocky Smooth	**bl**		38
Epidermal Polygonal	**ep**		16
Epidermal anticlinal	**ea**		5
P. ponderosa Type	**pp**		0
P. menziesii Type	**co**		0
Larix Type	**co**		0
Carex Type	**cx**		0
Thin Plate W/Wavy Margins	**wp**		0
Elongate Grainy	**el**		4
Diatoms	**di**		2
		Total:	**264**

Site/Locality: **SR27**			
Provenience: **240-250cm**			
Morphotype Descriptions			**Counts**
Poaceae Morphotypes			
Rectangular Plate	**pr**		5
Short Wavy <4 Lobes	**ws**		29
Long Wavy >4 Lobes	**wl**		1
Long Rectangular Parallel Sides	**lc**		5
Long Indented	**li**		12
Long Deeply Indented	**ld**		1
Long Angular Non-Parallel	**la**		6
Scutiform and Dendritic	**sd**		0
Rondel Oval	**ro**		36
Rondel Keeled	**rk**		7
Rondel Horned	**rh**		0
Rondel Pyramidal	**rp**		4
Stipa-type Bilobate	**bs**		0
Bilobate	**bi**		0
Saddle	**sa**		0
Tricome	**ht**		11
Hair/Base	**hh**		20
Non-Poaceae Morphotypes			
Blocky Grainy	**bg**		47
Blocky Smooth	**bl**		34
Epidermal Polygonal	**ep**		19
Epidermal anticlinal	**ea**		3
P. ponderosa Type	**pp**		1
P. menziesii Type	**co**		0
Larix Type	**co**		1
Carex Type	**cx**		0
Thin Plate W/Wavy Margins	**wp**		0
Elongate Grainy	**el**		11
Diatoms	**di**		4
		Total:	**257**

Site/Locality: **SR27**			
Provenience: **250-260cm**			
Morphotype Descriptions			**Counts**
Poaceae Morphotypes			
Rectangular Plate	**pr**		16
Short Wavy <4 Lobes	**ws**		27
Long Wavy >4 Lobes	**wl**		5
Long Rectangular Parallel Sides	**lc**		7
Long Indented	**li**		5
Long Deeply Indented	**ld**		0
Long Angular Non-Parallel	**la**		6
Scutiform and Dendritic	**sd**		0
Rondel Oval	**ro**		40
Rondel Keeled	**rk**		5
Rondel Horned	**rh**		0
Rondel Pyramidal	**rp**		3
Stipa-type Bilobate	**bs**		3
Bilobate	**bi**		0
Saddle	**sa**		0
Tricome	**ht**		4
Hair/Base	**hh**		23
Non-Poaceae Morphotypes			
Blocky Grainy	**bg**		44
Blocky Smooth	**bl**		28
Epidermal Polygonal	**ep**		14
Epidermal anticlinal	**ea**		4
P. ponderosa Type	**pp**		1
P. menziesii Type	**co**		0
Larix Type	**co**		0
Carex Type	**cx**		0
Thin Plate W/Wavy Margins	**wp**		0
Elongate Grainy	**el**		6
Diatoms	**di**		5
		Total:	**246**

Site/Locality: **SR27**			
Provenience: **280-290cm**			
Morphotype Descriptions			**Counts**
Poaceae Morphotypes			
Rectangular Plate	**pr**		11
Short Wavy <4 Lobes	**ws**		35
Long Wavy >4 Lobes	**wl**		4
Long Rectangular Parallel Sides	**lc**		13
Long Indented	**li**		8
Long Deeply Indented	**ld**		1
Long Angular Non-Parallel	**la**		9
Scutiform and Dendritic	**sd**		0
Rondel Oval	**ro**		28
Rondel Keeled	**rk**		5
Rondel Horned	**rh**		0
Rondel Pyramidal	**rp**		0
Stipa-type Bilobate	**bs**		1
Bilobate	**bi**		0
Saddle	**sa**		0
Tricome	**ht**		9
Hair/Base	**hh**		33
Non-Poaceae Morphotypes			
Blocky Grainy	**bg**		39
Blocky Smooth	**bl**		50
Epidermal Polygonal	**ep**		18
Epidermal anticlinal	**ea**		4
P. ponderosa Type	**pp**		2
P. menziesii Type	**co**		0
Larix Type	**co**		0
Carex Type	**cx**		0
Thin Plate W/Wavy Margins	**wp**		0
Elongate Grainy	**el**		7
Diatoms	**di**		4
		Total:	**281**

Site/Locality: **SR27**			
Provenience: **290-300cm**			
Morphotype Descriptions			**Counts**
Poaceae Morphotypes			
Rectangular Plate	**pr**		9
Short Wavy <4 Lobes	**ws**		27
Long Wavy >4 Lobes	**wl**		2
Long Rectangular Parallel Sides	**lc**		12
Long Indented	**li**		6
Long Deeply Indented	**ld**		0
Long Angular Non-Parallel	**la**		6
Scutiform and Dendritic	**sd**		0
Rondel Oval	**ro**		50
Rondel Keeled	**rk**		2
Rondel Horned	**rh**		0
Rondel Pyramidal	**rp**		0
Stipa-type Bilobate	**bs**		0
Bilobate	**bi**		0
Saddle	**sa**		0
Tricome	**ht**		12
Hair/Base	**hh**		23
Non-Poaceae Morphotypes			
Blocky Grainy	**bg**		37
Blocky Smooth	**bl**		33
Epidermal Polygonal	**ep**		17
Epidermal anticlinal	**ea**		3
P. ponderosa Type	**pp**		1
P. menziesii Type	**co**		0
Larix Type	**co**		0
Carex Type	**cx**		0
Thin Plate W/Wavy Margins	**wp**		0
Elongate Grainy	**el**		4
Diatoms	**di**		1
		Total:	**245**

Site/Locality: **SR34**			
Provenience: **0-10cm**			
Morphotype Descriptions			**Counts**
Poaceae Morphotypes			
Rectangular Plate	**pr**		19
Short Wavy <4 Lobes	**ws**		46
Long Wavy >4 Lobes	**wl**		9
Long Rectangular Parallel Sides	**lc**		14
Long Indented	**li**		12
Long Deeply Indented	**ld**		7
Long Angular Non-Parallel	**la**		9
Scutiform and Dendritic	**sd**		0
Rondel Oval	**ro**		62
Rondel Keeled	**rk**		3
Rondel Horned	**rh**		1
Rondel Pyramidal	**rp**		0
Stipa-type Bilobate	**bs**		0
Bilobate	**bi**		0
Saddle	**sa**		0
Tricome	**ht**		5
Hair/Base	**hh**		22
Non-Poaceae Morphotypes			
Blocky Grainy	**bg**		28
Blocky Smooth	**bl**		17
Epidermal Polygonal	**ep**		18
Epidermal anticlinal	**ea**		4
P. ponderosa Type	**pp**		0
P. menziesii Type	**co**		0
Larix Type	**co**		0
Carex Type	**cx**		0
Thin Plate W/Wavy Margins	**wp**		0
Elongate Grainy	**el**		13
Diatoms	**di**		9
		Total:	**298**

Site/Locality: **SR34**			
Provenience: **10-20cm**			
Morphotype Descriptions			**Counts**
Poaceae Morphotypes			
Rectangular Plate	**pr**		15
Short Wavy <4 Lobes	**ws**		50
Long Wavy >4 Lobes	**wl**		21
Long Rectangular Parallel Sides	**lc**		5
Long Indented	**li**		7
Long Deeply Indented	**ld**		7
Long Angular Non-Parallel	**la**		5
Scutiform and Dendritic	**sd**		1
Rondel Oval	**ro**		50
Rondel Keeled	**rk**		4
Rondel Horned	**rh**		2
Rondel Pyramidal	**rp**		0
Stipa-type Bilobate	**bs**		1
Bilobate	**bi**		0
Saddle	**sa**		0
Tricome	**ht**		8
Hair/Base	**hh**		19
Non-Poaceae Morphotypes			
Blocky Grainy	**bg**		24
Blocky Smooth	**bl**		14
Epidermal Polygonal	**ep**		11
Epidermal anticlinal	**ea**		2
P. ponderosa Type	**pp**		1
P. menziesii Type	**co**		0
Larix Type	**co**		0
Carex Type	**cx**		0
Thin Plate W/Wavy Margins	**wp**		0
Elongate Grainy	**el**		19
Diatoms	**di**		8
		Total:	**274**

Site/Locality: **SR34**			
Provenience: **20-30cm**			
Morphotype Descriptions			**Counts**
Poaceae Morphotypes			
Rectangular Plate	**pr**		13
Short Wavy <4 Lobes	**ws**		66
Long Wavy >4 Lobes	**wl**		7
Long Rectangular Parallel Sides	**lc**		6
Long Indented	**li**		12
Long Deeply Indented	**ld**		1
Long Angular Non-Parallel	**la**		2
Scutiform and Dendritic	**sd**		3
Rondel Oval	**ro**		53
Rondel Keeled	**rk**		0
Rondel Horned	**rh**		0
Rondel Pyramidal	**rp**		0
Stipa-type Bilobate	**bs**		0
Bilobate	**bi**		0
Saddle	**sa**		0
Tricome	**ht**		6
Hair/Base	**hh**		15
Non-Poaceae Morphotypes			
Blocky Grainy	**bg**		44
Blocky Smooth	**bl**		25
Epidermal Polygonal	**ep**		16
Epidermal anticlinal	**ea**		0
P. ponderosa Type	**pp**		0
P. menziesii Type	**co**		0
Larix Type	**co**		0
Carex Type	**cx**		1
Thin Plate W/Wavy Margins	**wp**		0
Elongate Grainy	**el**		9
Diatoms	**di**		9
		Total:	**288**

Site/Locality: **SR34**			
Provenience: **30-40cm**			
Morphotype Descriptions			**Counts**
Poaceae Morphotypes			
Rectangular Plate	**pr**		21
Short Wavy <4 Lobes	**ws**		59
Long Wavy >4 Lobes	**wl**		11
Long Rectangular Parallel Sides	**lc**		15
Long Indented	**li**		9
Long Deeply Indented	**ld**		9
Long Angular Non-Parallel	**la**		5
Scutiform and Dendritic	**sd**		2
Rondel Oval	**ro**		50
Rondel Keeled	**rk**		2
Rondel Horned	**rh**		0
Rondel Pyramidal	**rp**		0
Stipa-type Bilobate	**bs**		0
Bilobate	**bi**		1
Saddle	**sa**		0
Tricome	**ht**		7
Hair/Base	**hh**		28
Non-Poaceae Morphotypes			
Blocky Grainy	**bg**		24
Blocky Smooth	**bl**		17
Epidermal Polygonal	**ep**		13
Epidermal anticlinal	**ea**		1
P. ponderosa Type	**pp**		0
P. menziesii Type	**co**		0
Larix Type	**co**		0
Carex Type	**cx**		0
Thin Plate W/Wavy Margins	**wp**		0
Elongate Grainy	**el**		14
Diatoms	**di**		0
		Total:	**288**

Site/Locality: **SR34**			
Provenience: **40-50cm**			
Morphotype Descriptions			**Counts**
Poaceae Morphotypes			
Rectangular Plate	**pr**		10
Short Wavy <4 Lobes	**ws**		75
Long Wavy >4 Lobes	**wl**		7
Long Rectangular Parallel Sides	**lc**		10
Long Indented	**li**		16
Long Deeply Indented	**ld**		3
Long Angular Non-Parallel	**la**		8
Scutiform and Dendritic	**sd**		2
Rondel Oval	**ro**		54
Rondel Keeled	**rk**		7
Rondel Horned	**rh**		0
Rondel Pyramidal	**rp**		0
Stipa-type Bilobate	**bs**		0
Bilobate	**bi**		1
Saddle	**sa**		0
Tricome	**ht**		6
Hair/Base	**hh**		23
Non-Poaceae Morphotypes			
Blocky Grainy	**bg**		11
Blocky Smooth	**bl**		19
Epidermal Polygonal	**ep**		8
Epidermal anticlinal	**ea**		2
P. ponderosa Type	**pp**		0
P. menziesii Type	**co**		0
Larix Type	**co**		0
Carex Type	**cx**		0
Thin Plate W/Wavy Margins	**wp**		0
Elongate Grainy	**el**		10
Diatoms	**di**		4
		Total:	**276**

Site/Locality: **SR34**			
Provenience: **50-60cm**			
Morphotype Descriptions			**Counts**
Poaceae Morphotypes			
Rectangular Plate	**pr**		17
Short Wavy <4 Lobes	**ws**		54
Long Wavy >4 Lobes	**wl**		12
Long Rectangular Parallel Sides	**lc**		19
Long Indented	**li**		14
Long Deeply Indented	**ld**		12
Long Angular Non-Parallel	**la**		8
Scutiform and Dendritic	**sd**		1
Rondel Oval	**ro**		55
Rondel Keeled	**rk**		2
Rondel Horned	**rh**		0
Rondel Pyramidal	**rp**		0
Stipa-type Bilobate	**bs**		0
Bilobate	**bi**		1
Saddle	**sa**		0
Tricome	**ht**		7
Hair/Base	**hh**		19
Non-Poaceae Morphotypes			
Blocky Grainy	**bg**		27
Blocky Smooth	**bl**		9
Epidermal Polygonal	**ep**		14
Epidermal anticlinal	**ea**		0
P. ponderosa Type	**pp**		2
P. menziesii Type	**co**		0
Larix Type	**co**		0
Carex Type	**cx**		0
Thin Plate W/Wavy Margins	**wp**		0
Elongate Grainy	**el**		11
Diatoms	**di**		3
		Total:	**287**

Site/Locality: **SR34**			
Provenience: **60-70cm**			
Morphotype Descriptions			**Counts**
Poaceae Morphotypes			
Rectangular Plate	**pr**		20
Short Wavy <4 Lobes	**ws**		68
Long Wavy >4 Lobes	**wl**		11
Long Rectangular Parallel Sides	**lc**		12
Long Indented	**li**		7
Long Deeply Indented	**ld**		7
Long Angular Non-Parallel	**la**		2
Scutiform and Dendritic	**sd**		0
Rondel Oval	**ro**		70
Rondel Keeled	**rk**		6
Rondel Horned	**rh**		0
Rondel Pyramidal	**rp**		0
Stipa-type Bilobate	**bs**		0
Bilobate	**bi**		1
Saddle	**sa**		0
Tricome	**ht**		4
Hair/Base	**hh**		16
Non-Poaceae Morphotypes			
Blocky Grainy	**bg**		41
Blocky Smooth	**bl**		8
Epidermal Polygonal	**ep**		19
Epidermal anticlinal	**ea**		0
P. ponderosa Type	**pp**		0
P. menziesii Type	**co**		0
Larix Type	**co**		0
Carex Type	**cx**		1
Thin Plate W/Wavy Margins	**wp**		0
Elongate Grainy	**el**		18
Diatoms	**di**		2
		Total:	**313**

Site/Locality: **SR34**			
Provenience: **70-80cm**			
Morphotype Descriptions			**Counts**
Poaceae Morphotypes			
Rectangular Plate	**pr**		16
Short Wavy <4 Lobes	**ws**		48
Long Wavy >4 Lobes	**wl**		6
Long Rectangular Parallel Sides	**lc**		11
Long Indented	**li**		9
Long Deeply Indented	**ld**		4
Long Angular Non-Parallel	**la**		5
Scutiform and Dendritic	**sd**		0
Rondel Oval	**ro**		60
Rondel Keeled	**rk**		5
Rondel Horned	**rh**		2
Rondel Pyramidal	**rp**		0
Stipa-type Bilobate	**bs**		0
Bilobate	**bi**		3
Saddle	**sa**		0
Tricome	**ht**		1
Hair/Base	**hh**		14
Non-Poaceae Morphotypes			
Blocky Grainy	**bg**		23
Blocky Smooth	**bl**		10
Epidermal Polygonal	**ep**		7
Epidermal anticlinal	**ea**		0
P. ponderosa Type	**pp**		2
P. menziesii Type	**co**		0
Larix Type	**co**		0
Carex Type	**cx**		0
Thin Plate W/Wavy Margins	**wp**		0
Elongate Grainy	**el**		14
Diatoms	**di**		2
		Total:	**242**

Site/Locality: **SR34**			
Provenience: **80-90cm**			
Morphotype Descriptions			**Counts**
Poaceae Morphotypes			
Rectangular Plate	**pr**		16
Short Wavy <4 Lobes	**ws**		50
Long Wavy >4 Lobes	**wl**		7
Long Rectangular Parallel Sides	**lc**		5
Long Indented	**li**		10
Long Deeply Indented	**ld**		4
Long Angular Non-Parallel	**la**		6
Scutiform and Dendritic	**sd**		3
Rondel Oval	**ro**		82
Rondel Keeled	**rk**		8
Rondel Horned	**rh**		3
Rondel Pyramidal	**rp**		0
Stipa-type Bilobate	**bs**		0
Bilobate	**bi**		1
Saddle	**sa**		0
Tricome	**ht**		4
Hair/Base	**hh**		16
Non-Poaceae Morphotypes			
Blocky Grainy	**bg**		36
Blocky Smooth	**bl**		22
Epidermal Polygonal	**ep**		15
Epidermal anticlinal	**ea**		3
P. ponderosa Type	**pp**		0
P. menziesii Type	**co**		0
Larix Type	**co**		0
Carex Type	**cx**		0
Thin Plate W/Wavy Margins	**wp**		0
Elongate Grainy	**el**		12
Diatoms	**di**		2
		Total:	**305**

Site/Locality: **SR34**			
Provenience: **90-100cm**			
Morphotype Descriptions			**Counts**
Poaceae Morphotypes			
Rectangular Plate	**pr**		14
Short Wavy <4 Lobes	**ws**		59
Long Wavy >4 Lobes	**wl**		7
Long Rectangular Parallel Sides	**lc**		12
Long Indented	**li**		14
Long Deeply Indented	**ld**		4
Long Angular Non-Parallel	**la**		4
Scutiform and Dendritic	**sd**		4
Rondel Oval	**ro**		53
Rondel Keeled	**rk**		3
Rondel Horned	**rh**		1
Rondel Pyramidal	**rp**		0
Stipa-type Bilobate	**bs**		0
Bilobate	**bi**		0
Saddle	**sa**		0
Tricome	**ht**		3
Hair/Base	**hh**		18
Non-Poaceae Morphotypes			
Blocky Grainy	**bg**		26
Blocky Smooth	**bl**		30
Epidermal Polygonal	**ep**		19
Epidermal anticlinal	**ea**		2
P. ponderosa Type	**pp**		0
P. menziesii Type	**co**		0
Larix Type	**co**		0
Carex Type	**cx**		0
Thin Plate W/Wavy Margins	**wp**		0
Elongate Grainy	**el**		6
Diatoms	**di**		5
		Total:	**284**

Site/Locality: **SR34**			
Provenience: **100-110cm**			
Morphotype Descriptions			**Counts**
Poaceae Morphotypes			
Rectangular Plate	**pr**		19
Short Wavy <4 Lobes	**ws**		55
Long Wavy >4 Lobes	**wl**		6
Long Rectangular Parallel Sides	**lc**		8
Long Indented	**li**		16
Long Deeply Indented	**ld**		3
Long Angular Non-Parallel	**la**		7
Scutiform and Dendritic	**sd**		0
Rondel Oval	**ro**		65
Rondel Keeled	**rk**		2
Rondel Horned	**rh**		0
Rondel Pyramidal	**rp**		0
Stipa-type Bilobate	**bs**		0
Bilobate	**bi**		0
Saddle	**sa**		0
Tricome	**ht**		5
Hair/Base	**hh**		20
Non-Poaceae Morphotypes			
Blocky Grainy	**bg**		53
Blocky Smooth	**bl**		37
Epidermal Polygonal	**ep**		30
Epidermal anticlinal	**ea**		5
P. ponderosa Type	**pp**		0
P. menziesii Type	**co**		0
Larix Type	**co**		0
Carex Type	**cx**		0
Thin Plate W/Wavy Margins	**wp**		0
Elongate Grainy	**el**		16
Diatoms	**di**		6
		Total:	**353**

Site/Locality: **SR34**			
Provenience: **110-120cm**			
Morphotype Descriptions			**Counts**
Poaceae Morphotypes			
Rectangular Plate	**pr**		11
Short Wavy <4 Lobes	**ws**		69
Long Wavy >4 Lobes	**wl**		7
Long Rectangular Parallel Sides	**lc**		12
Long Indented	**li**		9
Long Deeply Indented	**ld**		4
Long Angular Non-Parallel	**la**		5
Scutiform and Dendritic	**sd**		0
Rondel Oval	**ro**		36
Rondel Keeled	**rk**		0
Rondel Horned	**rh**		0
Rondel Pyramidal	**rp**		0
Stipa-type Bilobate	**bs**		1
Bilobate	**bi**		0
Saddle	**sa**		0
Tricome	**ht**		2
Hair/Base	**hh**		19
Non-Poaceae Morphotypes			
Blocky Grainy	**bg**		63
Blocky Smooth	**bl**		53
Epidermal Polygonal	**ep**		32
Epidermal anticlinal	**ea**		2
P. ponderosa Type	**pp**		0
P. menziesii Type	**co**		0
Larix Type	**co**		0
Carex Type	**cx**		0
Thin Plate W/Wavy Margins	**wp**		0
Elongate Grainy	**el**		18
Diatoms	**di**		4
		Total:	**347**

Site/Locality: **SR34**			
Provenience: **120-130cm**			
Morphotype Descriptions			**Counts**
Poaceae Morphotypes			
Rectangular Plate	**pr**		10
Short Wavy <4 Lobes	**ws**		47
Long Wavy >4 Lobes	**wl**		8
Long Rectangular Parallel Sides	**lc**		14
Long Indented	**li**		9
Long Deeply Indented	**ld**		2
Long Angular Non-Parallel	**la**		5
Scutiform and Dendritic	**sd**		0
Rondel Oval	**ro**		31
Rondel Keeled	**rk**		1
Rondel Horned	**rh**		2
Rondel Pyramidal	**rp**		0
Stipa-type Bilobate	**bs**		2
Bilobate	**bi**		0
Saddle	**sa**		0
Tricome	**ht**		1
Hair/Base	**hh**		13
Non-Poaceae Morphotypes			
Blocky Grainy	**bg**		60
Blocky Smooth	**bl**		44
Epidermal Polygonal	**ep**		37
Epidermal anticlinal	**ea**		3
P. ponderosa Type	**pp**		1
P. menziesii Type	**co**		1
Larix Type	**co**		0
Carex Type	**cx**		0
Thin Plate W/Wavy Margins	**wp**		0
Elongate Grainy	**el**		9
Diatoms	**di**		7
		Total:	**307**

Site/Locality: **SR34**			
Provenience: **130-140cm**			
Morphotype Descriptions			**Counts**
Poaceae Morphotypes			
Rectangular Plate	**pr**		10
Short Wavy <4 Lobes	**ws**		60
Long Wavy >4 Lobes	**wl**		7
Long Rectangular Parallel Sides	**lc**		24
Long Indented	**li**		21
Long Deeply Indented	**ld**		8
Long Angular Non-Parallel	**la**		7
Scutiform and Dendritic	**sd**		0
Rondel Oval	**ro**		34
Rondel Keeled	**rk**		5
Rondel Horned	**rh**		0
Rondel Pyramidal	**rp**		0
Stipa-type Bilobate	**bs**		0
Bilobate	**bi**		0
Saddle	**sa**		1
Tricome	**ht**		8
Hair/Base	**hh**		10
Non-Poaceae Morphotypes			
Blocky Grainy	**bg**		25
Blocky Smooth	**bl**		16
Epidermal Polygonal	**ep**		8
Epidermal anticlinal	**ea**		1
P. ponderosa Type	**pp**		1
P. menziesii Type	**co**		0
Larix Type	**co**		0
Carex Type	**cx**		0
Thin Plate W/Wavy Margins	**wp**		1
Elongate Grainy	**el**		11
Diatoms	**di**		4
		Total:	**262**

Site/Locality: **SR34**			
Provenience: **140-150cm**			
Morphotype Descriptions			**Counts**
Poaceae Morphotypes			
Rectangular Plate	**pr**		7
Short Wavy <4 Lobes	**ws**		78
Long Wavy >4 Lobes	**wl**		18
Long Rectangular Parallel Sides	**lc**		25
Long Indented	**li**		16
Long Deeply Indented	**ld**		4
Long Angular Non-Parallel	**la**		4
Scutiform and Dendritic	**sd**		1
Rondel Oval	**ro**		50
Rondel Keeled	**rk**		4
Rondel Horned	**rh**		1
Rondel Pyramidal	**rp**		1
Stipa-type Bilobate	**bs**		1
Bilobate	**bi**		1
Saddle	**sa**		0
Tricome	**ht**		4
Hair/Base	**hh**		13
Non-Poaceae Morphotypes			
Blocky Grainy	**bg**		29
Blocky Smooth	**bl**		14
Epidermal Polygonal	**ep**		10
Epidermal anticlinal	**ea**		2
P. ponderosa Type	**pp**		2
P. menziesii Type	**co**		0
Larix Type	**co**		0
Carex Type	**cx**		0
Thin Plate W/Wavy Margins	**wp**		0
Elongate Grainy	**el**		7
Diatoms	**di**		5
		Total:	**297**

Site/Locality: **SR34**			
Provenience: **150-160cm**			
Morphotype Descriptions			**Counts**
Poaceae Morphotypes			
Rectangular Plate	**pr**		11
Short Wavy <4 Lobes	**ws**		63
Long Wavy >4 Lobes	**wl**		13
Long Rectangular Parallel Sides	**lc**		26
Long Indented	**li**		21
Long Deeply Indented	**ld**		11
Long Angular Non-Parallel	**la**		9
Scutiform and Dendritic	**sd**		4
Rondel Oval	**ro**		27
Rondel Keeled	**rk**		3
Rondel Horned	**rh**		2
Rondel Pyramidal	**rp**		3
Stipa-type Bilobate	**bs**		1
Bilobate	**bi**		0
Saddle	**sa**		0
Tricome	**ht**		3
Hair/Base	**hh**		18
Non-Poaceae Morphotypes			
Blocky Grainy	**bg**		36
Blocky Smooth	**bl**		22
Epidermal Polygonal	**ep**		13
Epidermal anticlinal	**ea**		0
P. ponderosa Type	**pp**		3
P. menziesii Type	**co**		0
Larix Type	**co**		0
Carex Type	**cx**		0
Thin Plate W/Wavy Margins	**wp**		0
Elongate Grainy	**el**		8
Diatoms	**di**		4
		Total:	**301**

Site/Locality: **SR34**			
Provenience: **180-190cm**			
Morphotype Descriptions			**Counts**
Poaceae Morphotypes			
Rectangular Plate	**pr**		6
Short Wavy <4 Lobes	**ws**		2
Long Wavy >4 Lobes	**wl**		0
Long Rectangular Parallel Sides	**lc**		6
Long Indented	**li**		2
Long Deeply Indented	**ld**		1
Long Angular Non-Parallel	**la**		1
Scutiform and Dendritic	**sd**		1
Rondel Oval	**ro**		0
Rondel Keeled	**rk**		0
Rondel Horned	**rh**		0
Rondel Pyramidal	**rp**		0
Stipa-type Bilobate	**bs**		0
Bilobate	**bi**		0
Saddle	**sa**		0
Tricome	**ht**		0
Hair/Base	**hh**		33
Non-Poaceae Morphotypes			
Blocky Grainy	**bg**		63
Blocky Smooth	**bl**		65
Epidermal Polygonal	**ep**		58
Epidermal anticlinal	**ea**		5
P. ponderosa Type	**pp**		4
P. menziesii Type	**co**		0
Larix Type	**co**		0
Carex Type	**cx**		0
Thin Plate W/Wavy Margins	**wp**		0
Elongate Grainy	**el**		0
Diatoms	**di**		1
		Total:	**248**

Site/Locality: **SR34**			
Provenience: **190-200cm**			
Morphotype Descriptions			**Counts**
Poaceae Morphotypes			
Rectangular Plate	**pr**		2
Short Wavy <4 Lobes	**ws**		4
Long Wavy >4 Lobes	**wl**		0
Long Rectangular Parallel Sides	**lc**		1
Long Indented	**li**		0
Long Deeply Indented	**ld**		0
Long Angular Non-Parallel	**la**		0
Scutiform and Dendritic	**sd**		0
Rondel Oval	**ro**		8
Rondel Keeled	**rk**		0
Rondel Horned	**rh**		0
Rondel Pyramidal	**rp**		0
Stipa-type Bilobate	**bs**		0
Bilobate	**bi**		0
Saddle	**sa**		0
Tricome	**ht**		0
Hair/Base	**hh**		28
Non-Poaceae Morphotypes			
Blocky Grainy	**bg**		72
Blocky Smooth	**bl**		67
Epidermal Polygonal	**ep**		54
Epidermal anticlinal	**ea**		3
P. ponderosa Type	**pp**		2
P. menziesii Type	**co**		0
Larix Type	**co**		0
Carex Type	**cx**		1
Thin Plate W/Wavy Margins	**wp**		0
Elongate Grainy	**el**		0
Diatoms	**di**		0
		Total:	**242**

Site/Locality: **SR34**			
Provenience: **200-210cm**			
Morphotype Descriptions			**Counts**
Poaceae Morphotypes			
Rectangular Plate	**pr**		4
Short Wavy <4 Lobes	**ws**		5
Long Wavy >4 Lobes	**wl**		1
Long Rectangular Parallel Sides	**lc**		5
Long Indented	**li**		1
Long Deeply Indented	**ld**		0
Long Angular Non-Parallel	**la**		2
Scutiform and Dendritic	**sd**		1
Rondel Oval	**ro**		13
Rondel Keeled	**rk**		0
Rondel Horned	**rh**		0
Rondel Pyramidal	**rp**		0
Stipa-type Bilobate	**bs**		0
Bilobate	**bi**		0
Saddle	**sa**		0
Tricome	**ht**		0
Hair/Base	**hh**		21
Non-Poaceae Morphotypes			
Blocky Grainy	**bg**		75
Blocky Smooth	**bl**		56
Epidermal Polygonal	**ep**		68
Epidermal anticlinal	**ea**		4
P. ponderosa Type	**pp**		3
P. menziesii Type	**co**		0
Larix Type	**co**		0
Carex Type	**cx**		0
Thin Plate W/Wavy Margins	**wp**		0
Elongate Grainy	**el**		0
Diatoms	**di**		5
		Total:	**264**

Site/Locality: **SR34**			
Provenience: **210-220cm**			
Morphotype Descriptions			**Counts**
Poaceae Morphotypes			
Rectangular Plate	**pr**		2
Short Wavy <4 Lobes	**ws**		2
Long Wavy >4 Lobes	**wl**		0
Long Rectangular Parallel Sides	**lc**		3
Long Indented	**li**		0
Long Deeply Indented	**ld**		1
Long Angular Non-Parallel	**la**		2
Scutiform and Dendritic	**sd**		0
Rondel Oval	**ro**		18
Rondel Keeled	**rk**		0
Rondel Horned	**rh**		0
Rondel Pyramidal	**rp**		0
Stipa-type Bilobate	**bs**		0
Bilobate	**bi**		0
Saddle	**sa**		0
Tricome	**ht**		1
Hair/Base	**hh**		19
Non-Poaceae Morphotypes			
Blocky Grainy	**bg**		77
Blocky Smooth	**bl**		64
Epidermal Polygonal	**ep**		65
Epidermal anticlinal	**ea**		5
P. ponderosa Type	**pp**		1
P. menziesii Type	**co**		0
Larix Type	**co**		0
Carex Type	**cx**		0
Thin Plate W/Wavy Margins	**wp**		0
Elongate Grainy	**el**		0
Diatoms	**di**		2
		Total:	**262**

Site/Locality: **SR34**			
Provenience: **220-230cm**			
Morphotype Descriptions			**Counts**
Poaceae Morphotypes			
Rectangular Plate	**pr**		6
Short Wavy <4 Lobes	**ws**		3
Long Wavy >4 Lobes	**wl**		0
Long Rectangular Parallel Sides	**lc**		1
Long Indented	**li**		0
Long Deeply Indented	**ld**		0
Long Angular Non-Parallel	**la**		0
Scutiform and Dendritic	**sd**		0
Rondel Oval	**ro**		13
Rondel Keeled	**rk**		0
Rondel Horned	**rh**		0
Rondel Pyramidal	**rp**		0
Stipa-type Bilobate	**bs**		1
Bilobate	**bi**		0
Saddle	**sa**		0
Tricome	**ht**		3
Hair/Base	**hh**		18
Non-Poaceae Morphotypes			
Blocky Grainy	**bg**		72
Blocky Smooth	**bl**		51
Epidermal Polygonal	**ep**		59
Epidermal anticlinal	**ea**		7
P. ponderosa Type	**pp**		2
P. menziesii Type	**co**		0
Larix Type	**co**		0
Carex Type	**cx**		1
Thin Plate W/Wavy Margins	**wp**		0
Elongate Grainy	**el**		0
Diatoms	**di**		3
		Total:	**240**

Site/Locality: **SR34**			
Provenience: **230-240cm**			
Morphotype Descriptions			**Counts**
Poaceae Morphotypes			
Rectangular Plate	**pr**		1
Short Wavy <4 Lobes	**ws**		8
Long Wavy >4 Lobes	**wl**		1
Long Rectangular Parallel Sides	**lc**		7
Long Indented	**li**		3
Long Deeply Indented	**ld**		2
Long Angular Non-Parallel	**la**		0
Scutiform and Dendritic	**sd**		0
Rondel Oval	**ro**		15
Rondel Keeled	**rk**		0
Rondel Horned	**rh**		0
Rondel Pyramidal	**rp**		0
Stipa-type Bilobate	**bs**		0
Bilobate	**bi**		0
Saddle	**sa**		0
Tricome	**ht**		5
Hair/Base	**hh**		16
Non-Poaceae Morphotypes			
Blocky Grainy	**bg**		74
Blocky Smooth	**bl**		48
Epidermal Polygonal	**ep**		52
Epidermal anticlinal	**ea**		5
P. ponderosa Type	**pp**		0
P. menziesii Type	**co**		0
Larix Type	**co**		0
Carex Type	**cx**		0
Thin Plate W/Wavy Margins	**wp**		0
Elongate Grainy	**el**		0
Diatoms	**di**		10
		Total:	**247**

Site/Locality: **SR34**			
Provenience: **240-250cm**			
Morphotype Descriptions			**Counts**
Poaceae Morphotypes			
Rectangular Plate	**pr**		5
Short Wavy <4 Lobes	**ws**		13
Long Wavy >4 Lobes	**wl**		0
Long Rectangular Parallel Sides	**lc**		5
Long Indented	**li**		4
Long Deeply Indented	**ld**		1
Long Angular Non-Parallel	**la**		0
Scutiform and Dendritic	**sd**		0
Rondel Oval	**ro**		55
Rondel Keeled	**rk**		4
Rondel Horned	**rh**		0
Rondel Pyramidal	**rp**		0
Stipa-type Bilobate	**bs**		1
Bilobate	**bi**		0
Saddle	**sa**		0
Tricome	**ht**		0
Hair/Base	**hh**		20
Non-Poaceae Morphotypes			
Blocky Grainy	**bg**		59
Blocky Smooth	**bl**		25
Epidermal Polygonal	**ep**		31
Epidermal anticlinal	**ea**		6
P. ponderosa Type	**pp**		2
P. menziesii Type	**co**		0
Larix Type	**co**		0
Carex Type	**cx**		0
Thin Plate W/Wavy Margins	**wp**		0
Elongate Grainy	**el**		0
Diatoms	**di**		10
		Total:	**241**

Site/Locality: **SR34**			
Provenience: **250-260cm**			
Morphotype Descriptions			**Counts**
Poaceae Morphotypes			
Rectangular Plate	**pr**		3
Short Wavy <4 Lobes	**ws**		13
Long Wavy >4 Lobes	**wl**		0
Long Rectangular Parallel Sides	**lc**		5
Long Indented	**li**		1
Long Deeply Indented	**ld**		0
Long Angular Non-Parallel	**la**		1
Scutiform and Dendritic	**sd**		0
Rondel Oval	**ro**		44
Rondel Keeled	**rk**		0
Rondel Horned	**rh**		0
Rondel Pyramidal	**rp**		0
Stipa-type Bilobate	**bs**		1
Bilobate	**bi**		1
Saddle	**sa**		0
Tricome	**ht**		2
Hair/Base	**hh**		15
Non-Poaceae Morphotypes			
Blocky Grainy	**bg**		66
Blocky Smooth	**bl**		27
Epidermal Polygonal	**ep**		44
Epidermal anticlinal	**ea**		4
P. ponderosa Type	**pp**		0
P. menziesii Type	**co**		0
Larix Type	**co**		0
Carex Type	**cx**		0
Thin Plate W/Wavy Margins	**wp**		1
Elongate Grainy	**el**		0
Diatoms	**di**		2
		Total:	**230**

Site/Locality: **SR34**			
Provenience: **260-270cm**			
Morphotype Descriptions			**Counts**
Poaceae Morphotypes			
Rectangular Plate	**pr**		2
Short Wavy <4 Lobes	**ws**		20
Long Wavy >4 Lobes	**wl**		0
Long Rectangular Parallel Sides	**lc**		11
Long Indented	**li**		2
Long Deeply Indented	**ld**		0
Long Angular Non-Parallel	**la**		0
Scutiform and Dendritic	**sd**		0
Rondel Oval	**ro**		60
Rondel Keeled	**rk**		2
Rondel Horned	**rh**		0
Rondel Pyramidal	**rp**		0
Stipa-type Bilobate	**bs**		1
Bilobate	**bi**		1
Saddle	**sa**		0
Tricome	**ht**		0
Hair/Base	**hh**		8
Non-Poaceae Morphotypes			
Blocky Grainy	**bg**		59
Blocky Smooth	**bl**		22
Epidermal Polygonal	**ep**		29
Epidermal anticlinal	**ea**		0
P. ponderosa Type	**pp**		1
P. menziesii Type	**co**		0
Larix Type	**co**		0
Carex Type	**cx**		0
Thin Plate W/Wavy Margins	**wp**		1
Elongate Grainy	**el**		0
Diatoms	**di**		8
		Total:	**227**

Site/Locality: **SR34**			
Provenience: **270-280cm**			
Morphotype Descriptions			**Counts**
Poaceae Morphotypes			
Rectangular Plate	**pr**		11
Short Wavy <4 Lobes	**ws**		32
Long Wavy >4 Lobes	**wl**		2
Long Rectangular Parallel Sides	**lc**		8
Long Indented	**li**		1
Long Deeply Indented	**ld**		0
Long Angular Non-Parallel	**la**		1
Scutiform and Dendritic	**sd**		0
Rondel Oval	**ro**		65
Rondel Keeled	**rk**		6
Rondel Horned	**rh**		0
Rondel Pyramidal	**rp**		0
Stipa-type Bilobate	**bs**		0
Bilobate	**bi**		0
Saddle	**sa**		0
Tricome	**ht**		4
Hair/Base	**hh**		11
Non-Poaceae Morphotypes			
Blocky Grainy	**bg**		52
Blocky Smooth	**bl**		17
Epidermal Polygonal	**ep**		22
Epidermal anticlinal	**ea**		0
P. ponderosa Type	**pp**		0
P. menziesii Type	**co**		0
Larix Type	**co**		0
Carex Type	**cx**		0
Thin Plate W/Wavy Margins	**wp**		0
Elongate Grainy	**el**		0
Diatoms	**di**		0
		Total:	**232**

Site/Locality: **SR34**			
Provenience: **280-290cm**			
Morphotype Descriptions			**Counts**
Poaceae Morphotypes			
Rectangular Plate	**pr**		4
Short Wavy <4 Lobes	**ws**		20
Long Wavy >4 Lobes	**wl**		3
Long Rectangular Parallel Sides	**lc**		2
Long Indented	**li**		6
Long Deeply Indented	**ld**		2
Long Angular Non-Parallel	**la**		0
Scutiform and Dendritic	**sd**		0
Rondel Oval	**ro**		62
Rondel Keeled	**rk**		5
Rondel Horned	**rh**		0
Rondel Pyramidal	**rp**		4
Stipa-type Bilobate	**bs**		2
Bilobate	**bi**		0
Saddle	**sa**		0
Tricome	**ht**		0
Hair/Base	**hh**		15
Non-Poaceae Morphotypes			
Blocky Grainy	**bg**		59
Blocky Smooth	**bl**		20
Epidermal Polygonal	**ep**		31
Epidermal anticlinal	**ea**		0
P. ponderosa Type	**pp**		0
P. menziesii Type	**co**		0
Larix Type	**co**		0
Carex Type	**cx**		0
Thin Plate W/Wavy Margins	**wp**		0
Elongate Grainy	**el**		0
Diatoms	**di**		1
		Total:	**236**

Site/Locality: **SR34**			
Provenience: **290-300cm**			
Morphotype Descriptions			**Counts**
Poaceae Morphotypes			
Rectangular Plate	**pr**		3
Short Wavy <4 Lobes	**ws**		27
Long Wavy >4 Lobes	**wl**		1
Long Rectangular Parallel Sides	**lc**		7
Long Indented	**li**		5
Long Deeply Indented	**ld**		0
Long Angular Non-Parallel	**la**		0
Scutiform and Dendritic	**sd**		0
Rondel Oval	**ro**		54
Rondel Keeled	**rk**		7
Rondel Horned	**rh**		0
Rondel Pyramidal	**rp**		2
Stipa-type Bilobate	**bs**		0
Bilobate	**bi**		0
Saddle	**sa**		0
Tricome	**ht**		2
Hair/Base	**hh**		12
Non-Poaceae Morphotypes			
Blocky Grainy	**bg**		47
Blocky Smooth	**bl**		15
Epidermal Polygonal	**ep**		36
Epidermal anticlinal	**ea**		0
P. ponderosa Type	**pp**		0
P. menziesii Type	**co**		0
Larix Type	**co**		0
Carex Type	**cx**		0
Thin Plate W/Wavy Margins	**wp**		0
Elongate Grainy	**el**		0
Diatoms	**di**		3
		Total:	**221**

Site/Locality: **SR34**			
Provenience: **300-310cm**			
Morphotype Descriptions			**Counts**
Poaceae Morphotypes			
Rectangular Plate	**pr**		10
Short Wavy <4 Lobes	**ws**		29
Long Wavy >4 Lobes	**wl**		2
Long Rectangular Parallel Sides	**lc**		5
Long Indented	**li**		4
Long Deeply Indented	**ld**		0
Long Angular Non-Parallel	**la**		0
Scutiform and Dendritic	**sd**		0
Rondel Oval	**ro**		41
Rondel Keeled	**rk**		5
Rondel Horned	**rh**		0
Rondel Pyramidal	**rp**		0
Stipa-type Bilobate	**bs**		1
Bilobate	**bi**		1
Saddle	**sa**		0
Tricome	**ht**		0
Hair/Base	**hh**		6
Non-Poaceae Morphotypes			
Blocky Grainy	**bg**		58
Blocky Smooth	**bl**		26
Epidermal Polygonal	**ep**		27
Epidermal anticlinal	**ea**		0
P. ponderosa Type	**pp**		0
P. menziesii Type	**co**		0
Larix Type	**co**		0
Carex Type	**cx**		0
Thin Plate W/Wavy Margins	**wp**		0
Elongate Grainy	**el**		0
Diatoms	**di**		1
		Total:	**216**

Site/Locality: **SR34**			
Provenience: **310-320cm**			
Morphotype Descriptions			**Counts**
Poaceae Morphotypes			
Rectangular Plate	**pr**		11
Short Wavy <4 Lobes	**ws**		23
Long Wavy >4 Lobes	**wl**		0
Long Rectangular Parallel Sides	**lc**		1
Long Indented	**li**		2
Long Deeply Indented	**ld**		0
Long Angular Non-Parallel	**la**		0
Scutiform and Dendritic	**sd**		0
Rondel Oval	**ro**		34
Rondel Keeled	**rk**		4
Rondel Horned	**rh**		0
Rondel Pyramidal	**rp**		2
Stipa-type Bilobate	**bs**		0
Bilobate	**bi**		0
Saddle	**sa**		0
Tricome	**ht**		2
Hair/Base	**hh**		8
Non-Poaceae Morphotypes			
Blocky Grainy	**bg**		52
Blocky Smooth	**bl**		30
Epidermal Polygonal	**ep**		37
Epidermal anticlinal	**ea**		8
P. ponderosa Type	**pp**		0
P. menziesii Type	**co**		0
Larix Type	**co**		0
Carex Type	**cx**		0
Thin Plate W/Wavy Margins	**wp**		0
Elongate Grainy	**el**		0
Diatoms	**di**		2
		Total:	**216**

Site/Locality: **SR34**			
Provenience: **320-330cm**			
Morphotype Descriptions			**Counts**
Poaceae Morphotypes			
Rectangular Plate	**pr**		7
Short Wavy <4 Lobes	**ws**		21
Long Wavy >4 Lobes	**wl**		3
Long Rectangular Parallel Sides	**lc**		7
Long Indented	**li**		4
Long Deeply Indented	**ld**		0
Long Angular Non-Parallel	**la**		0
Scutiform and Dendritic	**sd**		0
Rondel Oval	**ro**		49
Rondel Keeled	**rk**		9
Rondel Horned	**rh**		0
Rondel Pyramidal	**rp**		6
Stipa-type Bilobate	**bs**		0
Bilobate	**bi**		0
Saddle	**sa**		0
Tricome	**ht**		4
Hair/Base	**hh**		7
Non-Poaceae Morphotypes			
Blocky Grainy	**bg**		44
Blocky Smooth	**bl**		29
Epidermal Polygonal	**ep**		33
Epidermal anticlinal	**ea**		5
P. ponderosa Type	**pp**		1
P. menziesii Type	**co**		0
Larix Type	**co**		0
Carex Type	**cx**		0
Thin Plate W/Wavy Margins	**wp**		0
Elongate Grainy	**el**		0
Diatoms	**di**		4
		Total:	**233**

Site/Locality: **SR34**			
Provenience: **330-340cm**			
Morphotype Descriptions			**Counts**
Poaceae Morphotypes			
Rectangular Plate	**pr**		9
Short Wavy <4 Lobes	**ws**		5
Long Wavy >4 Lobes	**wl**		2
Long Rectangular Parallel Sides	**lc**		6
Long Indented	**li**		1
Long Deeply Indented	**ld**		0
Long Angular Non-Parallel	**la**		0
Scutiform and Dendritic	**sd**		0
Rondel Oval	**ro**		35
Rondel Keeled	**rk**		0
Rondel Horned	**rh**		0
Rondel Pyramidal	**rp**		0
Stipa-type Bilobate	**bs**		1
Bilobate	**bi**		1
Saddle	**sa**		0
Tricome	**ht**		2
Hair/Base	**hh**		18
Non-Poaceae Morphotypes			
Blocky Grainy	**bg**		69
Blocky Smooth	**bl**		24
Epidermal Polygonal	**ep**		51
Epidermal anticlinal	**ea**		7
P. ponderosa Type	**pp**		0
P. menziesii Type	**co**		0
Larix Type	**co**		0
Carex Type	**cx**		1
Thin Plate W/Wavy Margins	**wp**		1
Elongate Grainy	**el**		0
Diatoms	**di**		2
		Total:	**235**

Site/Locality: **SR34**			
Provenience: **340-350cm**			
Morphotype Descriptions			**Counts**
Poaceae Morphotypes			
Rectangular Plate	**pr**		5
Short Wavy <4 Lobes	**ws**		16
Long Wavy >4 Lobes	**wl**		0
Long Rectangular Parallel Sides	**lc**		4
Long Indented	**li**		2
Long Deeply Indented	**ld**		0
Long Angular Non-Parallel	**la**		0
Scutiform and Dendritic	**sd**		0
Rondel Oval	**ro**		47
Rondel Keeled	**rk**		10
Rondel Horned	**rh**		0
Rondel Pyramidal	**rp**		3
Stipa-type Bilobate	**bs**		0
Bilobate	**bi**		0
Saddle	**sa**		0
Tricome	**ht**		2
Hair/Base	**hh**		10
Non-Poaceae Morphotypes			
Blocky Grainy	**bg**		51
Blocky Smooth	**bl**		20
Epidermal Polygonal	**ep**		41
Epidermal anticlinal	**ea**		8
P. ponderosa Type	**pp**		2
P. menziesii Type	**co**		0
Larix Type	**co**		0
Carex Type	**cx**		0
Thin Plate W/Wavy Margins	**wp**		0
Elongate Grainy	**el**		0
Diatoms	**di**		0
		Total:	**221**

Site/Locality: **SR34**			
Provenience: **350-360cm**			
Morphotype Descriptions			**Counts**
Poaceae Morphotypes			
Rectangular Plate	**pr**		12
Short Wavy <4 Lobes	**ws**		22
Long Wavy >4 Lobes	**wl**		0
Long Rectangular Parallel Sides	**lc**		5
Long Indented	**li**		1
Long Deeply Indented	**ld**		0
Long Angular Non-Parallel	**la**		0
Scutiform and Dendritic	**sd**		0
Rondel Oval	**ro**		41
Rondel Keeled	**rk**		8
Rondel Horned	**rh**		0
Rondel Pyramidal	**rp**		4
Stipa-type Bilobate	**bs**		0
Bilobate	**bi**		0
Saddle	**sa**		0
Tricome	**ht**		1
Hair/Base	**hh**		7
Non-Poaceae Morphotypes			
Blocky Grainy	**bg**		44
Blocky Smooth	**bl**		18
Epidermal Polygonal	**ep**		35
Epidermal anticlinal	**ea**		12
P. ponderosa Type	**pp**		0
P. menziesii Type	**co**		0
Larix Type	**co**		0
Carex Type	**cx**		1
Thin Plate W/Wavy Margins	**wp**		0
Elongate Grainy	**el**		0
Diatoms	**di**		0
		Total:	**211**

Site/Locality: **SR34**			
Provenience: **350-360cm**			
Morphotype Descriptions			**Counts**
Poaceae Morphotypes			
Rectangular Plate	**pr**		8
Short Wavy <4 Lobes	**ws**		18
Long Wavy >4 Lobes	**wl**		0
Long Rectangular Parallel Sides	**lc**		10
Long Indented	**li**		5
Long Deeply Indented	**ld**		1
Long Angular Non-Parallel	**la**		0
Scutiform and Dendritic	**sd**		1
Rondel Oval	**ro**		53
Rondel Keeled	**rk**		8
Rondel Horned	**rh**		0
Rondel Pyramidal	**rp**		5
Stipa-type Bilobate	**bs**		0
Bilobate	**bi**		0
Saddle	**sa**		0
Tricome	**ht**		8
Hair/Base	**hh**		5
Non-Poaceae Morphotypes			
Blocky Grainy	**bg**		55
Blocky Smooth	**bl**		17
Epidermal Polygonal	**ep**		19
Epidermal anticlinal	**ea**		15
P. ponderosa Type	**pp**		1
P. menziesii Type	**co**		0
Larix Type	**co**		0
Carex Type	**cx**		1
Thin Plate W/Wavy Margins	**wp**		0
Elongate Grainy	**el**		0
Diatoms	**di**		0
		Total:	**230**

Site/Locality: **SR34**			
Provenience: **370-380cm**			
Morphotype Descriptions			**Counts**
Poaceae Morphotypes			
Rectangular Plate	**pr**		10
Short Wavy <4 Lobes	**ws**		25
Long Wavy >4 Lobes	**wl**		1
Long Rectangular Parallel Sides	**lc**		12
Long Indented	**li**		4
Long Deeply Indented	**ld**		0
Long Angular Non-Parallel	**la**		0
Scutiform and Dendritic	**sd**		0
Rondel Oval	**ro**		46
Rondel Keeled	**rk**		11
Rondel Horned	**rh**		0
Rondel Pyramidal	**rp**		2
Stipa-type Bilobate	**bs**		0
Bilobate	**bi**		0
Saddle	**sa**		0
Tricome	**ht**		1
Hair/Base	**hh**		4
Non-Poaceae Morphotypes			
Blocky Grainy	**bg**		52
Blocky Smooth	**bl**		21
Epidermal Polygonal	**ep**		22
Epidermal anticlinal	**ea**		10
P. ponderosa Type	**pp**		0
P. menziesii Type	**co**		0
Larix Type	**co**		0
Carex Type	**cx**		1
Thin Plate W/Wavy Margins	**wp**		0
Elongate Grainy	**el**		0
Diatoms	**di**		2
		Total:	**224**

Site/Locality: **SR34**			
Provenience: **380-390cm**			
Morphotype Descriptions			**Counts**
Poaceae Morphotypes			
Rectangular Plate	**pr**		17
Short Wavy <4 Lobes	**ws**		23
Long Wavy >4 Lobes	**wl**		3
Long Rectangular Parallel Sides	**lc**		11
Long Indented	**li**		2
Long Deeply Indented	**ld**		0
Long Angular Non-Parallel	**la**		0
Scutiform and Dendritic	**sd**		0
Rondel Oval	**ro**		34
Rondel Keeled	**rk**		5
Rondel Horned	**rh**		0
Rondel Pyramidal	**rp**		0
Stipa-type Bilobate	**bs**		1
Bilobate	**bi**		0
Saddle	**sa**		0
Tricome	**ht**		3
Hair/Base	**hh**		6
Non-Poaceae Morphotypes			
Blocky Grainy	**bg**		41
Blocky Smooth	**bl**		16
Epidermal Polygonal	**ep**		35
Epidermal anticlinal	**ea**		9
P. ponderosa Type	**pp**		0
P. menziesii Type	**co**		0
Larix Type	**co**		2
Carex Type	**cx**		1
Thin Plate W/Wavy Margins	**wp**		0
Elongate Grainy	**el**		0
Diatoms	**di**		1
		Total:	**210**

Site/Locality: **SR34**			
Provenience: **390-400cm**			
Morphotype Descriptions			**Counts**
Poaceae Morphotypes			
Rectangular Plate	**pr**		19
Short Wavy <4 Lobes	**ws**		12
Long Wavy >4 Lobes	**wl**		1
Long Rectangular Parallel Sides	**lc**		1
Long Indented	**li**		3
Long Deeply Indented	**ld**		1
Long Angular Non-Parallel	**la**		0
Scutiform and Dendritic	**sd**		0
Rondel Oval	**ro**		43
Rondel Keeled	**rk**		8
Rondel Horned	**rh**		0
Rondel Pyramidal	**rp**		3
Stipa-type Bilobate	**bs**		0
Bilobate	**bi**		0
Saddle	**sa**		0
Tricome	**ht**		3
Hair/Base	**hh**		25
Non-Poaceae Morphotypes			
Blocky Grainy	**bg**		48
Blocky Smooth	**bl**		10
Epidermal Polygonal	**ep**		31
Epidermal anticlinal	**ea**		6
P. ponderosa Type	**pp**		2
P. menziesii Type	**co**		0
Larix Type	**co**		0
Carex Type	**cx**		0
Thin Plate W/Wavy Margins	**wp**		0
Elongate Grainy	**el**		3
Diatoms	**di**		0
		Total:	**219**

Site/Locality: **SR34**			
Provenience: **400-410cm**			
Morphotype Descriptions			**Counts**
Poaceae Morphotypes			
Rectangular Plate	**pr**		16
Short Wavy <4 Lobes	**ws**		9
Long Wavy >4 Lobes	**wl**		1
Long Rectangular Parallel Sides	**lc**		2
Long Indented	**li**		3
Long Deeply Indented	**ld**		2
Long Angular Non-Parallel	**la**		1
Scutiform and Dendritic	**sd**		1
Rondel Oval	**ro**		31
Rondel Keeled	**rk**		5
Rondel Horned	**rh**		0
Rondel Pyramidal	**rp**		2
Stipa-type Bilobate	**bs**		1
Bilobate	**bi**		0
Saddle	**sa**		0
Tricome	**ht**		2
Hair/Base	**hh**		22
Non-Poaceae Morphotypes			
Blocky Grainy	**bg**		67
Blocky Smooth	**bl**		39
Epidermal Polygonal	**ep**		50
Epidermal anticlinal	**ea**		11
P. ponderosa Type	**pp**		0
P. menziesii Type	**co**		0
Larix Type	**co**		0
Carex Type	**cx**		0
Thin Plate W/Wavy Margins	**wp**		2
Elongate Grainy	**el**		1
Diatoms	**di**		0
		Total:	**268**

Site/Locality: **SR34**			
Provenience: **410-420cm**			
Morphotype Descriptions			**Counts**
Poaceae Morphotypes			
Rectangular Plate	**pr**		7
Short Wavy <4 Lobes	**ws**		5
Long Wavy >4 Lobes	**wl**		1
Long Rectangular Parallel Sides	**lc**		0
Long Indented	**li**		0
Long Deeply Indented	**ld**		0
Long Angular Non-Parallel	**la**		0
Scutiform and Dendritic	**sd**		0
Rondel Oval	**ro**		13
Rondel Keeled	**rk**		3
Rondel Horned	**rh**		0
Rondel Pyramidal	**rp**		0
Stipa-type Bilobate	**bs**		3
Bilobate	**bi**		0
Saddle	**sa**		0
Tricome	**ht**		1
Hair/Base	**hh**		16
Non-Poaceae Morphotypes			
Blocky Grainy	**bg**		57
Blocky Smooth	**bl**		32
Epidermal Polygonal	**ep**		58
Epidermal anticlinal	**ea**		9
P. ponderosa Type	**pp**		0
P. menziesii Type	**co**		0
Larix Type	**co**		0
Carex Type	**cx**		0
Thin Plate W/Wavy Margins	**wp**		1
Elongate Grainy	**el**		1
Diatoms	**di**		0
		Total:	**207**

Site/Locality: **SR34**			
Provenience: **420-430cm**			
Morphotype Descriptions			**Counts**
Poaceae Morphotypes			
Rectangular Plate	**pr**		10
Short Wavy <4 Lobes	**ws**		13
Long Wavy >4 Lobes	**wl**		2
Long Rectangular Parallel Sides	**lc**		5
Long Indented	**li**		0
Long Deeply Indented	**ld**		1
Long Angular Non-Parallel	**la**		0
Scutiform and Dendritic	**sd**		2
Rondel Oval	**ro**		8
Rondel Keeled	**rk**		4
Rondel Horned	**rh**		2
Rondel Pyramidal	**rp**		0
Stipa-type Bilobate	**bs**		0
Bilobate	**bi**		0
Saddle	**sa**		0
Tricome	**ht**		2
Hair/Base	**hh**		21
Non-Poaceae Morphotypes			
Blocky Grainy	**bg**		63
Blocky Smooth	**bl**		27
Epidermal Polygonal	**ep**		60
Epidermal anticlinal	**ea**		12
P. ponderosa Type	**pp**		0
P. menziesii Type	**co**		0
Larix Type	**co**		0
Carex Type	**cx**		0
Thin Plate W/Wavy Margins	**wp**		1
Elongate Grainy	**el**		1
Diatoms	**di**		2
		Total:	**236**

Site/Locality: **SR34**			
Provenience: **430-440cm**			
Morphotype Descriptions			**Counts**
Poaceae Morphotypes			
Rectangular Plate	**pr**		7
Short Wavy <4 Lobes	**ws**		6
Long Wavy >4 Lobes	**wl**		0
Long Rectangular Parallel Sides	**lc**		2
Long Indented	**li**		2
Long Deeply Indented	**ld**		1
Long Angular Non-Parallel	**la**		0
Scutiform and Dendritic	**sd**		1
Rondel Oval	**ro**		13
Rondel Keeled	**rk**		6
Rondel Horned	**rh**		0
Rondel Pyramidal	**rp**		0
Stipa-type Bilobate	**bs**		1
Bilobate	**bi**		1
Saddle	**sa**		0
Tricome	**ht**		4
Hair/Base	**hh**		20
Non-Poaceae Morphotypes			
Blocky Grainy	**bg**		65
Blocky Smooth	**bl**		30
Epidermal Polygonal	**ep**		64
Epidermal anticlinal	**ea**		10
P. ponderosa Type	**pp**		0
P. menziesii Type	**co**		0
Larix Type	**co**		0
Carex Type	**cx**		1
Thin Plate W/Wavy Margins	**wp**		3
Elongate Grainy	**el**		4
Diatoms	**di**		0
		Total:	**241**

Site/Locality: **SR34**			
Provenience: **440-450cm**			
Morphotype Descriptions			**Counts**
Poaceae Morphotypes			
Rectangular Plate	**pr**		5
Short Wavy <4 Lobes	**ws**		13
Long Wavy >4 Lobes	**wl**		1
Long Rectangular Parallel Sides	**lc**		2
Long Indented	**li**		6
Long Deeply Indented	**ld**		0
Long Angular Non-Parallel	**la**		0
Scutiform and Dendritic	**sd**		0
Rondel Oval	**ro**		10
Rondel Keeled	**rk**		2
Rondel Horned	**rh**		0
Rondel Pyramidal	**rp**		0
Stipa-type Bilobate	**bs**		1
Bilobate	**bi**		0
Saddle	**sa**		0
Tricome	**ht**		7
Hair/Base	**hh**		26
Non-Poaceae Morphotypes			
Blocky Grainy	**bg**		57
Blocky Smooth	**bl**		39
Epidermal Polygonal	**ep**		50
Epidermal anticlinal	**ea**		4
P. ponderosa Type	**pp**		0
P. menziesii Type	**co**		0
Larix Type	**co**		0
Carex Type	**cx**		1
Thin Plate W/Wavy Margins	**wp**		2
Elongate Grainy	**el**		6
Diatoms	**di**		0
		Total:	**232**

Site/Locality: **SR34**			
Provenience: **450-460cm**			
Morphotype Descriptions			**Counts**
Poaceae Morphotypes			
Rectangular Plate	**pr**		8
Short Wavy <4 Lobes	**ws**		7
Long Wavy >4 Lobes	**wl**		1
Long Rectangular Parallel Sides	**lc**		4
Long Indented	**li**		0
Long Deeply Indented	**ld**		0
Long Angular Non-Parallel	**la**		0
Scutiform and Dendritic	**sd**		0
Rondel Oval	**ro**		6
Rondel Keeled	**rk**		1
Rondel Horned	**rh**		0
Rondel Pyramidal	**rp**		2
Stipa-type Bilobate	**bs**		0
Bilobate	**bi**		0
Saddle	**sa**		0
Tricome	**ht**		5
Hair/Base	**hh**		21
Non-Poaceae Morphotypes			
Blocky Grainy	**bg**		65
Blocky Smooth	**bl**		33
Epidermal Polygonal	**ep**		43
Epidermal anticlinal	**ea**		11
P. ponderosa Type	**pp**		0
P. menziesii Type	**co**		0
Larix Type	**co**		0
Carex Type	**cx**		0
Thin Plate W/Wavy Margins	**wp**		1
Elongate Grainy	**el**		3
Diatoms	**di**		2
		Total:	**213**

Site/Locality: **SR34**			
Provenience: **460-470cm**			
Morphotype Descriptions			**Counts**
Poaceae Morphotypes			
Rectangular Plate	**pr**		6
Short Wavy <4 Lobes	**ws**		25
Long Wavy >4 Lobes	**wl**		0
Long Rectangular Parallel Sides	**lc**		6
Long Indented	**li**		11
Long Deeply Indented	**ld**		1
Long Angular Non-Parallel	**la**		0
Scutiform and Dendritic	**sd**		0
Rondel Oval	**ro**		5
Rondel Keeled	**rk**		4
Rondel Horned	**rh**		0
Rondel Pyramidal	**rp**		1
Stipa-type Bilobate	**bs**		0
Bilobate	**bi**		0
Saddle	**sa**		0
Tricome	**ht**		14
Hair/Base	**hh**		17
Non-Poaceae Morphotypes			
Blocky Grainy	**bg**		40
Blocky Smooth	**bl**		28
Epidermal Polygonal	**ep**		55
Epidermal anticlinal	**ea**		8
P. ponderosa Type	**pp**		0
P. menziesii Type	**co**		0
Larix Type	**co**		0
Carex Type	**cx**		0
Thin Plate W/Wavy Margins	**wp**		1
Elongate Grainy	**el**		1
Diatoms	**di**		0
		Total:	**223**

Site/Locality: **SR34**			
Provenience: **470-480cm**			
Morphotype Descriptions			**Counts**
Poaceae Morphotypes			
Rectangular Plate	**pr**		12
Short Wavy <4 Lobes	**ws**		23
Long Wavy >4 Lobes	**wl**		1
Long Rectangular Parallel Sides	**lc**		4
Long Indented	**li**		1
Long Deeply Indented	**ld**		1
Long Angular Non-Parallel	**la**		0
Scutiform and Dendritic	**sd**		0
Rondel Oval	**ro**		2
Rondel Keeled	**rk**		3
Rondel Horned	**rh**		0
Rondel Pyramidal	**rp**		0
Stipa-type Bilobate	**bs**		1
Bilobate	**bi**		1
Saddle	**sa**		0
Tricome	**ht**		12
Hair/Base	**hh**		11
Non-Poaceae Morphotypes			
Blocky Grainy	**bg**		51
Blocky Smooth	**bl**		36
Epidermal Polygonal	**ep**		40
Epidermal anticlinal	**ea**		10
P. ponderosa Type	**pp**		1
P. menziesii Type	**co**		0
Larix Type	**co**		0
Carex Type	**cx**		3
Thin Plate W/Wavy Margins	**wp**		0
Elongate Grainy	**el**		0
Diatoms	**di**		2
		Total:	**215**

Site/Locality: **SR34**			
Provenience: **480-490cm**			
Morphotype Descriptions			**Counts**
Poaceae Morphotypes			
Rectangular Plate	**pr**		6
Short Wavy <4 Lobes	**ws**		13
Long Wavy >4 Lobes	**wl**		2
Long Rectangular Parallel Sides	**lc**		4
Long Indented	**li**		1
Long Deeply Indented	**ld**		0
Long Angular Non-Parallel	**la**		0
Scutiform and Dendritic	**sd**		0
Rondel Oval	**ro**		8
Rondel Keeled	**rk**		3
Rondel Horned	**rh**		1
Rondel Pyramidal	**rp**		0
Stipa-type Bilobate	**bs**		0
Bilobate	**bi**		0
Saddle	**sa**		0
Tricome	**ht**		15
Hair/Base	**hh**		14
Non-Poaceae Morphotypes			
Blocky Grainy	**bg**		42
Blocky Smooth	**bl**		30
Epidermal Polygonal	**ep**		60
Epidermal anticlinal	**ea**		7
P. ponderosa Type	**pp**		1
P. menziesii Type	**co**		0
Larix Type	**co**		0
Carex Type	**cx**		0
Thin Plate W/Wavy Margins	**wp**		2
Elongate Grainy	**el**		5
Diatoms	**di**		1
		Total:	**215**

Site/Locality: **SR34**			
Provenience: **490-500cm**			
Morphotype Descriptions			**Counts**
Poaceae Morphotypes			
Rectangular Plate	**pr**		8
Short Wavy <4 Lobes	**ws**		24
Long Wavy >4 Lobes	**wl**		4
Long Rectangular Parallel Sides	**lc**		5
Long Indented	**li**		3
Long Deeply Indented	**ld**		0
Long Angular Non-Parallel	**la**		1
Scutiform and Dendritic	**sd**		0
Rondel Oval	**ro**		10
Rondel Keeled	**rk**		6
Rondel Horned	**rh**		1
Rondel Pyramidal	**rp**		2
Stipa-type Bilobate	**bs**		2
Bilobate	**bi**		1
Saddle	**sa**		0
Tricome	**ht**		5
Hair/Base	**hh**		12
Non-Poaceae Morphotypes			
Blocky Grainy	**bg**		29
Blocky Smooth	**bl**		34
Epidermal Polygonal	**ep**		67
Epidermal anticlinal	**ea**		6
P. ponderosa Type	**pp**		0
P. menziesii Type	**co**		0
Larix Type	**co**		0
Carex Type	**cx**		0
Thin Plate W/Wavy Margins	**wp**		1
Elongate Grainy	**el**		1
Diatoms	**di**		0
		Total:	**222**

Site/Locality: **10IH73**			
Provenience: **LU2**			
Morphotype Descriptions			**Counts**
Poaceae Morphotypes			
Rectangular Plate	**pr**		3
Short Wavy <4 Lobes	**ws**		4
Long Wavy >4 Lobes	**wl**		1
Long Rectangular Parallel Sides	**lc**		0
Long Indented	**li**		0
Long Deeply Indented	**ld**		0
Long Angular Non-Parallel	**la**		0
Scutiform and Dendritic	**sd**		0
Rondel Oval	**ro**		0
Rondel Keeled	**rk**		0
Rondel Horned	**rh**		0
Rondel Pyramidal	**rp**		0
Stipa-type Bilobate	**bs**		0
Bilobate	**bi**		0
Saddle	**sa**		0
Tricome	**ht**		4
Hair/Base	**hh**		8
Non-Poaceae Morphotypes			
Blocky Grainy	**bg**		45
Blocky Smooth	**bl**		60
Epidermal Polygonal	**ep**		63
Epidermal anticlinal	**ea**		17
P. ponderosa Type	**pp**		2
P. menziesii Type	**co**		0
Larix Type	**co**		1
Carex Type	**cx**		0
Thin Plate W/Wavy Margins	**wp**		1
Elongate Grainy	**el**		2
Diatoms	**di**		0
		Total:	**211**

Site/Locality: **10IH73**			
Provenience: **LU3**			
Morphotype Descriptions			**Counts**
Poaceae Morphotypes			
Rectangular Plate	**pr**		20
Short Wavy <4 Lobes	**ws**		39
Long Wavy >4 Lobes	**wl**		7
Long Rectangular Parallel Sides	**lc**		5
Long Indented	**li**		4
Long Deeply Indented	**ld**		1
Long Angular Non-Parallel	**la**		0
Scutiform and Dendritic	**sd**		0
Rondel Oval	**ro**		17
Rondel Keeled	**rk**		16
Rondel Horned	**rh**		1
Rondel Pyramidal	**rp**		3
Stipa-type Bilobate	**bs**		4
Bilobate	**bi**		3
Saddle	**sa**		1
Tricome	**ht**		7
Hair/Base	**hh**		15
Non-Poaceae Morphotypes			
Blocky Grainy	**bg**		18
Blocky Smooth	**bl**		11
Epidermal Polygonal	**ep**		29
Epidermal anticlinal	**ea**		7
P. ponderosa Type	**pp**		1
P. menziesii Type	**co**		0
Larix Type	**co**		0
Carex Type	**cx**		1
Thin Plate W/Wavy Margins	**wp**		0
Elongate Grainy	**el**		11
Diatoms	**di**		3
		Total:	**224**

Site/Locality: **10IH73**			
Provenience: **LU4**			
Morphotype Descriptions			**Counts**
Poaceae Morphotypes			
Rectangular Plate	**pr**		7
Short Wavy <4 Lobes	**ws**		38
Long Wavy >4 Lobes	**wl**		5
Long Rectangular Parallel Sides	**lc**		2
Long Indented	**li**		1
Long Deeply Indented	**ld**		0
Long Angular Non-Parallel	**la**		0
Scutiform and Dendritic	**sd**		0
Rondel Oval	**ro**		6
Rondel Keeled	**rk**		5
Rondel Horned	**rh**		19
Rondel Pyramidal	**rp**		2
Stipa-type Bilobate	**bs**		9
Bilobate	**bi**		0
Saddle	**sa**		0
Tricome	**ht**		10
Hair/Base	**hh**		18
Non-Poaceae Morphotypes			
Blocky Grainy	**bg**		33
Blocky Smooth	**bl**		15
Epidermal Polygonal	**ep**		35
Epidermal anticlinal	**ea**		4
P. ponderosa Type	**pp**		0
P. menziesii Type	**co**		0
Larix Type	**co**		0
Carex Type	**cx**		0
Thin Plate W/Wavy Margins	**wp**		0
Elongate Grainy	**el**		10
Diatoms	**di**		1
		Total:	**220**

Site/Locality: **10IH73**			
Provenience: **LU5**			
Morphotype Descriptions			**Counts**
Poaceae Morphotypes			
Rectangular Plate	**pr**		10
Short Wavy <4 Lobes	**ws**		40
Long Wavy >4 Lobes	**wl**		4
Long Rectangular Parallel Sides	**lc**		5
Long Indented	**li**		6
Long Deeply Indented	**ld**		0
Long Angular Non-Parallel	**la**		0
Scutiform and Dendritic	**sd**		0
Rondel Oval	**ro**		7
Rondel Keeled	**rk**		8
Rondel Horned	**rh**		5
Rondel Pyramidal	**rp**		4
Stipa-type Bilobate	**bs**		5
Bilobate	**bi**		1
Saddle	**sa**		0
Tricome	**ht**		7
Hair/Base	**hh**		13
Non-Poaceae Morphotypes			
Blocky Grainy	**bg**		27
Blocky Smooth	**bl**		30
Epidermal Polygonal	**ep**		40
Epidermal anticlinal	**ea**		7
P. ponderosa Type	**pp**		0
P. menziesii Type	**co**		0
Larix Type	**co**		0
Carex Type	**cx**		0
Thin Plate W/Wavy Margins	**wp**		2
Elongate Grainy	**el**		6
Diatoms	**di**		0
		Total:	**227**

Site/Locality: **10IH73**			
Provenience: **LU6**			
Morphotype Descriptions			**Counts**
Poaceae Morphotypes			
Rectangular Plate	**pr**		4
Short Wavy <4 Lobes	**ws**		50
Long Wavy >4 Lobes	**wl**		9
Long Rectangular Parallel Sides	**lc**		16
Long Indented	**li**		10
Long Deeply Indented	**ld**		1
Long Angular Non-Parallel	**la**		2
Scutiform and Dendritic	**sd**		2
Rondel Oval	**ro**		5
Rondel Keeled	**rk**		3
Rondel Horned	**rh**		0
Rondel Pyramidal	**rp**		4
Stipa-type Bilobate	**bs**		2
Bilobate	**bi**		0
Saddle	**sa**		0
Tricome	**ht**		10
Hair/Base	**hh**		19
Non-Poaceae Morphotypes			
Blocky Grainy	**bg**		13
Blocky Smooth	**bl**		20
Epidermal Polygonal	**ep**		26
Epidermal anticlinal	**ea**		2
P. ponderosa Type	**pp**		6
P. menziesii Type	**co**		0
Larix Type	**co**		0
Carex Type	**cx**		1
Thin Plate W/Wavy Margins	**wp**		4
Elongate Grainy	**el**		22
Diatoms	**di**		1
		Total:	**232**

Site/Locality: **10IH73**			
Provenience: **LU8a**			
Morphotype Descriptions			**Counts**
Poaceae Morphotypes			
Rectangular Plate	**pr**		10
Short Wavy <4 Lobes	**ws**		53
Long Wavy >4 Lobes	**wl**		4
Long Rectangular Parallel Sides	**lc**		20
Long Indented	**li**		7
Long Deeply Indented	**ld**		5
Long Angular Non-Parallel	**la**		1
Scutiform and Dendritic	**sd**		4
Rondel Oval	**ro**		9
Rondel Keeled	**rk**		10
Rondel Horned	**rh**		3
Rondel Pyramidal	**rp**		4
Stipa-type Bilobate	**bs**		0
Bilobate	**bi**		0
Saddle	**sa**		0
Tricome	**ht**		6
Hair/Base	**hh**		8
Non-Poaceae Morphotypes			
Blocky Grainy	**bg**		6
Blocky Smooth	**bl**		27
Epidermal Polygonal	**ep**		22
Epidermal anticlinal	**ea**		1
P. ponderosa Type	**pp**		3
P. menziesii Type	**co**		0
Larix Type	**co**		0
Carex Type	**cx**		0
Thin Plate W/Wavy Margins	**wp**		2
Elongate Grainy	**el**		17
Diatoms	**di**		0
		Total:	**222**

Site/Locality: **10IH73**			
Provenience: **LU8b**			
Morphotype Descriptions			**Counts**
Poaceae Morphotypes			
Rectangular Plate	**pr**		5
Short Wavy <4 Lobes	**ws**		32
Long Wavy >4 Lobes	**wl**		9
Long Rectangular Parallel Sides	**lc**		15
Long Indented	**li**		9
Long Deeply Indented	**ld**		1
Long Angular Non-Parallel	**la**		1
Scutiform and Dendritic	**sd**		3
Rondel Oval	**ro**		18
Rondel Keeled	**rk**		5
Rondel Horned	**rh**		0
Rondel Pyramidal	**rp**		3
Stipa-type Bilobate	**bs**		3
Bilobate	**bi**		1
Saddle	**sa**		1
Tricome	**ht**		2
Hair/Base	**hh**		10
Non-Poaceae Morphotypes			
Blocky Grainy	**bg**		21
Blocky Smooth	**bl**		32
Epidermal Polygonal	**ep**		20
Epidermal anticlinal	**ea**		2
P. ponderosa Type	**pp**		1
P. menziesii Type	**co**		0
Larix Type	**co**		0
Carex Type	**cx**		0
Thin Plate W/Wavy Margins	**wp**		0
Elongate Grainy	**el**		20
Diatoms	**di**		2
		Total:	**216**